DISCLAIMER NOTICE

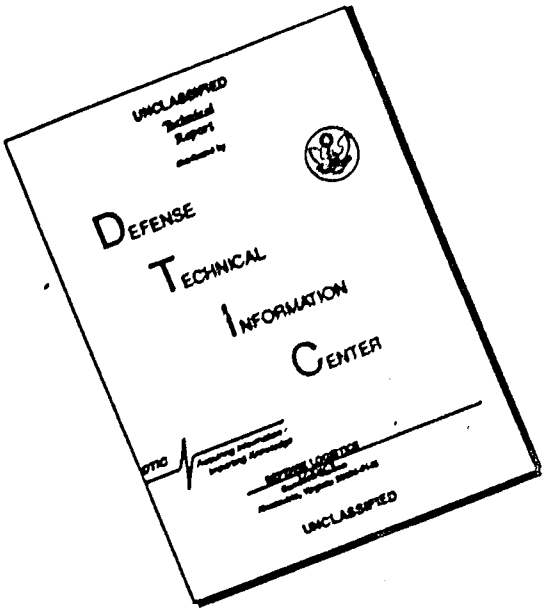

THIS DOCUMENT IS BEST QUALITY AVAILABLE. THE COPY FURNISHED TO DTIC CONTAINED A SIGNIFICANT NUMBER OF PAGES WHICH DO NOT REPRODUCE LEGIBLY.

AF TECHNICAL REPORT 5867

Drop Tests of 16,000-Square-Inch Model Parachutes

Volume I

F. J. Stimler and R. S. Ross

Goodyear Aircraft Corporation
Akron, Ohio

GER-5108

April 1960

Aeronautical Accessories Laboratory
Contract No. AF33(616)-2310
RDO No. 672-160

Wright Air Development Division
Air Research and Development Command
United States Air Force
Wright-Patterson Air Force Base, Ohio

AF-WP-B-AUG 60 200

AF TECHNICAL REPORT 5867

Drop Tests of 16,000-Square-Inch Model Parachutes

Volume I

F. J. Stimler and R.S. Ross

Goodyear Aircraft Corporation

Akron, Ohio

APRIL 1960

Wright Air Development Division

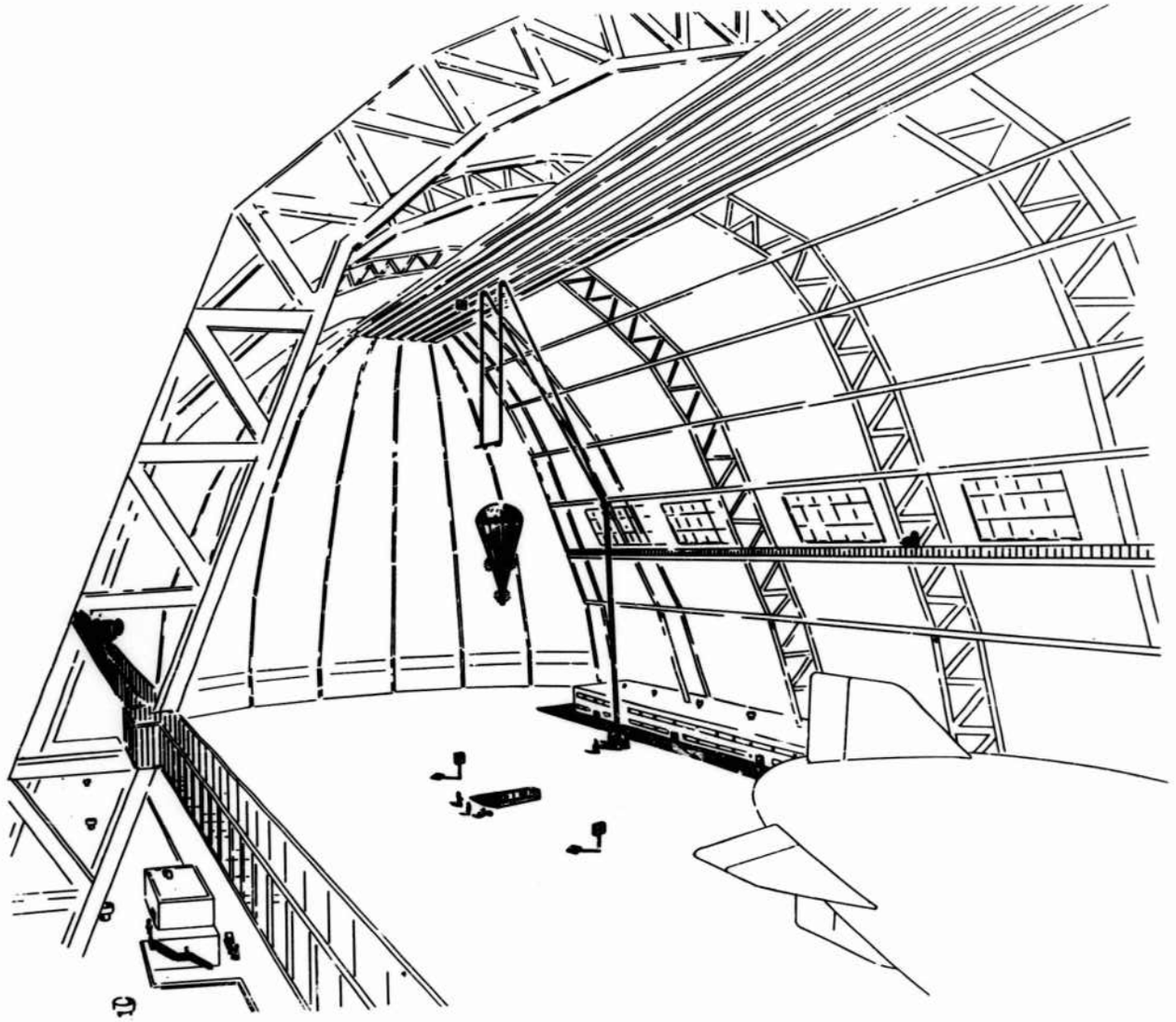

Frontispiece - Goodyear Aircraft Corporation Parachute Drop-Test Setup

FOREWORD

This unclassified report was prepared by Goodyear Aircraft Corporation of Akron, Ohio for the Parachute Branch of the Equipment Laboratory of Air Materiel Command at Wright-Patterson Air Force Base, Dayton, Ohio. The research program was authorized under Purchase Request No. 108280 and Contract No. AF33(038)11979. The parachute drop-test models were constructed at Wingfoot Lake Airship Base in accordance with AMC Exhibit MCREXE-6B-26, and the directions of Mr. G. E. Aichinger, the AMC project engineer. The tests included in this report are an extension of the work described in Memorandum Report No. MCREXE-672-12-B, OS-USAF Wright-Patterson No. 175. This program was initiated at Goodyear Aircraft Corporation under Manufacturing-Order No. 379 and Project No. GA335.

Excellent cooperation was received from the personnel of the Air Materiel Command related to this project, particularly Mr. G. E. Aichinger, Dr. Helmut, G. Heinrich and Captain Sterling K. Hight who were directly affiliated with the program.

ABSTRACT

Performance in free fall of 27 model parachutes of various designs was determined by drop tests conducted in the Goodyear Aircraft Corporation airship dock at Akron, Ohio. Models of approximately 16,000 square inches of cloth surface area were tested to determine the influence of the shape of the canopy (type) and the rate of descent on the drag and stability of specific types of parachutes. The influence of the shroud-line length on the aerodynamic characteristics and the stability of the solid-flat 10% extended-skirt parachute was also investigated. All models were tested at vertical terminal velocitiesof approximately 10, 15, 25, and 40 feet per second for both vertical and horizontal types of release.

Over 700 drop tests were conducted at different intervals between February 1951 and February 1952 with the following types of parachute models:

a. Solid flat parachutes - circular, square with pockets, and triangular with pockets.

b. Solid extended-skirt parachutes - 10%, 12½% and full extension.

c. Airfoil parachute with 50% vent.

d. Solid spherical parachutes - ½ sphere circular, ¼ sphere circular, ¼ sphere square, and ¼ sphere triangular.

e. Solid conical parachutes (30° angle) - circular, square and triangular.

f. Guide-surface parachutes - medium-construction brake, stabilization, universal riblese, and personnel type.

g. Exeter Type - 12 parachute.

h. FIST-type ribbon parachutes - circular (λ_T = 20%, 25%, and 26%), square, and triangular.

i. Ring-slot parachutes - circular (λ_T = 10%, 13.5% and 17%).

The results of the drop tests are inserted in the appendices and include a copy of the originaldata sheets giving the space coordinates of the parachute throughout the descent along with a descriptive remark on the parachute performance. The appendices also include

ABSTRACT (CONT.)

a plan-view, oscillation, and trajectory curve for each of the drop tests analyzed completely, followed by a representative sketch of the parachute canopy in question.

The geometric and aerodynamic characteristics of all the parachutes have been tabulated, and only the drag-coefficient information was directly correlated with descent velocity variation. In general, most of the parachutes tested showed an increase in C_{D_o} for a decrease in descent velocity; however, above a critical V_v value the drag coefficient became constant in most cases. Only for the very stable parachutes did the drag coefficient remain approximately constant for the V_v range tested. No constant C_{D_o} region was detected for the parachutes with inconsistent descent characteristics.

At the low V_v conditions the unstable parachutes tended to glide with moderate or large oscillations. As the descent velocity was increased these parachutes approximated straight vertical descent characteristics with little or no oscillation in most cases. The logarithmic decrement could not be calculated because of the incomplete nature of the oscillation curves in most cases and because some parachutes displayed undamped oscillation characteristics. The frequency of oscillation was calculated for a number of the parachutes and usually ranged between [illegible] and 0.5 cycles per second showing an increase in value for an increase in V_v over the range tested.

The shroud-line length of the solid-flat 10% extended-skirt parachute was varied from an L_S/D_o ratio of 0.60 to 1.40 in six equal steps and drop tests were made on each configuration. The resulting drag curves indicated that a substantial decrease in C_{D_o} was effected for a decrease in L_S/D_o below a value of approximately 0.9 for the range tested.

A method for determing the instantaneous angle of attack of the parachute system during descents was derived and calculations were made with the drop-test results of the solid flat-circular parachute. The angle-of-attack curves were oscillatory in nature, increasing in frequency as V_v was increased.

In most cases the results of the horizontal and vertical conditions of release were nearly the same. Conducting drop tests using the horizontal type of release for determining the frequency of oscillation and damping characteristic of the parachutes indicated the possibility of obtaining all of the important information from a straight vertical release.

This report has been reviewed and is approved.

FOR THE COMMANDER:

W. P. Shepardson

W.P. SHEPARDSON
Chief, Parachute Branch
Aeronautical Accessories Laboratory

TABLE OF CONTENTS

VOLUME I - SUMMARY REPORT

TABLE OF CONTENTS (CONT)

TABLE OF CONTENTS (CONT)

TABLE OF CONTENTS (CONT)

LIST OF TABLES

LIST OF TABLES (CONT)

LIST OF TABLES (CONT)

LIST OF FIGURES

LIST OF FIGURES (CONT)

LIST OF FIGURES (CONT)

LIST OF FIGURES (CONT.)

LIST OF FIGURES (CONT)

LIST OF FIGURES (CONT)

LIST OF FIGURES (CONT)

LIST OF SYMBOLS

C_D — Drag coefficient based on vertical velocity of the load and the canopy projected area; $C_D = \frac{2W}{\rho V_v^2 S_p}$.

C_{D_o} — Drag coefficient based on vertical velocity of the load and the canopy total-surface area; $C_{D_o} = \frac{2W}{\rho V_v^2 S_o}$.

$C_{D_{or}}$ — Drag coefficient based on resultant velocity of the load and the canopy total-surface area; $C_{D_{or}} = \frac{2W \cos\phi}{\rho V_r^2 S_o}$.

D_o — Nominal diameter of the parachute canopy, ft., $D_o = 1.128 \sqrt{S_o}$.

D_p — Projected diameter of the inflated parachute canopy, ft. (design diameter on guide-surface parachutes and two-thirds of deflated diameter on solid-flat parachutes).

f — Frequency of oscillation, cycles per second.

H — Vertical displacement of load from release point in feet, where $H = 74.1 - Z$.

L_s — Free shroud-line or suspension-line length measured from the canopy skirt to the shroud-line confluence point.

S_o — Total surface area of parachute canopy, square feet (includes vent area if smaller than 1% of total and for ribbon models includes space between ribbons);

$$S_o = \frac{\pi D_o^2}{4}.$$

S_p — Projected area of the inflated parachute canopy, square feet.

t — Time since release, seconds.

V_h — Horizontal velocity along the trajectory of the suspended load of the parachute, ft/sec.

V_r — Resultant velocity along the trajectory of the suspended load of the parachute, ft/sec.

V_v — Vertical velocity of the suspended load of the parachute, ft/sec.

W — Total weight of parachute system, lbs. (including parachute, instrumentation, and suspended load).

x,y,z — Coordinates of the representative shroud-line point.

X,Y,Z — Coordinates of the load point.

α — Angle of attack of the parachute measured at the load, degrees (angle between the resultant velocity of the load and the parachute axis).

γ — Angle of oscillation measured between the vertical and the axis of the parachute, degrees.

δ — Logarithmic decrement which is an indication of the damping of the angle of oscillation curves, defined as $\log_e N_1/N_2$ where N_1 and N_2 are the amplitudes of consecutive oscillations one cycle apart.

λ_T Total porosity in percent (equals actual material porosity for solid fabric designs and the sum of material and geometric porosity for ribbon designs) (1% of geometric porosity = 27.4 cu. ft/sq. ft/min at ½" water pressure).

ρ Mass density of air, slugs per cubic foot

ϕ Glide angle of the parachute measured at the load, degrees (angle between resultant velocity of the load and the vertical);

$$\phi = \tan^{-1} \frac{V_h}{V_v}$$

NOTE: Primed symbols will refer to measurements made at the parachute-canopy reference point.

INTRODUCTION

Although the inception of the parachute occurred many years ago it was not until the past few decades that any systematic effort was made to develop a completely satisfactory design. The essential characteristics to be considered in fulfilling the requirements of the ideal parachute system are low weight, low bulk, simplicity, reliable opening, low opening shock, high drag, and good stability. Even though several parachute designs have many of the before-mentioned characteristics, no one type of parachute seems to possess all of them simultaneously when compared with other designs. The actual choice of parachute type depends entirely on the intended use, since in general some characteristics are more important than others in the various phases of application.

Considerable parachute research has been conducted relatively recently with full-scale and model tests in the United States and abroad. Most of the tests were conducted under limited conditions, thus offering data which are not comparable and transferable in many respects. In general, no definite trends had been established satisfactorily as to the effects of the parachute geometry on the aerodynamic and stability characteristics of the system. In order to combat this problem, the Parachute Branch, Equipment Laboratory, AMC, initiated a parachute test program to study the influence of various design factors on parachute performance (Reference 1). Model and full-size parachutes having different types of canopies were tested in wind tunnels and free-fall drops under transferable conditions in an effort to establish design criteria. The variation of drag coefficient with rate of descent and shroud-line length was determined for these different types of parachutes.

The present report concerns a free-fall drop-test program on different types of parachute models of 16,000-square-inch canopy surface area and is considered a continuation and extension of the before-mentioned AMC parachute work. The general purpose of the overall coordinated research effort is to de-

termine completely the design criteria of parachutes for various applications based entirely on full-size and model parachute tests in free-fall and wind-tunnel research work under comparable conditions. The present work is the second step in the model phase of this general program. The future contemplated schedule includes wind-tunnel tests to be conducted on these 16,000-square-inch models, following which full-size parachutes are to be tested in free-fall and wind-tunnel tests. At the completion of the coordinated program it is hoped to be able to predict intelligently the effect of parachute size and Reynolds number on the drag and stability characteristics for any of the types of parachute designs considered to date.

The investigation of the effect of shroud-line length on the drag and stability of the solid-flat 10% extended-skirt parachute for an L_s/D_o range of 0.6 to 1.4 is also an extension of the general program. A definite approach for measuring the different velocities, the frequency of oscillation, the oscillation damping, the angle of attack, and the glide angle of the parachute system in free fall has been determined in the present report.

Terminology and definitions used in this report correspond to AMC standards as noted in the USAF Parachute Handbook (Reference 2).

DESCRIPTION OF EQUIPMENT

A free-drop space with a height of approximately 172 feet and a suitable floor area was supplied inside the Goodyear Aircraft Corporation airship dock where a minimum amount of air disturbance from thermals and drafts existed. Adequate instrumentation was required to measure and record the test data within the requested tolerances. Measurements of the vertical velocity, the horizontal and resultant velocities along the trajectory, the glide angle, the angle of attack, the angle and frequency of oscillation (where applicable), the drag coefficient, and the trajectory plan view were desired from the drop tests of the various types of parachutes under all test conditions of speed and release.

In order to facilitate accurate, economical, and efficient measurement during the drop tests, it was decided to utilize the two-camera system of recording, giving test data in the form of "sequence-still-photographs". It was also necessary to have the test equipment as automatic as possible since the program was long and it was imperative to maintain consistency in the test procedure.

The general layout for the equipment used in the drop-test program is shown in the schematic view of the airship dock in Figure 1. A special hoist assembly was erected along a main arch of the airship dock making it possible to obtain a free-drop height of approximately 172 feet. Two Eastman D-2, 8" x 10" cameras were mounted equidistant from the drop point at approximately 98 feet above the floor.

A hygrograph recording continuous relative-humidity readings and a thermometer for temperature measurements were located at the control panel. Thermometers were also located at each camera station to measure average air conditions in the overall drop area. The prevailing barometric pressure reading along with the average temperature in the drop-test area permitted the determination of the actual air density for each drop.

Hoist System

From the standpoint of safety and efficiency it was necessary to utilize a mechanical hoist system to raise the parachute to the top of the dock and provide automatic release at this point. The horizontal hoist bar shown on Figure 2 was employed in order to simulate systematically the two desired conditions of release defined in Figure 3. Figure 2 shows the actual installation of the parachute system on the hoist bar assembly for both the vertical and horizontal release conditions. The hoist bar consisted of aluminum, channel-type construction and was approximately 24 feet long. Two 1/8-inch stainless steel cables were attached to the bar at points approximately 21 feet apart. The automatic release unit was located on the north end of the horizontal hoist bar and was actuated by a buffer plate located on Arch 2 near the top of the dock. The buffer plate depresses two vertical pins acting against springs to effect the release of the parachute system. The north cable establishes the centerline of drop for the test program and the contact point of the two horizontal retaining pins of the release mechanism when held against the buffer plate is defined as the point of release or drop.

Since the distance between the apex of the collapsed canopy and the suspended load connection varied for the different types of parachutes tested it was necessary to provide a movable hook near the south end of the hoist bar for the efficient manipulation of the horizontal release condition.

Using a system of pulleys, the two cables went from the horizontal bar to the top of the dock, then down along Arch 2, and finally were connected to separate sections of the hoist drum which was approximately 8 inches in diameter. Figure 4 shows this hoist drum installation which allows the hoist bar to be raised horizontally from the floor to the top of the dock at a speed of approximately 2.4 ft/sec. The belt connection between the one-horsepower electric motor and the speed reducer acted as a flexible coupling to allow slippage as the release mechanism became engaged by the buffer plate at the top of the dock. The magnetic-type brake controlled the start and stop characteristics of the hoist system.

Data Recording System

The two 8" x 10" cameras were located as shown on Figure 1 and designated east and west cameras because of their position in the airship dock. There is a system of catwalks on the sides of the dock running the full axial length. In order to position the cameras at the approximate mean distance of the free-fall height, it was necessary to locate them off the second catwalk on each side of the dock. Figures 5 and 6 show the installation of the east and west cameras respectively. The camera mounts were constructed of heavy steel members securely connected to the dock structure. The critical parts of the cameras were locked in position and firmly fastened to prevent any calibration change during the test program. A telephone head set installed at each of the camera positions and at the control panel located at the dock floor permitted continuous contact between the three test stations and facilitated safe and efficient operation of the drop-test program. Figure 7 shows the control panel and the remote-control switches utilized in the tests.

In order to obtain efficiently the test quantities desired it was necessary to have a simple, accurate, and economical method of data recording. Figure 8 is a composite view of the complete photographic system of recording used for the tests. As the result of a thorough analysis of several methods which were considered for obtaining the drop-test data, it was decided to employ a constant light source on the parachute system and have the timing mechanism located at the fixed camera positions. Small light bulbs were fastened to the parachute system to define the location and attitude of the parachute axis throughout the drop. For timing purposes it was decided to use constantly rotating perforated circular discs in front of the open camera shutters. With this arrangement, it was necessary to conduct the drop tests at night while the inside of the airship dock was relatively dark.

A 1/16th-inch aluminum disc 19.75 inches in diameter was used as the timing means. Eight truncated radial slots approximately 3 inches long were located symmetrically about the disc at an inner radius of 7 inches. Seven of the slots had a central angle of 4.5 degrees while one slot had a central angle of 13.5 degrees. The disc was rotated at a constant speed of 30 rpm in front of the camera lens.

Since there was a constant light source on the parachute system, it can be seen that there would be eight sets of marks defining the parachute system produced on the film for every two seconds of drop test time during one rotation of the disc. The dash produced by the large slot provided an easy means of coordinating the photographs taken by the east and west cameras for each drop test. The circular hole opposite the large slot was intended for balancing purposes only and did not pass in front of the lens. Each disc was directly connected to a synchro-motor (similar to a Selsyn) and mounted underneath the camera in such a way as to permit covering and uncovering of the lens by the rotating disc with its radial slots.

Each Eastman D-2, 8" x 10" camera had a Kodak Wide-Field Ektar 190-mm Ilex Acme Synchro shutter (f6.3). The shutter solenoid of each camera, utilizing a 6-volt battery source and a 110-volt relay, was controlled at the floor panel by an "on"- "off" dial switch thus making it necessary for the camera operator only to load and unload the camera and cock the lens shutter. Electrical lines between the control panel and each camera terminated at quick-disconnect type plugs which permitted the use of the camera cover as protection of the photograph equipment when not in use.

In order to provide constant reference points on each photographic negative it was necessary to install in the airship dock fixed markers in the field of view of both cameras to establish the exact location of the center of drop on every photograph. The fields of view of the east and west cameras are shown in Figures 9 and 10 respectively and accentuate the clear drop-test area. Three position signs of the type shown in Figure 11, located at widely scattered points, were used for this photographic coordination. Each illuminated cross remained fixed in position for the drop-test program.

The large number of drop tests in the program necessitated an accurate and simple method of drop identification along with camera distinction on each negative. Figure 12 shows the marking or identification sign employed for these tests. The sign was positioned in the drop-test area in such a way that the identifying letters E and W, fastened at a 45-degree angle to the main board were seen only by their respective cameras.

Three groups of two numbers each(as shown on the photograph) were used to designate the month of the year, the day of the month and the drop-test number (reading from left to right), i.e., Figure 12 identifies the seventh drop made on October 12th. The illumination of the marking sign as well as the position signs was controlled from the operator's panel.

Parachute System

The parachute models were constructed basically with 16,000 square inches of total canopy surface area and free shroud-line or suspension-line lengths of 12 feet. Rip-Stop nylon cloth defined in Bureau of Aeronautics Specification 27M4 (Aer) and 100-pound tensile strength nylon shroud lines (specification AN-C-63a Type I) were used on all the solid canopy type parachutes. The ribbon parachutes were constructed of nylon ribbon and webbing determined by specifications MIL-R-5608A and MIL-T-5038 respectively. In general, sizes A and E nylon thread following specification AN-T-9a were used in sewing the parachute models. Individual construction details of the parachute models are given in the appendices at the end of the report by sketches of the complete parachute or a representative gore pattern which excludes allowances for the seams.

Standard sewing practice was employed in the fabrication of the model parachutes as much as possible. Figure 13 shows a few of the construction details defined early in the program thus insuring consistency of design. Reinforcing webbing 9/16 inches wide was inserted into all the radial load-bearing, vent, and skirt seams while a standard 1/2-inch French-fell seam was used for the general gore construction of the solid-type canopies. The construction details of the skirt and vent seams were identical. The sewed shroud-line loops provided an efficient means of attaching the suspended load. The shroud lines were attached to the outer edge of the canopy for a distance of 5 inches above the skirt with both a straight and zig-zag type stitches for added strength. The shroud-line attachments were made at radial seams except for the square and the triangular solid canopy-type parachutes, where it was necessary to strengthen the fabric in the immediate vicinity of the attachment points with ribbon material placed in a finger-like manner to distribute the stresses.

The suspended load of the parachute system consisted of a fabric bag for variable loadings of lead shot and a top unit housing the battery power source for the lighting arrangement, as shown on Figure 14. United Carr fasteners were used to fasten the reinforced bag to the top unit thus facilitating addition or removal of the lead shot bags between the drop tests. This type of suspended load arrangement was used because of ease of construction combined with ruggedness, efficient use of space, and negligible drag effect when compared with that of the parachute canopy. No interference effect was anticipated between the suspended load unit and the parachute canopy. The harness snap provided an efficient connection of the suspended load to the shroud-line loop.

Figure 15 shows the construction of the fabric weight bag into which lead-shot sacks were placed to obtain the weight variation desired for the drop-test program. The top part of the suspended load is shown in Figure 16 accentuating the battery supply for the electrical system of the parachute along with the location of the flashlight bulbs defining the parachute load point for the drop-test program. A toggle switch increased efficiency by permitting the lights of the parachute to be turned off while getting ready for each drop test. Photoflash type dry-cell batteries were used because of their large current capacity, thus giving a brighter light and having a longer life than ordinary flashlight batteries.

In order to establish the parachute axis location at any time during the drop tests, flashlight bulbs were added to some of the shroud lines of the parachute system in addition to having them located on the suspended load unit. For the circular and square-type parachutes a flashlight bulb was mounted to each of two diametrically opposite shroud lines at a point eight feet above the shroud-line confluence point as shown on Figure 17. For the square-type parachute the lights were mounted on the shroud lines fastened to the center of opposite sides of the canopy since there appeared to be more uniform tension in these lines throughout the complete drop test. For the triangular-type parachute a light was mounted at the end of an eight-foot line located along the axis of the parachute system as shown on Figure 18. The lower end of this line was fastened to the shroud-line loop while the upper end was held on the parachute centerline during inflation by three flat rubber bands 1/8 inch wide which ran from three symmetrically located shroud lines to the light socket. The attachment points for the rubber bands were 9 feet above the confluence point of the shroud lines.

In order to connect the shroud-line flashlight bulbs to the battery source in the suspended load two strands of 26-gage enameled copper wire were wound around each respective shroud line from the shroud-line loop to the light attachment point. The upper ends of the wires were connected to a screw-base type electrical socket while the lower ends were fastened to quick disconnects. The sockets permitted replacement of the light bulbs with a minimum of trouble. The quick disconnects permitted easy disengaging of the lines from the power source every time the weight unit was removed from the parachute system. The shroud-line lights consisted of one or two 2.3-volt flashlight bulbs while the load unit had three, 3.8-volt flashlight bulbs symmetrically located about the strut of the weight top. This arrangement of flashlight bulbs resulted in maximum, uniform brilliance for the power source supplied. Each light socket was taped to its respective shroud line to eliminate interference with the parachute opening process.

The average bulk in cubic inches of each canopy and complete parachute was determined with the instrument shown in Figure 19. The cylinder of the bulk tester consists of a 3/32-inch-thick fiber tube approximately 5-3/4 inches in outside diameter and 21-1/2 inches long with one end closed. The wooden piston has a calibrated scale mounted on one side giving volumes directly from 0 to 400 cubic inches. The notch in the side of the piston head permitted bulk readings of the parachute to be taken with and without shroud lines included.

An average porosity value of the parachute canopies was determined on a Sherman W. Frazier Company fabric permeability machine which is shown on Figure 20. Porosity readings in cubic feet of air per minute per square foot of cloth at a static head of 1/2 inch water pressure were required for at least every separate piece of cloth in the canopy with a desired minimum of approximately 16 points.

Analysis System

For purposes of evaluating the photographic drop-test data a mechanical analyzer as shown in Figures 21 and 22 was developed, giving the coordinates of the parachute lights according to an established 3-plane orthogonal system of axes. The general principle of the analyzer design is explained in Reference 3. By use of these coordinates, the instantaneous location and attitude of the parachute axis becomes available.

The instrument basically consists of a system of simple levers whose location and length are determined by the angle between the line of sight of the two cameras and the camera focal length. Two grid levers give the plan-view location with respect to the drop point while the third grid lever is used to determine the distance from the drop point. The actual drop-test-camera setup is duplicated in a similar manner by the analyzer and thus it is possible to graphically locate a point on the parachute system by lining up representative dots on the two photographs with the given levers.

Both negatives must be laid flat on the analyzer board in such a manner that the same view is obtained as would be seen by looking through the rear of the cameras at the ground-glass projection. The plastic levers and indicators have thin lines accurately marked on both sides as a means for preventing parallax in locating the position of the parachute lights. In this two-dimensional setup, Figure 22, the indicators extending in the direction of the longer side of the negative are used to determine the plan-view location of the parachute with reference to the center line of drop. When the grid levers are at zero the negatives must be positioned so that the hairline on the indicators is on the center line of drop. When the instrument is in its zero position (grid levers crossing the grid origin) the distance between the sliding junction of the negative indicator assembly with the rod extension of the grid lever and the pivot point of the grid lever is equal to the focal length of the cameras of 7.48 inches as defined in Figure 22. The sliding parts utilized ball bushings while the rotating parts utilized precision ball bearing assemblies. Accurate motion perpendicular to the centerline of drop is provided for the plan-view indicator used to align the negative. Reversible electric motors with integral gearboxes facilitate rapid movement of the levers with the fine adjustment being obtained by rotation of the knurled knob placed in the sliding plate. Each circuit has a DPDT center-off-position toggle switch for the rapid manipulation of the levers and indicators.

Provisions for graphically measuring height from the negative necessitated that an indicator moving along the center line of drop be installed over either negative. The general construction of the height indicator arrangement is similar to that of the other indicators and sliding plates. The motion of this sliding plate is transferred by cable and pulleys to a sliding carriage located under the grid table where motion is provided parallel to that of the respective plan-view sliding plate of the same

negative. Here again the distance between the fulcrum point and the sliding junction is equal to the camera focal length of 7.48 inches when the grid lever is at its zero position.

Both the plan-view and height indicators associated with the east camera negative are connected to a differential gearbox with a one-to-one ratio. In order to determine the height graphically it is basically necessary to duplicate the similar triangle relationship established in the vertical plane of projection by the measured photograph height, the camera line of sight, the camera center line of sight and the actual height of the point in question. In the analyzer, the correct projection angle is preserved and then the vertical height is measured by placing a calibrated scale perpendicular to the east camera plan-view lever and the distance measured between the intersection of the plan-view levers of both cameras and the intersection of the height lever and the calibrated grid axis. (Figure 22). The gearbox is arranged in such a manner that the height lever and the east plan-view lever move together whenever rotation of the east plan-view lever is effected; however, only the height lever moves when its rotation is initiated. The scales of the plan-view and height grid are designed to permit readings directly in feet according to the full-scale airship dock setup. The grid axes definitions and their correlation with the actual drop-test setup can be seen in Figures 1 and 22.

METHOD OF PROCEDURE

Because of the inherent instability of some of the parachute models in sideslip, the requirement of making horizontal releases, and the heavy weights needed to obtain a descent speed of 40 ft/sec many difficulties were encountered in trying to select a suitable drop-test site in the Goodyear Aircraft Corporation airship dock on the basis of safety and efficiency. Fortunately the design of the airship dock (embodying unusual unobstructed interior height and a series of axial catwalks along the sides of the building) lends itself quite readily to the test requirements of the present research program.

Based on past experience, the decision was made to utilize a two-camera system of data recording which would give a complete drop test on each sheet of film. This, so called, "sequence-still-photograph" system of recording was chosen for reasons of economy and ease of data reduction when compared with other photographic systems in use today. Since the cameras had to be located accurately it was necessary to first establish the center line of drop by installation of the hoist system and the corresponding cables.

An electric light and a communication system were installed at each camera position for convenience, efficiency, economy, and safety since all drop tests were conducted at night with the inside of the airship dock in a semi-dark condition. The thermometers located at each camera station and at the floor panel were read at the beginning, middle, and end of every test period as was the hygrograph located at the floor panel. Charts of daily barometric pressure were obtained from the U. S. Weather Bureau to determine the true mass density of the air during each drop test.

Hoist System

The hoist drive (including a one-horsepower electric motor, a speed reducer, a magnetic brake, the required flexible couplings, and a winding drum assembly) was fastened to a mounting bed and located at the outer periphery of the drop-test area directly under a main

structural arch of the airship dock. The control panel and storage cabinet were set up near the hoist drive as a matter of convenience and efficiency. The two 1/8-inch cables were threaded along Arch No. 2 through a system of pulleys and ultimately connected to the horizontal hoist bar. Because of the horizontal-release condition and the high suspended-weight requirements for the 40-ft/sec drops it was necessary to construct a light, sturdy beam from which the parachutes could be released automatically at the top of the dock for both specified conditions of parachute release. The variation in design of the parachute canopies and the length of some of the shroud lines necessitated that a movable attachment point be established to hold the parachutes taut in a horizontal manner. This was achieved by utilizing a rectangular, aluminum plug movable between two aluminum beams of channel-type construction placed back-to-back with the appropriate spacers inserted. The two cables were separated at the pulley plate on the arch eventually to be connected to the hoist bar at two points approximately 21 feet apart. One cable was connected directly to the release mechanism at the north end of the bar and was designated as the center line of drop.

Data Recording System

The cameras were positioned equidistant from this center line of drop at the second catwalk up from the airship dock floor as explained previously. All measurements were made with a transit and checked against the available structural drawings of the airship dock. The camera lenses were located 174.5 feet from the drop center line and 98.3 feet above the dock floor. The original intention was to have the included angle between the camera lines of sight equal to 90 degrees; however, because of structural interference it was necessary to make this angle equal to 95.8 degrees. It is important to note that once the cameras were fastened to the dock structure and properly adjusted all the vital parts were locked in position to prevent any change in calibration of the drop-test setup.

Considerable research was initiated in finding a system of data recording which offered economy, simplicity, and accuracy. For purposes of measuring the desired descent velocities of the parachute, it was decided to attach some small electric lights at several defined key points of the parachute system and to take all test photographs at night in the darkened airship dock. Since the cameras were

located approximately half way between the floor and the point of release it was necessary to establish a light system capable of being detected by the cameras throughout the complete range of the parachute free fall, especially in the lower half or terminal velocity zone. For this reason it was decided to attach a light to each of two diametrically opposite shroud lines (for all but the triangular type parachutes) approximately 4 feet below the skirt of the parachute canopy as described previously to prevent shielding of the lights by the canopy itself. The three other flashlight bulbs located in the weight-unit top made it possible to detect two load lights simultaneously throughout the complete drop irrespective of any rotation.

A dozen different types of small light bulbs were tested for brilliance under various conditions of normal overload; however, it was found that apparently the best dots and dashes were produced on the negatives by using 2.3-volt flashlight bulbs on the shroud lines and 3.8-volt flashlight bulbs at the suspended-load point. The resistance of the electrical lines connecting the shroud-line lights to the battery power source in the suspended load prevented failure of the 2.3-volt flashlight bulbs. For obvious reasons every effort was made to keep the time of illumination down to a minimum during the drop tests and this resulted in the installation of a toggle switch in the weight unit.

In an effort to obtain a direct measurement of the parachute angle of oscillation during descent, ideas concerning the possible use of a gyroscope and a scratch-gage system were investigated. It must be remembered that the gyroscope would have to be erected and activated from a power source at the floor and would be under coasting conditions during the ascent and descent of the parachute. Experiments showed that the gyroscope equipment available for these tests would not operate within the angle-accuracy requirements of $\pm$ 2 degrees during the coasting condition for the times involved. The delicateness and expense of the equipment required in an operation of this type was another reason why this development was discontinued. Excessive and repeated impact loads were expected during these drop tests and would have required the design of an expensive shock-absorption system for this type of recording mechanism.

The next important decision was to determine just how the element of time would be correlated with the drop-test negatives. Initial attempts were made to design an accurate light-blinking system by use of a small d-c motor, cam, and microswitch assembly. Considerable difficulty was encountered in obtaining a constant-speed motor capable of being mounted satisfactorily in the suspended load unit. The number of blinks per second was limited by the necessity of distinct dots appearing on the photographic negative. An intricate system was designed to blink the lights four times per second; however, this method was discontinued in favor of the timing process used in the actual drop tests at the request of the Air Forces.

The timing system used in the drop tests essentially involved a perforated disc rotating at a constant speed in front of the open camera lens. The discs were mounted as close to the camera lens as possible and were directly connected to electrical synchro-motors. The east camera synchro was connected to a synchronous a-c motor which rotated the disc at 30 rpm. Experiments conducted to determine the amount of angular lag of the driven disc behind the driver disc showed that the follower disc was approximately 7 degrees behind the driven disc. This lag angle remained the same when electrical resistance was inserted into the connecting lines in an effort to duplicate the effect of the very long electrical lines needed between the cameras and the control panel. After advancing the follower disc the necessary 7 degrees, the synchronization was verified by measurements of photographs taken with the discs running side-by-side. The discs were carefully balanced about their axis of rotation to insure consistent motion.

After installation of the camera assemblies in the dock the disc synchronization was accomplished in a simple and accurate manner. In the dark, a flashlight bulb was attached to the north end of the hoist bar near the cable establishing the center line of drop. After the rotating discs had attained a constant speed, the camera shutters were opened and photographs taken as the light was raised vertically on the hoist from its starting position near the floor. At approximately five equal intervals the hoist was stopped and a stationary point of more than usual brilliance was picked up on the photographs. Comparison of the photographs taken by both cameras by matching the respective dots, dashes, and stationary points indicated the degree of synchronization attained during the test. At least one or two

synchronization checks were made during each test period particularly whenever the power source had been turned off or the follower disc accidentally disturbed. In this way it was possible to determine the reliability before starting the analysis of the photographic test data.

In order to control the opening of the camera shutters from the floor panel it was necessary to install a solenoid arrangement on each camera. The proper adjustments were made so that both camera shutters could be opened simultaneously at the beginning of a drop test and closed by the panel operator after the parachute had completed its descent. A 110-volt a-c electrical line was installed between the floor panel and the camera stations along with the necessary electrical connections for the synchros. This 110-volt a-c source was used to energize an electrical relay thereby closing the d-c circuit needed to operate the camera shutters. Since the cameras were operated under time-exposure conditions during the drop tests it was necessary to trigger the shutter mechanism twice for each test negative, once to open the shutter and once to close it. This was accomplished by installation of a rotary type switch at the floor panel. This switch rotated through an angle of approximately 60 degrees and closed the 110-volt a-c circuit at the mid point of travel. In order to prevent the solenoid from burning out because of prolonged switch contact at the panel a buzzer was inserted into the circuit and became energized at the same time the solenoids were energized. Therefore, the sequence of operation consisted of rotating the switch knob clockwise through its full travel for opening the shutters at the beginning of each drop test and then returning the dial to its original position upon completion of the descent to close the shutters, each time energizing the electrical circuit as the mid-point is passed and thus initiating the buzzer warning. By observing the switch position at any time it was possible to detect whether the shutters were open or closed.

Tests were conducted to determine whether any distortion existed in the field of the wide-angle lenses used. Photographs of grids were taken and analyzed for consistency. All results indicated that no corrections for distortion would be required for the present tests.

Several lighting systems were tested for the identification and position signs in order to get satisfactory exposure for the time range involved.

Drop-times ranged from approximately 4 to 20 seconds depending on the descent velocity and flight characteristics of the parachute system. On this basis cumulative exposure times of approximately 1/4 to 1-1/4 seconds were involved since the film was exposed 1/8 of a second for each revolution of the synchronizing disc. A 7-1/2 watt bulb properly shaded with masking tape provided sufficient light for the position signs which were illuminated during the complete test period. The three position signs were placed at strategic locations in the drop-test area and could be detected by each of the cameras. One sign was located at the top of the dock, and the two other signs were located near the floor level at the north and south ends of the drop-test area. Several locations of these signs were investigated in an effort to spread these important reference points as far apart as possible in the field of view of both cameras. For any position signs designed in the future, efforts should be made toward stressing more clearness of the lighted cross-points but it was found that the present simple setup was satisfactory. Each exposed cross consisted of two black stripes approximately 2 inches wide and 12 inches long painted at right angles on a white background.

Similar investigations were made to determine the appropriate letter size and lighting for the marking or identification sign. The black stripes were 2 inches wide and made into letters and numbers approximately 13 inches high. A continuous beam of light across the full length of the sign was produced by a single row of fluorescent light tubes placed end to end. Experimentation resulted in the proper amount of masking tape being placed on the glass cover plate above the light tubes in order to eliminate unwanted high spots or glare on the lighted background. The marking sign was located on the floor in the drop-test area to facilitate changing the drop and date numbers as the tests were conducted. The lights were controlled by the panel operator and were illuminated during the complete test run.

A simple and accurate method of calibrating the camera setup was devised. A flashlight with its bulb illuminated and exposed was fastened to the hoist bar near the release mechanism at the north end of the bar. A transit was set up at a known location on the catwalk near one of the cameras and used to measure the distance of the flashlight bulb above the floor at various points along the center line of drop by determining the angle the line of projection made with the horizontal.

At approximately equal intervals along the centerline of drop between the floor and ceiling of the airship dock the flashlight bulb and hoist were held stationary and exposures made with each camera. A single sheet of film was used in each camera and multiple exposures made of approximately one second duration, one for each light-bulb location. Each timing disk was held stationary throughout the calibration and positioned so that the large radial slot uncovered the camera lens. The exposure time and light location was controlled by the operator at the floor panel. Usually seven to nine exposures were made on any one sheet of film for the calibration and a transit angle reading was also taken at each point. It was immaterial whether the data were taken with the light moving up or down from the starting position; however, both methods were used during the extensive drop-test period and similar results were obtained in each case. The height of the test point closest to the floor was measured by the operators which in turn made it possible to determine the actual height of each point above the floor by use of the transit angular measurements. After two exposures during any one calibration the lights of the position and marking signs were turned off to prevent over-exposure on the film.

Using the light position closest to the floor as the zero point, the distance in inches was measured between this zero point and the other test points on each negative. In turn, the actual height in feet of each of these points above the floor was determined from the transit measurements, since the exact location of the transit lens pivot with reference to the zero test point was known. A typical calibration curve of the drop-test photographic setup is given in Figure 23 which is a plot of measured height (inches) on the photograph against the actual height (feet) above the floor. The straight-line curve indicated that one inch of measurement on the drop-test negative equaled 23.7 feet of actual measurement at the drop-test site. After the cameras were positioned so that their principal line of sight was horizontal and centered on the centerline of drop it was only necessary to calibrate this particular setup once. Whenever the cameras or position signs were disturbed from this original setup a check calibration was made; however, because of the rigidity and accuracy of the clamping units the calibration curve remained constant.

Several types of film, developers, and processing methods were investigated during the early stages of the drop-test program in order to obtain test negatives which accentuated the minute dots and dashes. Ex-

tremely clear test negatives were desired to simplify the analysis by eliminating any unnecessary eye strain for the operators of the analyzer.

Experimentation indicated that Tri-X, Panchromatic film developed for ten minutes in D-11 developer accentuated the dots and dashes in a very satisfactory manner. It must be appreciated that the flashlight bulbs which produced the dots were approximately 200 feet or more from the camera lenses during the drop tests and that the exposure time on the film was in the neighborhood of less than one-fortieth of a second. Another important factor influencing the selection of the proper film was the descent velocity range of 10 to 40 ft/sec which was to be investigated during the program.

Throughout the test program it was required to measure any thermal or gust conditions that might exist in the drop-test area. As a first approximation several weighted conical paper drinking cups were dropped into the drop-test area from the catwalk at the top of the dock and their flight path observed in the plan and side view. Results indicated that little or no air disturbance was present in the dock area investigated. In order to determine quantitatively the air disturbances possibly existing at night during the actual drop tests, a right circular cone was constructed of fiberglas laminate material approximately 0.010 inches thick with a base diameter of approximately 34 inches and a height of 19 inches. The cone was instrumented with a flashlight bulb at its apex mounted in a balsa-wood plug. The cone was hung from the hoist-release mechanism and photographs taken of it following its automatic release and descent from the top of the dock. By the use of the analyzer, it was possible to determine the descent velocity and sideslip of the cone and thus to detect any effect of vertical and horizontal gusts on its flight path. For the minimum descent velocity of approximately 10 to 15 ft/sec of the cone no apparent disturbances were detected during the drop-test program. Before the check for gusts and during the drop tests, it was imperative that all outside doors leading into the neighboring dock area be closed thus eliminating the cause for air distrubances in the drop-test area.

Although the cone tests covered the lower velocity range investigated in the drop-test program and seemed to give satisfactory results it was suggested that better equipment or some system of suspended particles such as a smoke column or bubbles filled with a gas be utilized in an effort to detect extremely minute air disturbances that could be present in the drop-test area. A commercial vane-type anemometer capable of de-

tecting air flows as low as approximately one foot per second was attached to the hoist bar and lifted to several heights between the floor and the top of the airship dock. No movement of the vane was detected indicating the apparent absence of air disturbances in this area. As a further check, a smoke column extending from the floor to near the release point was created by the use of titanium tetrachloride and observations showed that there was no visible movement of the smoke for several minutes before its final dissipation. This smoke-column method was used during the remainder of the drop-test program to insure that the surrounding air possessed stable conditions for accurate determination of the aerodynamic characteristics of the parachutes.

Parachute System

All the parachute models were constructed from sketches similar to those exhibited in the appendices of this report, where usually the gore pattern or the complete canopy pattern is given. These pattern sketches do not include the seam allowances but give only the center line or overall dimensions of the canopies or their components. The various nylon panels used in assembling the parachute gores were connected with French fell seams 1/2 inch wide. Both left- and right-twist type nylon thread was used in the double-needle machines so as to obtain a tight seam connection.

In order to check the strength of a typical radial load-bearing French fell seam perpendicular to the direction of the included webbing, tensile tests were performed until rupture of the fabric or the seam. The loads were applied to the fabric through standard wooden clamps. A few seconds of time were permitted to elapse before the addition of each new load, since the time of load application itself is a critical factor in testing the strength of any fabric. Results indicated that the seam strength in this direction was greater than that of the actual canopy fabric.

Tests were also conducted to check the strength of a typical connection between a shroud line and the skirt of the canopy. The element of time was again considered during the loading of the specimen by permitting the load to remain constant for a few seconds after each addition. The joint proved to be approximately as strong as the shroud line which itself operated under a substantial margin of safety for the load conditions imposed during the drop-test program.

In addition to using reinforcing webbing in the radial, skirt, and vent seams for the solid-canopy type of parachute models, the square and triangular designs utilized finger-like patches of ribbon to distribute the loads exerted by the suspension lines to the canopy at the skirt and vent. A minimum of four vent lines, sewed to the parachute in a manner similar to that used for the suspension line, were used on the parachute models to facilitate attachment of the parachute to the hoist bar for the two required conditions of release. The vent lines were threaded through a small metal ring made of 1/8-inch material approximately one inch in diameter. For the vertical-release condition this ring was placed in the hoist-bar release mechanism while the parachute system hung limp below the bar along the center line of drop. For the horizontal-release condition the weight unit was attached to the hoist release mechanism while the ring was hooked on a bent metal pin near the opposite end of the hoist. In this manner the parachute model was held taut in an approximately horizontal position between these two points of attachment of the hoist bar. Experimentation verified that satisfactory horizontal release of the parachute was effected when a release pin was used with its axis at 45 degrees to the hoist bar.

The total cloth area of the solid-type parachute canopies used in the determination of the drag coefficients (C_{D_o}) also included the areas of the vent, pockets, skirt extensions, ribs, and guide-surface panels. The total cloth area of the ribbon and ring-slot parachute canopies included the areas of the vent and the voids between ribbons. These voids between ribbons are accounted for in the total porosity value given for the ribbon-type canopies. All parachute models were measured and the corresponding dimensions checked with the design drawings. In the cases where the important dimensions were within the 2-percent tolerance requirements the design total area was used in the drag coefficient (C_{D_o}) determination. Several parachute models had radial dimensions sufficiently different from the design values to warrant a re-evaluation of the canopy surface area. In general the vent areas were approximately one percent of the total canopy surface area. The vent areas of the guide surface parachutes were approximately one percent of the canopy roof total area. For strength purposes, one nylon cloth was used on the bias in the solid-type parachute canopy construction with the direction of warp or fill placed at 45 degrees with the center line of the gores or the skirt of the canopy.

Following completion each of the parachute models was inspected and checked with the design specifications, and the various construction features

investigated for consistency of manufacture. The models were weighed and their bulk or volume determined. By using the bulk tester described previously, the average bulk of each parachute canopy and of each complete parachute (shroud lines included) was determined as the result of three readings for each of these conditions. After arrangement of the canopy in the tube of the bulk tester the piston was inserted and a constant weight applied to the top of the piston. The bulk or volume of the canopy was determined in cubic inches by reading the attached scale at the side of the piston. Bulks were determined by using both 10 and 25 pounds of weight on the piston and the average of these readings taken. These weights represented piston pressures of approximately 0.4 and 1.0 lbs/sq. in. respectively. The average bulk values obtained when using the 25-pound weight have been recorded in Table I. For purposes of information the average bulk values obtained using the 10-pound weight were approximately 8 cubic inches larger than the tabulated values. The bulk of the parachute-model shroud lines was approximately 14 cubic inches. For purposes of obtaining consistant results only one person was responsible for making the bulk tests.

The porosity of the cloth of each parachute canopy was determined by a Frazier fabric permeability machine and recorded in terms of cubic feet of airflow per minute through one square foot of the fabric for a pressure drop across the fabric of 0.5 inches of water. An effort was made to obtain a reading in every panel of the parachute canopies with a minimum number of approximately 16 test points for the triangular and square types of parachutes. By the use of consistent material and fabrication methods, in general, the porosity values were kept within the range of 80 to 120 cubic feet/min/sq. ft. as given in the specification on rip-stop nylon parachute cloth (MIL-C-7020). For the ribbon and ring-slot parachutes the total porosity is given in percent and includes the material and geometric porosity. The accepted conversion factor of one percent of geometric porosity equal to 27.4 cubic feet per min per sq. ft. material porosity (Reference 4) was used in the present report.

Considerable difficulty was encountered during the preliminary drop tests because of tangling of the suspension lines in retrieving the parachutes after their descent, storage of models between tests, and the system of instrumentation utilized. A very effective means of eliminating this trouble was developed by installing thin circular wooden disks approximately

3 inches diameter into the shroud-line system as close to their confluence point as practicable. Around the outer periphery of these disks was located a series of small holes of 1/16 inch diameter into which the shroud lines were placed in the same sequence as they were attached to the skirt of the parachute. Therefore, after every drop test the parachute with load was suspended vertically from the hoist bar and the shroud lines untangled merely by tugging at the lines in a systematic manner. By beginning at one point of the disk and tugging successive shroud lines the trouble was easily detected and rectified. While the parachute system was suspended vertically from the hoist bar the disk installation caused the shroud lines to hang in a "bird-cage" manner which eliminated interference with instrumented shroud lines and also facilitated the inflation of the parachutes during the drop tests.

The installation of the lights on the shroud lines as well as on the weight unit is the result of many investigations to determine an efficient, inexpensive, and accurate method of defining the axis of the parachute system during the complete descent from the top of the dock. The light sockets were taped to the shroud lines in order to minimize tangling of the suspension lines and interference with the inflation characteristics of the parachute.

Several items of importance considered during the design of the suspended load unit were the necessity of rapid weight variation in obtaining the descent velocity range required for the tests, the time needed to replace batteries and light bulbs after failure and ruggedness needed to withstand the repeated impact loads at landing. For the high-speed tests where approximately 200-lb loads were required round-headed screws and appropriate washers were used in place of the quick-disconnect fasteners to attach the weight bag to the weight-unit top in a safe manner. Also for the higher loads the efficient harness snap used to connect the suspended load to the parachute was replaced by a more positive cable shackle. One extra weight-unit top and seven extra fabric weight bags were constructed to eliminate unnecessary delay between drop tests.

Analysis System

During the construction of the analyzer, precision machining and proper alignment were the important considerations. All sliding and rotating parts were made with a tight fit using bearings in order to increase

the accuracy of the machine. Efforts were made to eliminate slack in the cable for the system which determines height. The analyzer levers and dimensions simulated the camera setup used in the drop-test program and provided a graphical means of determining the location of the parachute in the airship dock at any time during its descent. All the components were fastened to a common board of 3/4-inch plywood to facilitate accurate location and eliminate the need of constant adjustment.

The order to calibrate the analyzer, including its levers and the grid, the camera calibration films were used. From Figure 23 it was found that one inch on the test negative equaled 23.7 ft of actual distance in the drop-test area. The zero on the grid of the analyzer was represented by the intersection of the principal line of sight of the cameras with the center line of drop. This zero point was marked on the camera calibration films since it was known that the principal axis of each camera was 98.3 ft above the floor measured along the center line of drop which was 172.4 ft long. Each lever on the analyzer was calibrated separately with these camera calibration films by setting the film zero point (98.3 ft above floor) under the respective zeroed indicator with the center line of drop at right angles to the indicator. As the indicator was moved from point to point the deflections of the grid lever from the grid zero were measured perpendicular to the zeroed lever axis in terms of grid divisions. These analyzer readings were plotted against the actual distance in feet from the zero point on the camera calibration film (98.3 ft from the dock floor). Figure 24 is an example of a typical analyzer calibration curve indicating that one grid division represents one foot of actual distance in the drop-test area. This was accomplished by producing a grid such that 0.615 inches (10 divisions) represented 10 ft of distance in the drop area. The grid-axis definitions and their correlation with the drop-test setup can be seen on Figure 1 and 22.

In order to offer a better understanding of the function of the analyzer the following method of procedure in data analysis is presented: Referring to Figure 22, after the grid levers were placed on zero the camera calibration negatives were inserted under the proper indicators. All films were placed on the analyzer board in the same manner that they were viewed if looking at the ground-glass projection from the rear of each camera. A set of camera calibration films were used in order to define

the center line of drop and the principal axis location of the camera. The center line of drop on each film was aligned with its respective plan-view indicator while the principal axis of the camera was aligned with the height indicator. After positioning this calibration film as accurately as possible it was taped to the analyzer board. The drop-test films were placed under the indicators and over the calibration film and then fixed in place with tape after the position signs on the two films were mated. In this way, once the calibration films were fixed on the analyzer, it was possible to locate accurately any of the drop-test negatives by the use of the position signs, correlating the center of drop on each film with the zero grid reading of the plan-view levers.

The coordinates of the "load" dots were determined first, starting with points near the floor (top of negative) and ending near the top of the dock where the parachute inflation was incomplete. The indicators were always aligned on the test dots from the same direction to improve the analyzer accuracy by eliminating any play in the mechanical system. When the center line of the same set of load dots in both films was covered by the hairline of each of the plan-view indicators the location of the load from the center line of drop was given directly in feet by the coordinates at the intersection of the plan-view grid levers. After aligning the height indicator with the center of this same set of load dots on the east film the height of the load above (positive) or below (negative) the principal axis of the cameras was determined by measuring the distance between the intersection of the plan-view grid levers and the height grid lever in a direction perpendicular to the east plan-view grid lever. This was conveniently accomplished by the use of a movable scale whose divisions were the same size as those of the fixed grid. The scale was marked on transparent paper so that coordinate readings could be determined with a minimum of movement of the scale when traversing between test points. This same procedure was followed for each set of load points through the acceptable range of points on the test negative.

Whenever a complete analysis was desired of any set of test negatives the coordinates of the center of the shroud-line lights were also determined in a manner similar to that described above. For these complete tests, therefore, the parachute axis location and attitude was defined throughout the descent from the top of the dock. It

was important to analyze only the test points where the parachute was completely inflated and in free fall in order to get consistent terminal velocity curves. The plan-view indicators had an extra pair of parallel lines scribed one eighth of an inch apart and equidistant from the original hairline to facilitate the location of the center of the shroud-line points. These three parallel lines were extremely helpful in determining the center of the load and shroud-line points in an accurate and efficient manner.

The electric motors were used for expeditious traversing over the test film between dots and dashes; however, the final adjustment of the hairline at any point was made by rotating the knurled knobs by hand. Although the dots and dashes were of variable length depending on the speed of parachute descent the height-indicator hairline was always aligned with the center of the point for the analysis.

Typical Drop-Test Procedure

In order to understand better the method of procedure of drop-testing the parachute models and the use of the allied equipment it seems advisable to present the program for a typical testing period from start to finish. After obtaining a maximum supply of film for the holders available, the camera operators manned their stations, uncovered the cameras, and connected the electrical instrumentation and communication lines. The timing discs were set in rotation immediately by a switch at the floor panel in order to provide ample time for warmup while the rest of the equipment was readied for the tests. The parachutes scheduled for testing during this period were removed from the storage cabinet and the canopy and shroud lines set in proper order. In general, the parachute models were tested in two phases, the first phase including the drop conditions of approximately 10, 15, and 25 ft/sec for both vertical and horizontal releases while the second phase consisted of all 40-ft/sec drops. The obvious reason for this phasing procedure was that the high speeds necessitated very heavy suspended loads which highly stressed the parachutes and their instrumentation and caused failure in many cases during the violent descents. The weight unit and the required lead-shot bags were also assembled in the test area.

The next step was to prepare the drop area and make some routine checks of equipment before drop testing could proceed. The position and photo-identification signs were illuminated and readied for the tests. The floor of the drop area was cleared as much as practicable to prevent damage to the parachutes and injury to the retrieving personnel. All outside doors in the immediate neighborhood were closed and a test for gusts or thermals conducted by one of the previously explained methods. During this period the temperature was reported from each test station and recorded by the panel operator along with the relative humidity.

Before actual drop tests could proceed it was necessary to check the synchronization of the timing discs. This condition of synchronization could usually be verified by visual observation of the follower disc by experienced personnel; however, a standard synchronization check was always made in the manner described previously. At the same time it was found convenient to check the operation of the camera shutters.

After the parachute system was connected to the hoist bar in its proper position and with the desired weight, the instrumentation lights were turned on and the parachute started on its ascent to the top of the dock. During this ascent the proper numbers were displayed on the illuminated identification sign, film was loaded into the camera, the film-holder slides were removed, the camera shutters were cocked, and all the lights in the immediate drop area were turned off to prevent fogging of the test films. When the hoist was near the top of the dock the camera shutters were opened by the panel operator. The parachute was then automatically released and started its descent. After the parachute landed, the camera shutters were closed by the floor-panel operator and the area lights were turned on to facilitate recovery of the parachute system. The instrumentation lights were turned off immediately and the parachute again hung from the hoist upon its return from the top of the dock. The parachute canopy and shroud lines were straightened and readied for the next scheduled test. After the shutters were closed the film-holder slides were replaced and the exposed film removed from the camera. During the descent of the parachute the east camera operator timed each descent for approximately the last 100 feet of height with an electrical stop watch, thus enabling the panel operator to check the velocities attained with the various weights used. These measurements

of velocity were only used for facilitating the selection of the proper suspended weight and were not used in the drag-coefficient calculations. The drop tests were continued in this manner until either the film supply was exhausted at the camera stations or mechanical difficulties were encountered with the parachutes or the drop-test equipment. The last film of the drop-test period was usually reserved for a synchronization check. In addition to recording the relative humidity and temperatures periodically the time was also marked on the data sheet. After the films were developed, dried, and prominently marked they were processed through the analyzer. Although the identification sign provided an excellent means of permanently marking each test film it was decided to transfer this information to a piece of masking tape for convenience of filing. The parachute number, the nominal descent velocity, and the type of release were also marked on this masking tape, which was then placed on the proper test negative.

Figure 24a is a photographic copy of a set of representative drop-test negatives showing the actual dots produced by the data recording system explained previously. The complexity of the data along with the enormous amount of data to be analyzed necessitated the design and construction of a machine to cut calculation costs to a minimum. It was found that with the present analyzer the data reduction time for any representative test negative was less than one-twelfth the time needed to measure the distances by hand on the negatives and calculate the coordinates of the parachute system during descent.

ACCURACY OF RESULTS

Because of the large amount of data that was to be analyzed, great care was taken to provide a system by which both the experimental and human errors could be reduced to a minimum. Besides being accurate, the system had to be practical, efficient, and relatively inexpensive to build and to operate. A reasonable compromise of all of these requirements was accomplished in the combination photographic and mechanical drop-test system previously described. It might therefore be interesting to note the degree of accuracy which was attained.

Since photographic film was to be used in the process, the problem of possible errors due to film shrinkage in the developing process was considered. Although this error appeared to be small, the possibility of its occurring at all was eliminated by calibrating the test negative after it was developed and placed on the analyzer. To make sure that all negatives remained the same size as the calibrated negative, each new drop-test negative was checked against previously marked stations on the original negative. The error which could occur because of negative stretch or shrinkage was always found to be smaller than could be detected on the mechanical analyzer.

The equations upon which the design of the mechanical analyzer was based assumed that the camera lens was perfect for its entire field of view. Errors which could be due to the lens were therefore checked by taking a picture of a grid and examining the distortions resulting in the negative. It was found that in the extreme corners of the picture the distortions, when compared to the center part, were less than $\pm \frac{1}{4}$ of one percent. Since almost all of the drop measurements were made along the centerline of the negative, the error from the lens system of the camera was considered to be negligible.

The shutters of the two cameras used in this system had to operate in unison and at a definitely known speed in order to provide a basis for timing the parachute drops. The rate of rotation of one

of the shutter disks was determined by a synchronous motor operating off a standard 60-cycle supply line, making the timing accuracy as close to perfect as possible. The synchronization between the two cameras was checked by photographing a light source moving along the drop centerline. Comparison between the negatives of the two cameras indicated that the error in the synchronization was less than the analyzer operator could detect.

A shutter opening of 1/40 of a second was required to provide sufficient lighting during the high-speed drops. The records obtained from these tests could be read to within $\frac{1}{4}$ of the length of the mark on the negative or to within approximately $\pm$ 1/160 of a second. This indicates the timing accuracy which is important in the determination of the accuracy of the velocity measurements.

Perhaps the largest errors which existed in the system were those human and mechanical errors which occurred in the operation of the analyzer itself. The mechanical design and operation of the machine appeared to follow the calculated predictions exactly. However, it was possible to check only the combination of human and mechanical errors by calibrating the analyzer through the actual measurement of the locations of known stations photographed by the two cameras. Repeated checks of the calibration negatives by different people at different times indicated that a known point in space could be located at least to within $\pm$ 3 inches. This value includes the summation of all the errors in the determination of a position in space and on the average would be about one half as large as this.

Using 3 inches as the worst possible error which would be recorded, and observing that the terminal velocity was determined from the slope of the vertical distance-vs-time curve for a period of at least three seconds, it can be stated that the velocity was accurate to within approximately $\pm$ 1/12 ft/sec. The determination of the angle of oscillation of the parachute depended on the location of the relative position of the lights on the shroud line with respect to those on the weight unit. Since these lights were approximately $8\frac{1}{2}$ feet apart for almost all of the parachutes tested, and an accuracy of 3 inches could be obtained in the $8\frac{1}{2}$ foot distance, an average angle of oscillation error of approximately $\pm$ 1-2/3 degrees could be expected. The only drop test in which this error would have been increased would be the drops on the parachute using the smallest shroud-line lengths where it could have been as high as two and one half times this amount.

The accuracy of the geometric characteristics of the parachute could be generally divided into three parts; the material itself, the construction and the measurements made. The porosity and weight of the cloth purchased for the construction of the majority of the parachutes followed specification MIL-C- 7020. The finished weight of the parachute was measured and is accurate to within $\pm$ 1%. The average bulk of the parachute is accurate to within $\pm$ 2% based on the method described elsewhere in the report. An attempt was made to keep all the dimensions of the parachutes within $\pm$ 2% of the design values. Any variation from this was noted.

It is apparent, therefore, that the determination of all basic data was accomplished well within the allowable error usually obtained in experimental tests. The use of the basic data to obtain derived information is as accurate as the judgment of those who analyzed the information. The accuracy of the actual drag-coefficient points plotted on the curve sheets depends primarily on the accuracy of the parachute weight and velocity measurements and is estimated to be within $\pm$ 2.25%. The average glide angle was found from the slope of the vertical vs horizontal velocity curve and is based entirely on the portion of the curve analyzed. An attempt was made to consider only the section at which terminal-velocity conditions existed. In most cases this is within $\pm$ 1°. Each curve is marked so that the reason for the choice of angle is indicated. The frequency of oscillation was taken from the oscillation curves and, as explained previously, was an engineering evaluation which would be accurate to within $\pm$ 10%.

The maximum angle of oscillation was based entirely on the estimate of the analyst regarding the nature of the oscillation curve giving careful consideration to both ends and was probably accurate to within $\pm$ 10% for most of the conditions. The average or constant angle of oscillation was not calculated at all, only estimated, and should serve only as an indication of the apparent angle exhibited by that drop. The logarithmic decrement is based on the peak angles which are of the same order of accuracy as the maximum angle mentioned earlier.

It should be pointed out that many of these measurements are being made for the first time and that in the future, when trends are more readily recognized, better engineering evaluations will be possible.

PRESENTATION OF RESULTS

In view of the fact that over 700 drop tests were made during this project it became necessary to establish in addition to the main report a system of appendices which included the drop-test data, miscellaneous curve sheets, and design sketches for the parachutes tested.

The number, type of design, shape, and cross-section of each parachute model tested are defined in Table 1 and it is in this order that the appendices, parachute photographs, and general curve sheets are presented and discussed in the text. In all, there were 27 different parachutes (and 32 different configurations) tested during this drop-test program. The additional configurations were a result of varying the length of the suspension lines of the solid-flat 10% extended-skirt parachute in six equal increments between $0.6D_o$ and $1.4D_o$.

Theoretically, 24 drop tests were to have been conducted on each configuration during this program; however, for reasons of unsatisfactory parachute performance, high suspended load requirements, and extensive damage to the models, some of the high-speed drops were eliminated. A drop number has been allocated in sequence for each drop-test condition beginning with parachute No. 1 and ending with parachute No. 31 on the basis of twenty-four drops per configuration bringing the theoretical total number of drop tests to 768. The drop numbers for parachutes No. 7 and 8 were reversed accidentally during the analysis and were not changed during checking of the data and test results. The drop conditions of each parachute were tabulated first according to the vertical type of release for nominal descent velocities of 10, 15, 25 and 40 feet/sec respectively and then for the horizontal type of release in the same terminal-velocity arrangement. Three drop tests were planned for each condition of terminal velocity and release.

Because of the bulkiness of the complete report it was decided to separate the material into seven volumes in which Volume I would include the text of the report and Volumes II through VII would contain the appendices grouped in the following manner:

Volume Number	Appendices Included
II	A, B, C
III	D
IV	E, F, G, H, I, J
V	K, L, M, N, O, P
VI	Q, R, S, T, U, V
VII	W, X, Y, Z, AA

Volume III contains the data for all six configurations of the solid-flat 10% extended-skirt parachute (No. 4). The grouping of appendices chosen for these volumes was based entirely on convenience providing a reasonable number of volumes in a size not too difficult to handle.

Each appendix contains a list of the tables and figures included for each parachute configuration. The data, tables, and figures are identified by the drop numbers and are numbered consecutively according to the sequence of nominal velocity and release conditions mentioned previously. It is important to note that the respective table and figure numbers for the various appendices represent similar conditions of nominal descent velocity and release, thus making it easier to compare the similar data of the different parachutes. Wherever drop tests have been eliminated from the test program the respective table or figure numbers are replaced by a dash and the numbering sequence retained.

All of the tables of geometric and aerodynamic characteristics summarizing the data of the appendices are included in Volume I. It is important to note that Table 5 giving the aerodynamic characteristics of the solid-flat 10% extended skirt parachute contains six sections from (5a) through (5f) to account for the various shroud-line configurations tested for this type of parachute.

Figures 25 through 51 are photographs of the parachutes taken during descent to accentuate the inflated form of the various types of parachutes tested. Wherever possible a side-view and a plan-view projection are presented. These photographs were all taken during one drop-test period for economy reasons and suspended loads were used to give approximately 20-ft/sec vertical descent velocity for each parachute.

Geometric Characteristics

The geometric characteristics of the model parachutes are given in Table 1 where the parachute numbers used in the present report are associated with the design terminology and the canopy shape of the parachutes tested during this drop-test program. The columns on parachute shape and cross section show schematically the plan view and cross-sectional view respectively of the parachute canopy when all the crimp is taken out of the cloth in essentially the uninflated condition. This procedure accentuates the difference between preformed and flat-type canopies as usually defined in the literature of today.

The total surface area is the actual cloth area used in the construction of the parachute canopy neglecting any internal seam structure and includes such items as the roof panels, rib panels, pockets, vents, guide panels and the spaces between ribbons for the designs tested. In general, the vent areas were one percent of the total surface area or of the roof-panel area. The nominal diameter is calculated as the equivalent diameter of a disk whose area is equal to the canopy surface area of the parachute. The construction diameter is a designation of the size of the parachute based upon actual design dimensions. For the square and triangular types of parachutes the construction diameter represents the length of a side of the canopy. The constructed skirt dimension is another indication of parachute canopy size and represents the average distance on the skirt between the shroud-line attachment points. For the circular-type parachutes this distance equals the base of the canopy gore while for the square and triangular types this distance represents a segment of the parachute side which is divided equally by the shroud-line attachment points. For the circular-type parachutes the number of gores and number of shroud-lines were the same and ranged from 10 to 24 as shown on Table 1. The square-type parachutes had 16 shroud lines and the triangular type parachutes had 15 shroud lines equally spaced around the skirt periphery.

The average porosity of each parachute canopy is given in cubic feet per square foot per minute measured at 1/2-inch water pressure differential for the solid canopy designs, while for the ribbon types the total porosity is given in percent. The porosities of the ribbons of the ring-slot parachutes were also measured in cubic feet per square feet per minute terms and are included in parentheses in the table.

The average bulk of the complete parachute, including canopy and shroud lines, and that of the parachute canopy alone is given in cubic inches for the models tests. The weight of each complete parachute is given in pounds. Calculations of the specific density of these parachute models, weight divided by bulk, give values ranging from 0.010 to 0.012 lbs per cu. in.

Aerodynamic Characteristics

The aerodynamic characteristics of the parachute models are presented in Tables 2 through 28 where the results are catalogued according to the drop-number scheme explained previously. The ambient air temperature, air relative humidity, and barometric pressure prevalent in the drop area at the time of the tests were recorded and used to determine the mass density of the air in slugs per cu. ft. The total weight, W, includes the weight of the parachute, the instrumentation, and the suspended load. The instrumentation consisted of the flashlight bulbs, sockets, wires, and electrical clips mounted to the shroud lines and the plywood disc used to facilitate untangling of the parachute. The average weight of all the instrumentation was approximately 0.10 lbs. The suspended load included the weight unit and the miscellaneous lead weight used inside the fabric bag.

The velocities, drag coefficients, and miscellaneous flight characteristics of the parachutes as explained in the remainder of these tables of aerodynamic terms were determined from the data and curve sheets contained in the appendices of the report. The tables of drop-test data show the coordinates of the load point and also those of the shroud-line point, for complete analysis as defined on the analyzer grid of Figure 22. The x and y terms define the plan-view location of the desired point from the center of drop. The z term gives the distance of the desired point above or below the height of the cameras with a positive z defining points above the plane of the cameras. The load point is defined as the geometric center of the three lights mounted on the weight-unit top while the shroud-line point represents the geometric center of the light or lights fastened either along the axis or to the shroud lines of the parachutes respectively, as described previously.

Station No. 1 represents the parachute system close to the floor while still in the terminal or constant-velocity region. The highest station number represents a location close to the top of the dock or during the early part of the drop-test flight path where the parachute inflation is such that the terminal-velocity condition has not yet been reached. The station numbers marked with an asterisk represent the parachute system as defined by dashes on the film for purposes of coordinating the two test negatives of each drop test. Also included in the tables is the number of seconds elapsing between the release of the parachute and arrival at the parachute location defined by the highest tabulated station number of the drop test. Remarks covering the observed descent characteristics of the parachute system were also recorded on the tables of data. Each system of points was numbered consecutively in ascending order taking No. 1 for the starting point near the floor.

For the lower velocities of descent it was only necessary to analyze every other station number to obtain the required curves and data because of the large number of test points obtained. Also included in the tables is the vertical displacement (H) of the load point from the release point near the top of the dock. Since the plane of the camera lines of sight was 74.1 feet below the release point, the following formula was used to calculate H:

$$H = 74.1 - Z$$

In order to determine the vertical terminal velocity of the parachute system as requested, the vertical distance of the suspended load from release point, H, was plotted against time since release, and the slope of the straight line or terminal velocity portion of the curve determined and recorded. Each station number represents one quarter of a second of time since the camera discs rotated once every two seconds and possessed eight radial slots.

Three drop tests were to be conducted for each of the defined conditions of release and nominal terminal velocity of the parachute. It was only necessary to analyze completely (determine both the coordinates of the load and shroud-line points) one representative drop of the three. For the drop tests where just the load-point coordinates were determined, the vertical terminal velocity, V_v, and the drag coefficient, C_{D_o}, were the only dynamic properties recorded in the table of the aerodynamic characteristics of the parachutes. The tables of drop-test data for each parachute were placed in consecutive order according to the drop numbers.

Flight Paths

The three following curves are presented in the appendices for all the drop tests which were analysed completely:

1) Plan view of the path of the suspended load.
2) Top view of the oscillation of the parachute with the suspended load as the origin.
3) Vertical displacement vs horizontal displacement along trajectory.

These figures are presented in the order mentioned above according to drop numbers. In each appendix the list of figures explains the method of grouping and numbering the curve sheets so that similar conditions of descent velocity and release for the different types of parachutes can be compared by using the same figure number between appendices. An attempt was made to use only one scale size for each type of curve throughout the report for convenience in making comparisons however, it was found necessary to use two different scales for the plan-view curves because of the extreme limits of flight-path variation existing for the types of parachute tested with the two methods of release.

The plan-view curves of the path of the load were plotted on the (X, Y) axes as defined and correlated with the drop-test area in Figures 1 and 22. (The position of North was inserted for correlation purposes only). On all the curves of the appendices the measured test points are identified by the intersection of small dashes with the curve itself. Points representing the synchronization dash on the drop-test films (station numbers with asterisk in drop-test data tables) are differentiated from the other test points by increasing the length of the identifying dash on the curves. Each plan-view curve includes the horizontal projection of the parachute axis at intervals of one second. This projection of the axis is accomplished by plotting the plan-view location of the shroud-line point for any desired load point and is identified by a cross symbol. The line drawn between the load point and the respective shroud-line point represents the parachute axis and thus defines the parachute attitude throughout the descent. An arrow has been added near the curve wherever needed to clarify the data to show the direction of flight of the parachute. The method of point representation utilized in the curves of the appendices facilitates correlation of test points between curves. In the drop tests when the parachutes had essentially a vertical descent the plan-view

curves were plotted even though a congestion of points resulted. There may seem to be some discrepancy between the final point on the plan-view curve and the remark on the drop-test data table concerning the landing point of the parachute; however, it must be remembered that the plan-view data do not include points very near to the floor in all cases in order to eliminate any ground effect from the parachute drag data. The important item considered in analyzing the drop-test data was to reproduce the flight path of the parachute during the terminal-velocity range, omitting as much as possible the conditions where the parachute was opening or approaching the airship dock floor during the drop tests.

Curves showing the top view of the oscillation of the parachute using the suspended load point as the origin were obtained by plotting the (x-X, y-Y) coordinates of the parachute axis. These coordinates were determined by subtracting the plan-view coordinates of the load point from the corresponding coordinates of the shroud-line point of the parachute system. Here again the method of point representation explained previously was used for correlation purposes. The distance between the load and shroud-line points was calculated for every type of parachute tested and circles were drawn on the oscillation curves giving the range of oscillation angles (γ) for the parachute axis in 10-degree increments. The maximum and average or constant angles of oscillation, if definable, have been determined and added to the tables of aerodynamic characteristics of the parachutes. Wherever the parachute oscillation essentially takes place in one plane (two-dimensional motion) the frequency of oscillation and logarithmic decrement have also been determined and tabulated.

Finally, a curve of vertical displacement vs horizontal displacement along the trajectory for the suspended load was plotted for each drop test analyzed completely, incorporating the previously described method of point representation along with the time scale. The horizontal displacement along the trajectory was determined from the plan-view curve by summation of the trajectory increments between the measured test points. This horizontal displacement curve was plotted against time on a work sheet and the average horizontal velocity of the suspended load (V_h) determined by taking the slope of the curve. The initial point on the curve was located by assuming the horizontal distance to be equal to the length of the radius vector of the corresponding point on the respective plan-view curve. The average glide angle for the parachute during descent was determined by taking the slope of the trajectory curve such that by definition the glide angle becomes

$$\phi = \tan^{-1} \frac{V_h}{V_v}$$

Therefore, it can be seen that a parachute possessing a vertical trajectory curve is said to have zero glide angle. The value of the average glide angle in degrees was noted on each trajectory curve and also tabulated in the tables of aerodynamic characteristics.

Initially the resultant velocity along the trajectory of the suspended load was obtained by first graphically determining the resultant distance along the trajectory at each test point from the known horizontal and vertical distance quantities and then taking the slope of the resultant distance curve when plotted against time. In view of the fact that the average resultant velocity obtained in this manner was for all practical purposes the same as the value obtained by the formula

$$V_r = \sqrt{V_h^2 + V_v^2}$$

it was decided to utilize the latter method for the majority of the drop tests. The values for V_r were recorded on the tables of aerodynamic characteristics for the drop tests analyzed completely.

The drag coefficient, C_{D_o}, was determined and tabulated for every drop test, where a vertical terminal velocity was established, according to the following formula:

$$C_{D_o} = \frac{2W}{\rho V_v^2 S_o}$$

The drag coefficient, $C_{D_{or}}$, was determined and tabulated only for the drop tests which were analyzed completely according to the following formula:

$$C_{D_{or}} = \frac{2W \cos \phi}{\rho V_r^2 S_o}$$

Drag Coefficients

In view of the fact that this drop-test program was an extension of research work conducted previously (Reference 1) it was decided to present the drag-coefficient data in a similar manner by first displaying the drag-coefficient curve for each model tested of a particular parachute family or general type on a summary-curve figure, then following with a separate drag-coefficient versus vertical-velocity curve for

each of these parachutes tested. This method of presentation offers an excellent means for comparing the different parachute designs belonging essentially to the same type or parachute family. The actual test points will be shown with the drag-coefficient curve for a particular parachute model, whereas the summary-curve sheet will present the average C_{D_o} curve determined from the average of these test points.

Figure 52 shows the summary curves of C_{D_o} vs. V_v for the models of the solid-flat parachute family. Figures 53, 54, and 55 are the drag-coefficient curves for the circular (No. 1), square (No. 2), and triangular (No. 3) parachutes, respectively, and include the test points obtained from both horizontal and vertical types of release. In general, one suspended load was used to determine the six drag coefficients at any nominal descent-velocity condition for a parachute. This is characterized by the test points being positioned in a definite line, provided the air density remains the same during the tests. In some cases it was necessary to adjust the suspended load during the test run in order to obtain a velocity closer to the desired nominal velocity thus causing these test points to be in a jumbled group rather than in a definite line.

Figure 56 gives the summary curves of C_{D_o} vs. V_v for the solid, extended-skirt parachute family where the models range from 10% to full extension and the L_s/D_o ratio is equal to 1.0. Figure 57 presents the summary curves of drag coefficient for the 10% extended-skirt parachute (No. 4) for the suspension-line ratios investigated ranging for L_s/D_o from 1.40 to 0.60. Figure 58 gives the relationship of drag coefficient with the suspension line ratio for parachute No. 4 on the basis of the constant C_{D_o} obtained at the higher speed range from Figure 57. Figures 59 through 64 are the C_{D_o} vs. V_v curves of the various configurations tested of parachute No. 4 giving the drop-test points. Wherever the drawn curve deviates noticeably from the calculated average of the test points, the curve is dotted. It must be noted that considerable difficulty was encountered during the 40-ft/sec drop tests and that since the parachute system was very heavily loaded the C_{D_o} value should probably not be as representative of the parachute characteristics as that obtained near a velocity of 30 ft. sec. Figures 65 and 66 are the drag coefficient curves for the 12½% (No. 5) and fully (No. 6) extended-skirt parachutes, respectively.

Figure 67 is the drag-coefficient curve for the airfoil parachute (No. 7). Considerable difficulty was encountered obtaining test data at speeds above 15 ft/sec because of the inconsistent opening characteristics of the parachute at the high speeds. The dotted part of the curve was drawn on the basis of published data from previous tests on this type of parachute.

Figure 68 gives the summary curves of the drag coefficient for the four models of the solid-spherical parachute family investigated during the test program. Figures 69 through 72 present the C_{D_o} vs. V_v curves for 1/2-sphere circular (No. 8), 1/4-sphere circular (No. 9), 1/2-sphere square (No. 10), and 1/4-sphere triangular (No. 11) parachutes, respectively.

Figure 73 presents the summary curves of drag coefficient for the three models of the 30° solid-conical parachute family. Figures 74 through 76 are the C_{D_o} vs V_v curves for the circular (No. 12), square (No. 13), and triangular (No. 14) parachutes, repsectively, belonging to this family.

Figure 77 gives the C_D vs V_v summary curves for the four types of guide-surface parachute models tested. The C_D curve was presented here rather than that of the C_{D_o} values since it is more common in the literature and this facilitates making comparisons with other test data. Figures 78 through 81 are the drag-coefficient curves, both C_{D_o} and C_D, for the medium-construction brake-type (No. 16), stabilization-type (No. 17), universal-type riblese (No. 25), and the personnel-type (No. 26) guide-surface parachute models respectively. The actual test points were used to determine an average C_{D_o} vs V_v curve in each case. The C_D curves were obtained from the C_{D_o} curves with the following formula for each of these parachutes:

$$C_D = \frac{S_o}{S_p} C_{D_o}$$

Figure 82 gives the C_{D_o} vs V_v curve for the Exeter Type-12 shaped parachute model (No. 24) as determined from vertical and horizontal types of release in the drop tests.

Figure 83 presents the summary drag-coefficient curves for the five models tested of the FIST ribbon-parachute family including variations of canopy shape and porosity. Figures 84 through 88 contain the C_{D_o} vs V_v curves for the circular brake (No. 21), square (No. 22), triangular (No. 23), 20% porosity circular (No. 27), and 25% porosity circular (No. 28) FIST type ribbon parachutes. The three circular parachutes (Nos. 21, 27, and 28) were used to investigate the effect of porosity variation for λ_v between 20% and 26%.

Figure 89 gives the summary drag curves for the three circular models of the ring-slot parachute family. Figures 90 through 92 are curves of C_{D_o} vs. V_v for the parachutes with 10% total porosity (No. 29), 13.5% total porosity (No. 30), and 17% total porosity (No. 31), respectively.

In general, the C_{D_o} vs V_v curves were drawn through the average values of the test points for the various nominal descent-velocity conditions for the parachutes tested. Whenever a considerable spread of test points existed for any one nominal-descent condition due to the erratic motion of the parachute, an attempt was made to obtain help in drawing the C_{D_o} curves on the basis of previously published data.

Angle of Attack

A method was devised for determining the angle of attack of the descending parachute throughout its complete flight path. Figure 93 defines the axes and vector terminology used in this calculation and also includes the actual vector formulas. When determining the angle of attack of the parachute (angle between the instantaneous resultant velocity V_r of the load and the parachute axis A) at any point "n", it is more accurate for the velocity vector to be obtained by using the coordinates of the (n-1) and (n + 1) points. In the present test program the consecutive points considered in the calculations were 1/4 second apart. Standard vector notation is used in the formulas (Reference 5) where the letter with the dash above it signifies a vector quantity while the letter alone signifies a scalar quantity, vector magnitude. The angle α was determined by the use of the "dot" product of the parachute axis and resultant velocity vector. This method of calculating angle of attack can be applied to any of the drop tests which were analyzed completely.

The angle of attack was determined for all eight drop-test conditions of the solid-flat-circular parachute model during the complete descent. Figures 94 through 101 represent the angle of attack versus time curves for the nominal 10, 15, 25 and 40-ft/sec vertical-release and the nominal 10, 15, 25, and 40-ft/sec horizontal-release drop tests, respectively. The angle of attack was calculated at the various stations as given in the tables of drop-test data in the appendices of the report. Each calculated point is marked by an open circular symbol while those representing the synchronization point (marked with asterisk in tables of drop-test data) is a solid or "filled" circular symbol. This again facilitates comparison of points between the various curve sheets and tables of data. An average curve was drawn through the test points and showed the oscillating nature of the angle of attack for the parachute during its descent.

ANALYSIS AND DISCUSSION

This drop-test information, collected under controlled conditions for approximately 700 drops, provides a wealth of data which can be readily analyzed to indicate overall parachute performance. To show the potentialities of the test method employed, a partial analysis has been made of typical drops and is presented in tabular and curve form.

Space coordinates for the weight unit of the parachute system were determined for all the drops so that parachute drag coefficients could be evaluated. Each different drop condition was further analyzed in regard to parachute stability to establish typical flight operational trends for all the designs tested. A sample analysis was made of parachute angles of attack. Although the analysis presented in this report is perhaps the most extensive of its type ever attempted, it should by no means be considered to exhaust the possibilities, but merely to indicate the value of the data, and what can be done in several types of evaluations.

Because of the many different solid and ribbon types of parachutes tested it is considered desirable to catalogue them according to canopy design characteristics as an aid for discussion purposes. The term "solid" refers to parachutes possessing no interruptions in the main canopy surface other than the vent. The term "flat" signifies that the uninflated canopy can be spread out on a flat surface with all the crimp taken out of the material. Several of the parachutes tested had a "shaped" canopy such as the conical and spherical designs and these will only spread out evenly over a predetermined form or pattern and not on a flat surface.

During the drop tests, the descent characteristics of the parachutes were observed and the corresponding remarks entered on the data sheet by the test engineer at the floor panel. The term "drift" in the remarks designates the horizontal distance of the parachute landing spot measured from the center of drop location on the floor. Also in the remarks on the data sheets will be found the term "sideslip" which is synonymous with glide. It is suggested that more emphasis be placed on the actual test results and plotted curves than on the remarks of the data sheets for reliability and completeness.

In general, there did not seem to be any significant difference between the tabulated test results of the parachutes for the two conditions or types of release used in the program except in a few special cases. Some of the presented curves have features characteristic of the type of release used on the parachute system and must be interpreted with the following limitations in mind: All the flight-path curves for the vertical release usually start near the centerline of drop or (X, Y) = (0, 0). For the horizontal condition of release the plan-view-curve starting point varies somewhat but usually begins in the neighborhood of (X, Y) = (30,-10). Because of the high drift characteristics of some of the parachutes it became necessary to use two different scales for the plan-view curves. It is important to keep this fact in mind when comparing the characteristics of the various parachutes by just observing the flight-path curves. The starting point of the oscillation curves for the horizontal release condition depends on how close to the drop position the test points are analyzed. Usually the starting point of this curve lies in the second quadrant indicating a large angle, and this fact was taken into account when the maximum and minimum angles of oscillation were determined for the parachutes. The plotted trajectory curves for the horizontal release condition look approximately the same as those of the vertical types of release except for a displacement of the curves about 30 feet from the drop centerline. The average glide angle was determined by taking the slope of the lower part of the trajectory curve, since this section of the curve was usually fairly straight and represented the terminal velocity condition of the descent. In many cases for the parachutes with erratic descent characteristics the trajectory curves seemed to indicate two different slopes, depending on how far up the curve the terminal velocity condition of the descent prevailed. This fact was considered when analyzing the trajectory data, and the glide-angle line was put on the curve only after the complete history of the drop was known. For the trajectory curves of the horizontal release conditions the tendency was to consider more of the complete curve when obtaining the necessary slope. It is believed that in some of the high-speed drops only a small portion of the terminal-velocity condition may have been attained, thus complicating the velocity and glide-angle determination. This was particularly true for the horizontal types of release where the parachute seemed to lob into the impact point on the floor, never reaching straight vertical descent. In some cases, during the horizontal release condition, the parachute became disengaged prematurely during the first quadrant of its swing. This has

been termed in "improper release" on the data sheets. Drop tests completed under these conditions were used for drag determination; however, efforts were made always to attain a good horizontal release for the representative drop which was analyzed completely. Whenever the remark on the data sheet referred to an inflation irregularity for any particular drop test, the information was analyzed only if it was felt that the parachute had reached the terminal velocity condition and thus give satisfactory drag information.

Since the logarithmic decrement usually describes the damping characteristics of a system and is obtained from the measurement of successive amplitudes of oscillation, this term was used to describe the motion of those parachutes which showed a reduction in oscillation amplitude in any one complete cycle. If an increase of amplitude was experienced, the term "negative" was used to describe this unstable tendency. This term usually indicated that a small angle of oscillation of the parachute system early in the drop steadily grew to a larger angle where it remained throughout the rest of the test.

Both the frequency of oscillation and the logarithmic decrement as obtained from these data indicate order of magnitude rather than absolute value. Still it is interesting to note how consistent this information is for any one type of parachute and how narrow a range encompasses all the types tested.

In order to determine a value for the oscillation frequency and logarithmic decrement of any particular drop, it was necessary to establish a meaning for these terms in regard to the parachute action. If the parachute axis tended to remain essentially in one plane, the frequency was based on the amount of time it took the parachute to travel from a position of maximum angular deflection through a complete cycle and back to the original position. If the parachute axis followed a conical motion, the oscillation frequency was based on the time it took for the parachute axis to traverse the entire motion from any starting position around the cone and back to the original point. If only half a cycle was available an estimate was still made of the probable frequency of the system.

The terms "maximum angle of oscillation" and "average angle of oscillation" used in the description of the parachute attitude during its descent refer to the angle the parachute axis makes with the

vertical. This includes all motion of the parachute system except the initial angle imparted to the parachute in the horizontal release.

If the parachute axis tended to follow a conical motion, the average angle was defined as one half of the cone angle. If it was a two-dimensional motion, the arithmetic average of the sum of the oscillation amplitudes was used. In the analysis of the data the oscillation range of the parachute is taken to be from the minimum value of the average or constant angle of oscillation to the maximum value of the tabulated maximum angle of oscillation experienced by the parachute during the drop tests (see tables).

In general, the very stable parachutes possessed straight vertical descent with little or no oscillation. The unstable parachutes tended to glide at the low V_v range and possessed a trend toward straight vertical descent as the descent velocity was increased. At the lower V_v range the unstable parachutes seemed to oscillate about a point near the canopy skirt; however, as the suspended load was increased for the higher V_v range the parachutes oscillated with high frequency about the load. In general, as the descent velocity was increased the average glide angle became smaller for the parachutes which possessed sideslip characteristics.

In an effort to submit all the test curves required, it was necessary to include some curves for the very stable parachutes which when plotted did not seem to show much or lend themselves to further analysis. Although these plan-view and oscillation curves appear as a mass of points about the origin of the axes they serve as documentary evidence of the good descent characteristics of the particular parachutes involved. For many of the drop tests analyzed fully it was either impossible or impractical to determine some of the required data; therefore, these voids were noted on the tables of aerodynamic characteristics as dashes (-). Although the spread of the data was greater for the unstable parachutes or the ones with erratic descent characteristics, it was found that, in general, the data spread was within the accepted limits of experimental test results. Except where mentioned, all parachutes tested had an L_s/D_o ratio equal to one.

The unstable parachutes showed a significant increase in drag coefficient for decrease in descent velocity, sometimes not ever reaching a constant C_{D_o} value throughout the velocity range tested. The stable parachutes either presented a moderate increase in drag coefficient for a decrease in descent velocity or approximately had a constant C_{D_o} value for the V_v range tested. In cases where the drag coefficent based on the projected area is better known than that based on the surface area both the C_D and C_{D_o} curves were presented along with the conversion formulas used.

The maximum and average spread of the test points from the estimated drag curve were calculated and the values of each recorded in the analysis section of the respective parachutes. In general the average spread of the test points is in the neighborhood of $\pm$ 15% for the parachutes with erratic descent characteristics, $\pm$ 10% for most of the parachutes, and $\pm$ 5% for some of the very stable parachute systems. Except for the special series of tests on the 10% extended-skirt parachute (No. 4), the drag coefficients recorded were for parachutes with a suspension-line ratio equal to unity. Since no points are shown on the summary drag curves presented for each parachute family it should be noted that the curves were drawn exactly as their respective drag curves plotted with all the test points. Whenever the plotted curve did not go through the average values of the test points obtained for the separate velocity conditions the estimated curve was dotted, this being particularly true at the higher V_v range tested. Although $C_{D_{or}}$ was recorded on the tables of aerodynamic characteristics of the parachutes, the results were not discussed in the present report, and no trends were investigated.

Solid-Flat Parachutes

The drop-test results for the circular (No. 1), square (No. 2) and triangular (No. 3) parachutes of the solid-flat family are presented in Tables 2 through 4. The square and triangular parachutes had pockets on each of their corners whose area was approximately nine percent of the total canopy surface area. The summary drag curves of Figure 52 indicate that the C_{D_o} values for the circular parachute are larger than those of the square and triangular parachutes. This apparent higher efficiency of the circular design may be due to the canopy pockets used with the square and triangular canopies. No definite differences appear between the C_{D_o} curves of the square and triangular parachutes. For the solid-flat type parachutes there seems to be a substantial increase in C_{D_o} for a decrease of descent velocity particularly below V_v of 30 feet per second for the range tested.

The average horizontal velocity varied from 9 to 3 feet per second for the average resultant velocity range of 12 to 47 feet per second. In general, the horizontal velocity, V_h, decreased for an increase in descent velocity except for the square parachute (No. 2) which seemed to have a constant V_h value of approximately 7 feet per second for all conditions of V_v tested. The average glide angles varied from approximately 40 to 3 degrees with the higher angles prevalent at the lower V_v conditions. Although each of these parachutes had flight characteristics peculiar to the design of the canopy, the ranges of their maximum and average angles of oscillation seemed to be approximately the same. The maximum angles of oscillation varied from 16 to 40 degrees while the average angles of oscillation ranged from 10 to 32 degrees for the V_v range tested.

In general, the oscillation frequencies of these parachutes ranged from approximately 0.2 to 0.5 cycles per second for the descent velocity range tested, an increased frequency resulting for an increase in V_v. The frequency results obtained for the circular parachute (No. 1) seemed to be the same for both conditions of release. The frequency of oscillation for the square parachute (No. 2) apparently remained fairly constant around 0.3 cycles per second for the lower descent speeds tested, no values being readily available for the 40-foot-per-second conditions. The frequency of oscillation for the triangular parachute (No. 3) although within the range of values mentioned previously was not as consistent as that for the circular design of canopy. Here again some difficulty was encountered for the high-speed descent condition.

It was not possible to obtain any conclusive information concerning the damping characteristics (logarithmic decrement) of these three parachutes on the basis of the recorded test data. The oscillation curves presented no consistent pattern needed for calculations of this kind.

Figure 53 gives the constant value of C_{D_o} as 0.97 for the circular parachute while Figures 54 and 55 give constant C_{D_o} values of 0.75 and 0.82 for the square and triangular parachutes respectively. The spread of the drag data averages about ± 12% for the velocity range tested with most of the point spread occurring at the lower V_v values. The maximum spread for these points from the curve ranges from 15 to 18%.

These parachutes all tended to sideslip and oscillate at the lower V_v range, then exhibited straight vertical descent with high-frequency oscillation about the load for the upper V_v range tested. In general, good inflation characteristics were found except for the slow inflating of the tips of the triangular parachute at the lower descent speeds. For both the circular and triangular parachutes there was a tendency toward conical-type oscillations for the horizontal release conditions.

The curves of angle of attack vs time (Figures 94 through 101) determined for the circular parachute are oscillating in nature and show an increase in frequency for an increase in parachute descent velocity. In general, better results seem to be available for the vertical release conditions of the drop-test program. The average angle of attack was determined for each test condition and varied between 40 to 20 degrees, decreasing for an increased V_v for the range tested. It was noted that whenever the parachute oscillated in the plane of the flight path the average angle of attack was approximately equal to the average glide angle of the drop test. This will naturally be true so long as the parachute axis swings about the vertical and does not oscillate out past the glide path where the angle of attack would become negative. According to the definitions established earlier in the report, the angle of attack (because of the complications of conical motion) is not calculated as negative. Most unstable parachutes exhibit large glide angles at the low usable V_v range, and the observation that the average angle of attack equals the glide angle becomes applicable.

Solid, Extended-Skirt Parachutes

The drop-test results for the three solid-flat extended-skirt parachutes tested - 10% extension (No. 4), 12½% extension (No. 5), and full extension (No. 6) - are presented in Tables 5 through 7 respectively. Although the 10% extended-skirt parachute (No. 4) was not tested with an L_s/D_o ratio equal to unity, a general comparison of this parachute with the results of the other extended-skirt parachutes was determined by interpolating the data of the 10% extended-skirt parachutes with L_s/D_o equal to 1.08 and 0.92. For the extended-skirt range tested in this program, 10% to full extension, the overall flight-path characteristics of the three parachutes seem to be the same with no definite pattern being indicated. The usual gliding tendency decrease with increase of V_v was observed. Although only a limited number of logarithmic decrements were calculated for these parachutes because of the undamped characteristics of the oscillation curves it was possible to determine the oscillation frequencies in most cases. No inflation difficulties were encountered during these drop tests.

The average horizontal velocities varied between 3 and 10 feet per second at random while the average resultant velocities ranged from 12 to 52 feet per second. The average glide angles decreased from approximately 34 to 3 degrees as V_v was increased over the tested range. The frequencies of oscillation varied from approximately 0.2 to 0.5 cycles per second as V_v was increased for the tests. The few logarithmic decrements calculated varied between 0.5 and 0.7 and signify only order of magnitude to be expected for parachtes of this type when damping does occur.

The summary drag curves for the extended-skirt parachute family are given in Figure 56. Although the C_{D_o} curve for the 12½% extended-skirt parachute is lower than the others it must be pointed out that no constant trend can be determined. Probably an average C_{D_o} of 0.77 would be acceptable for design purposes above a V_v of 25 feet per second. There seems to be a sharp decline of C_{D_o} for an increase of V_v over the lower tested range after which a constant C_{D_o} is attained. An average spread of about ± 10% was detected for the drag-curve test points for all the parachutes of thie family tested during the program except in a few extreme cases.

A series of tests was conducted with the 10% extended-skirt parachute wherein the L_s/D_o ratio was varied from 1.40 to 0.60 in six equal steps for the same nominal descent-velocity range used throughout the overall test program.

All the configurations tested of this parachute seemed to possess a gliding tendency at the low V_v range combined with moderate angles of oscillation. As V_v was increased the parachutes approached straight vertical descent combined with moderate oscillations. Several cases of conical-type oscillation were noted during the test. In general, undamped oscillations prevailed and the angles of oscillation grew larger as V_v was increased.

For the configuration with the smallest shroud-line length ($L_s/D_o = 0.60$) the parachute canopy had decided breathing tendencies particularly for the heavier suspended loads used. In addition erratic oscillation patterns were noticed. As the shroud-line length is decreased it is important to note that the coordinate distances on the oscillation curves represent larger values of angle of oscillation. Also the frequencies of oscillation are more difficult to determine for the configurations with the shorter line lengths.

In general the average horizontal velocity varies between 3 to 10 feet per second for the average resultant velocity range of approximately 11 to 53 feet per second obtained with tests of the various configurations of the 10% extended-skirt parachute. The average glide angles varied from approximately 34 to 5 degrees for an increase in V_v over the tested range. The summary drag curves for the configuration of the 10% extended-skirt parachute are presented in Figure 57 and show a consistent pattern for the L_s/D_o range. There is a definite increase in C_{D_o} for a decrease in V_v at the lower values. A constant C_{D_o} value for each curve seems to be reached in most cases above a V_v of approximately 24 feet per second. These constant values of the drag coefficients are plotted against the suspension-line ratio (L_s/D_o) in Figure 58 which indicates that C_{D_o} ranges from 0.65 to 0.85 for the tests, increasing in value for an increase in L_s/D_o. The drag coefficient becomes fairly constant above an L_s/D_o of approximately 0.95. This indicates that above a critical suspension-line ratio the increase in drag coefficient of the parachute system is apparently only due to the drag of the increased length of the suspension lines, which is small. As L_s/D_o is decreased below the critical value the canopy projected diameter appears to have been made smaller and this results in a decided drag decrease of the parachute system.

In the following statements an attempt is made to describe the properties peculiar to the various configurations of the 10% extended-skirt parachute wherein shroud-line or suspension-line lengths were varied from 16 feet 8

inches to 7 feet 2 inches to cover an L_s/D_o range from 1.40 to 0.60 respectively:

The configuration with a shroud-line length of 16 feet 8 inches (L_s/D_o = 1.40) oscillated between 20 and 42 degrees in an unstable manner particularly for the vertical types of release making it impossible to determine any logarithmic decrement values. For the vertical types of release the angles of oscillation seemed to become smaller for an increase in descent velocity. The frequencies of oscillation increased from approximately 0.2 to 0.4 cycles per second as V_v was increased for the tests. The drag-coefficient curve shown on Figure 59 depicts a constant C_{D_o} of 0.85 above a V_v of 24 feet per second. The increase in C_{D_o} for a decrease of V_v is not as large as experienced with the rest of the configurations of the 10% extended-skirt parachute used in the tests. The curve is dotted above a descent velocity of 30 feet per second whenever it doesn't coincide with the average values of the test points recorded for the higher V_v range. The point spread of the data seems fairly consistent, the maximum value being around 13% for the highest V_v condition.

The model with a shroud-line length of 14 feet 9 inches (L_s/D_o = 1.24) oscillated between 12 to 35 degrees with frequencies ranging from 0.21 to 0.45 cycles per second as V_v was increased for the tests. While the unstable type oscillations seem fairly constant for the vertical types of release, there seems to be a tendency for the oscillation to increase for an increase in V_v for the horizontal condition of release. The erratic pattern of the oscillation curves permitted the calculation of limited logarithmic decrement data. The drag-coefficient curve in Figure 60 shows a constant C_{D_o} of 0.84 above a V_v of approximately 25 feet per second. The point spread seems fairly regular for the curve with a maximum of about 14% being measured at the high V_v range.

The configuration with a shroud-line length of 12 feet 10 inches (L_s/D_o = 1.08) oscillated between 12 to 40 degrees with frequencies of oscillation ranging from approximately 0.3 to 0.50 cycles per second increasing for a descent velocity increase during the tests. The angle of oscillation tends to increase as V_v is increased, particularly for the vertical release conditions. Since no definite damping characteristics were observed it was not possible to calculate any logarithmic decrement for this configuration. Figure 61 shows that a constant C_{D_o} of 0.83 exists above a V_v of about 26 feet per second. Here again the drag curve was

dotted at the higher V_v range because it was not drawn through the average point indicated by the test data. A maximum point spread from the curve of 16% was measured at a low V_v value.

For a shroud-line length of 10 feet, 11 inches (L_s/D_o = 0.92) the 10% extended skirt parachute oscillated between 22 and 35 degrees in most cases and exhibited undamped characteristics. It was only possible to determine the frequency of oscillation for the vertical conditions of release which varied from approximately 0.3 to 0.45 cycles per second as V_v was increased over the test range. In general, it was not possible to determine much information on the logarithmic decrement of this parachute system. A constant C_{D_o} of 0.82 above a V_v of 27 feet per second is shown in Figure 62. The curve is dotted in the upper V_v region for reasons mentioned earlier. A maximum point spread from the curve of about 15% was determined at the lower V_v range

The configuration with a shroud-line length of 9 feet, 1 inch (L_s/D_o = 0.76) oscillated between 10 and 50 degrees for the tests. In most cases the angle of oscillation remained between 20 and 40 degrees and its undamped characteristics permitted limited calculations of the logarithmic decrement. Although a slight increase in frequency of oscillation seems evident for an increase in V_v, the average value seems to be around 0.30 cycles per second. Figure 63 shows a constant C_{D_o} of about 0.76 above a V_v of 28 feet per second. A maximum point spread from the curve of about 11% was detected at the low V_v values.

The 10% extended-skirt parachute with a shroud-line length of 7 feet, 2 inches (L_s/D_o = 0.60) oscillated between 10 and 45 degrees in an erratic pattern and displayed undamped characteristics throughout the test range. A limited amount of oscillation frequency data was calculated, but no logarithmic decrements were determined. Figure 64 shows a constant C_{D_o} of 0.66 above 29 feet per second. A maximum point spread of about 20% was calculated in the intermediate V_v range.

The 12½% extended-skirt parachute (No. 5) oscillated between 12 and 36 degrees and displayed undamped characteristics thus permitting only a limited calculation of the logarithmic decrement. For the vertical release condition the oscillation angle tended to remain the same independent of a V_v change. For the horizontal release condition there seems to be an increase in oscillation angle for an increase in V_v over the range tested. The frequency of oscillation tends to increase from

about 0.22 to 0.40 cycles per second for an increase in V_v during the tests. Figure 65 shows a constant C_{D_o} of 0.66 above a V_v of 28 feet per second. In general, the scatter of test points seems to be small, with a maximum spread of about 18% being calculated at the upper V_v range. The drag curve for this parachute has practically the same shape as those obtained for the 10% and fully extended-skirt parachutes except that the constant C_{D_o} value is about 20 percent lower.

The fully extended-skirt parachute (No. 6) oscillated between 15 and 50 degrees and also displayed undamped characteristics in flight. There seemed to be no consistent trend of oscillation angle variation with descent velocity for the vertical type of release; however, an increase in angle of oscillation seemed apparent for an increase in V_v over the tested range for the horizontal release condition. The oscillation frequencies varied from about 0.18 to 0.45 cycles per second respectively for an increase of V_v during the tests. The erratic nature of the oscillation curves permitted only a limited analysis of the logarithmic decrement. Figure 66 defines a constant C_{D_o} of about 0.83 for a V_v above 24 feet per second. The maximum point scatter was calculated as about 17% at the upper V_v range. In general, the drag coefficient curves for the 10% and fully extended-skirt parachutes are almost identical and indications are that the drag coefficient is independant of extended-skirt length for the range tested.

Airfoil Parachute

The drop-test results for the 50% vent airfoil parachute (No. 7) are presented in Table 8. Considerable difficulty was encountered during the testing of this parachute since it descended in an erratic manner and had critical opening characteristics. Several attempts were made to shorten the vent-line lengths to eliminate this difficulty, with some success. However, the scope of the project did not permit further work along these lines. Since the actual test data were limited, no specific trends were established. In general, the flight-path characteristics were approximately the same as measured for other circular canopy designs tested except that no definite oscillation pattern seemed predominant. Several values of 0.3 cycles per second oscillation frequency were calculated; however, the determination of the damping characteristics was not possible.

Because only a limited amount of drag data was determined for this parachute during the present program it was thought advisable to rely on previous test results for constructing the C_{D_o} curve presented in Figure 67 as was mentioned earlier in this report. Results indicated that a decided increase in C_{D_o} exists for a decrease in V_v. A constant value of C_{D_o} equal to 0.83 seems to exist above approximately 40 feet per second. The average point spread for this C_{D_o} curve seemed to be about $\pm$ 10% with a maximum of 19% being measured for these tests made only at the lower V_v.

Although the tested airfoil parachute design was not satisfactory it is felt that a little more investigation on the proper vent-line length might help create a dependable system. Several different vent-line lengths were tried in the present program, each showing a slight improvement in performance. However, none of the combinations proved entirely successful and the drop tests had to be eliminated for lack of time.

Solid Spherical Parachutes

The drop-test results for the ½ sphere circular (No. 8), ¼ sphere circular (No. 9), ¼ sphere square (No. 10), and the ¼ sphere triangular (No. 11) parachutes are given in Tables 9 through 12. In general, these parachutes had a tendency to sideslip with moderate oscillation during descent at the lower V_v range; however, in the upper descent-velocity range the parachutes possessed approximately straight vertical-descent characteristics with slight oscillation. No inflation difficulties were encountered with these parachutes except as noted with the square canopy design. While hanging on the test bar of the drop-test setup in an uninflated condition only four shroud lines of the square-type parachute supported the suspended load, resulting in a large number of shroud lines hanging limp with varying loop lengths. The tangling of these unloaded shroud lines could well be the reason for the inflation difficulties encountered, rather than the actual canopy design. In some cases there was a tendency for the parachutes of this family to execute conical-type oscillations at the lower V_v range tested.

The average horizontal velocities ranged from 4 to 15 feet per second with no consistent pattern being established. The average resultant velocities varied from 11 to 43 feet per second for these parachutes. The average glide angles showed an apparent decrease from approximately 42 to 6 degrees for an increase in V_v over the tested range. The parachutes of this family seemed to oscillate between 20 to 30 degrees from the vertical unless otherwise noted. In general the frequencies of oscillation varied between 0.25 and 0.40 cycles per second for the range of descent velocities tested, increasing in value for an increase in velocity. In a few noted cases it was not possible to calculate the frequency values because of the nature of the oscillation curves. It was impractical to determine the logarithmic decrement for almost all test conditions completely analyzed for these parachutes.

The summary C_{D_o} curves given in Figure 68 show that the ¼ sphere circular parachute is more efficient than the ½ sphere circular design. In the ¼ sphere parachute group the triangular canopy design seems to have the best drag characteristics, followed in order, by the square and circular canopies. There is a substantial increase in C_{D_o} for a decrease of V_v for these parachutes, the drag curves reaching a constant value only after approximately 28 feet per second. The average spread of data for the drag curves of the solid-spherical parachutes is almost $\pm$ 10%.

The ½ sphere circular parachute (No. 8) oscillated between 20 and 30 degrees during most of the drop tests for both conditions of release. Figure 69 indicates a C_{D_o} of 0.78 above the critical V_v value of the curve. A maximum spread of 20% was detected at the intermediate speeds on the C_{D_o} curve.

The ¼ sphere circular parachute (No. 9) oscillated between 20 and 30 degrees in most tests particularly for the vertical types of release, while for the horizontal types of release several cases of small oscillation angles of 10 degrees or less were measured. Figure 70 gives a constant value of $C_{D_o} = 0.85$ for this parachute and indicates a maximum point spread of about 13% in the intermediate velocity range.

The ¼ sphere square parachute (No. 10) in the different tests oscillated with amplitudes between 12 and 40 degrees, but the range in amplitude for each particular case was small, thus showing poor damping characteristics. No definite tendencies of oscillation-magnitude variation with descent velocity can be presented. Figure 71 gives a constant value of $C_{D_o} = 0.88$ and shows a maximum point spread of approximately 21% at the low V_v range.

The ¼ sphere triangular parachute (No. 11) oscillated within the range of 15 to 25 degrees during most of the tests, tending toward conical oscillation at some of the lower V_v values. Since no consistant oscillation patterns were established it was only possible to obtain limited oscillation-frequency data and no damping data for this parachute. Figure 72 gives a constant C_{D_o} of 0.92 and indicates a maximum point spread of about 20%.

Solid Conical Parachutes

A circular (No. 12), a square (No. 13), and a triangular (No. 14) parachute with 30-degree cone angles were tested and the results presented in Tables 13 through 15 respectively. In general the motion of the parachutes during descent is two-dimensional with undamped types of oscillations prevalent. There seemed to be a tendency to glide considerably at the lower V_v range along with a slight oscillating motion. As the descent speed was increased the angles of oscillation tended to increase particularly for the vertical types of release. No inflation difficulties were encountered with these solid conical parachutes.

The average horizontal velocities varied from 4 to 13 feet per second in no consistent pattern as the average resultant velocities ranged from 13 to 42 feet per second. The average glide angles decreased from approximately 42 to 6 degrees as V_v was increased through the test range. The circular parachute had smaller glide angles than the square and triangular type canopies for most of the V_v conditions tested. Since undamped types of oscillation existed in most cases it was only possible to determine the oscillation frequency values and not the logarithmic decrements for the parachutes. The frequencies of oscillation varied from approximately 0.2 to 0.4 cycles per second, usually increasing in value for an increase in V_v.

The summary C_{D_o} curves presented in Figure 73 indicate that the triangular canopy is slightly more efficient than the circular and square canopies which follow in the order mentioned for the constant section of drag curves. The drag curves for the circular and square parachutes are practically the same for the lower V_v conditions and differ substantially only after a V_v of approximately 28 feet per second. Here again there is in evidence a considerable increase in C_{D_o} for a decrease in V_v for the range tested. For the triangular and circular design the C_{D_o} becomes approximately constant above a V_v of about 30 feet per second while for the square parachute this constant condition only seems to exist at the extreme end of the test curve near a V_v of around 44 feet per second. In general, the average spread of test points for these drag curves is about $\pm$ 13% with a larger spread being experienced at the low V_v range.

The 30° circular conical parachute (No. 12) oscillated between 20 and 40 degrees in almost all of the tests the magnitude of oscillation tending to increase for an increase in V_v particularly for the vertical release

condition. In general this parachute exhibited two-dimensional motion with regard to oscillation and possessed a tendency toward conical motion for the horizontal conditions of release. Figure 74 indicates a constant C_{D_o} of approximately 0.87 above a V_v of 34 feet per second. A maximum point spread of approximately 23% exists at the extreme ends of the tested V_v range.

The 30° square conical parachute (No. 13) oscillated between approximately 10 and 30 degrees for the vertical types of release, the angle increasing for an increase of V_v. In several of the horizontal release tests the oscillation angles show no apparent change with V_v particularly at the lower range investigated. The C_{D_o} curve given in Figure 75 tends toward a constant value only at the extreme end of the V_v range. A C_{D_o} of 0.815 seems to be indicated above a V_v of 44 feet per second. A maximum point spread of approximately 30% was measured at the low V_v end of the drag curve.

The 30° triangular conical parachute (No. 14) oscillated between approximately 5 to 25 degrees for the vertical release condition, increasing for an increase in V_v. For the horizontal types of release the oscillation angles ranged approximately between 20 to 40 degrees, again displaying no definite damping characteristics. Figure 76 indicates a C_{D_o} of about 0.89 above a V_v of 30 feet per second. A maximum point spread of approximately 24% was measured at the lower V_v range.

Guide-Surface Parachutes

The drop-test results of the medium-construction brake-type (No. 16), the stabilization-type (No. 17), the universal-type ribless (No. 25), and the personnel-type (No. 26) guide-surface parachutes are given in Tables 16 and 17 and Tables 22 and 23 respectively. In general, the parachutes exhibited practically straight vertical descent with slight or moderate oscillation during the drop tests. The small magnitude and nature of the oscillation curves prevented the calculation of the oscillation frequencies and the logarithmic decrements in many cases. No inflation difficulties were encountered with these parachutes during almost all the drop tests.

Average horizontal velocities up to 6 feet per second were determined; however, no consistent variation with V_v seems readily evident. The average resultant velocities ranged from 11 to 54 feet per second for these tests. The glide angles varied from 13 to 2 degrees for the tested V_v increase for most of the parachutes; however, they increased to a range of 22 to 6 degrees for the personnel-type guide-surface parachutes which during the tests seemed to be a little more unstable than the other parachutes of the guide-surface family in many respects. These parachutes oscillated from approximately 3 to 30 degrees during the tests; however, the logarithmic decrement could be calculated for only the stabilization-type parachute.

The summary drag curves of Figure 77 are presented in the form of C_D vs V_v rather than C_{D_o} vs V_v, since the drag coefficient based on the projected area is more familiar for guide-surface parachutes. On the individual drag curves of the parachutes both the C_D and C_{D_o} curves are presented along with the necessary conversion formula used. The constant term in these formulas represents the ratio of the parachute surface area to its projected area. Generally the C_{D_o} curve was determined from the test points and then converted to C_D by the given formula. As can be seen from Figure 77, the stabilization-type guide-surface parachute tested seems to have the highest drag efficiency, followed in order by the medium-brake, the universal ribless, and the personnel guide-surface parachutes. The drag curves range from a negligible C_{D_o} change (for the tested V_v values) to a considerable C_{D_o} variation, for the family of guide-surface parachutes investigated. The medium brake (No. 16) and

the universal ribless (No. 25) guide surface parachutes have drag curves with a fairly constant C_D and seemed to be the most stable members of this parachute family during these tests. The average speed of the test points from which these curves were determined range from ± 8% to ± 15%. It seems that larger point spreads occur at the intermediate V_v values of the tests for the drag curves in general.

The medium-construction brake-type guide-surface parachute (No. 16) oscillated between 11 and 25 degrees for the first three V_v conditions for both types of release in such a manner that only the frequency properties could be calculated. The oscillation frequencies ranged from 0.2 to 0.4 cycles per second, increasing for an increase in V_v. Figure 78 shows a constant C_D of 1.01 above a V_v of about 35 feet per second. An average point spread of ± 10% was determined for this curve while a maximum spread of 18% was detected at the intermediate V_v range.

The stabilization-type guide-surface parachute (No. 17) oscillated up to 22 degrees during the drop tests, the oscillations getting smaller for an increase in V_v. The frequencies of oscillation varied from about 0.3 to 0.6 cycles per second as V_v was increased. Although several logarithmic decrements ranging from about 0.2 to 0.9 were calculated no definite trend could be detected for a V_v increase. The oscillation frequencies and damping characteristics could not be calculated at the higher V_v conditions. Figure 79 shows no tendency toward a constant drag coefficient for the range of V_v tested. Although the results of the C_D curve may seem high the test-point average spread of ± 15% is within reason and all the calculations have been checked in an effort to verify the results. A maximum point spread of 30% was determined for the intermediate V_v range.

The universal-type ribless guide-surface parachute (No. 25) oscillated between 3 and 19 degrees in no consistent manner with the V_v variation of the tests. Although this parachute exhibited very good descent and damping characteristics no values of logarithmic decrement could be determined. The limited number of calculated values of oscillation frequency showed a variation between 0.2 and 0.3 cycles per second for the two lower V_v conditions. Figure 80 shows a negligible increase in C_D for the V_v range tested. The average point spread was about ± 8% with a maximum of 10% recorded for the lower V_v values.

The personnel-type guide-surface parachute (No. 26) oscillated between 5 and 31 degrees for the tests, the angle of oscillation tending to increase for an increase in V_v. The frequencies of oscillation increase from 0.2 to 0.5 cycles per second for an increase of V_v over the range tested. The undamped oscillation curves made it impossible to calculate the logarithmic decrement values. This parachute exhibited more gliding tendencies than any other parachute tested of the guide-surface family. Delayed opening characteristics were detected for some of the horizontal releases; however, in general most of the drop tests performed satisfactorily. Figure 81 indicates a constant C_D of 0.8 above a V_v of about 34 feet per second and shows a moderate increase in C_D for a decrease in V_v at the lower descent-velocity range tested. An average point spread of $\pm$ 10% was calculated while a maximum spread of about 20% existed in the intermediate V_v range of the tests.

Exeter Type-12 Parachute

The drop-test results for the Exeter Type-12 shaped parachute (No. 24) are presented in Table 21. This parachute exhibited large glide-angle characteristics with moderate oscillation at the low V_v range; however, as V_v was increased the flight path approximated straight vertical descent and the angles of oscillation became larger with increased frequency. No inflation difficulties were encountered during the drop tests conducted with this parachute.

The average horizontal velocities ranged from approximately 8 to 3 feet per second in no consistent pattern while the average resultant velocity varied from 9 to 40 feet per second for the drop tests. The glide angles varied from about 35 to 4 degrees as V_v was increased through the tested range. The parachutes oscillated between 8 and 37 degrees, the angles increasing for an increase in V_v. The oscillation curves did not display any damping characteristics; therefore, no logarithmic decrement values were calculated. Only a few oscillation frequencies were calculated and they ranged from approximately 0.25 to 0.40 cycles per second, showing an increase in value for an increase in V_v.

Figure 82 defines a C_{D_o} of 0.80 for a V_v above 23 feet per second. There is a considerable increase in C_{D_o} for a decrease in V_v. A maximum point spread of approximately 26% was calculated near the upper limit of the V_v range while the average spread is near $\pm$ 8% for the drag curve in general.

FIST-Type Ribbon Parachutes

The drop-test results for the three FIST circular (Nos 21, 27 and 28), the square (No. 22) and the triangular (No. 23) ribbon parachutes are given in Tables 18 through 20 and Tables 24 and 25. In general, the parachutes exhibited approximately straight vertical descent with little or no oscillation. For the square and triangular parachutes moderate glide angles were detected at the lower V_v range. The ribbon parachutes appeared to have good oscillation damping characteristics, particularly the circular-type canopies. Because of the nature of the oscillation curves in exhibiting small angles of oscillation it was difficult to obtain any conclusive information concerning the frequency of oscillation and the logarithmic decrement or damping characteristics of the parachutes. The parachutes of this family tended to lob from release to the impact point for the higher-speed horizontal conditions and this made it impossible to derive any oscillation information in most cases. Observations indicated that once an oscillation was initiated with these parachutes the motion seemed to damp completely in about one-half of a cycle in most instances. Generally these parachutes had characteristics of slow inflation in the normal operating range, and some tendencies to squid at the high V_v range were noted. Because of the lower suspended-load requirements for these parachutes it was possible to conduct 24 tests on each, of which 8 different test conditions were completely analyzed.

The average horizontal velocities ranged from 0 to 4 feet per second with apparently no consistent pattern in most cases. For the vertical release condition the average horizontal velocity seemed to decrease for the square parachute and increase for the triangular parachute as V_v was increased over the tested range. The average resultant velocities varied between approximately 9 and 52 feet per second while the average glide angles ranged from 1 to 10 degrees for the circular designs and 2 to 20 degrees for the square and triangular canopies. The parachutes on occasion oscillated as high as 20 degrees but in general the angles of oscillation were small, particularly for the circular-type parachutes.

The summary drag-coefficent curves of Figure 83 indicate that the triangular and square parachutes have a higher drag than the circular designs at the low V_v range; however, taking into account the porosity

values, it seems that no significant differences in drag characteristics exist for all these ribbon parachutes over the range of V_v tested. There is an increase in C_{D_o} for a decrease in V_v over the range tested and a tendency for C_{D_o} to become constant above a V_v of approximately 30 feet per second in most cases. The average spread of the test data varies from $\pm$ 5% to $\pm$ 15% for the five ribbon parachutes tested.

The circular brake-type FIST ribbon parachute (No. 21) usually oscillated between 0 and 5 degrees except at the lowest V_v conditions where a maximum angle of oscillation of about 14 degrees was recorded. No values of oscillation frequency and logarithmic decrement were obtained. Figure 84 shows a constant C_{D_o} of 0.44 above a descent velocity of about 35 feet per second, but in general there is a substantial increase in C_{D_o} for a decrease in V_v over the tested range. An average point spread of $\pm$ 15% was calculated, with most of the spread at the high V_v range. One test point was recorded for a V_v of about 59 feet per second and, although it seemed out of line on the drag curve, the drop-test notes and corresponding data substantiated its accuracy.

The square ribbon parachute (No. 22) oscillated between 5 and 16 degrees showing no particular trend for the V_v range tested. No values of oscillation frequency and logarithmic decrement were obtained. The parachute exhibited moderate glide angles at the low V_v range, particularly for the horizontal conditions of release. Figure 85 gives a constant C_{D_o} of 0.45 above a V_v of 36 feet per second but displays a decided increase in C_{D_o} for a decrease in descent velocity over most of the tested range. The average point spread amounts to about $\pm$ 15%, with a maximum spread of approximately 27% occurring at both ends of the V_v range tested. The square ribbon parachute had slow inflation characteristics, but once fully opened appeared stable and consistent. This inflation difficulty may have been the reason for the large point spread of the drag data.

The triangular ribbon parachute (No. 23) oscillated between 4 and 12 degrees, but showed a definite tendency toward undamped oscillations at approximately 10 degrees for all conditions of horizontal release investigated and for the low V_v range of the vertical release condition. A conical type of oscillation was detected for the

low V_v condition for both types of release. From these comparatively large oscillation curves it was possible to determine oscillation frequencies ranging between 0.2 and 0.3 cycles per second for the first three V_v conditions of the test program. A logarithmic decrement of 0.66 was calculated for the low V_v range of the vertical release condition. In several cases it was impractical to determine an angle of oscillation from the recorded data. For the horizontal release condition there was a tendency for the glids angle to decrease for an increase in V_v for the range tested. Figure 86 shows a constant C_{D_o} of 0.4 above a descent velocity of 46 feet per second. The high-speed drops with the horizontal release condition, being erratic in nature, show considerable spread on the drag-coefficient curve. Neglecting this data an average point spread of $\pm$ 10% exists on Figure 86 while a maximum spread of 25% exists near the upper V_v range. This point spread of the drag-coefficient curve may be due to the erratic descent characteristics of the triangular paracute which had a tendency to squid at the high V_v range and whose tips were reluctant to inflate at the low V_v range.

In general the circular FIST ribbon parachute with a total porosity of 20% (No.27) oscillated up to 13 degrees for the horizontal release condition and 5 degrees for the vertical release condition. No values of oscillation frequency and logarithmic decrement could be determined from the oscillation curves. A trend toward decrease in glide angle for an increase in V_v was detected. Figure 87 gives a constant C_{D_o} of 0.48 above a V_v of 40 feet per second and shows a moderate increase in drag coefficient for a decrease in descent velocity over the range tested. The average point spread is about $\pm$ 5%, with a maximum of 12% existing for the higher V_v condition, where delayed inflation was noticed several times.

The circular FIST ribbon parachute with a total porosity of 25% (No. 28) descended along an approximately straight vertical path and oscillated up to 7 degrees in most cases. Larger oscillation angles near 16 degrees were detected with a few of the horizontal-release drop tests. An oscillation frequency of about 0.3 cycles per second and a logarithmic decrement of 0.7 were determined for the low-speed drop with the horizontal release condition. Figure 88 indicates a constant C_{D_o} of 0.47 above a V_v of 40 feet per second and shows an increase in drag coefficent for a decrease in descent velocity over the lower V_v range. Having a maximum point spread of only 7% indicates thatthis parachute had excellent descent characteristics.

Ring-Slot Parachutes

The drop-test results for three circular ring-slot parachutes, with 10% total porosity (No. 29), with 13.5% total porosity (No. 30), and with 17% total porosity (No. 31), are presented in Tables 26, 27 and 28 respectively. These parachutes descended with small or moderate glide angles, which decreased for an increase of V_v and also tended to oscillate in an undamped manner in most cases. As the parachute porosity was increased there seemed to be a decrease in the magnitude of the oscillation. The limited calculations of oscillation frequency ranged from approximately 0.1 to 0.5 cycles per second for an increase of V_v over the range tested. Very little information was obtained on the logarithmic decrement of the parachutes from the drop tests. The pattern of the oscillation curves for the high V_v condition of the horizontal type of release was such that no conclusive oscillation information could be tabulated. In general each of the three parachutes tested had its own peculiar descent characteristics; however, no special trend was detected from the drop tests conducted.

The average horizontal velocities showed inconsistent variations up to 4 feet per second for the measured average resultant-velocity range from 11 to 49 feet per second. The average glide angles varied from 25 degrees to straight vertical descent, decreasing both for an increase in V_v and an increase in parachute porosity for the range tested.

The summary drag coefficient curves of Figure 89 show a consistent effect of C_{D_o} decrease for an increase in parachute porosity; however, they indicate no constant C_{D_o} value for any of the curves over the range of V_v tested. There seems to be a decided C_{D_o} increase for a V_v decrease for the entire drag-coefficent curves of the three parachute tested.

In general, the ring-slot parachute with a total porosity of 10% (No. 29) oscillated between 4 and 30 degrees in a two-dimensional manner. Although unstable and undamped oscillations prevailed for most of the drops a few oscillation frequencies and logarithmic decrements were determined. Frequencies of oscillation ranging from about 0.2 to 0.3 cycles per second and logarithmic decrements

of from 0.3 to 0.4 were calculated. The average horizontal velocity seems to remain constant around 4 feet per second for most of the drops, while the glide angle decreases from 25 to 5 degrees as V_v is increased over the tested range. The average point spread of the drag coefficient curve of Figure 90 is approximately $\pm$ 5%, while a maximum of 17% was calculated for the high V_v range.

The ring-slot parachute with a total porosity of 13.5% (No. 30) oscillated up to 25 degrees during the tests. For the horizontal release conditions the angle of oscillation tended to decrease for an increase in V_v over the range tested. At low V_v conditions the oscillations were usually unstable while at the high V_v conditions the parachute descent characteristics became unpredictable. The glide angle varied from 19 degrees to zero for straight vertical descent, in general, decreasing in value for an increase in V_v. The frequency of oscillation varied from 0.1 to 0.5 cycles per second, increasing for a V_v increase over the tested range while no logarithmic decrements were calculated. The average point spread of the drag-coefficient curve of Figure 91 is about $\pm$ 8% with a maximum of 13% being measured at the high V_v condition.

The ring-slot parachute with a total porosity of 17% (No. 31) oscillated in an undamped manner between 4 and 16 degrees during the tests. The oscillations seem to be slightly higher for the horizontal release conditions. Late opening and collapsing of the bottom ring seem to be a characteristic of the parachute at the high V_v condition. Frequencies of oscillation averaged about 0.23 cycles per second but no logarithmic decrements were determined for this parachute. The glide angles varied from a maximum of 15 degrees, decreasing as V_v was increased for the range tested. Small average horizontal velocities ranging between 1 and 3 feet per second were experienced by this parachute during the tests. The average point spread of the drag coefficient curve of Figure 92 is about $\pm$ 5%, with a maximum of 9% being detected at the low V_v range.

CONCLUSIONS AND RECOMMENDATIONS

Early in this program it became apparent that the amount of data which was to be collected would have to be organized so that a person interested in just the general operational characteristics of all parachutes as well as one interested in the particular behavior of one type could readily find the information he wanted. For this reason the report was prepared in seven volumes, the summary volume providing a complete but brief story of the entire project, and the other six volumes showing the detailed information for each parachute. It is important to note that the data sheets containing the drop-test space coordinates for each parachute were obtained by the use of the analyzer and are already in a form which can be used directly for further evaluation. Many of the statements made in the summary volume concerning the indicated trends of any particular parachute or family of parachutes were obtained from the curves furnished in the appendices and can therefore be readily checked. Constant reference to the six detailed volumes is recommended for clarification of those items which have been determined for the first time in this report.

The relatively wide spread of drag-coefficient data obtained from these carefully controlled drop tests is consistent with what has been obtained in the past and is an indication of the necessity for trying to find a more representative term with which to define parachute drag. Descent characteristics obtained by the system employed in this program are of sufficiently high accuracy to provide an ideal means for this further investigation. By careful analysis of these data it may be possible to define some "effective inflated area" or other criterion which would provide a constant coefficient for any one type of parachute. It is also recommended that the data in this report be compared with other existing and future data to see if similar parachutes exhibit the same trends. Quantitative drag-coefficient and stability values could also be investigated to eradicate any possible effects due to model size.

Much of the drag data collected indicated a change of drag coefficient with velocity in the low velocity or usable range. This tends to increase the difficulty of predicting full-scale parachute performance from model data. It is therefore recommended that further controlled drop tests be considered using full-scale parachutes, dropped in the vertical-release condition so that terminal velocity could be assured in a relatively short dropping distance. This could be done on relatively few parachute types, establishing a correlation which could then be applied to the others.

From these tests it appears that parachutes of a particular family or design seemed to indicate specific tendencies such as gliding or oscillating rates which did not vary substantially when the parachute shape was changed. It is recommended that a careful study be made of these tendencies in an effort to determine the exact aerodynamic forces responsible for this action. Engineering evaluations of why a parachute behaves as it does,

combined with the wealth of empirical data constantly being gathered would aid the parachute designer considerably in attempting to provide a newparachute design with predetermined flight characteristics.

The determination of instantaneous angle of attack of the parachute system has been handled in this report for one parachute to indicate how this value can be obtained from the available data. Whether this newly obtained information will help solve some of the parachute problems cannot be fully determined until this angle of attack is evaluated for several more parachute drops and the results carefully studied. It is therefore recommended that the method established in this report be applied to several of the other types of parachutes tested in this program. All required information is available and need only be treated by the suggested procedure. It is further recommended that all the data provided by these drop tests be carefully examined to see if any other combination of this information can lead to further knowledge of the parachutes. As an example, such characteristics as opening rate, canopy rotations or even the effect of shroud-line stretch at high loads might be available.

Aerodynamic data on parachutes have been collected from wind-tunnel and drop tests but very few actual measurements of the apparent mass of the parachute system have ever been made. Techniques for determining apparent mass in a wind tunnel have not been developed because of the relatively small part this term plays in the stability of aircraft and because of the difficulty which would be involved in trying to obtain an accurate system of measurement. In the case of the parachute, however, the apparent-mass term is essential to the theoretical evaluation of parachute stability because the mass of air accelerated by the parachute canopy is of the order of magnitude of the mass of the parachute system itself. At present, estimates of apparent mass are the only values which the theoretical aerodynamicist can use for his stability equations. Yet, apparent mass of a parachute system might be very easily determined by employing the controlled drop-test method used on this project. It is recommended that a study be made of the possibility of conducting drop tests on basic parachute types with this in mind. Such methods as releasing a known portion of the parachute load after terminal velocity is once reached and measuring the momentary change in parachute flight characteristics could be one of the methods employed. More knowledge of the theoretical basis of parachute aerodynamics would assure a better understanding of the operating difficulties of parachute systems.

It is apparent from a study of this report that through the joint efforts of the Equipment Laboratory Parachute Branch at Wright-Patterson Air Force Base and the Goodyear Aircraft Corporation Research and Development Department a controlled drop-test system of high accuracy has been devised which is both economical and efficient to operate. It is also evident that the data collected in this program together with the experience of the

Air Force with full-scale parachutes would make possible the determination of the basic flight characteristics which are required of any good parachute. It is recommended that such standards and trends be established and that all new parachute designs which are to be given further consideration be first made to fulfill these requirements by actual drop-test evaluation under controlled conditions. This would provide an inexpensive and efficient means of screening new parachute designs or applications before permitting expenditures for advanced development or actual use.

REFERENCES

1. Knacke, Theodor W.: Comparison Tests of Various Types Parachute Models AMC Memorandum Report No. MCREXE-672-12B, GS-USAF-Wright-Patterson #175, 12 January 1949.

2. USAF Parachute Handbook, AMC, Wright-Patterson Air Force Base, Engineering Division, Equipment Laboratory, December 1947.

3. Sharp, H. Oakley: Photogrammetry. John Wiley and Sons, 1943, Pages 20-21.

4. Knacke, Theodor W.: Design, Use and Construction of FIST-Type Parachute. AMC Memorandum Report No. MCREXE-672-19LL, GS-USAF-Wright-Patterson #139, 30 June 1948.

5. Burington, R. S. & and Torrance, C. C. Higher Mathematics. McGraw-Hill Book Company, Incorporated, New York, 1939, Page 685.

TABLE 1 - Geometric Characteristics of Model Parachutes Tested*

1

Parachute Number	Design of Parachute	Parachute Shape	Parachute Cross Section	Total Surface Area S_o (Sq. In.)	Vent Area[4] (Sq. In.)	Nominal Diameter[5] D_o (In.)	Construction Diameter[6] (In.)	Constructed Skirt Dimension[7] (In.)	N... A...
1	Solid Flat	○	—	15,625[1]	160	141.00	144.6	28.20	
2	Solid Flat	□	—	16,000	145	142.68	120.6	30.15	
3	Solid Flat	△	—	16,000	145	142.68	183.3	36.67	
4	Solid Extended Skirt, 10%	○	⟍⟋	16,000	160	142.68	123.8	19.20	
5	Solid Extended Skirt, 12½%	○	⟍⟋	16,000	160	142.68	120.2	17.50	
6	Solid Extended Skirt, Full	○	⟍⟋	16,000	160	142.68	116.1	20.31	
7	Airfoil, 50% Vent	◎	( )	16,000	-	142.68	147.8	29.00	
8	Solid Spherical, ½ Sphere	○	½	16,000	160	142.68	102.2	19.95	
9	Solid Spherical, ¼ Sphere	○	¼	16,000	160	142.68	133.4	23.90	
10	Solid Spherical, ¼ Sphere	□	¼	16,000	160	142.68	116.2	29.05	
11	Solid Spherical, ¼ Sphere	△	¼	16,000	160	142.68	176.9	35.38	
12	Solid Conical, 30° Angle	○	30°	16,000	186	142.68	134.2	26.20	
13	Solid Conical, 30° Angle	□	30°	16,000	185	142.68	117.7	29.42	
14	Solid Conical, 30° Angle	△	30°	16,000	160	142.68	179.0	35.80	
16	Guide Surface, Med. Brake	○	⌒	16,290[1]	80	143.99	98.0	20.00	
17	Guide Surface, Stabilization	○	⌒	17,550	59	149.43	82.0	15.45	
21	FIST Ribbon, Brake	○	.....	16,000	160	142.68	145.0	28.21	
22	Square Ribbon	□	.....	16,000	0	142.68	126.5	31.62	
23	Triangular Ribbon	△	.....	16,000	0	142.68	192.25	38.45	
24	Shaped, Exeter Type 12	○	⌒	16,000	160	142.68	97.1	21.40	
25	Guide Surface, Univ'l Ribless	⬡	⌒	16,000	110	142.68	99.04	21.60	
26	Guide Surface, Personnel	◎	⌒	16,000	25	142.68	134.32	15.14	
27	FIST Ribbon	○	.....	15,730[1]	126	141.48	144.6	28.21	
28	FIST Ribbon	○	.....	15,570[1]	160	140.76	144.6	28.21	
29	Ring Slot, 4 Slots	○	---	15,550[1]	116	140.66	145.6	28.20	
30	Ring Slot, 4 Slots	○	---	15,760[1]	116	141.61	145.6	28.20	
31	Ring Slot, 4 Slots	○	---	15,760[1]	116	141.61	145.6	28.20	

* Definition of Superscripts on next page

Vent Area[4] q. In.)	Nominal Diameter[5] D_o (In.)	Construction Diameter[6] (In.)	Constructed Skirt Dimension[7] (In.)	Number of Shroud Lines[2] And Gores	Average Porosity Of Canopy[8] ($Ft^3/Ft^2/Min.$)	Average Bulk of Complete Parachute (Cu. In.)	Average Bulk of Parachute Canopy (Cu. In.)	Weight of Complete Parachute (Lbs)
160	141.00	144.6	28.20	16	98	154	140	1.90
145	142.68	120.6	30.15	16	93	134	121	1.52
145	142.68	183.3	36.67	15	102	135	121	1.67
160	142.68	123.8	19.20	16	91	159	142	1.94
160	142.68	120.2	17.50	16	108	141	125	1.96
160	142.68	116.1	20.31	16	105	148	134	1.90
-	142.68	147.8	29.00	16	95	167	150	1.96
160	142.68	102.2	19.95	16	111	156	142	1.91
160	142.68	133.4	23.90	16	103	152	136	1.90
160	142.68	116.2	29.05	16	104	127	118	1.56
160	142.68	176.9	35.38	15	108	137	126	1.55
186	142.68	134.2	26.20	16	105	147	129	1.96
185	142.68	117.7	29.42	16	92	126	111	1.58
160	142.68	179.0	35.80	15	98	132	119	1.56
80	143.99	98.0	20.00	12	103	153	136	1.79
59	149.43	82.0	15.45	10	101	159	142	1.75
160	142.68	145.0	28.21	16	26%	227	210	2.34
0	142.68	126.5	31.62	16	15%	223	211	2.32
0	142.68	192.25	38.45	15	15%	225	204	2.38
160	142.68	97.1	21.40	16	107	149	137	1.78
110	142.68	99.04	21.60	10	154	127	121	1.39
25	142.68	134.32	15.14	24	157	149	136	1.62
126	141.48	144.6	28.21	16	20%	240	227	2.38
160	140.76	144.6	28.21	16	25%	229	215	2.30
116	140.66	145.6	28.20	16	10% (130)	201	184	2.41
116	141.61	145.6	28.20	16	13.5% (121)	206	192	2.42
116	141.61	145.6	28.20	16	17% (118)	202	190	2.40

2

DEFINITIONS OF SUPERSCRIPTS FOR TABLE 1

1. Radial seams are slightly smaller than design dimensions necessitating a surface area correction.

2. All models had free shroud line lengths of 144 inches except as noted.

   No. 2 - Length of shroud lines to corner pockets was 134 inches.

   No. 3 - Length of shroud lines to corner pockets was 132 inches.

   No. 4 - Length of shroud lines was 200 inches for special testing purposes.

3. The porosity of the parachutes of solid fabric design is given in cu. ft./sq. ft./min. measured at $\frac{1}{2}$ inch water pressure. The total porosity of the ribbon type parachutes is given in percent and includes the geometric and ribbon porosity of the canopy. The ribbon porosity of the ring-slot parachutes is included in perentheses in terms of cu. ft./sq. ft./min. at $\frac{1}{2}$ inch water pressure.

4. Vent areas are approximately one percent of the design canopy or roof panel cloth area for most parachutes.

5. $D_o = 1.128 \sqrt{S_o}$

6. Construction diameter designates the size of the parachute based upon design dimensions: Canopy diameter for flat type parachutes, form diameter for formed type parachutes. For square and triangular type parachutes this represents the dimensions of a side of the canopy.

7. Constructed skirt dimension represents the distance between shroud lines at the canopy skirt except for the personnel guide surface parachute where the measurements are made at the base of the roof panel.

TABLE 2 - Aerodynamic Characteristics as Determined from Model Drop Tests.
Solid-Flat Circular Parachute (No. 1)

1

Drop No.	Type of Release	Ambient Air Temp. (° F)	Air Relative Humidity (%)	Barometric Pressure (In. of Hg)	Mass Density of Air ρ (Slugs/cu ft)	Total Weight W (Lbs)	Vertical Terminal Velocity V_v (Ft/Sec)	Average Horizontal Velocity V_h (Ft/Sec)	Average Resultant Velocity V_r (Ft/Sec)	Avera Glid Angl ϕ (Degr
1	V	76	56	29.00	0.00223	20.4	10.4	7.8	13.0	36.
2	V	76	56	29.00	0.00223	20.4	11.1			
3	V	76	56	29.00	0.00223	20.4	10.8			
4	V	76	56	29.00	0.00223	35.4	16.8	9.4	19.3	24.
5	V	76	56	29.00	0.00223	35.4	16.2			
6	V	76	56	29.00	0.00223	35.4	17.7			
7	V	76	56	29.00	0.00223	80.4	25.4			
8	V	76	56	29.00	0.00223	80.4	26.8	5.3	27.3	11.
9	V	76	56	29.00	0.00223	80.4	25.5			
10	V	47	70	28.78	0.00234	202.0	39.8			
11	V	52	75	29.08	0.00234	205.0	41.1	3.7	41.2	5.
12	V	52	75	29.08	0.00234	205.0	40.6			
13	H	70	57	29.00	0.00226	20.4	12.1			
14	H	70	57	29.00	0.00226	20.4	11.7			
15	H	70	57	29.00	0.00226	20.4	11.2	8.7	14.2	37.
16	H	70	57	29.00	0.00226	35.4	15.2	9.2	17.8	35.
17	H	70	57	29.00	0.00226	35.4	14.8			
18	H	70	57	29.00	0.00226	35.4	15.3			
19	H	70	57	29.00	0.00226	80.4	26.8			
20	H	70	57	29.00	0.00226	80.4	27.2	3.6	27.4	5.
21	H	70	57	29.00	0.00226	80.4	25.3			
22	H	50	75	28.29	0.00229	179.0	38.5	4.0	38.7	6
23	H	50	75	28.29	0.00229	179.0	54.2			
24	H									

p Tests.

2

sal nal ity ec)	Average Horizontal Velocity V_h (Ft/Sec)	Average Resultant Velocity V_r (Ft/Sec)	Average Glide Angle ϕ (Degrees)	C_D or	C_D e	Frequency of Oscillation (f) (Cycles/Sec)	Maximum Angle of Oscillation (Degrees)	Average or Constant Angle of Oscillation (Degrees)	Logarithmic Decrement
4	7.8	13.0	36.1	0.805	1.558	0.222	22	12	-
1					1.368				
8					1.445				
8	9.4	19.3	24.8	0.713	1.036	0.267	40	30	-
2					1.115				
7					0.934				
4					1.029				
8	5.3	27.3	11.0	0.875	0.925	0.333	37	30	-
.5					1.022				
.8					1.003				
.1	3.7	41.2	5.5	0.946	0.957	0.40	33	30	-
.6					0.979				
.1					1.136				
.7					1.215				
.2	8.7	14.2	37.6	0.654	1.326	0.267	23	20	-
.2	9.2	17.8	35.8	0.739	1.249	0.267	27	15	-
.8					1.318				
.3					1.233				
.8					0.913				
.2	3.6	27.4	5.0	0.870	0.886	0.364	36	25	-
.3					1.025				
.5	4.0	38.7	6.2	0.958	0.974	0.40	35	25	-
.2					0.492				

TABLE 3 - Aerodynamic Characteristics as Determined from Model Drop Tests.
Solid-Flat-Square Pocketed Parachute (No. 2)

Drop No.	Type of Release	Ambient Air Temp. (° F)	Air Relative Humidity (%)	Barometric Pressure (In. of Hg)	Mass Density of Air ρ (Slugs/cu ft)	Total Weight W (Lbs)	Vertical Terminal Velocity V_v (Ft/Sec)	Average Horizontal Velocity V_h (Ft/Sec)
25	V	66	59	29.11	0.00228	15.0	9.9	7.0
26	V	66	59	29.11	0.00228	15.0	9.9	
27	V	66	59	29.11	0.00228	15.0	9.7	
28	V	66	59	29.11	0.00228	30.0	16.3	7.0
29	V	66	59	29.11	0.00228	30.0	15.9	
30	V	66	59	29.11	0.00228	30.0	16.6	
31	V	66	59	29.11	0.00228	80.0	27.7	
32	V	66	59	29.11	0.00228	80.0	28.1	
33	V	66	59	29.11	0.00228	80.0	28.2	6.2
34	V	52	75	28.57	0.00230	196.6	42.5	
35	V	44	70	28.36	0.00232	200.6	46.8	
36	V	44	70	28.36	0.00232	200.6	46.4	6.7
37	H	62	62	29.11	0.00230	15.0	10.9	6.5
38	H	62	62	29.11	0.00230	15.0	10.5	
39	H	62	62	29.11	0.00230	15.0	9.2	
40	H	62	62	29.11	0.00230	25.0	12.5	
41	H	62	62	29.11	0.00230	25.0	13.9	
42	H	62	62	29.11	0.00230	25.0	12.7	8.3
43	H	62	62	28.95	0.00226	80.0	27.6	
44	H	50	73	28.68	0.00232	80.0	29.1	7.7
45	H	50	73	28.68	0.00232	80.0	28.8	
46	H	51	73	28.60	0.00231	202.6	46.4	
47	H							
48	H							

ed from Model Drop Tests.
o. 2)

ft)	Total Weight W (Lbs)	Vertical Terminal Velocity V_V (Ft/Sec)	Average Horizontal Velocity V_h (Ft/Sec)	Average Resultant Velocity V_r (Ft/Sec)	Average Glide Angle ϕ (Degrees)	C_D or	C_D e	Frequency of Oscillation (f) (Cycles/Sec)	Maximum Angle of Oscillation (Degrees)	Average or Constant Angle of Oscillation (Degrees)	Logarithmic Decrement
28	15.0	9.9	7.0	12.1	34.7	0.662	1.209	0.308	20	15	0.405
28	15.0	9.9					1.209				
28	15.0	9.7					1.259				
28	30.0	16.3	7.0	17.7	23.0	0.696	0.893	0.25	35	23	-
28	30.0	15.9					0.938				
28	30.0	16.6					0.861				
28	80.0	27.7					0.824				
28	80.0	28.1					0.800				
28	80.0	28.2	6.2	28.9	11.4	0.742	0.795	0.286	40	32	-
30	196.6	42.5					0.852				
32	200.6	46.8					0.708				
32	200.6	46.4	6.7	46.8	8.0	0.701	0.721	-	>30	25	-
30	15.0	10.9	6.5	12.7	31.1	0.623	0.988	0.286	30	23	-
30	15.0	10.5					1.063				
30	15.0	9.2					1.389				
30	25.0	12.5					1.252				
30	25.0	13.9					1.011				
30	25.0	12.7	8.3	15.2	37.0	0.676	1.212	0.286	16	13	-
26	80.0	27.6					0.837				
32	80.0	29.1	7.7	30.1	13.8	0.666	0.734	0.286	30	25	-
32	80.0	28.8					0.749				
31	202.6	46.4					0.734	-	-	-	-

2

TABLE 4 - Aerodynamic Characteristics as Determined from Model Drop Tests.
Solid-Flat-Triangular Pocketed Parachute (No. 3)

Drop No.	Type of Release	Ambient Air Temp. (° F)	Air Relative Humidity (%)	Barometric Pressure (In. of Hg)	Mass Density of Air ρ (Slugs/cu ft)	Total Weight W (Lbs)	Vertical Terminal Velocity V_v (Ft/Sec)	Average Horizontal Velocity V_h (Ft/Sec)	Average Resultant Velocity V_r (Ft/Sec)	Aver Gli Ang (De
49	V	82	68	28.68	0.00218	15.4	11.2			
50	V	74	73	28.68	0.00222	15.4	9,9			
51	V	74	73	28.68	0.00222	15.4	10.8	6,3	12.5	30
52	V	74	73	28.68	0.00222	25.4	14.5	7.1	16.1	26
53	V	74	73	28.68	0.00222	30.4	15.8			
54	V	74	73	28.68	0.00222	30.4	16.0			
55	V	74	73	28.68	0.00222	80.4	27.4			
56	V	74	73	28.68	0.00222	70.4	25.3	5.8	26.0	13
57	V	74	73	28.68	0.00222	70.4	24.4			
58	V	41	71	28.95	0.00239	201.0	40.7	2.6	40.8	3
59	V	41	71	28.95	0.00239	201.0	46.1			
60	V	41	71	28.95	0.00239	201.0	42.2			
61	H	74	73	28.68	0.00222	15.4	12.0	7.1	13.9	30
62	H	74	73	28.68	0.00222	15.4	10.6			
63	H	74	73	28.68	0.00222	15.4	10.2			
64	H	74	73	28.68	0.00222	30.4	15.9			
65	H	74	73	28.68	0.00222	30.4	15.3	7.0	16.8	2
66	H	74	73	28.68	0.00222	30.4	16.1			
67	H	72	79	28.68	0.00222	70.4	27.4	4.6	27.8	1
68	H	72	79	28.68	0.00222	70.4	27.0			
69	H	72	79	28.68	0.00222	70.4	28.6			
70	H	51	73	28.60	0.00231	203.0	45.2			
71	H									
72	H									

Drop Tests.

rtisal rminal locity V_v t/Sec)	Average Horisontal Velocity V_h (Ft/Sec)	Average Resultant Velocity V_r (Ft/Sec)	Average Glide Angle ϕ (Degrees)	C_D or	C_D e	Frequency of Oscillation (f) (Cycles/Sec)	Maximum Angle of Oscil-lation (Degrees)	Average or Constant Angle of Oscillation (Degrees)	Loga-rithmic Decrement
11.2					1.012				
9,9					1.275				
10.8	6,3	12.5	30.8	0.699	1.070	0.250	22	18	-
14.5	7.1	16.1	26.9	0.723	0.982	0.267	20	16	-
15.8					0.987				
16.0					0.965				
27.4					0.870				
25.3	5.8	26.0	13.7	0.824	0.892	0.333	33	26	-
24.4					0.958				
40.7	2.6	40.8	3.2	0.907	0.913	0.50	25	15	-
46.1					0.712				
42.2					0.850				
12.0	7.1	13.9	30.3	0.559	0.868	0.286	18	12	-
10.6					1.111				
10.2					1.199				
15.9					0.977				
15.3	7.0	16.8	25.2	0.790	1.053	0.286	19	10	-
16.1					0.952				
27.4	4.6	27.8	11.2	0.731	0.760	0.40	33	20	-
27.0					0.784				
28.6					0.698				
45.2					0.774	-	-	-	-

2

TABLE 5a - Aerodynamic Characteristics as Determined from Model Drop Tests.
Solid-Flat 10% Extended-Skirt Parachute (No. 4)
Shroud-Line Length - 16 Ft. 8 In. (L_s/D_o = 1.40)

Drop No.	Type of Release	Ambient Air Temp. (° F)	Air Relative Humidity (%)	Barometric Pressure (In. of Hg)	Mass Density of Air ρ (Slugs/cu ft)	Total Weight W (Lbs)	Vertical Terminal Velocity V_v (Ft/Sec)	Average Horizontal Velocity V_h (Ft/Sec)	A R V (F
73	V	61	54	28.92	0.00229	20.4	12.8		
74	V	61	54	28.92	0.00229	20.4	12.8		
75	V	61	54	28.92	0.00229	20.4	13.1	7.6	1
76	V	61	54	28.92	0.00229	30.4	16.4		
77	V	61	54	28.92	0.00229	30.4	16.3		
78	V	61	54	28.92	0.00229	30.4	16.2	7.0	1
79	V	61	54	28.92	0.00229	75.4	25.9		
80	V	61	54	28.92	0.00229	75.4	26.2	4.6	2
81	V	61	54	28.92	0.00229	75.4	26.2		
82	V	55	87	28.91	0.00232	200.0	42.8		
83	V	51	75	28.29	0.00229	185.0	38.9		
84	V	51	75	28.29	0.00229	185.0	39.6	4.2	3
85	H	59	60	28.92	0.00230	20.4	13.5		
86	H	59	60	28.92	0.00230	20.4	13.4	7.1	1
87	H	59	60	28.92	0.00230	20.4	13.8		
88	H	59	60	28.92	0.00230	30.4	15.3	9.1	1
89	H	59	60	28.92	0.00230	30.4	16.8		
90	H	59	60	28.92	0.00230	30.4	15.3		
91	H	59	60	28.92	0.00230	75.4	25.9	5.3	2
92	H	59	60	28.92	0.00230	75.4	27.8		
93	H	59	60	28.92	0.00230	75.4	27.0		
94	H								
95	H								
96	H								

ned from Model Drop Tests.
e (No. 4)
D_o = 1.40)

ft)	Total Weight W (Lbs)	Vertical Terminal Velocity V_v (Ft/Sec)	Average Horizontal Velocity V_h (Ft/Sec)	Average Resultant Velocity V_r (Ft/Sec)	Average Glide Angle ϕ (Degrees)	C_D or	C_D e	Frequency of Oscillation (f) (Cycles/Sec)	Maximum Angle of Oscillation (Degrees)	Average or Constant Angle of Oscillation (Degrees)	Logarithmic Decrement
9	20.4	12.8					0.979				
9	20.4	12.8					0.979				
9	20.4	13.1	7.6	15.1	29.3	0.614	0.934	0.235	42	35	Neg
9	30.4	16.4					0.889				
9	30.4	16.3					0.900				
9	30.4	16.2	7.0	17.6	23.7	0.708	0.911	0.222	33	26	Neg
9	75.4	25.9					0.885				
9	75.4	26.2	4.6	26.6	10.1	0.825	0.864	0.333	30	26	Neg
9	75.4	26.2					0.864				
2	200.0	42.8					0.848				
9	185.0	38.9					0.962				
9	185.0	39.6	4.2	39.8	6.8	0.911	0.928	0.364	26	20	-
0	20.4	13.5					0.878				
0	20.4	13.4	7.1	15.2	27.5	0.613	0.890	0.222	30	25	Neg
0	20.4	13.8					0.842				
0	30.4	15.3	9.1	17.8	29.6	0.654	1.016	0.182	27	26	-
0	30.4	16.8					0.845				
0	30.4	15.3					1.016				
0	75.4	25.9	5.3	26.4	10.8	0.832	0.880	0.333	31	30	-
0	75.4	27.8					0.763				
0	75.4	27.0					0.810				

2

TABLE 5b - Aerodynamic Characteristics as Determined from Model Drop Tests.
Solid-Flat 10% Extended-Skirt Parachute (No. 4)
Shroud-Line Length - 14 Ft. 9 Inc. (L_s/D_o = 1.24)

Drop No.	Type of Release	Ambient Air Temp. (° F)	Air Relative Humidity (%)	Barometric Pressure (In. of Hg)	Mass Density of Air ρ (Slugs/cu ft)	Total Weight W (Lbs)	Vertical Terminal Velocity V_v (Ft/Sec)	Average Horizontal Velocity V_h (Ft/Sec)	Average Resultant Velocity V_r (Ft/Sec)	A (?
97	V	63	53	28.82	0.00227	15.4	10.2	4.7	11.2	
98	V	63	53	28.82	0.00227	15.4	10.6			
99	V	63	53	28.82	0.00227	15.4	10.6			
100	V	63	53	28.82	0.00227	30.4	16.4			
101	V	63	53	28.82	0.00227	30.4	17.3			
102	V	63	53	28.82	0.00227	30.4	16.4	7.0	17.8	
103	V	63	53	28.82	0.00227	75.4	25.6			
104	V	63	53	28.82	0.00227	75.4	25.8	4.0	26.1	
105	V	63	53	28.82	0.00227	75.4	25.5			
106	V	40	65	29.08	0.00240	167.5	40.9			
107	V	40	65	29.08	0.00240	167.5	41.5			
108	V	52	75	29.08	0.00234	205.0	41.8	4.2	42.0	
109	H	58	58	28.82	0.00229	15.4	10.0			
110	H	58	58	28.82	0.00229	15.4	10.1	6.8	12.2	
111	H	58	58	28.82	0.00229	15.4	10.6			
112	H	58	58	28.82	0.00229	30.4	16.9	10.4	19.8	
113	H	58	58	28.82	0.00229	30.4	15.0			
114	H	58	58	28.82	0.00229	30.4	17.0			
115	H	58	58	28.82	0.00229	75.4	26.7			
116	H	58	58	28.82	0.00229	75.4	26.0			
117	H	58	58	28.82	0.00229	75.4	26.4	5.7	27.0	
118	H									
119	H									
120	H									

Drop Tests.

2

rtical rminal locity V_v t/Sec)	Average Horizontal Velocity V_h (Ft/Sec)	Average Resultant Velocity V_r (Ft/Sec)	Average Glide Angle ϕ (Degrees)	C_D or	C_D e	Frequency of Oscillation (f) (Cycles/Sec)	Maximum Angle of Oscil- lation (Degrees)	Average or Constant Angle of Oscillation (Degrees)	Loga- rithmic Decrement
10.2	4.7	11.2	32.1	0.825	1.172	0.222	25	18	.770
10.6					1.087				
10.6					1.087				
16.4					0.896				
17.3					0.807				
16.4	7.0	17.8	22.6	0.702	0.896	0.266	35	30	Neg
25.6					0.912				
25.8	4.0	26.1	9.6	0.865	0.898	0.333	35	30	Neg
25.5					0.920				
40.9					0.751				
41.5					0.729				
41.8	4.2	42.0	5.5	0.890	0.903	0.445	27	25	-
10.0					1.210				
10.1	6.8	12.2	33.8	0.676	1.185	0.235	14	12	-
10.6					1.077				
18.9	10.4	19.8	21.7	0.567	0.837	0.21	25	20	-
15.0					1.062				
17.0					0.827				
26.7					0.831				
26.0					0.877				
26.4	5.7	27.0	11.7	0.796	0.850	0.333	34	30	-

TABLE 5c - Aerodynamic Characteristics as Determined from Model Drop Tests.
Solid-Flat 10% Extended-Skirt Parachute (No. 4)
Shroud-Line Length - 12 Ft. 10 In. (L_s/D_o = 1.08)

Drop No.	Type of Release	Ambient Air Temp. (° F)	Air Relative Humidity (%)	Barometric Pressure (In. of Hg)	Mass Density of Air ρ (Slugs/cu ft)	Total Weight W (Lbs)	Vertical Terminal Velocity V_v (Ft/Sec)	Average Horizontal Velocity V_h (Ft/Sec)	Average Resultant Velocity V_r (Ft/Sec)
121	V	55	60	28.82	0.00231	15.4	10.3	6.9	12.4
122	V	55	60	28.82	0.00231	15.4	10.5		
123	V	55	60	28.82	0.00231	15.4	9.8		
124	V	55	60	28.82	0.00231	30.4	16.6	9.5	19.1
125	V	55	60	28.82	0.00231	30.4	15.5		
126	V	55	60	28.82	0.00231	30.4	16.5		
127	V	55	60	28.82	0.00231	75.4	25.8	4.5	26.2
128	V	55	60	28.82	0.00231	75.4	26.4		
129	V	55	60	28.82	0.00231	75.4	27.2		
130	V	44	62	29.08	0.00238	197.0	52.7	4.9	52.9
131	V	44	62	29.08	0.00238	195.0	45.0		
132	V	44	62	29.08	0.00238	192.0	41.0		
133	H	55	60	28.82	0.00231	15.4	10.6		
134	H	55	60	28.82	0.00231	15.4	10.8		
135	H	55	60	28.82	0.00231	15.4	11.4	7.2	13.5
136	H	55	60	28.82	0.00231	30.4	15.1		
137	H	55	60	28.82	0.00231	30.4	17.3	8.5	19.7
138	H	55	60	28.82	0.00231	30.4	15.2		
139	H	55	60	28.82	0.00231	75.4	26.3	10.0	28.6
140	H	55	60	28.82	0.00231	75.4	27.3		
141	H	55	60	28.82	0.00231	75.4	25.3		
142	H								
143	H								
144	H								

d from Model Drop Tests.
(No. 4)
$_{o}$ = 1.08)

t)	Total Weight W (Lbs)	Vertical Terminal Velocity V_v (Ft/Sec)	Average Horizontal Velocity V_h (Ft/Sec)	Average Resultant Velocity V_r (Ft/Sec)	Average Glide Angle ϕ (Degrees)	C_D or	C_D e	Frequency of Oscillation (f) (Cycles/Sec)	Maximum Angle of Oscillation (Degrees)	Average or Constant Angle of Oscillation (Degrees)	Logarithmic Decrement
	15.4	10.3	6.9	12.4	33.2	0.653	1.130	0.286	16	12	-
	15.4	10.5					1.088				
	15.4	9.8					1.249				
	30.4	16.6	9.5	19.1	24.9	0.589	0.860	0.267	23	18	-
	30.4	15.5					0.986				
	30.4	16.5					0.870				
	75.4	25.8	4.5	26.2	7.6	0.848	0.883	0.364	34	25	-
	75.4	26.4					0.843				
	75.4	27.2					0.794				
	197.0	52.7	4.9	52.9	3.3	0.532	0.536	0.50	30	-	-
	195.0	45.0					0.728				
	192.0	41.0					0.863				
l	15.4	10.6					1.067				
l	15.4	10.8					1.028				
l	15.4	11.4	7.2	13.5	30.3	0.568	0.923	0.286	18	15	-
l	30.4	15.1					1.038				
l	30.4	17.3	8.5	19.7	27.0	0.547	0.748	0.296	40	30	-
l	30.4	15.2					1.023				
l	75.4	26.3	10.0	28.6	20.3	0.673	0.818	0.40	30	20	-
l	75.4	27.3					0.788				
l	75.4	25.9					0.876				

2

TABLE 5d - Aerodynamic Characteristics as Determined from Model Drop Tests.

Solid-Flat 10% Extended-Skirt Parachute (No. 4)
Shroud-Line Length - 10 Ft. 11 In. (L_s/D_o = 0.92)

Drop No.	Type of Release	Ambient Air Temp. (° F)	Air Relative Humidity (%)	Barometric Pressure (In. of Hg)	Mass Density of Air ρ (Slugs/cu ft)	Total Weight W (Lbs)	Vertical Terminal Velocity V_v (Ft/Sec)	Average Horisontal Velocity V_h (Ft/Sec)	Average Resultant Velocity V_r (Ft/Sec)	Ave Gl An (De
145	V	55	54	28.82	0.00231	15.4	10.7	6.0	12.3	2
146	V	55	54	28.82	0.00231	15.4	10.7			
147	V	55	54	28.82	0.00231	15.4	10.3			
148	V	55	54	28.82	0.00231	30.4	16.1			
149	V	55	54	28.82	0.0023[illegible]	30.4	16.5	5.2	17.3	2
150	V	55	54	28.82	0.00231	30.4	17.0			
151	V	63	54	28.87	0.00228	75.4	27.1			
152	V	63	54	28.87	0.00228	75.4	25.7			
153	V	63	54	28.87	0.00228	75.4	27.0	8.7	28.4	1
154	V	46	71	28.57	0.00232	202.0	41.5	4.6	41.7	
155	V	46	71	28.57	0.00232	202.0	43.4			
156	V	52	80	28.42	0.00238	197.0	41.9			
157	H	63	54	28.87	0.00228	15.4	10.2	7.3	12.5	1
158	H	63	54	28.87	0.00228	15.4	11.9			
159	H	63	54	28.87	0.00228	15.4	10.9			
160	H	63	54	28.87	0.00228	30.4	16.3			
161	H	63	54	28.87	0.00228	30.4	16.2			
162	H	63	54	28.87	0.00228	30.4	15.9	7.0	17.4	
163	H	63	54	28.87	0.00228	75.4	26.3	8.1	27.5	
164	H	63	54	28.87	0.00228	75.4	28.7			
165	H	63	54	28.87	0.00228	75.4	27.9			
166	H									
167	H									
168	H									

2

tical minal ocity V_v /Sec)	Average Horizontal Velocity V_h (Ft/Sec)	Average Resultant Velocity V_r (Ft/Sec)	Average Glide Angle ϕ (Degrees)	C_D or	C_D e	Frequency of Oscillation (f) (Cycles/Sec)	Maximum Angle of Oscil-lation (Degrees)	Average or Constant Angle of Oscillation (Degrees)	Loga-rithmic Decrement
.0.7	6.0	12.3	29.8	0.688	1.048	0.286	25	25	.693
.0.7					1.048				
10.3					1.130				
16.1					0.915				
16.5	5.2	17.3	20.9	0.740	0.870	0.286	31	22	-
17.0					0.820				
27.1					0.810				
25.7					0.902				
27.0	8.7	28.4	18.0	0.701	0.817	0.40	33	27	-
41.5	4.6	41.7	6.0	0.895	0.908	0.445	31	27	-
43.4					0.832				
41.9					0.850				
10.2	7.3	12.5	33.5	0.648	1.168	-	13	7	-
11.9					0.858				
10.9					1.022				
16.3					0.905				
16.2					0.915				
15.9	7.0	17.4	24.1	0.723	0.950	-	30	25	-
26.3	8.1	27.5	16.5	0.755	0.860	-	35	30	-
23.7					0.723				
27.9					0.765				

TABLE 5e - Aerodynamic Characteristics as Determined from Model Drop Tests.

Solid-Flat 10% Extended-Skirt Parachute (No. 4)
Shroud-Line Length-3 Ft. 1 In (L_s/D_o = 0.76)

Drop No.	Type of Release	Ambient Air Temp. (° F)	Air Relative Humidity (%)	Barometric Pressure (In. of Hg)	Mass Density of Air ρ (Slugs/cu ft)	Total Weight W (Lbs)	Vertical Terminal Velocity V_v (Ft/Sec)	Average Horizontal Velocity V_h (Ft/Sec)	Average Resultant Velocity V_r (Ft/Sec)
169	V	59	57	28.87	0.00230	15.4	10.9		
170	V	59	57	28.87	0.00230	15.4	11.6	6.5	13.3
171	V	59	57	28.87	0.00230	15.4	12.2		
172	V	59	57	28.87	0.00230	30.4	17.5	6.2	18.6
173	V	59	57	28.87	0.00230	30.4	16.0		
174	V	59	57	28.87	0.00230	30.4	17.8		
175	V	59	57	28.87	0.00230	75.4	23.5	3.0	28.7
176	V	59	57	28.87	0.00230	75.4	27.2		
177	V	59	57	28.87	0.00230	75.4	28.8		
178	V	52	80	28.42	0.00238	202.0	45.3	9.8	46.3
179	V	52	80	28.42	0.00238	203.0	46.2		
180	V	52	80	28.42	0.00238	201.0	43.5		
181	H	59	57	28.87	0.00230	15.4	12.2	5.7	13.5
182	H	59	57	28.87	0.00230	15.4	11.1		
183	H	59	57	28.87	0.00230	15.4	11.3		
184	H	59	57	28.87	0.00230	30.4	16.8	6.8	18.1
185	H	59	57	28.87	0.00230	30.4	17.1		
186	H	59	57	28.87	0.00230	30.4	16.8		
187	H	44	58	29.06	0.00237	75.4	27.8	6.5	28.6
188	H	44	58	29.06	0.00237	75.4	28.3		
189	H	44	58	29.06	0.00237	75.4	28.1		
190	H								
191	H								
192	H								

d from Model Drop Tests.

(No. 4)
.76)

t)	Total Weight W (Lbs)	Vertical Terminal Velocity V_v (Ft/Sec)	Average Horizontal Velocity V_h (Ft/Sec)	Average Resultant Velocity V_r (Ft/Sec)	Average Glide Angle ϕ (Degrees)	C_D or	C_D o	Frequency of Oscillation (f) (Cycles/Sec)	Maximum Angle of Oscillation (Degrees)	Average or Constant Angle of Oscillation (Degrees)	Logarithmic Decrement
	15.4	10.9					1.013	0.286	24	10	-
	15.4	11.6	6.5	13.3	31.0	0.585	0.895				
	15.4	12.2					0.810				
	30.4	17.5	6.2	18.6	19.2	0.649	0.777	0.308	38	28	.642
	30.4	16.0					0.930				
	30.4	17.8					0.751				
	75.4	23.5	3.0	28.7	8.0	0.710	0.727	0.333	35	25	-
	75.4	27.2					0.797				
	75.4	28.8					0.711				
	202.0	45.3	9.8	46.3	9.6	0.702	0.744	-	25	20	-
	203.0	46.2					0.718				
	201.0	43.5					0.831				
	15.4	12.2	5.7	13.5	26.4	0.592	0.810	-	30	-	-
	15.4	11.1					0.979				
	15.4	11.3					0.945				
)	30.4	16.8	6.8	18.1	21.9	0.675	0.844	-	30	25	-
	30.4	17.1					0.813				
)	30.4	16.8					0.844				
'	75.4	27.8	6.5	28.6	12.4	0.710	0.768	0.40	50	40	-
'	75.4	28.3					0.742				
'	75.4	28.1					0.753				

TABLE 5f - Aerodynamic Characteristics as Determined from Model Drop Tests.
Solid-Flat 10% Extended-Skirt Parachute (No. 4)
Shroud-Line Length - 7 Ft. 2 In. (L_s/D_o = 0.60)

Drop No.	Type of Release	Ambient Air Temp. (° F)	Air Relative Humidity (%)	Barometric Pressure (In. of Hg)	Mass Density of Air ρ (Slugs/cu ft)	Total Weight W (Lbs)	Vertical Terminal Velocity V_v (Ft/Sec)	Average Horizontal Velocity V_h (Ft/Sec)	Average Resultant Velocity V_r (Ft/Sec)	Av G A (D
193	V	54	59	28.87	0.00232	15.4	11.9	6.7	13.7	2
194	V	54	59	28.87	0.00232	15.4	11.5			
195	V	54	59	28.87	0.00232	15.4	11.8			
196	V	54	59	28.87	0.00232	30.4	17.5			
197	V	66	59	29.11	0.00228	30.4	17.7	8.5	19.6	2
198	V	66	59	29.11	0.00228	30.4	18.2			
199	V	54	59	28.87	0.00232	75.4	29.2	7.4	30.1	1
200	V	69	57	28.95	0.00226	75.4	29.4			
201	V	52	81	28.14	0.00227	75.4	29.2			
202	V	50	75	28.29	0.00229	182.0	45.2	8.8	46.0	1
203	V	50	75	28.29	0.00229	182.0	44.6			
204	V	50	75	28.29	0.00229	182.0	48.0			
205	H	69	57	28.95	0.00226	15.4	12.1	6.0	13.5	
206	H	69	57	28.95	0.00226	15.4	11.6			
207	H	69	57	28.95	0.00226	15.4	12.1			
208	H	69	57	28.95	0.00226	30.4	17.1			
209	H	69	57	28.95	0.00226	30.4	17.3	7.8	19.0	
210	H	69	57	28.95	0.00226	30.4	18.2			
211	H	69	57	28.95	0.00226	75.4	32.1	5.4	32.6	
212	H	69	57	28.95	0.00226	75.4	31.9			
213	H	69	57	28.95	0.00226	75.4	33.6			
214	H									
215	H									
216	H									

Drop Tests.

2

rtical rminal locity V_v t/Sec)	Average Horizontal Velocity V_h (Ft/Sec)	Average Resultant Velocity V_r (Ft/Sec)	Average Glide Angle ϕ (Degrees)	C_D or	C_D e	Frequency of Oscillation (f) (Cycles/Sec)	Maximum Angle of Oscillation (Degrees)	Average or Constant Angle of Oscillation (Degrees)	Logarithmic Decrement
11.9	6.7	13.7	28.1	0.562	0.845	0.20	23	20	-
11.5					0.903				
11.8					0.858				
17.5					0.770				
17.7	8.5	19.6	25.4	0.564	0.766	-	18	10	-
18.2					0.725				
29.2	7.4	30.1	13.9	0.627	0.686	0.333	28	25	-
29.4					0.694				
29.2					0.701				
45.2	8.8	46.0	11.6	0.663	0.700	-	17	-	-
44.6					0.719				
48.0					0.621				
12.1	6.0	13.5	26.7	0.601	0.838	-	20	15	-
11.6					0.910				
12.1					0.838				
17.1					0.828				
17.3	7.8	19.0	24.4	0.611	0.809	-	.5	-	-
18.2					0.731				
32.1	5.4	32.6	9.5	0.556	0.582	0.333	45	35	-
31.9					0.590				
33.6					0.532				

TABLE 6 -- Aerodynamic Characteristics as Determined from Model Drop Tests.
Solid-Flat 12½% Extended-Skirt Parachute (No. 5)

Drop No.	Type of Release	Ambient Air Temp. (° F)	Air Relative Humidity (%)	Barometric Pressure (In. of Hg)	Mass Density of Air ρ (Slugs/cu ft)	Total Weight W (Lbs)	Vertical Terminal Velocity V_v (Ft/Sec)	Average Horizontal Velocity V_h (Ft/Sec)	Average Resultant Velocity V_r (Ft/Sec)	A
217	V	79	76	28.58	0.00219	15.5	12.9			
218	V	79	76	28.58	0.00219	15.5	12.4			
219	V	79	76	28.58	0.00219	15.5	12.6	6.8	14.3	
220	V	46	81	28.24	0.00231	20.5	14.9	5.3	15.8	
221	V	46	81	28.24	0.00231	22.5	15.4			
222	V	80	70	28.61	0.00219	25.5	17.4			
223	V	46	81	28.24	0.00231	65.5	28.9	5.8	29.5	
224	V	80	70	28.61	0.00219	70.5	29.1			
225	V	80	70	28.61	0.00219	70.5	28.3			
226	V	44	70	28.36	0.00232	199.1	51.0			
227	V	44	70	28.36	0.00232	199.1	46.3	5.8	46.6	
228	V	55	87	28.91	0.00232	202.1	45.3			
229	H	80	70	28.61	0.00219	15.5	13.2			
230	H	80	70	28.61	0.00219	15.5	12.4			
231	H	80	70	28.61	0.00219	15.5	12.4	6.3	13.9	
232	H	80	70	28.61	0.00219	25.5	16.0	7.3	17.6	
233	H	80	70	28.61	0.00219	25.5	17.2			
234	H	80	70	28.61	0.00219	25.5	17.6			
235	H	46	81	28.24	0.00231	65.5	29.6	7.7	30.6	
236	H	46	81	28.24	0.00231	65.5	27.9			
237	H	80	70	28.61	0.00219	70.5	30.5			
238	H	51	73	28.60	0.00231	203.1	51.9	2.8	52.0	
239	H									
240	H									

ed from Model Drop Tests.
e (No. 5)

2

ft)	Total Weight W (Lbs)	Vertical Terminal Velocity V_v (Ft/Sec)	Average Horizontal Velocity V_h (Ft/Sec)	Average Resultant Velocity V_r (Ft/Sec)	Average Glide Angle ϕ (Degrees)	C_D or	C_D e	Frequency of Oscillation (f) (Cycles/Sec)	Maximum Angle of Oscillation (Degrees)	Average or Constant Angle of Oscillation (Degrees)	Logarithmic Decrement
)	15.5	12.9					0.767				
)	15.5	12.4					0.829				
)	15.5	12.6	6.8	14.3	28.3	0.548	0.804	0.228	27	18	0.602
L	20.5	14.9	5.3	15.8	22.7	0.591	0.720	0.235	28	20	-
L	22.5	15.4					0.740				
)	25.5	17.4					0.693				
L	65.5	28.9	5.8	29.5	11.2	0.577	0.612	0.286	30	28	.-
9	70.5	29.1					0.685				
9	70.5	28.3					0.699				
2	199.1	51.0					0.594				
2	199.1	46.3	5.8	46.6	7.2	0.705	0.720	0.364	25	-	-
2	202.1	45.3					0.764				
9	15.5	13.2					0.732				
.9	15.5	12.4					0.830				
.9	15.5	12.4	6.3	13.9	26.6	0.591	0.830	0.25	15	12	0.662
.9	25.5	16.0	7.3	17.6	23.5	0.621	0.818	0.308	20	13	-
.9	25.5	17.2					0.708				
.9	25.5	17.6					0.677				
51	65.5	29.6	7.7	30.6	14.5	0.528	0.582	0.40	28	20	-
51	65.5	27.9					0.655				
19	70.5	30.5					0.623				
51	203.1	51.9	2.8	52.0	6.7	0.581	0.588	-	36	-	-

TABLE 7 - Aerodynamic Characteristics as Determined from Model Drop Tests.
Solid-Flat Fully Extended-Skirt Parachute (No. 6)

Drop No.	Type of Release	Ambient Air Temp. (° F)	Air Relative Humidity (%)	Barometric Pressure (In. of Hg)	Mass Density of Air ρ (Slugs/cu ft)	Total Weight W (Lbs)	Vertical Terminal Velocity V_v (Ft/Sec)	Average Horizontal Velocity V_h (Ft/Sec)	Average Resultant Velocity V_r (Ft/Sec)	Aver Gli Ang ϕ (Deg
241	V	85	67	28.61	0.00217	15.4	10.7			
242	V	85	67	28.61	0.00217	15.4	10.8	6.4	12.6	30.
243	V	75	77	28.58	0.00220	15.4	10.4			
244	V	85	67	28.61	0.00217	30.4	17.0	6.1	18.1	19.
245	V	85	67	28.61	0.00217	30.4	17.0			
246	V	85	37	28.61	0.00217	30.4	16.5			
247	V	85	67	28.61	0.00217	80.4	28.4	5.7	29.0	10.
248	V	85	67	28.61	0.00217	80.4	29.2			
249	V	82	68	28.68	0.00218	80.4	29.6			
250	V	43	71	29.11	0.00238	202.0	41.1			
251	V	43	71	29.11	0.00238	202.0	40.1	4.0	40.3	5
252	V	43	71	29.11	0.00238	202.0	40.9			
253	H	79	76	28.58	0.00220	15.4	11.0			
254	H	75	77	28.58	0.00220	15.4	10.9	7.0	13.0	34
255	H	75	77	28.58	0.00220	15.4	9.9			
256	H	82	68	28.68	0.00218	30.4	17.2			
257	H	75	77	28.58	0.00220	30.4	15.7			
258	H	82	68	28.68	0.00218	30.4	16.6	9.4	19.1	28
259	H	82	68	28.68	0.00218	80.4	30.0	3.7	30.2	6
260	H	82	68	28.68	0.00218	80.4	31.0			
261	H	82	68	28.68	0.00218	80.4	28.4			
262	H	51	73	28.60	0.00231	203.0	45.0			
263	H									
264	H									

Drop Tests.

2

rtical rminal locity V_v t/Sec)	Average Horizontal Velocity V_h (Ft/Sec)	Average Resultant Velocity V_r (Ft/Sec)	Average Glide Angle ϕ (Degrees)	C_D or	C_D e	Frequency of Oscillation (f) (Cycles/Sec)	Maximum Angle of Oscil-lation (Degrees)	Average or Constant Angle of Oscillation (Degrees)	Loga-rithmic Decrement
10.7					1.112				
10.8	6.4	12.6	30.0	0.402	1.093	0.182	25	15	-
10.4					1.163				
17.0	6.1	18.1	19.5	0.726	0.874	0.25	44	30	Neg
17.0					0.874				
16.5					0.927				
28.4	5.7	29.0	10.9	0.780	0.827	0.286	36	28	-
29.2					0.783				
29.6					0.757				
41.1					0.905				
40.1	4.0	40.3	5.2	0.936	0.950	0.445	29	24	-
40.9					0.913				
11.0					1.041				
10.9	7.0	13.0	34.4	0.615	1.061	0.250	22	19	-
9.9					1.287				
17.2					0.849				
15.7					1.007				
16.6	9.4	19.1	28.3	0.606	0.912	0.267	32	31	-
30.0	3.7	30.2	6.9	0.722	0.738	0.40	50	40	0.511
31.0					0.690				
28.4					0.822				
45.0					0.781				

TABLE 8 - Aerodynamic Characteristics as Determined from Model Drop Tests.
50% Vent Airfoil Parachute (No. 7)

Drop No.	Type of Release	Ambient Air Temp. ($^{\circ}$ F)	Air Relative Humidity (%)	Barometric Pressure (In. of Hg)	Mass Density of Air ρ (Slugs/cu ft)	Total Weight W (Lbs)	Vertical Terminal Velocity V_v (Ft/Sec)	Average Horizontal Velocity V_h (Ft/Sec)	Average Resultant Velocity V_r (Ft/Sec)
289	V	46	70	28.94	0.00236	10.5	8.4	5.0	9.8
290	V	46	70	28.94	0.00236	15.5	9.7		
291	V	46	70	28.94	0.00236	15.5	9.5		
292	V	46	70	28.94	0.00236	25.5	13.7		
293	V	46	70	28.94	0.00236	25.5	13.7	8.5	16.1
294	V								
295	V								
296	V								
297	V								
298	V								
299	V								
300	V								
301	H	47	70	28.78	0.00234	15.5	10.6	8.2	13.4
302	H	47	70	28.78	0.00234	15.5	10.4		
303	H	47	70	28.78	0.00234	15.5	10.7		
304	H	47	70	28.78	0.00234	25.5	14.0		
305	H	47	70	28.78	0.00234	25.5	13.2		
306	H	47	70	28.78	0.00234	25.5	14.7	6.2	15.9
307	H								
308	H								
309	H								
310	H								
311	H								
312	H								

ed from Model Drop Tests.

ft)	Total Weight W (Lbs)	Vertical Terminal Velocity V_v (Ft/Sec)	Average Horizontal Velocity V_h (Ft/Sec)	Average Resultant Velocity V_r (Ft/Sec)	Average Glide Angle ϕ (Degrees)	C_D or	C_{D_o}	Frequency of Oscillation (f) (Cycles/Sec)	Maximum Angle of Oscillation (Degrees)	Average or Constant Angle of Oscillation (Degrees)	Logarithmic Decrement
;	10.5	8.4	5.0	9.8	35.9	0.675	1.133	-	8	4	-
;	15.5	9.7					1.257				
;	15.5	9.5					1.310				
;	25.5	13.7					1.036				
;	25.5	13.7	8.5	16.1	20.1	0.704	1.036	0.286	15	5	-
4	15.5	10.6	8.2	13.4	27.5	0.603	1.061	-	9	5	-
4	15.5	10.4					1.102				
4	15.5	10.7					1.042				
4	25.5	14.0					1.000				
4	25.5	13.2					1.123				
4	25.5	14.7	6.2	15.9	26.2	0.696	0.908	0.308	22	15	-

2

TABLE 9 - Aerodynamic Characteristics as Determined from Model Drop Tests.

½ Sphere Circular Parachute (No. 8)

Drop No.	Type of Release	Ambient Air Temp. (° F)	Air Relative Humidity (%)	Barometric Pressure (In. of Hg)	Mass Density of Air ρ (Slugs/cu ft)	Total Weight W (Lbs)	Vertical Terminal Velocity V_v (Ft/Sec)	Average Horizontal Velocity V_h (Ft/Sec)	Average Resultant Velocity V_r (Ft/Sec)	Averag Glide Angle ϕ (Degr
265	V	80	73	28.53	0.00220	25.4	15.6			
266	V	80	73	28.53	0.00220	25.4	16.3			
267	V	80	73	28.53	0.00220	25.4	16.0	7.9	17.8	27.
268	V	80	73	28.53	0.00220	30.4	17.4			
269	V	80	73	28.53	0.00220	30.4	17.9			
270	V	80	73	28.53	0.00220	30.4	18.0	8.7	20.1	24.
271	V	80	73	28.53	0.00220	70.4	27.1	6.1	27.8	10.
272	V	85	67	28.61	0.00217	75.4	27.5			
273	V	85	67	28.61	0.00217	75.4	27.8			
274	V	44	70	28.36	0.00232	199.0	42.4	5.2	42.7	6.
275	V	41	71	28.95	0.00239	199.0	43.1			
276	V	41	71	28.95	0.00239	198.0	43.5			
277	H	56	53	28.47	0.00227	10.4	8.8	6.8	11.1	38.
278	H	56	53	28.47	0.00227	10.4	8.4			
279	H	56	53	28.47	0.00227	10.4	8.2			
280	H	56	53	28.47	0.00227	22.4	13.2	6.4	14.7	26.
281	H	56	53	28.47	0.00227	22.4	13.0			
282	H	80	70	28.61	0.00219	35.4	16.9			
283	H	47	65	28.47	0.00231	65.4	28.5	6.8	29.3	14.
284	H	47	65	28.47	0.00231	65.4	26.4			
285	H	47	65	28.47	0.00231	65.4	27.4			
286	H									
287	H									
288	H									

rop Tests.

2

tical minal ocity V_v t/Sec)	Average Horizontal Velocity V_h (Ft/Sec)	Average Resultant Velocity V_r (Ft/Sec)	Average Glide Angle ϕ (Degrees)	C_D or	C_D o	Frequency of Oscillation (f) (Cycles/Sec)	Maximum Angle of Oscil-lation (Degrees)	Average or Constant Angle of Oscillation (Degrees)	Loga-rithmic Decrement
15.6					0.855				
16.3					0.782				
16.0	7.9	17.8	27.8	0.580	0.812	0.250	31	20	-
17.4					0.821				
17.9					0.778				
18.0	8.7	20.1	24.3	0.562	0.769	0.250	30	20	-
27.1	6.1	27.8	10.6	0.732	0.785	0.308	35	30	Neg
27.5					0.826				
27.8					0.808				
42.4	5.2	42.7	6.5	0.840	0.860	0.40	30	27	-
43.1					0.807				
43.5					0.788				
8.8	6.8	11.1	38.5	0.522	1.064	0.25	26	18	-
8.4					1.168				
8.2					1.227				
13.2	6.4	14.7	26.3	0.736	1.019	-	24	10	-
13.0					1.050				
16.9					1.019				
28.5	6.8	29.3	14.4	0.575	0.628	0.308	35	-	-
26.4					0.732				
27.4					0.678				

TABLE 10 - Aerodynamic Characteristics as Determined from Model Drop Tests.
¼ Sphere Circular Parachute (No. 9)

Drop No.	Type of Release	Ambient Air Temp. (° F)	Air Relative Humidity (%)	Barometric Pressure (In. of Hg)	Mass Density of Air ρ (Slugs/cu ft)	Total Weight W (Lbs)	Vertical Terminal Velocity V_v (Ft/Sec)	Average Horizontal Velocity V_h (Ft/Sec)	Average Resultant Velocity V_r (Ft/Sec)	Av G A (D
313	V	60	52	28.87	0.00226	20.3	12.7	6.8	14.4	2
314	V	60	52	28.87	0.00226	20.3	12.7			
315	V	60	52	28.87	0.00226	20.3	12.2			
316	V	60	52	28.87	0.00226	35.3	17.7			
317	V	60	52	28.87	0.00226	35.3	16.7	6.3	17.9	2
318	V	46	65	28.47	0.00232	35.3	18.7			
319	V	46	68	28.23	0.00230	75.3	27.1	6.1	27.8	1
320	V	46	68	28.23	0.00230	65.3	24.3			
321	V	46	68	28.23	0.00230	65.3	25.4			
322	V	52	80	28.42	0.00238	182.0	39.6	4.4	39.8	
323	V	52	80	28.42	0.00238	182.0	39.3			
324	V	52	80	28.42	0.00238	182.0	40.4			
325	H	56	53	28.47	0.00227	20.3	12.5			
326	H	56	53	28.47	0.00227	20.3	12.0	7.2	14.0	
327	H	56	53	28.47	0.00227	20.3	12.5			
328	H	60	52	28.87	0.00226	35.3	16.4	9.1	18.8	
329	H	46	65	28.47	0.00232	30.3	15.6			
330	H	46	65	28.47	0.00232	30.3	16.5			
331	H	47	68	28.23	0.00230	65.3	25.8			
332	H	47	68	28.23	0.00230	65.3	24.8			
333	H	47	68	28.23	0.00230	65.3	23.7	14.6	27.8	
334	H									
335	H									
336	H									

d from Model Drop Tests.

t)	Total Weight W (Lbs)	Vertical Terminal Velocity V_v (Ft/Sec)	Average Horizontal Velocity V_h (Ft/Sec)	Average Resultant Velocity V_r (Ft/Sec)	Average Glide Angle ϕ (Degrees)	C_D or	C_{D_o}	Frequency of Oscillation (f) (Cycles/Sec)	Maximum Angle of Oscillation (Degrees)	Average or Constant Angle of Oscillation (Degrees)	Logarithmic Decrement
	20.3	12.7	6.8	14.4	27.0	0.695	1.002	0.276	33	20	-
	20.3	12.7					1.002				
	20.3	12.2					1.085				
	35.3	17.7					0.897				
	35.3	16.7	6.3	17.9	28.8	0.769	1.007	0.308	32	20	-
	35.3	18.7					0.784				
	75.3	27.1	6.1	27.8	11.4	0.721	0.803	0.308	34	20	-
	65.3	24.3					0.867				
	65.3	25.4					0.792				
	182.0	39.6	4.4	39.8	6.8	0.862	0.877	0.40	30	25	-
	182.0	39.3					0.892				
	182.0	40.4					0.843				
	20.3	12.5					1.029				
	20.3	12.0	7.2	14.0	32.0	0.735	1.179	-	8	5	-
	20.3	12.5					1.029				
3	35.3	16.4	9.1	18.8	27.9	0.704	1.043	-	10	5	-
2	30.3	15.6					0.967				
2	30.3	16.5					0.863				
0	65.3	25.8					0.768				
0	65.3	24.8					0.830				
0	65.3	23.7	14.6	27.8	23.8	0.605	0.910	0.40	31	20	-

TABLE 11 - Aerodynamic Characteristics as Determined from Model Drop Tests.
¼ Sphere Square Parachute (No. 10)

Drop No.	Type of Release	Ambient Air Temp. (° F)	Air Relative Humidity (%)	Barometric Pressure (In. of Hg)	Mass Density of Air ρ (Slugs/cu ft)	Total Weight W (Lbs)	Vertical Terminal Velocity V_v (Ft/Sec)	Average Horizontal Velocity V_h (Ft/Sec)	Average Resultant Velocity V_r (Ft/Sec)	A (I
337	V	50	72	28.68	0.00232	20.1	11.0	5.9	12.5	
338	V	44	58	29.06	0.00237	20.1	10.0			
339	V	44	58	29.06	0.00237	20.1	9.8			
340	V	47	68	28.23	0.00230	35.1	16.1	10.2	19.1	
341	V	47	68	28.23	0.00230	35.1	17.0			
342	V	50	73	28.68	0.00232	35.1	16.2			
343	V	50	73	28.68	0.00232	80.1	27.3			
344	V	50	73	28.68	0.00232	80.1	26.9			
345	V	50	73	28.68	0.00232	80.1	27.1	6.7	27.8	
346	V	46	72	28.57	0.00232	196.7	40.2			
347	V	44	62	29.08	0.00238	176.7	38.5			
348	V	55	87	28.91	0.00232	204.7	42.4	6.5	42.8	
349	H	44	58	29.06	0.00237	20.1	11.0	8.3	13.8	
350	H	44	58	29.06	0.00237	20.1	12.0			
351	H	44	58	29.06	0.00237	20.1	10.4			
352	H	47	68	28.23	0.00230	30.1	13.3	10.4	16.9	
353	H	47	68	28.23	0.00230	30.1	13.9			
354	H	46	71	28.23	0.00230	30.1	15.2			
355	H	50	73	28.68	0.00232	80.1	27.0	8.9	28.4	
356	H	50	73	28.68	0.00232	80.1	25.7			
357	H	50	73	28.68	0.00232	80.1	29.0			
358	H									
359	H									
360	H									

Drop Tests.

rtical rminal locity V_v t/Sec)	Average Horizontal Velocity V_h (Ft/Sec)	Average Resultant Velocity V_r (Ft/Sec)	Average Glide Angle ϕ (Degrees)	C_D or	C_D e	Frequency of Oscillation (f) (Cycles/Sec)	Maximum Angle of Oscil-lation (Degrees)	Average or Constant Angle of Oscillation (Degrees)	Loga-rithmic Decrement
11.0	5.9	12.5	32.2	0.845	1.290	0.267	13	12	-
10.0					1.525				
9.8					1.589				
16.1	10.2	19.1	33.0	0.631	1.060	0.308	28	23	-
17.0					0.951				
16.2					1.038				
27.3					0.835				
26.9					0.860				
27.1	6.7	27.8	13.0	0.785	0.848	0.308	40	30	-
40.2					0.944				
38.5					0.901				
42.4	6.5	42.8	8.3	0.856	0.883	0.40	28	20	-
11.0	8.3	13.8	37.6	0.634	1.290	0.25	32	27	0.336
12.0					1.059				
10.4					1.410				
13.3	10.4	16.9	36.7	0.661	1.331	0.333	15	13	Neg
13.9					1.218				
15.2					1.021				
27.0	8.9	28.4	11.9	0.755	0.854	0.333	38	33	-
25.7					0.942				
29.0					0.740				

TABLE 12 - Aerodynamic Characteristics as Determined from Model Drop Tests.
¼ Sphere Triangular Parachute (No. 11)

Drop No.	Type of Release	Ambient Air Temp. (° F)	Air Relative Humidity (%)	Barometric Pressure (In. of Hg)	Mass Density of Air ρ (Slugs/cu ft)	Total Weight W (Lbs)	Vertical Terminal Velocity V_v (Ft/Sec)	Average Horizontal Velocity V_h (Ft/Sec)	Average Resultant Velocity V_r (Ft/Sec)	A C A (D
361	V	56	64	28.82	0.00231	20.1	10.6			
362	V	56	54	28.82	0.00231	20.1	10.2			
363	V	56	54	28.82	0.00231	20.1	10.1	6.6	12.1	
364	V	56	54	28.82	0.00231	40.1	15.3	12.2	19.6	
365	V	50	73	28.68	0.00232	40.1	17.1			
366	V	50	73	28.68	0.00232	40.1	17.1			
367	V	51	59	28.14	0.00228	80.1	25.3			
368	V	51	59	28.14	0.00228	80.1	26.4	14.9	30.3	
369	V	51	59	28.14	0.00228	80.1	25.7			
370	V	44	70	28.36	0.00232	198.7	42.9	6.6	43.4	
371	V	44	70	28.36	0.00232	198.7	39.0			
372	V	44	62	29.08	0.00238	187.1	39.9			
373	H	73	56	28.95	0.00224	20.1	12.2	10.5	16.1	
374	H	73	56	28.95	0.00224	20.1	9.7			
375	H	73	56	28.95	0.00224	20.1	11.8			
376	H	73	56	28.96	0.00224	35.1	16.7	12.5	20.9	
377	H	73	56	28.95	0.00224	35.1	14.6			
378	H	73	56	28.95	0.00224	35.1	15.8			
379	H	73	56	28.95	0.00224	80.1	27.3	12.9	30.2	
380	H	73	56	28.95	0.00224	80.1	30.0			
381	H	51	59	28.14	0.00228	80.1	26.3			
382	H									
383	H									
384	H									

d from Model Drop Tests.

t)	Total Weight W (Lbs)	Vertical Terminal Velocity V_v (Ft/Sec)	Average Horizontal Velocity V_h (Ft/Sec)	Average Resultant Velocity V_r (Ft/Sec)	Average Glide Angle ϕ (Degrees)	C_D or	C_D o	Frequency of Oscillation (f) Cycles/Sec	Maximum Angle of Oscillation (Degrees)	Average or Constant Angle of Oscillation (Degrees)	Logarithmic Decrement
	20.1	10.6					1.392				
	20.1	10.2					1.505				
	20.1	10.1	6.6	12.1	40.5	0.812	1.533	-	10	5	-
	40.1	15.3	12.2	19.6	38.4	0.637	1.334	-	23	18	-
	40.1	17.1					1.063				
	40.1	17.1					1.063				
	80.1	25.3					0.989				
	80.1	26.4	14.9	30.3	40.6	0.522	0.908	-	25	18	-
	80.1	25.7					0.958				
	198.7	42.9	6.6	43.4	11.8	0.801	0.838	-	28	-	-
	198.7	39.0					1.011				
	187.1	39.9					0.989				
	20.1	12.2	10.5	16.1	41.5	0.467	1.083	-	22	15	-
	20.1	9.7					1.718				
	20.1	11.8					1.160				
	35.1	16.7	12.5	20.9	37.6	0.512	1.010	0.286	20	15	-
	35.1	14.6					1.321				
	35.1	15.8					1.130				
	80.1	27.3	12.9	30.2	25.6	0.636	0.863	0.333	25	20	-
	80.1	30.0					0.715				
	80.1	26.3					0.915				

2

TABLE 13 - Aerodynamic Characteristics as Determined from Model Drop Tests.
30° Circular Conical Parachute (No. 12)

Drop No.	Type of Release	Ambient Air Temp. (° F)	Air Relative Humidity (%)	Barometric Pressure (In. of Hg)	Mass Density of Air ρ (Slugs/cu ft)	Total Weight W (Lbs)	Vertical Terminal Velocity V_v (Ft/Sec)	Average Horizontal Velocity V_h (Ft/Sec)	Average Resultant Velocity V_r (Ft/Sec)	Average Glide Angle ϕ (Degr
385	V	60	52	28.87	0.00226	20.5	10.8	7.2	13.0	33.5
386	V	60	52	28.87	0.00226	20.5	11.6			
387	V	60	78	28.14	0.00228	20.5	12.9			
388	V	60	52	28.87	0.00226	35.5	16.8	6.2	17.9	21.2
389	V	60	52	28.87	0.00226	35.5	16.5			
390	V	60	52	28.87	0.00226	35.5	16.8			
391	V	50	78	28.14	0.00228	75.5	26.2			
392	V	50	78	28.14	0.00228	75.5	25.3	6.0	26.0	10.7
393	V	50	78	28.14	0.00228	75.5	26.1			
394	V	52	75	28.57	0.00230	197.1	39.0	4.2	39.2	5.7
395	V	52	75	28.57	0.00230	197.1	40.0			
396	V	52	75	29.08	0.00234	205.1	49.5			
397	H	55	53	28.47	0.00229	20.5	12.2	7.7	14.4	29.8
398	H	55	53	28.47	0.00229	20.5	10.4			
399	H	55	53	28.47	0.00229	20.5	10.4			
400	H	56	53	28.47	0.00227	35.5	16.4			
401	H	56	53	28.47	0.00227	35.5	15.4			
402	H	56	53	28.47	0.00227	35.5	16.2	9.6	18.8	29.5
403	H	55	53	28.47	0.00229	75.5	25.7	6.5	26.5	13.8
404	H	55	53	28.47	0.00229	75.5	24.0			
405	H	50	78	28.14	0.00228	75.5	26.5			
406	H									
407	H									
408	H									

rop Tests.

2

tical minal ocity V_v /Sec)	Average Horizontal Velocity V_h (Ft/Sec)	Average Resultant Velocity V_r (Ft/Sec)	Average Glide Angle ϕ (Degrees)	C_D or	C_D e	Frequency of Oscillation (f) (Cycles/Sec)	Maximum Angle of Oscil-lation (Degrees)	Average or Constant Angle of Oscillation (Degrees)	Loga-rithmic Decrement
0.8	7.2	13.0	33.5	0.806	1.400	0.222	22	15	0.604
1.6					1.212				
2.9					0.974				
3.8	6.2	17.9	21.2	0.823	1.001	0.25	36	25	Neg.
3.5					1.038				
3.8					1.001				
3.2					0.869				
5.3	6.0	26.0	10.7	0.867	0.932	0.364	40	30	-
6.1					0.875				
9.0	4.2	39.2	5.7	0.999	1.013	0.364	30	26	-
0.0					0.965				
9.5					0.643				
2.2	7.7	14.4	29.8	0.674	1.081	0.286	24	20	-
0.4					1.487				
0.4					1.487				
6.4					1.045				
5.4					1.186				
16.2	9.6	18.8	29.5	0.694	1.072	0.20	22	6	-
25.7	6.5	26.5	13.8	0.821	0.899	0.364	35	30	-
24.0					1.030				
26.5					0.849				

TABLE 14 - Aerodynamic Characteristics as Determined from Model Drop Tests.

30° Square Conical Parachute (No. 13)

Drop No.	Type of Release	Ambient Air Temp. ($^{\circ}$ F)	Air Relative Humidity (%)	Barometric Pressure (In. of Hg)	Mass Density of Air ρ (Slugs/cu ft)	Total Weight W (Lbs)	Vertical Terminal Velocity V_v (Ft/Sec)	Average Horizontal Velocity V_h (Ft/Sec)	Average Resultant Velocity V_r (Ft/Sec)
409	V	66	59	29.11	0.00228	20.1	10.5		
410	V	66	59	29.11	0.00228	20.1	9.7	8.3	12.7
411	V	66	59	29.11	0.00228	20.1	10.1		
412	V	62	62	29.11	0.00230	40.1	17.2		
413	V	62	62	29.11	0.00230	40.1	15.0		
414	V	62	62	29.11	0.00230	40.1	17.0	11.3	20.4
415	V	62	62	29.11	0.00230	90.1	26.9		
416	V	62	62	29.11	0.00230	80.1	26.6	11.2	28.9
417	V	62	62	29.11	0.00230	80.1	26.2		
418	V	52	75	28.57	0.00230	196.7	41.6	7.8	42.3
419	V	55	87	28.91	0.00232	204.7	45.9		
420	V	51	75	28.29	0.00229	201.7	44.0		
421	H	62	62	29.11	0.00230	20.1	13.2		
422	H	62	62	29.11	0.00230	20.1	11.6	9.3	14.9
423	H	62	62	29.11	0.00230	20.1	10.8		
424	H	62	62	29.11	0.00230	40.1	15.3		
425	H	71	54	28.96	0.00225	40.1	18.4	7.1	19.7
426	H	71	54	28.96	0.00225	40.1	18.5		
427	H	52	81	28.14	0.00227	80.1	26.3		
428	H	52	81	28.14	0.00227	80.1	28.0	12.0	30.5
429	H	44	58	29.06	0.00237	80.1	26.6		
430	H								
431	H								
432	H								

ad from Model Drop Tests.

ht)	Total Weight W (Lbs)	Vertical Terminal Velocity V_v (Ft/Sec)	Average Horizontal Velocity V_h (Ft/Sec)	Average Resultant Velocity V_r (Ft/Sec)	Average Glide Angle ϕ (Degrees)	$C_{D_{cr}}$	C_{D_o}	Frequency of Oscillation (f) (Cycles/Sec)	Maximum Angle of Oscillation (Degrees)	Average cr Constant Angle of Oscillation (Degrees)	Logarithmic Decrement
	20.1	10.5					1.438				
	20.1	9.7	8.3	12.7	37.4	0.780	1.685	0.25	10	7	-
	20.1	10.1					1.553				
	40.1	17.2					1.060				
	40.1	15.0					1.392				
	40.1	17.0	11.3	20.4	33.7	0.627	1.083	0.25	19	10	-
	90.1	26.9					0.974				
	80.1	26.6	11.2	28.9	21.9	0.695	0.885	0.267	33	27	-
	80.1	26.2					0.914				
	196.7	41.6	7.8	42.3	9.1	0.849	0.888	0.40	30	28	-
2	204.7	45.9					0.754				
9	201.7	44.0					0.819				
0	20.1	13.2					0.903				
0	20.1	11.6	9.3	14.9	42.0	0.526	1.168	0.267	37	33	-
0	20.1	10.8					1.348				
0	40.1	15.3					1.338				
5	40.1	18.4	7.1	19.7	21.3	0.769	0.947	0.308	42	35	-
5	40.1	18.5					0.938				
7	80.1	26.3					0.920				
7	80.1	28.0	12.0	30.5	22.3	0.631	0.810	0.333	21	-	-
7	80.1	26.6					0.897				

2

TABLE 15 - Aerodynamic Characteristics as Determined from Model Drop Tests. 30° Triangular Conical Parachute (No. 14)

Drop No.	Type of Release	Ambient Air Temp. (° F)	Air Relative Humidity (%)	Barometric Pressure (In. of Hg)	Mass Density of Air ρ (Slugs/cu ft)	Total Weight W (Lbs)	Vertical Terminal Velocity V_v (Ft/Sec)	Average Horizontal Velocity V_h (Ft/Sec)	Average Resultant Velocity V_r (Ft/Sec)	Average Glide Angle ϕ (Degrees
433	V	61	54	28.82	0.00231	20.1	9.9	8.3	12.9	40.0
434	V	61	54	28.82	0.00231	20.1	10.1			
435	V	61	54	28.82	0.00231	20.1	9.9			
436	V	69	57	28.95	0.00226	35.1	14.5	11.1	18.3	37.8
437	V	69	57	28.95	0.00226	35.1	13.2			
438	V	69	57	28.95	0.00226	35.1	15.9			
439	V	69	57	28.95	0.00226	80.1	26.5	9.4	28.1	29.7
440	V	69	57	28.95	0.00226	80.1	25.7			
441	V	69	57	28.95	0.00226	80.1	26.0			
442	V	43	70	28.36	0.00232	198.7	45.0			
443	V	43	70	28.36	0.00232	198.7	40.7			
444	V	43	70	28.36	0.00232	198.7	39.7	12.7	41.5	18.6
445	H	70	57	29.00	0.00226	20.1	10.6			
446	H	70	57	29.00	0.00226	20.1	11.5	9.9	15.2	38.0
447	H	70	57	29.00	0.00226	20.1	10.0			
448	H	70	57	29.00	0.00226	35.9	13.7	12.1	18.3	41.3
449	H	67	57	29.00	0.00227	35.9	15.2			
450	H	67	57	29.00	0.00227	35.9	17.2			
451	H	64	57	28.95	0.00228	80.1	26.5			
452	H	67	57	29.00	0.00227	80.1	28.3	9.3	29.8	16.5
453	H	67	57	29.00	0.00227	80.1	24.1			
454	H									
455	H									
456	H									

Drop Tests.

2

rtical rminal locity V_v t/Sec)	Average Horizontal Velocity V_h (Ft/Sec)	Average Resultant Velocity V_r (Ft/Sec)	Average Glide Angle ϕ (Degrees)	C_D or	C_D e	Frequency of Oscillation (f) Cycles/Sec)	Maximum Angle of Oscil- lation (Degrees)	Average or Constant Angle of Oscillation (Degrees)	Loga- rithmic Decrement
9.9	8.3	12.9	40.0	0.722	1.599	-	10	5	-
.0.1					1.533				
9.9					1.599				
.4.5	11.1	18.3	37.8	0.660	1.330	0.286	17	13	-
.3.2					1.603				
.5.9					1.103				
26.5	9.4	28.1	29.7	0.702	0.908	0.333	24	18	-
25.7					0.966				
26.0					0.943				
45.0					0.761				
40.7					0.930				
39.7	12.7	41.5	18.6	0.847	0.977	0.333	24	12	-
10.6					1.423				
11.5	9.9	15.2	38.0	0.546	1.210	0.286	32	29	-
10.0					1.600				
13.7	12.1	18.3	41.3	0.640	1.520	0.235	29	20	-
15.2					1.232				
17.2					0.963				
26.5					0.901				
28.3	9.3	29.8	16.5	0.685	0.793	0.308	43	42	-
24.1					1.093				

TABLE 16 - Aerodynamic Characteristics as Determined from Model Drop Tests.

Medium-Construction Brake-Type Guide-Surface Parachute (No. 16)

Drop No.	Type of Release	Ambient Air Temp. (° F)	Air Relative Humidity (%)	Barometric Pressure (In. of Hg)	Mass Density of Air ρ (Slugs/cu ft)	Total Weight W (Lbs)	Vertical Terminal Velocity V_v (Ft/Sec)	Average Horizontal Velocity V_h (Ft/Sec)	Average Resultant Velocity V_r (Ft/Sec)	Av C A (D
457	V	41	59	28.76	0.00237	15.3	15.4			
458	V	41	59	28.76	0.00237	15.3	15.0	3.3	15.4	
459	V	41	59	28.76	0.00237	10.3	13.2			
460	V	41	59	28.76	0.00237	20.3	17.8	2.4	18.0	
461	V	41	59	28.76	0.00237	20.3	16.6			
462	V	41	59	28.76	0.00237	20.3	18.2			
463	V	41	59	28.76	0.00237	40.3	23.7	2.0	23.8	
464	V	41	59	28.76	0.00237	40.3	23.6			
465	V	41	71	28.95	0.00239	40.3	24.3			
466	V	47	80	28.42	0.00238	101.9	40.4	1.8	40.4	
467	V	47	80	28.42	0.00238	101.9	42.5			
468	V	47	80	28.42	0.00238	101.9	40.7			
469	H	41	59	28.68	0.00236	10.3	13.0			
470	H	41	59	28.68	0.00236	10.3	13.3	2.2	13.5	
471	H	41	59	28.68	0.00236	10.3	12.8			
472	H	41	59	28.68	0.00236	20.3	17.1			
473	H	41	59	28.68	0.00236	20.3	16.5			
474	H	41	59	28.68	0.00236	20.3	17.3	3.6	17.7	
475	H	41	59	28.76	0.00237	40.3	23.0	2.3	23.1	
476	H	41	59	28.76	0.00237	40.3	25.6			
477	H	41	59	28.75	0.00237	40.3	27.4			
478	H	51	73	28.60	0.00231	131.9	47.4			
479	H									
480	H									

d from Model Drop Tests.

face Parachute (No. 16)

t)	Total Weight W (Lbs)	Vertical Terminal Velocity V_v (Ft/Sec)	Average Horizontal Velocity V_h (Ft/Sec)	Average Resultant Velocity V_r (Ft/Sec)	Average Glide Angle ϕ (Degrees)	C_D or	C_D e	Frequency of Oscillation (f) (Cycles/Sec)	Maximum Angle of Oscillation (Degrees)	Average or Constant Angle of Oscillation (Degrees)	Logarithmic Decrement
	15.3	15.4					0.482				
	15.3	15.0	3.3	15.4	12.3	0.471	0.508	0.286	20	15	-
	10.3	13.2					0.442				
	20.3	17.3	2.4	18.0	7.7	0.464	0.479	0.286	19	11	-
	20.3	16.6					0.550				
	20.3	18.2					0.458				
	40.3	23.7	2.0	23.8	4.4	0.529	0.536	0.364	20	15	-
	40.3	23.6					0.540				
	40.3	24.3					0.505				
	101.9	40.4	1.8	40.4	2.5	0.464	0.465	-	7	4	-
	101.9	42.5					0.420				
	101.9	40.7					0.457				
3	10.3	13.0					0.457				
3	10.3	13.3	2.2	13.5	10.6	0.417	0.437	0.235	19	15	-
3	10.3	12.8					0.472				
3	20.3	17.1					0.522				
3	20.3	16.5					0.560				
3	20.3	17.3	3.6	17.7	10.7	0.479	0.509	0.286	25	15	-
7	40.3	23.0	2.3	23.1	4.5	0.562	0.569	0.364	19	12	-
7	40.3	25.6					0.460				
7	40.3	27.4					0.401				
1	131.9	47.4					0.450				

2

TABLE 17 - Aerodynamic Characteristics as Determined from Model Drop Tests.
Stabilization-Type Guide-Surface Parachute (No. 17)

Drop No.	Type of Release	Ambient Air Temp. (° F)	Air Relative Humidity (%)	Barometric Pressure (In. of Hg)	Mass Density of Air ρ (Slugs/cu ft)	Total Weight W (Lbs)	Vertical Terminal Velocity V_v (Ft/Sec)	Average Horizontal Velocity V_h (Ft/Sec)	Average Resultant Velocity V_r (Ft/Sec)	A (I
481	V	41	59	28.68	0.00236	10.3	14.0	3.0	14.3	
482	V	41	59	28.68	0.00236	10.3	12.8			
483	V	41	59	28.68	0.00236	10.3	12.3			
484	V	41	59	28.68	0.00236	20.3	16.7	1.8	16.8	
485	V	41	59	28.68	0.00236	20.3	19.5			
486	V	41	59	28.68	0.00236	20.3	18.5			
487	V	41	59	28.68	0.00236	40.3	26.5	1.2	26.7	
488	V	44	58	29.06	0.00237	35.3	23.6			
489	V	44	58	29.06	0.00237	35.3	23.0			
490	V	47	70	28.78	0.00234	101.9	41.9			
491	V	47	70	28.78	0.00234	101.9	44.8			
492	V	47	70	28.78	0.00234	101.9	43.9	1.9	43.9	
493	H	41	59	28.68	0.00236	10.3	12.2	3.6	12.7	
494	H	41	59	28.68	0.00236	10.3	12.7			
495	H	44	58	29.06	0.00237	10.3	12.4			
496	H	44	58	29.06	0.00237	20.3	18.6	1.7	18.7	
497	H	44	58	29.06	0.00237	20.3	17.6			
498	H	44	58	29.06	0.00237	20.3	20.2			
499	H	44	58	29.06	0.00237	35.3	24.7			
500	H	41	59	28.68	0.00236	40.3	22.7	1.9	22.7	
501	H	41	59	28.68	0.00236	40.3	26.0			
502	H	56	75	28.60	0.00228	131.9	53.4	5.5	53.5	
503	H									
504	H									

Drop Tests.

rtical rminal locity V_v t/Sec)	Average Horisontal Velocity V_h (Ft/Sec)	Average Resultant Velocity V_r (Ft/Sec)	Average Glide Angle ϕ (Degrees)	C_D or	C_D o	Frequency of Oscillation (f) (Cycles/Sec)	Maximum Angle of Oscil-lation (Degrees)	Average or Constant Angle of Oscillation (Degrees)	Loga-rithmic Decrement
4.0	3.0	14.3	12.4	0.343	0.366	0.296	17	15	0.888
12.8					0.437				
12.3					0.473				
16.7	1.8	16.8	5.0	0.499	0.507	0.40	16	13	0.166
19.5					0.372				
18.5					0.413				
26.5	1.2	26.7	2.3	0.392	0.399	0.572	11	9	0.498
23.6					0.439				
23.0					0.462				
41.9					0.407				
44.8					0.356				
43.9	1.9	43.9	2.1	0.370	0.370	-	5	3	-
12.2	3.6	12.7	13.2	0.433	0.482	0.286	22	18	0.36
12.7					0.445				
12.4					0.464				
18.6	1.7	18.7	3.4	0.401	0.407	0.50	12	9	0.694
17.6					0.455				
20.2					0.345				
24.7					0.401				
22.7	1.9	22.7	4.9	0.542	0.544	-	16	13	-
26.0					0.417				
53.4	5.5	53.5	7.9	0.328	0.332	-	0	0	-

2

TABLE 18 - Aerodynamic Characteristics as Determined from Model Drop Tests.
Circular Brake-Type FIST Ribbon Parachute (No. 21)

Drop No.	Type of Release	Ambient Air Temp. (° F)	Air Relative Humidity (%)	Barometric Pressure (In. of Hg)	Mass Density of Air ρ (Slugs/cu ft)	Total Weight W (Lbs)	Vertical Terminal Velocity V_v (Ft/Sec)	Average Horizontal Velocity V_h (Ft/Sec)	Average Resultant Velocity V_r (Ft/Sec)	Av Gl Ar (De
505	V	46	64	29.10	0.00232	8.7	10.6	1.3	10.7	7
506	V	46	64	29.10	0.00232	8.7	10.3			
507	V	46	64	29.10	0.00232	8.7	10.6			
508	V	63	58	28.74	0.00227	15.8	14.2	3.2	14.6	9
509	V	63	58	28.74	0.00227	15.8	14.2			
510	V	63	58	28.74	0.00227	15.8	14.0			
511	V	46	64	29.10	0.00232	29.4	23.6			
512	V	46	64	29.10	0.00232	29.4	23.4	0.8	23.4	2
513	V	63	58	28.74	0.00227	30.8	20.3			
514	V	63	58	28.74	0.00227	70.8	33.7	1.5	33.7	2
515	V	74	81	28.60	0.00221	70.8	36.5			
516	V	74	81	28.60	0.00221	70.8	35.7			
517	H	63	58	28.74	0.00227	8.7	10.2	1.0	10.3	5
518	H	74	81	28.60	0.00221	8.7	9.9			
519	H	74	81	28.60	0.00221	8.7	10.0			
520	H	74	81	28.60	0.00221	15.8	14.1	1.4	14.2	6
521	H	72	83	28.60	0.00222	15.8	14.3			
522	H	72	83	28.60	0.00222	15.8	13.8			
523	H	72	83	28.60	0.00222	30.8	23.2	1.5	23.3	4
524	H	72	83	28.60	0.00222	30.8	22.6			
525	H	80	70	28.58	0.00218	30.8	21.9			
526	H	73	85	28.60	0.00222	70.8	58.6			
527	H	73	85	28.60	0.00222	70.8	39.6	2.2	39.7	5
528	H	80	70	28.58	0.00218	70.8	35.9			

d from Model Drop Tests.
e (No. 21)

t)	Total Weight W (Lbs)	Vertical Terminal Velocity V_v (Ft/Sec)	Average Horizontal Velocity V_h (Ft/Sec)	Average Resultant Velocity V_r (Ft/Sec)	Average Glide Angle ϕ (Degrees)	$C_{D_{or}}$	C_{D_o}	Frequency of Oscillation (f) (Cycles/Sec)	Maximum Angle of Oscillation (Degrees)	Average or Constant Angle of Oscillation (Degrees)	Logarithmic Decrement
	8.7	10.6	1.3	10.7	7.3	0.584	0.600	-	15	5	-
	8.7	10.3					0.636				
	8.7	10.6					0.600				
	15.8	14.2	3.2	14.6	9.6	0.580	0.622	-	5	4	-
	15.8	14.2					0.622				
	15.8	14.0					0.639				
	29.4	23.6					0.409				
	29.4	23.4	0.8	23.4	2.7	0.413	0.413	-	6	3	-
	30.8	20.3					0.592				
	70.8	33.7	1.5	33.7	2.7	0.493	0.494	-	5	4	-
	70.8	36.5					0.432				
	70.8	35.7					0.451				
	8.7	10.2	1.0	10.3	5.4	0.648	0.664	-	13	5	-
	8.7	9.9					0.722				
	8.7	10.0					0.708				
	15.8	14.1	1.4	14.2	6.0	0.635	0.647	-	8	5	-
?	15.8	14.3					0.626				
?	15.8	13.8					0.672				
?	30.8	23.2	1.5	23.3	4.3	0.460	0.464	-	3	-	-
?	30.8	22.6					0.489				
3	30.8	21.9					0.530				
2	70.8	58.6					0.167				
2	70.8	39.6	2.2	39.7	5.6	0.362	0.366	-	-		-
.8	70.8	35.9					0.454				

2

TABLE 19 - Aerodynamic Characteristics as Determined from Model Drop Tests.
Square Ribbon Parachute (No. 22)

Drop No.	Type of Release	Ambient Air Temp. (° F)	Air Relative Humidity (%)	Barometric Pressure (In. of Hg)	Mass Density of Air ρ (Slugs/cu ft)	Total Weight W (Lbs)	Vertical Terminal Velocity V_v (Ft/Sec)	Average Horizontal Velocity V_h (Ft/Sec)	Average Resultant Velocity V_r (Ft/Sec)	Ave Gl An (De
529	V	58	69	28.75	0.00229	8.7	10.2			
530	V	58	69	28.75	0.00229	8.7	10.2	3.3	10.7	2(
531	V	74	76	28.53	0.00220	8.7	11.5			
532	V	58	69	28.75	0.00229	20.8	17.0	2.6	17.2	
533	V	58	69	28.75	0.00229	20.8	16.4			
534	V	74	76	28.53	0.00220	20.8	15.4			
535	V	58	69	28.75	0.00229	27.8	20.8	2.0	20.9	
536	V	74	76	28.53	0.00220	30.8	19.6			
537	V	74	76	28.53	0.00220	30.8	22.2			
538	V	80	70	28.61	0.00219	60.8	31.8	1.7	31.8	
539	V	71	79	28.68	0.00223	70.8	34.0			
540	V	71	79	28.68	0.00223	70.8	36.3			
541	H	74	76	28.58	0.00220	8.7	9.0			
542	H	74	76	28.58	0.00220	8.7	9.7	2.5	10.0	1(
543	H	74	76	28.58	0.00220	8.7	10.0			
544	H	81	74	28.58	0.00218	20.8	15.7			
545	H	81	74	28.58	0.00218	20.8	15.4	3.4	15.8	1(
546	H	81	74	28.58	0.00218	20.8	15.4			
547	H	78	76	28.58	0.00219	30.8	19.8			
548	H	78	76	28.58	0.00219	30.8	20.4	3.8	20.8	1(
549	H	78	76	28.58	0.00219	30.8	22.5			
550	H	71	79	28.68	0.00223	70.8	31.0			
551	H	71	79	28.68	0.00223	70.8	43.2			
552	H	71	79	28.68	0.00223	70.8	38.0	1.9	38.0	

Drop Tests.

2

rtical rminal locity V_v t/Sec)	Average Horizontal Velocity V_h (Ft/Sec)	Average Resultant Velocity V_r (Ft/Sec)	Average Glide Angle ϕ (Degrees)	C_D or	C_D e	Frequency of Oscillation (f) (Cycles/Sec)	Maximum Angle of Oscil-lation (Degrees)	Average or Constant Angle of Oscillation (Degrees)	Loga-rithmic Decrement
10.2					0.656				
10.2	3.3	10.7	20.5	0.559	0.656	-	13	5	-
11.5					0.538				
17.0	2.6	17.2	8.3	0.547	0.566	-	11	8	-
16.4					0.608				
15.4					0.718				
20.8	2.0	20.9	6.2	0.497	0.506	-	8	7	-
19.6					0.656				
22.2					0.512				
31.8	1.7	31.8	3.5	0.492	0.493	-	11	7	-
34.0					0.495				
36.3					0.434				
9.0					0.879				
9.7	2.5	10.0	15.1	0.687	0.756	-	16	10	-
10.0					0.712				
15.7					0.697				
15.4	3.4	15.8	12.8	0.671	0.725	-	9	5	-
15.4					0.725				
19.8					0.647				
20.4	3.8	20.8	10.5	0.575	0.608	-	9	6	-
22.5					0.500				
31.0					0.595				
43.2					0.307				
38.0	1.9	38.0	2.1	0.396	0.396	-	7	-	-

TABLE 20 - Aerodynamic Characteristics as Determined from Model Drop Tests.
Triangular Ribbon Parachute (No. 23)

Drop No.	Type of Release	Ambient Air Temp. (° F)	Air Relative Humidity (%)	Barometric Pressure (In. of Hg)	Mass Density of Air ρ (Slugs/cu ft)	Total Weight W (Lbs)	Vertical Terminal Velocity V_v (Ft/Sec)	Average Horizontal Velocity V_h (Ft/Sec)	Average Resultant Velocity V_r (Ft/Sec)	Aver Gli Ang ϕ (Deg
553	V	61	49	28.82	0.00228	8.73	9.2	1.3	9.3	12
554	V	61	49	28.82	0.00228	8.73	9.2			
555	V	61	49	28.82	0.00228	8.73	9.2			
556	V	61	49	28.82	0.00228	15.9	14.2			
557	V	56	54	28.82	0.00231	15.9	13.1			
558	V	56	54	28.82	0.00231	15.9	13.8	2.2	14.0	8
559	V	56	54	28.82	0.00231	35.9	25.8			
560	V	56	54	28.82	0.00231	35.9	21.4	3.5	21.6	10
561	V	56	54	28.82	0.00231	35.9	21.5			
562	V	64	62	28.95	0.00228	70.9	30.9			
563	V	64	62	28.95	0.00228	80.9	37.1	3.8	37.2	4
564	V	64	62	28.95	0.00228	80.9	44.9			
565	H	56	64	29.11	0.00233	8.73	9.5	3.2	10.0	18
566	H	56	64	29.11	0.00233	8.73	9.3			
567	H	69	57	28.95	0.00226	8.73	9.5			
568	H	69	57	28.95	0.00226	15.9	13.3			
569	H	64	62	28.95	0.00228	15.9	13.0	2.6	13.3	12
570	H	64	62	28.95	0.00228	15.9	13.0			
571	H	56	54	28.82	0.00231	35.9	20.9	3.4	21.2	9
572	H	56	54	28.82	0.00231	35.9	56.8			
573	H	56	54	28.82	0.00231	35.9	21.6			
574	H	64	62	28.95	0.00228	80.9	67.5			
575	H	70	57	29.00	0.00226	80.9	61.7			
576	H	70	57	29.00	0.00226	80.9	51.3	4.0	51.5	6

i from Model Drop Tests.

t)	Total Weight W (Lbs)	Vertical Terminal Velocity V_v (Ft/Sec)	Average Horizontal Velocity V_h (Ft/Sec)	Average Resultant Velocity V_r (Ft/Sec)	Average Glide Angle ϕ (Degrees)	C_D or	C_D e	Frequency of Oscillation (f) (Cycles/Sec)	Maximum Angle of Oscillation (Degrees)	Average or Constant Angle of Oscillation (Degrees)	Logarithmic Decrement
	8.73	9.2	1.3	9.3	12.6	0.778	0.815	0.222	12	8	0.663
	8.73	9.2					0.815				
	8.73	9.2					0.815				
	15.9	14.2					0.623				
	15.9	13.1					0.723				
	15.9	13.8	2.2	14.0	8.0	0.627	0.652	-	4	4	-
	35.9	25.9					0.420				
	35.9	21.4	3.5	21.6	10.4	0.588	0.610	-	-	-	-
	35.9	21.5					0.603	-			
	70.9	30.9					0.587				
	80.9	37.1	3.8	37.2	4.9	0.461	0.465	-	5	5	-
3	80.9	44.9					0.317				
5	8.73	9.5	3.2	10.0	18.7	0.639	0.747	0.267	12	8	-
5	8.73	9.3					0.780				
3	8.73	9.5					0.747				
6	15.9	13.3					0.717				
8	15.9	13.0	2.6	13.3	12.1	0.694	0.744	0.286	12	10	-
8	15.9	13.0					0.744				
1	35.9	20.9	3.4	21.2	9.0	0.613	0.639	0.308	11	8	-
1	35.9	56.8					0.086				
1	35.9	21.6					0.598				
8	80.9	67.5					0.140				
6	80.9	61.7					0.169				
6	80.9	51.3	4.0	51.5	6.7	0.241	0.245	-	-	-	-

2

TABLE 21 - Aerodynamic Characteristics as Determined from Model Drop Tests.
Exeter Type-12 Shaped Parachute (No.24)

Drop No.	Type of Release	Ambient Air Temp. (^{o} F)	Air Relative Humidity (%)	Barometric Pressure (In. of Hg)	Mass Density of Air ρ (Slugs/cu ft)	Total Weight W (Lbs)	Vertical Terminal Velocity V_v (Ft/Sec)	Average Horizontal Velocity V_h (Ft/Sec)	Average Resultant Velocity V_r (Ft/Sec)
577	V	46	81	28.24	0.00231	10.3	8.3		
578	V	46	81	28.24	0.00231	10.3	7.8	5.3	9.4
579	V	46	81	28.24	0.00231	15.3	11.4		
580	V	46	78	28.23	0.00231	20.3	12.8		
581	V	46	78	28.23	0.00231	20.3	13.6	6.5	15.1
582	V	46	78	28.23	0.00231	20.3	12.4		
583	V	46	78	28.23	0.00231	55.3	24.8		
584	V	46	78	28.23	0.00231	65.3	24.5	4.6	24.9
585	V	46	78	28.23	0.00231	65.3	25.2		
586	V	43	71	29.11	0.00238	201.9	39.8	3.1	39.8
587	V	43	71	29.11	0.00238	201.9	38.9		
588	V	43	71	29.11	0.00238	201.9	41.6		
589	H	46	81	28.24	0.00231	15.3	11.1		
590	H	46	81	28.24	0.00231	15.3	10.0		
591	H	46	81	28.24	0.00231	15.3	11.0	5.2	12.1
592	H	46	78	28.23	0.00231	20.3	12.5		
593	H	46	78	28.23	0.00231	20.3	13.6		
594	H	46	78	28.23	0.00231	20.3	12.3	7.5	14.4
595	H	46	78	28.23	0.00231	65.3	26.0	4.6	26.4
596	H	46	78	28.23	0.00231	65.3	26.3		
597	H	46	81	28.24	0.00231	65.3	26.3		
598	H								
599	H								
600	H								

Drop Tests.

2

ertical erminal elocity V_v Ft/Sec)	Average Horizontal Velocity V_h (Ft/Sec)	Average Resultant Velocity V_r (Ft/Sec)	Average Glide Angle ϕ (Degrees)	C_D or	C_D e	Frequency of Oscillation (f) Cycles/Sec)	Maximum Angle of Oscil-lation (Degrees)	Average or Constant Angle of Oscillation (Degrees)	Loga-rithmic Decrement
8.3					1.164				
7.8	5.3	9.4	35.5	0.740	1.320	-	10	8	-
11.4					0.917				
12.8					0.967				
13.6	6.5	15.1	27.2	0.618	0.857	0.267	19	15	-
12.4					1.029				
24.8					0.700				
24.5	4.6	24.9	11.1	0.804	0.847	0.333	37	30	-
25.2					0.801				
39.8	3.1	39.8	4.4	0.961	0.964	0.400	28	25	-
38.9					1.008				
41.6					0.882				
11.1					0.968				
10.0					1.192				
11.0	5.2	12.1	26.0	0.732	0.985	-	17	12	-
12.5					1.012				
13.6					0.856				
12.3	7.5	14.4	30.4	0.658	1.050	-	26	18	-
26.0	4.6	26.4	10.1	0.718	0.753	0.333	37	30	-
26.3					0.735				
26.3					0.735				

TABLE 22 - Aerodynamic Characteristics as Determined from Model Drop Tests.
Universal-Type Ribless Guide-Surface Parachute (No. 25)

Drop No.	Type of Release	Ambient Air Temp. (° F)	Air Relative Humidity (%)	Barometric Pressure (In. of Hg)	Mass Density of Air ρ (Slugs/cu ft)	Total Weight W (Lbs)	Vertical Terminal Velocity V_v (Ft/Sec)	Average Horizontal Velocity V_h (Ft/Sec)	Average Resultant Velocity V_r (Ft/Sec)	Av G A (D
601	V	46	55	28.84	0.00236	7.74	11.2	2.4	11.4	11
602	V	46	55	28.84	0.00236	7.74	11.7			
603	V	46	55	28.84	0.00236	7.74	11.8			
604	V	46	55	28.84	0.00236	14.9	15.5	1.5	15.6	
605	V	46	55	28.84	0.00236	14.9	15.2			
606	V	46	55	28.84	0.00236	14.9	16.3			
607	V	46	55	28.84	0.00236	29.9	22.8			
608	V	46	55	28.84	0.00236	39.9	27.1	2.3	27.2	
609	V	46	55	28.84	0.00236	39.9	27.1			
610	V	47	70	29.11	0.00237	131.5	47.3	2.3	47.3	
611	V	47	70	29.11	0.00237	131.5	46.3			
612	V	47	70	29.11	0.00237	131.5	45.8			
613	H	46	55	28.84	0.00236	7.74	11.6			
614	H	46	55	28.84	0.00236	7.74	11.4	2.2	11.6	1
615	H	46	55	28.84	0.00236	7.74	11.8			
616	H	46	55	28.84	0.00236	14.9	15.7	3.1	16.0	
617	H	46	55	28.84	0.00236	14.9	15.2			
618	H	46	55	28.84	0.00236	14.9	16.4			
619	H	46	55	28.84	0.00236	39.9	25.9			
620	H	46	55	28.84	0.00236	39.9	26.1			
621	H	46	55	28.84	0.00236	39.9	25.3	0.4	25.3	0
622	H	51	73	28.60	0.00231	131.5	49.8	1.0	49.8	3
623	H									
624	H									

d from Model Drop Tests.
achute (No. 25)

2

t)	Total Weight W (Lbs)	Vertical Terminal Velocity V_v (Ft/Sec)	Average Horizontal Velocity V_h (Ft/Sec)	Average Resultant Velocity V_r (Ft/Sec)	Average Glide Angle ϕ (Degrees)	$C_{D_{or}}$	C_{D_o}	Frequency of Oscillation (f) (Cycles/Sec)	Maximum Angle of Oscillation (Degrees)	Average or Constant Angle of Oscillation (Degrees)	Logarithmic Decrement
	7.74	11.2	2.4	11.4	11.3	0.445	0.471	0.235	10	8	-
	7.74	11.7					0.432				
	7.74	11.8					0.424				
	14.9	15.5	1.5	15.6	2.9	0.466	0.473	0.308	19	10	-
	14.9	15.2					0.492				
	14.9	16.3					0.427				
	29.9	22.8					0.439				
	39.9	27.1	2.3	27.2	4.9	0.411	0.415	-	7	4	-
	39.9	27.1					0.415				
	131.5	47.3	2.3	47.3	2.9	0.447	0.447	-	6	3	-
	131.5	46.3					0.465				
	131.5	45.8					0.477				
	7.74	11.6					0.439				
	7.74	11.4	2.2	11.6	10.1	0.432	0.454	0.267	10	8	-
	7.74	11.8					0.424				
	14.9	15.7	3.1	16.0	9.1	0.438	0.460	0.250	18	15	-
	14.9	15.2					0.492				
	14.9	16.4					0.422				
	39.9	25.9					0.454				
	39.9	26.1					0.447				
	39.9	25.3	0.4	25.3	0.9	0.476	0.476	-	16	5	-
	131.5	49.8	1.0	49.8	3.2	0.412	0.413	-	-	-	-

TABLE 23 - Aerodynamic Characteristics as Determined from Model Drop Tests.
Personnel-Type Guide-Surface Parachute (No. 26)

Drop No.	Type of Release	Ambient Air Temp. (° F)	Air Relative Humidity (%)	Barometric Pressure (In. of Hg)	Mass Density of Air ρ (Slugs/cu ft)	Total Weight W (Lbs)	Vertical Terminal Velocity V_v (Ft/Sec)	Average Horizontal Velocity V_h (Ft/Sec)	Average Resultant Velocity V_r (Ft/Sec)	Av G A (D
625	V	48	55	29.06	0.00236	15.1	11.9	5.2	13.0	
626	V	48	55	29.06	0.00236	15.1	12.1			
627	V	48	55	29.06	0.00236	15.1	12.0			
628	V	48	55	29.06	0.00236	20.1	13.8	5.8	15.0	
629	V	48	55	29.06	0.00236	20.1	13.8			
630	V	48	55	29.06	0.00236	20.1	14.3			
631	V	48	55	29.06	0.00236	50.1	22.6	4.1	23.0	
632	V	48	55	29.06	0.00236	50.1	22.7			
633	V	48	55	29.06	0.00236	50.1	24.5			
634	V	47	70	29.11	0.00237	131.7	38.0	3.0	38.1	
635	V	47	70	29.11	0.00237	131.7	37.1			
636	V	47	70	29.11	0.00237	131.7	37.4			
637	H	55	87	28.91	0.00232	16.2	11.8	4.0	12.5	
638	H	55	87	28.91	0.00232	16.2	14.0			
639	H	55	87	28.91	0.00232	16.2	12.0			
640	H	55	87	28.91	0.00232	21.2	14.1	5.6	15.2	
641	H	55	87	28.91	0.00232	21.2	13.9			
642	H	55	87	28.91	0.00232	21.2	13.6			
643	H	55	87	28.91	0.00232	51.2	21.4			
644	H	55	87	28.91	0.00232	51.2	21.9			
645	H	55	87	28.91	0.00232	51.2	23.1	4.7	23.6	
646	H	56	75	28.60	0.00228	131.7	39.9	6.2	40.3	
647	H									
648	H									

Drop Tests.

2

·tical ·minal locity V_v t/Sec)	Average Horizontal Velocity V_h (Ft/Sec)	Average Resultant Velocity V_r (Ft/Sec)	Average Glide Angle ϕ (Degrees)	C_D or	C_D o	Frequency of Oscillation (f) (Cycles/Sec)	Maximum Angle of Oscil-lation (Degrees)	Average or Constant Angle of Oscillation (Degrees)	Loga-rithmic Decrement
11.9	5.2	13.0	17.3	0.651	0.815	0.21	21	15	-
12.1					0.787				
12.0					0.801				
13.8	5.8	15.0	17.0	0.652	0.808	0.267	18	10	-
13.8					0.808				
14.3					0.751				
22.6	4.1	23.0	8.9	0.713	0.749	0.236	28	20	-
22.7					0.742				
24.5					0.637				
38.0	3.0	38.1	5.6	0.687	0.695	0.40	25	22	-
37.1					0.727				
37.4					0.717				
11.8	4.0	12.5	18.5	0.762	0.902	-	10	5	-
14.0					0.640				
12.0					0.872				
14.1	5.6	15.2	21.9	0.661	0.827	0.25	22	20	-
13.9					0.851				
13.6					0.889				
21.4					0.867				
21.9					0.828				
23.1	4.7	23.6	11.6	0.699	0.744	0.308	31°	25	-
39.9	6.2	40.3	6.9	0.634	0.652	0.50	28	18	-

TABLE 24 - Aerodynamic Characteristics as Determined from Model Drop Tests.
FIST Ribbon Parachute (20% Total Porosity) (No. 27)

Drop No.	Type of Release	Ambient Air Temp. (° F)	Air Relative Humidity (%)	Barometric Pressure (In. of Hg)	Mass Density of Air ρ (Slugs/cu ft)	Total Weight W (Lbs)	Vertical Terminal Velocity V_v (Ft/Sec)	Average Horizontal Velocity V_h (Ft/Sec)	Average Resultant Velocity V_r (Ft/Sec)
649	V	40	65	29.08	0.00240	10.9	11.0		
650	V	40	65	29.08	0.00240	10.9	11.2		
651	V	40	65	29.08	0.00240	10.9	11.2	1.9	11.4
652	V	40	65	29.08	0.00240	20.9	16.4	2.1	16.5
653	V	40	65	29.08	0.00240	20.9	16.5		
654	V	40	65	29.08	0.00240	20.9	16.2		
655	V	40	65	29.08	0.00240	50.9	27.0	1.2	27.0
656	V	40	65	29.08	0.00240	50.9	27.5		
657	V	54	66	29.08	0.00234	50.9	27.4		
658	V	54	66	29.08	0.00234	127.5	44.7	0	44.7
659	V	54	66	29.08	0.00234	127.5	44.8		
660	V	54	66	29.08	0.00234	127.5	43.5		
661	H	52	70	29.08	0.00234	12.0	12.0	2.0	12.2
662	H	52	70	29.08	0.00234	12.0	12.3		
663	H	52	70	29.08	0.00234	12.0	12.2		
664	H	52	70	29.08	0.00234	22.0	16.8	1.9	16.9
665	H	52	70	29.08	0.00234	22.0	16.7		
666	H	52	70	29.08	0.00234	22.0	16.6		
667	H	52	70	29.08	0.00234	52.0	27.9	2.2	28.0
668	H	52	70	29.08	0.00234	52.0	27.7		
669	H	52	70	29.08	0.00234	52.0	29.4		
670	H	55	87	28.91	0.00232	127.5	48.8	3.4	48.9
671	H	55	87	28.91	0.00232	127.5	46.7		
672	H	55	87	28.91	0.00232	127.5	46.3		

ained from Model Drop Tests.
osity) (No. 27)

ity r cu ft)	Total Weight W (Lbs)	Vertical Terminal Velocity V_v (Ft/Sec)	Average Horizontal Velocity V_h (Ft/Sec)	Average Resultant Velocity V_r (Ft/Sec)	Average Glide Angle ϕ (Degrees)	$C_{D_{or}}$	C_{D_o}	Frequency of Oscillation (f) (Cycles/Sec)	Maximum Angle of Oscillation (Degrees)	Average or Constant Angle of Oscillation (Degrees)	Logarithmic Decrement
240	10.9	11.0					0.687				
240	10.9	11.2					0.664				
240	10.9	11.2	1.9	11.4	9.5	0.632	0.663	-	5	3	-
240	20.9	16.4	2.1	16.5	7.5	0.580	0.592	-	8	5	-
240	20.9	16.5					0.585				
240	20.9	16.2					0.607				
240	50.9	27.0	1.2	27.0	3.2	0.532	0.532	-	4	2	-
240	50.9	27.5					0.514				
234	50.9	27.4					0.517				
234	127.5	44.7	0	44.7	0.7	0.499	0.499	-	0	0	-
234	127.5	44.8					0.497				
234	127.5	43.5					0.527				
234	12.0	12.0	2.0	12.2	8.9	0.624	0.652	-	13	8	-
234	12.0	12.3					0.620				
234	12.0	12.2					0.631				
234	22.0	16.8	1.9	16.9	6.4	0.599	0.610	-	9	4	-
234	22.0	16.7					0.617				
234	22.0	16.6					0.625				
234	52.0	27.9	2.2	28.0	3.3	0.518	0.522	-	8	4	-
234	52.0	27.7					0.530				
234	52.0	29.4					0.471				
232	127.5	48.8	3.4	48.9	8.0	0.417	0.422	-	-	-	-
232	127.5	46.7					0.461				
232	127.5	46.3					0.469				

TABLE 25 - Aerodynamic Characteristics as Determined from Model Drop Tests.
FIST Ribbon Parachute (25% Total Porosity) (No. 28)

Drop No.	Type of Release	Ambient Air Temp. (° F)	Air Relative Humidity (%)	Barometric Pressure (In. of Hg)	Mass Density of Air ρ (Slugs/cu ft)	Total Weight W (Lbs)	Vertical Terminal Velocity V_v (Ft/Sec)	Average Horizontal Velocity V_h (Ft/Sec)	Average Resultant Velocity V_r (Ft/Sec)	Ave Gl Ar (De
673	V	58	77	28.91	0.00230	8.65	11.2	0.4	11.2	2
674	V	58	77	28.91	0.00230	8.65	11.1			
675	V	58	77	28.91	0.00230	8.65	10.7			
676	V	58	77	28.91	0.00230	16.9	15.3	1.2	15.4	3
677	V	58	77	28.91	0.00230	16.9	15.4			
678	V	58	77	28.91	0.00230	16.9	15.4			
679	V	58	77	28.91	0.00230	41.9	25.2	0.8	25.2	1
680	V	58	77	28.91	0.00230	41.9	25.8			
681	V	58	77	28.91	0.00230	41.9	26.3			
682	V	58	77	28.91	0.00230	91.9	38.5	0	38.5	
683	V	58	77	28.91	0.00230	91.9	39.3			
684	V	58	77	28.91	0.00230	91.9	38.2			
685	H	57	83	28.91	0.00231	8.65	10.8			
686	H	57	83	28.91	0.00231	8.65	10.8	2.1	11.0	
687	H	57	83	28.91	0.00231	8.65	10.5			
688	H	57	83	28.91	0.00231	16.9	15.2			
689	H	57	83	28.91	0.00231	16.9	15.5	1.4	15.6	
690	H	57	83	28.91	0.00231	16.9	15.5			
691	H	57	83	28.91	0.00231	41.9	26.1			
692	H	57	83	28.91	0.00231	41.9	25.9			
693	H	57	83	28.91	0.00231	41.9	26.9	2.7	27.0	
694	H	58	77	28.91	0.00230	91.9	41.1			
695	H	58	77	28.91	0.00230	91.9	39.5			
696	H	58	77	28.91	0.00230	91.9	40.9	2.9	41.0	

Drop Tests.

2

rtical rminal locity V_v Ft/Sec)	Average Horizontal Velocity V_h (Ft/Sec)	Average Resultant Velocity V_r (Ft/Sec)	Average Glide Angle ϕ (Degrees)	C_D or	C_D o	Frequency of Oscillation (f) (Cycles/Sec)	Maximum Angle of Oscillation (Degrees)	Average or Constant Angle of Oscillation (Degrees)	Logarithmic Decrement
11.2	0.4	11.2	2.2	0.554	0.555	-	7	4	-
11.1					0.565				
10.7					0.609				
15.3	1.2	15.4	3.6	0.572	0.581	-	6	4	-
15.4					0.574				
15.4					0.574				
25.2	0.8	25.2	1.6	0.530	0.531	-	3	2	-
25.8					0.506				
26.3					0.487				
38.5	0	38.5	0.9	0.498	0.498	-	3	1	-
39.3					0.478				
38.2					0.506				
10.8					0.595				
10.8	2.1	11.0	10.4	0.563	0.595	0.286	20	10	0.693
10.5					0.628				
15.2					0.586				
15.5	1.4	15.6	4.1	0.555	0.564	-	7	3	-
15.5					0.564				
26.1					0.492				
25.9					0.500				
26.9	2.7	27.0	5.3	0.458	0.463	-	16	16	-
41.1					0.437				
39.5					0.473				
40.9	2.9	41.0	6.0	0.437	0.441	-	-	-	-

TABLE 26 - Aerodynamic Characteristics as Determined from Model Drop Tests.
Ring-Slot Parachute (10% Total Porosity)(No. 29)

Drop No.	Type of Release	Ambient Air Temp. (° F)	Air Relative Humidity (%)	Barometric Pressure (In. of Hg)	Mass Density of Air ρ (Slugs/cu ft)	Total Weight W (Lbs)	Vertical Terminal Velocity V_v (Ft/Sec)	Average Horizontal Velocity V_h (Ft/Sec)	Average Resultant Velocity V_r (Ft/Sec)	Ave Gl Ar (De
697	V	52	68	28.90	0.00233	10.9	9.8	4.4	10.7	2
698	V	52	68	28.90	0.00233	15.9	12.4			
699	V	52	68	28.90	0.00233	15.9	12.5			
700	V	52	68	28.90	0.00233	20.9	14.3	3.6	14.7	1
701	V	52	68	28.90	0.00233	20.9	14.5			
702	V	52	68	28.90	0.00233	20.9	14.6			
703	V	52	68	28.90	0.00233	50.9	24.1	3.8	24.4	
704	V	52	68	28.90	0.00233	50.9	23.8			
705	V	52	68	28.90	0.00233	50.9	22.7			
706	V	47	70	29.11	0.00237	132.5	38.6	4.0	38.8	
707	V	47	70	29.11	0.00237	132.5	45.3			
708	V	47	70	29.11	0.00237	132.5	39.1			
709	H	50	70	28.90	0.00234	15.9	12.6	3.4	13.1	1
710	H	50	70	28.90	0.00234	15.9	12.2			
711	H	50	70	28.90	0.00234	15.9	12.2			
712	H	50	70	28.90	0.00234	20.9	15.2			
713	H	50	70	28.90	0.00234	20.9	14.4			
714	H	50	70	28.90	0.00234	20.9	14.5	3.7	14.9	1
715	H	50	70	28.90	0.00234	50.9	24.6			
716	H	50	70	28.90	0.00234	50.9	22.7			
717	H	50	70	28.90	0.00234	50.9	24.5	2.8	24.6	
718	H	51	73	28.60	0.00231	132.5	41.3	2.2	41.3	
719	H									
720	H									

i from Model Drop Tests.
(No. 29)

2

PAGE I-127
MODEL AFTR-5867
GER- 5108
REF NO. R-621

t)	Total Weight W (Lbs)	Vertical Terminal Velocity V_v (Ft/Sec)	Average Horizontal Velocity V_h (Ft/Sec)	Average Resultant Velocity V_r (Ft/Sec)	Average Glide Angle ϕ (Degrees)	C_D or	C_D o	Frequency of Oscillation (f) (Cycles/Sec)	Maximum Angle of Oscil-lation (Degrees)	Average or Constant Angle of Oscillation (Degrees)	Loga-rithmic Decrement
	10.9	9.8	4.4	10.7	24.9	0.687	0.902	0.222	27	20	0.412
	15.9	12.4					0.822				
	15.9	12.5					0.809				
	20.9	14.3	3.6	14.7	14.4	0.744	0.812	0.286	28	25	Neg
	20.9	14.5					0.789				
	20.9	14.6					0.780				
	50.9	24.1	3.8	24.4	8.7	0.671	0.696	-	7	4	-
	50.9	23.8					0.714				
	50.9	22.7					0.785				
	132.5	38.6	4.0	38.8	5.5	0.686	0.696	-	15	12	-
	132.5	45.3					0.505				
	132.5	39.1					0.678				
	15.9	12.6	3.4	13.1	14.7	0.710	0.792	0.235	16	12	0.266
	15.9	12.2					0.846				
	15.9	12.2					0.846				
	20.9	15.2					0.716				
	20.9	14.4					0.797				
	20.9	14.5	3.7	14.9	14.1	0.722	0.787	0.308	30	25	Neg
	50.9	24.6					0.665				
	50.9	22.7					0.781				
4	50.9	24.5	2.8	24.6	6.6	0.661	0.671	0.333	20	18	0.447
1	132.5	41.3	2.2	41.3	4.6	0.621	0.623	-	-	-	-

TABLE 27 - Aerodynamic Characteristics as Determined from Model Drop Tests.
Ring-Slot Parachute (13.5% Total Porosity) (No. 30)

Drop No.	Type of Release	Ambient Air Temp. (° F)	Air Relative Humidity (%)	Barometric Pressure (In. of Hg)	Mass Density of Air ρ (Slugs/cu ft)	Total Weight W (Lbs)	Vertical Terminal Velocity V_v (Ft/Sec)	Average Horizontal Velocity V_h (Ft/Sec)	Average Resultant Velocity V_r (Ft/Sec)	Aver Gli Ang φ (Deg
721	V	48	71	28.90	0.00235	10.9	10.5	2.6	10.9	16
722	V	48	71	28.90	0.00235	10.9	10.1			
723	V	48	71	28.90	0.00235	10.9	10.2			
724	V	50	54	28.84	0.00234	20.9	15.4			
725	V	50	54	28.84	0.00234	20.9	14.6	4.0	15.1	14
726	V	50	54	28.84	0.00234	20.9	15.5			
727	V	50	54	28.84	0.00234	50.9	24.9	1.4	25.0	4
728	V	50	54	28.84	0.00234	50.9	24.5			
729	V	50	54	28.84	0.00234	50.9	22.9			
730	V	47	70	29.11	0.00237	132.5	39.8			
731	V	47	70	29.11	0.00237	132.5	41.7			
732	V	47	70	29.11	0.00237	132.5	38.0	1.2	38.0	2
733	H	50	54	28.84	0.00234	10.9	10.3			
734	H	50	54	28.84	0.00234	10.9	10.2	3.4	10.7	19
735	H	50	54	28.84	0.00234	10.9	10.1			
736	H	50	54	28.84	0.00234	20.9	14.2			
737	H	50	54	28.84	0.00234	20.9	14.3	2.4	14.5	9
738	H	50	54	28.84	0.00234	20.9	14.8			
739	H	50	54	28.84	0.00234	50.9	24.1	0.8	24.1	1
740	H	44	62	29.08	0.00238	50.9	24.2			
741	H	44	62	29.08	0.00238	50.9	22.9			
742	H	57	75	28.60	0.00228	132.5	47.7	2.5	47.8	6
743	H									
744	H									

Drop Tests.

2

rtical rminal locity V_v t/Sec)	Average Horizontal Velocity V_h (Ft/Sec)	Average Resultant Velocity V_r (Ft/Sec)	Average Glide Angle ϕ (Degrees)	C_D or	C_D o	Frequency of Oscillation (f) (Cycles/Sec)	Maximum Angle of Oscil-lation (Degrees)	Average or Constant Angle of Oscillation (Degrees)	Loga-rithmic Decrement
10.5	2.6	10.9	16.2	0.685	0.769	0.238	15	12	Neg
10.1					0.830				
10.2					0.814				
15.4					0.688				
14.6	4.0	15.1	14.2	0.694	0.766	0.242	26	20	Neg
15.5					0.679				
24.9	1.4	25.0	4.4	0.634	0.641	-	8	4	-
24.5					0.662				
22.9					0.758				
39.8					0.645				
41.7					0.587				
38.0	1.2	38.0	2.5	0.707	0.707	0.50	16	10	-
10.3					0.803				
10.2	3.4	10.7	19.4	0.701	0.818	0.138	20	16	Neg
10.1					0.834				
14.2					0.810				
14.3	2.4	14.5	9.5	0.765	0.799	-	13	7	-
14.8					0.745				
24.1	0.8	24.1	1.8	0.684	0.684	-	4	2	-
24.2					0.667				
22.9					0.746				
47.7	2.5	47.8	6.6	0.461	0.467	-	-	-	-

TABLE 28 - Aerodynamic Characteristics as Determined from Model Drop Tests.
Ring-Slot Parachute (17% Total Porosity) (No. 31)

Drop No.	Type of Release	Ambient Air Temp. (° F)	Air Relative Humidity (%)	Barometric Pressure (In. of Hg)	Mass Density of Air ρ (Slugs/cu ft)	Total Weight W (Lbs)	Vertical Terminal Velocity V_v (Ft/Sec)	Average Horizontal Velocity V_h (Ft/Sec)	Average Resultant Velocity V_r (Ft/Sec)	Ave Gl An (De
745	V	50	70	28.90	0.00234	15.9	13.4	2.6	13.6	1
746	V	50	70	28.90	0.00234	10.9	10.6			
747	V	50	70	28.90	0.00234	10.9	10.5			
748	V	50	70	28.90	0.00234	20.9	15.2	2.3	15.4	
749	V	50	70	28.90	0.00234	20.9	15.3			
750	V	50	70	28.90	0.00234	20.9	15.3			
751	V	50	70	28.90	0.00234	40.9	22.2	1.7	22.3	
752	V	50	70	28.90	0.00234	50.9	24.3			
753	V	50	70	28.90	0.00234	50.9	24.8			
754	V	47	70	29.11	0.00237	132.5	44.9	1.3	44.9	
755	V	47	70	29.11	0.00237	132.5	42.7			
756	V	47	70	29.11	0.00237	132.5	42.4			
757	H	48	71	28.90	0.00235	10.9	10.7			
758	H	48	71	28.90	0.00235	10.9	10.6	2.8	11.0	1
759	H	48	71	28.90	0.00235	10.9	10.1			
760	H	48	71	28.90	0.00235	20.9	15.4	2.8	15.6	
761	H	48	71	28.90	0.00235	20.9	15.0			
762	H	48	71	28.90	0.00235	20.9	15.4			
763	H	48	71	28.90	0.00235	50.9	24.4			
764	H	48	71	28.90	0.00235	50.9	24.2			
765	H	48	71	28.90	0.00235	50.9	24.6	3.0	24.8	
766	H	51	73	28.60	0.00231	132.5	44.0	1.9	44.0	
767	H									
768	H									

d from Model Drop Tests.
(No. 31)

2

PAGE I-129
MODEL AETR-5867
GER 5108
REF NO. R-621

t)	Total Weight W (Lbs)	Vertical Terminal Velocity V_v (Ft/Sec)	Average Horizontal Velocity V_h (Ft/Sec)	Average Resultant Velocity V_r (Ft/Sec)	Average Glide Angle ϕ (Degrees)	$C_{D_{or}}$	C_{D_o}	Frequency of Oscillation (f) (Cycles/Sec)	Maximum Angle of Oscillation (Degrees)	Average or Constant Angle of Oscillation (Degrees)	Logarithmic Decrement
	15.9	13.4	2.6	13.6	11.9	0.657	0.692	0.20	10	9	-
	10.9	10.6					0.758				
	10.9	10.5					0.772				
	20.9	15.2	2.3	15.4	7.5	0.682	0.707	0.25	11	9	-
	20.9	15.3					0.698				
	20.9	15.3					0.698				
	40.9	22.2	1.7	22.3	5.2	0.639	0.648	-	10	6	-
	50.9	24.3					0.673				
	50.9	24.8					0.647				
	132.5	44.9	1.3	44.9	1.5	0.507	0.507	-	9	4	-
	132.5	42.7					0.560				
	132.5	42.4					0.569				
5	10.9	10.7					0.741				
5	10.9	10.6	2.8	11.0	15.2	0.676	0.755	0.25	14	12	-
5	10.9	10.1					0.831				
5	20.9	15.4	2.8	15.6	9.8	0.658	0.686	0.235	16	16	-
5	20.9	15.0					0.723				
5	20.9	15.4					0.686				
5	50.9	24.4					0.664				
5	50.9	24.2					0.676				
5	50.9	24.6	3.0	24.8	6.2	0.639	0.654	-	6	-	-
1	132.5	44.0	1.9	44.0	7.5	0.538	0.542	-	-	-	-

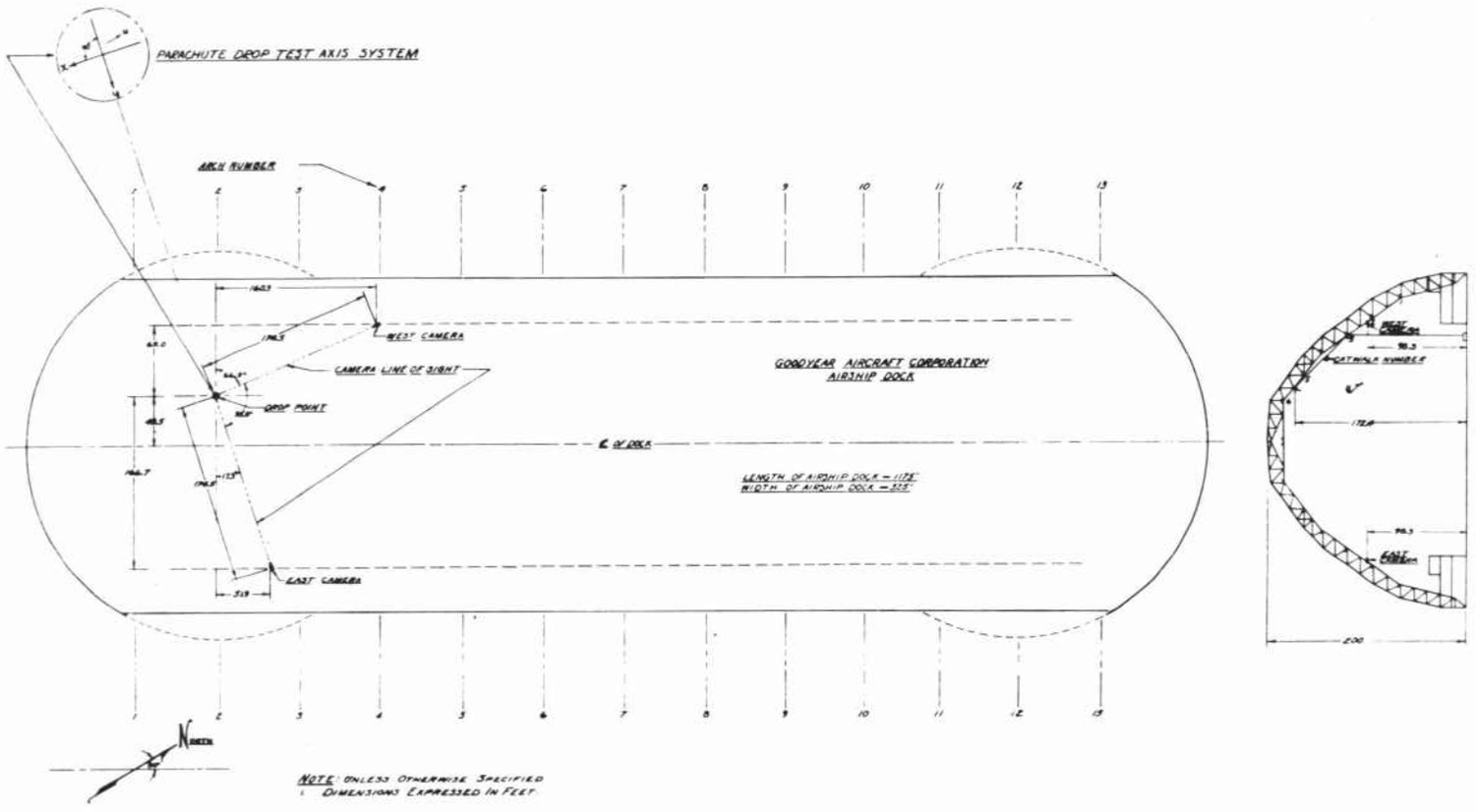

Figure 1 - Schematic view of parachute drop-test setup in the Goodyear Aircraft Corporation airship dock showing characteristic dimensions.

a) Vertical release condition

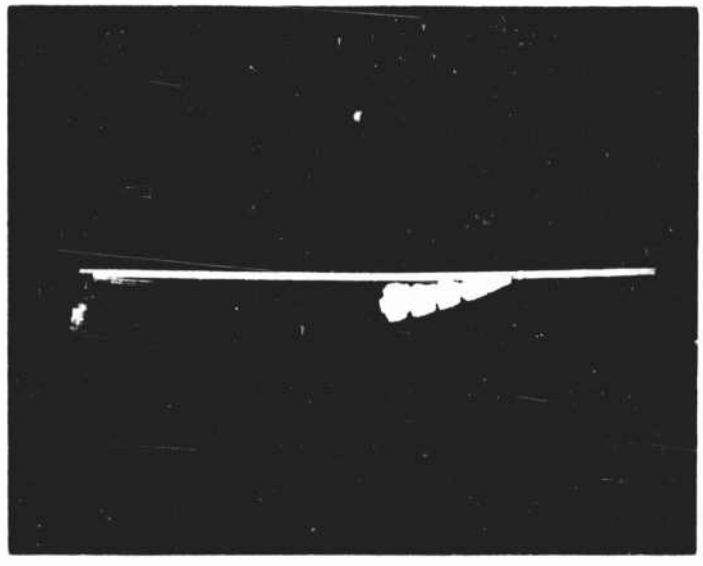

b) Horizontal release condition

Figure 2 - View of parachute hoist bar assembly showing the two methods of release employed in the drop-test program.

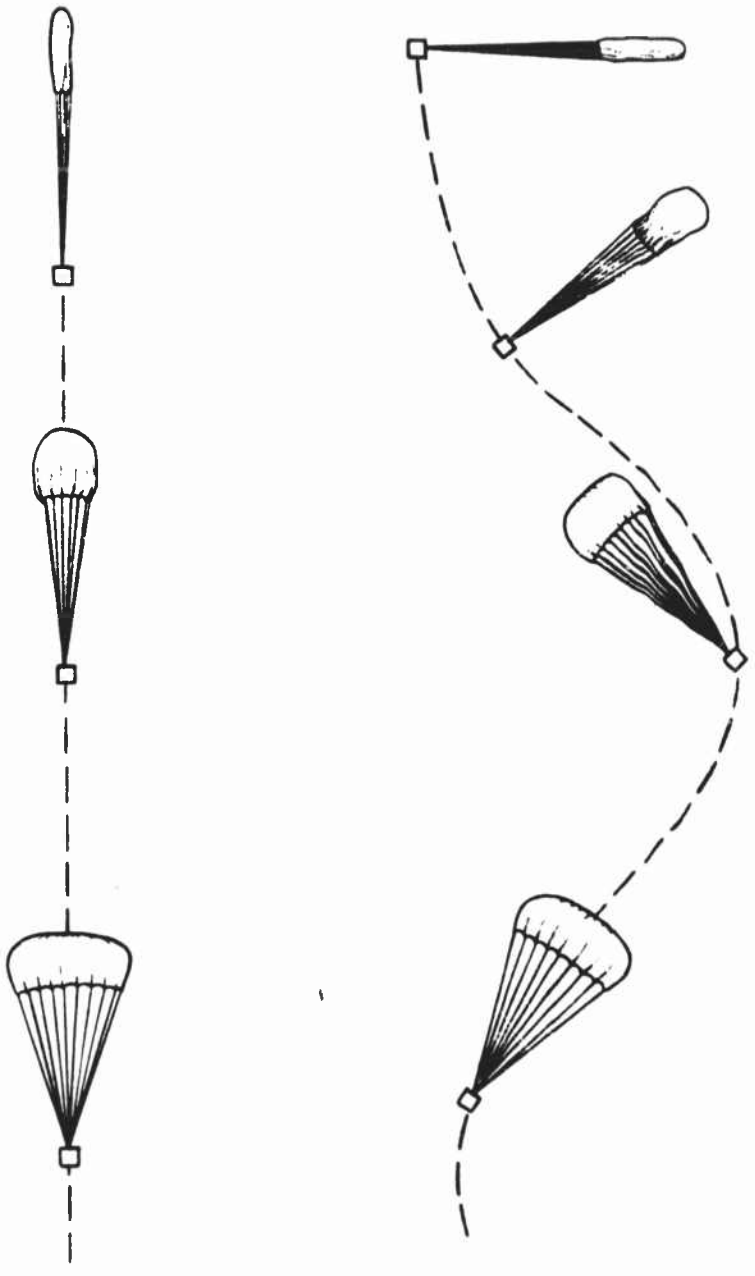

Vertical Release

Horizontal Release

Figure 3 - Schematic diagram of the two release conditions as employed in the parachute drop-test program.

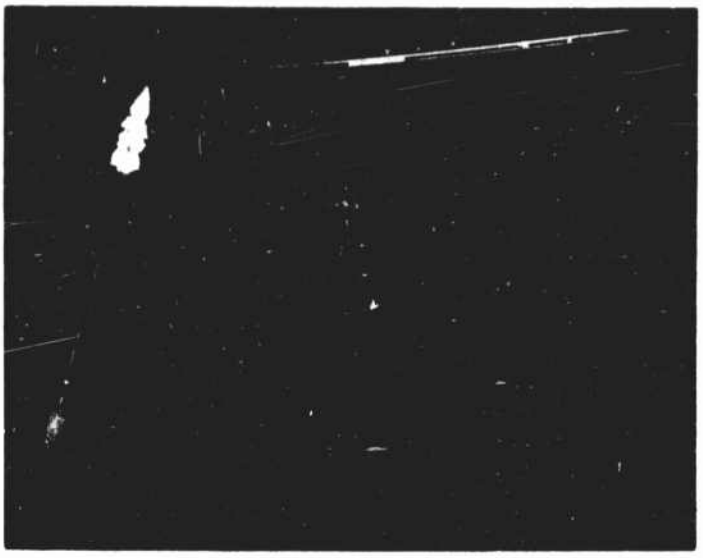

a) Vertical release condition

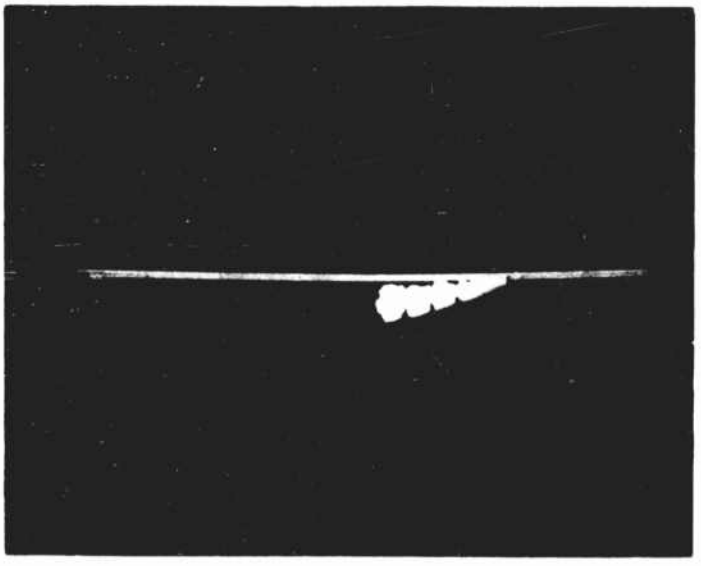

b) Horizontal release condition

Figure 2 - View of parachute hoist bar assembly showing the two methods of release employed in the drop-test program.

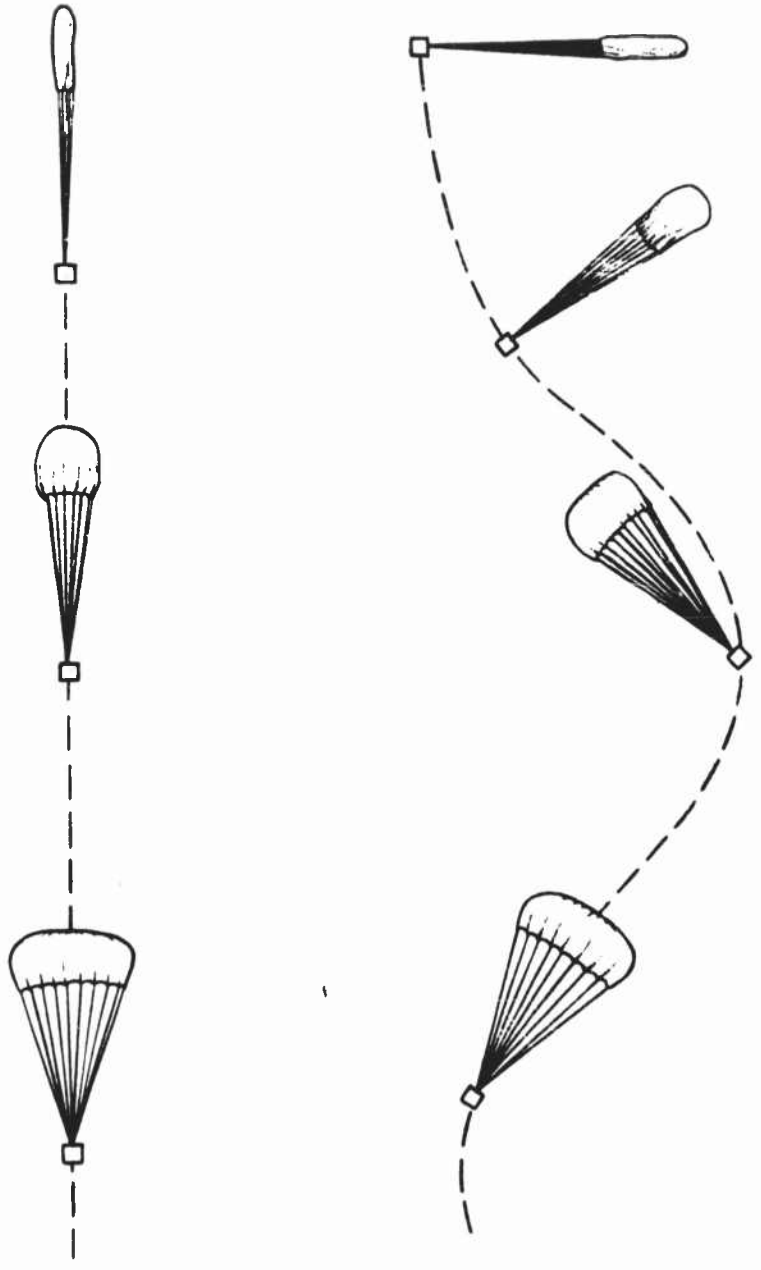

Vertical Release

Horizontal Release

Figure 3 - Schematic diagram of the two release conditions as employed in the parachute drop-test program.

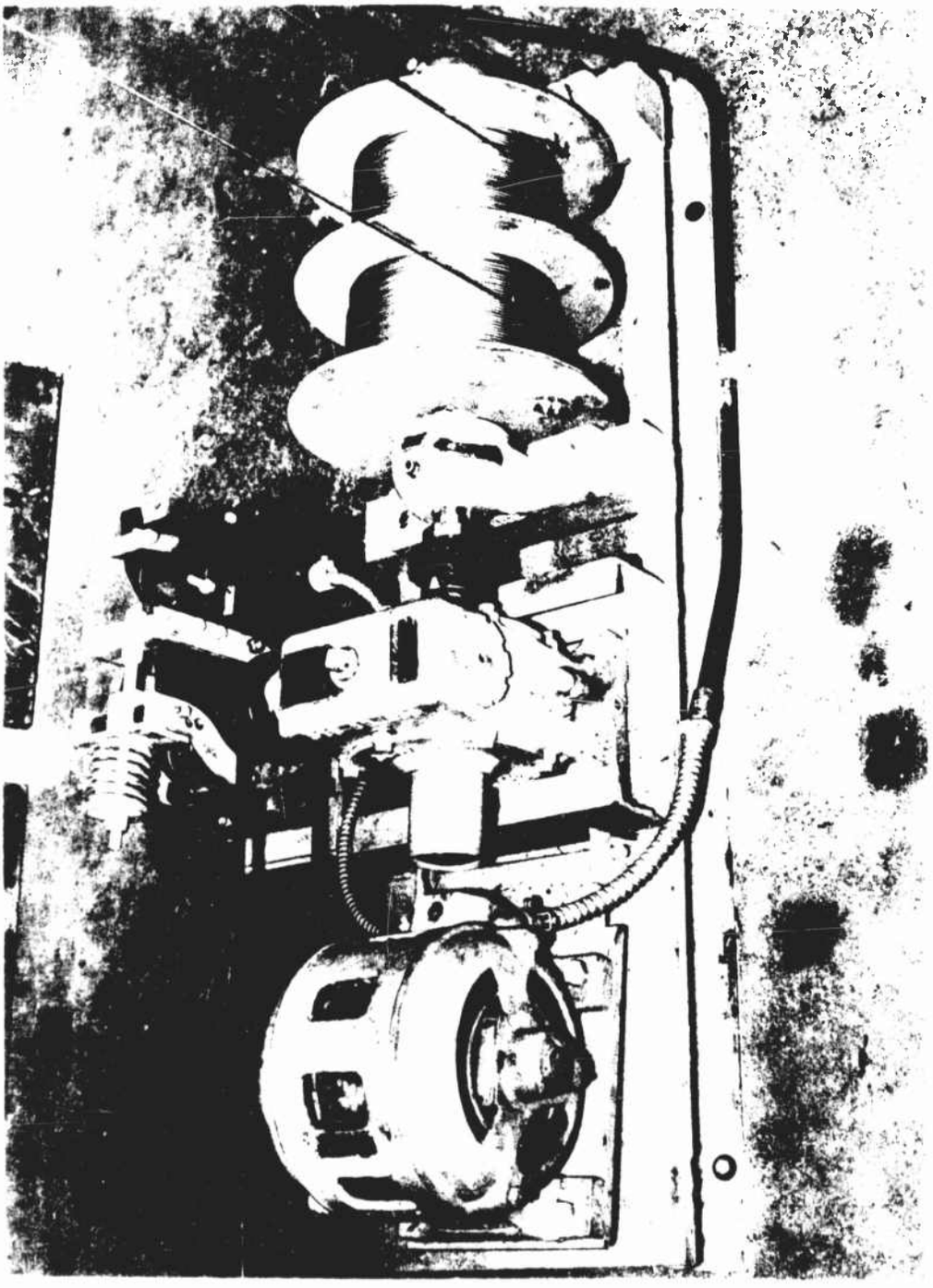

Figure 4 - View of hoist-drive mechanism for the parachute drop-test program.

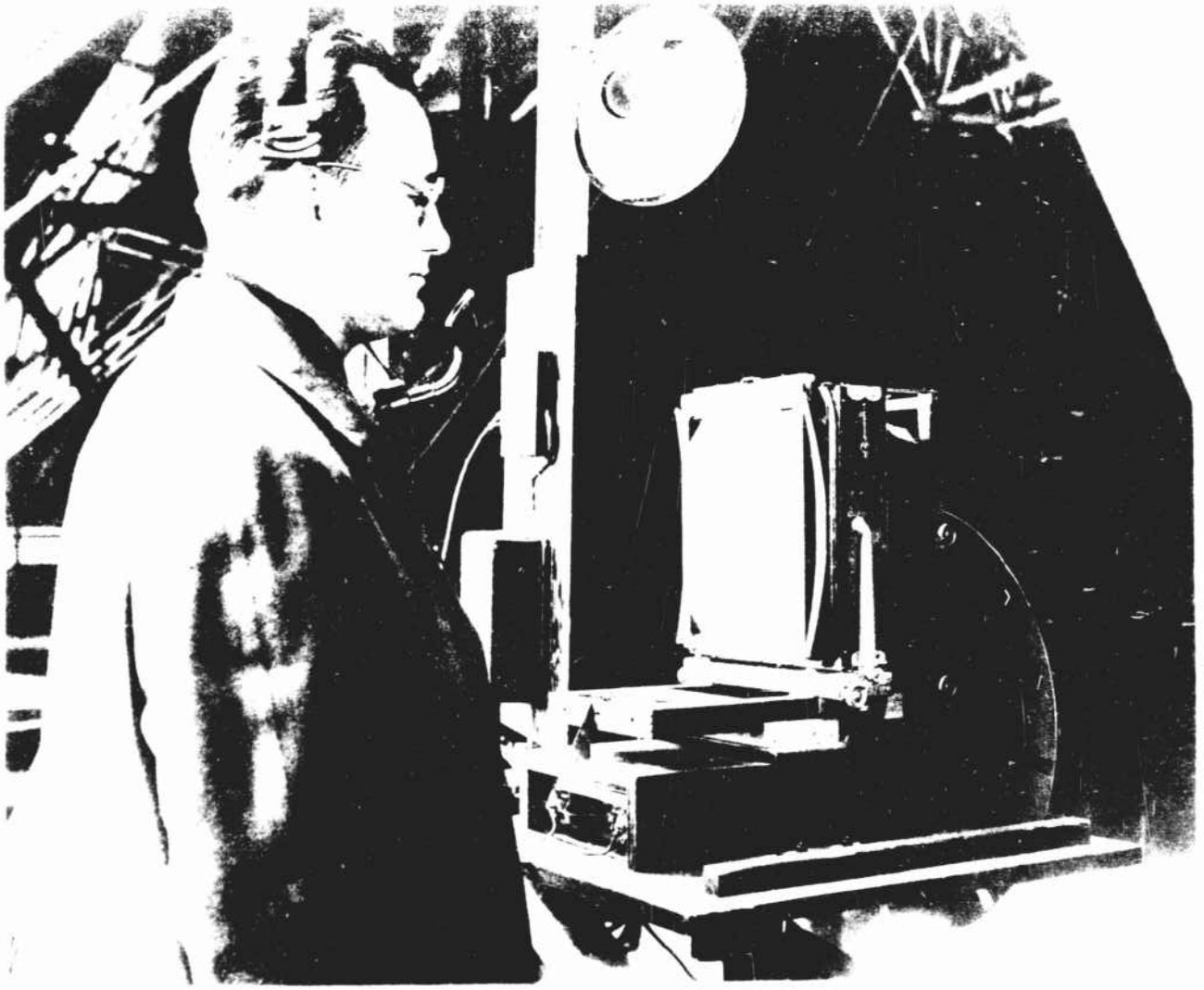

Figure 5 - View of east camera installation in the GAC airship dock.

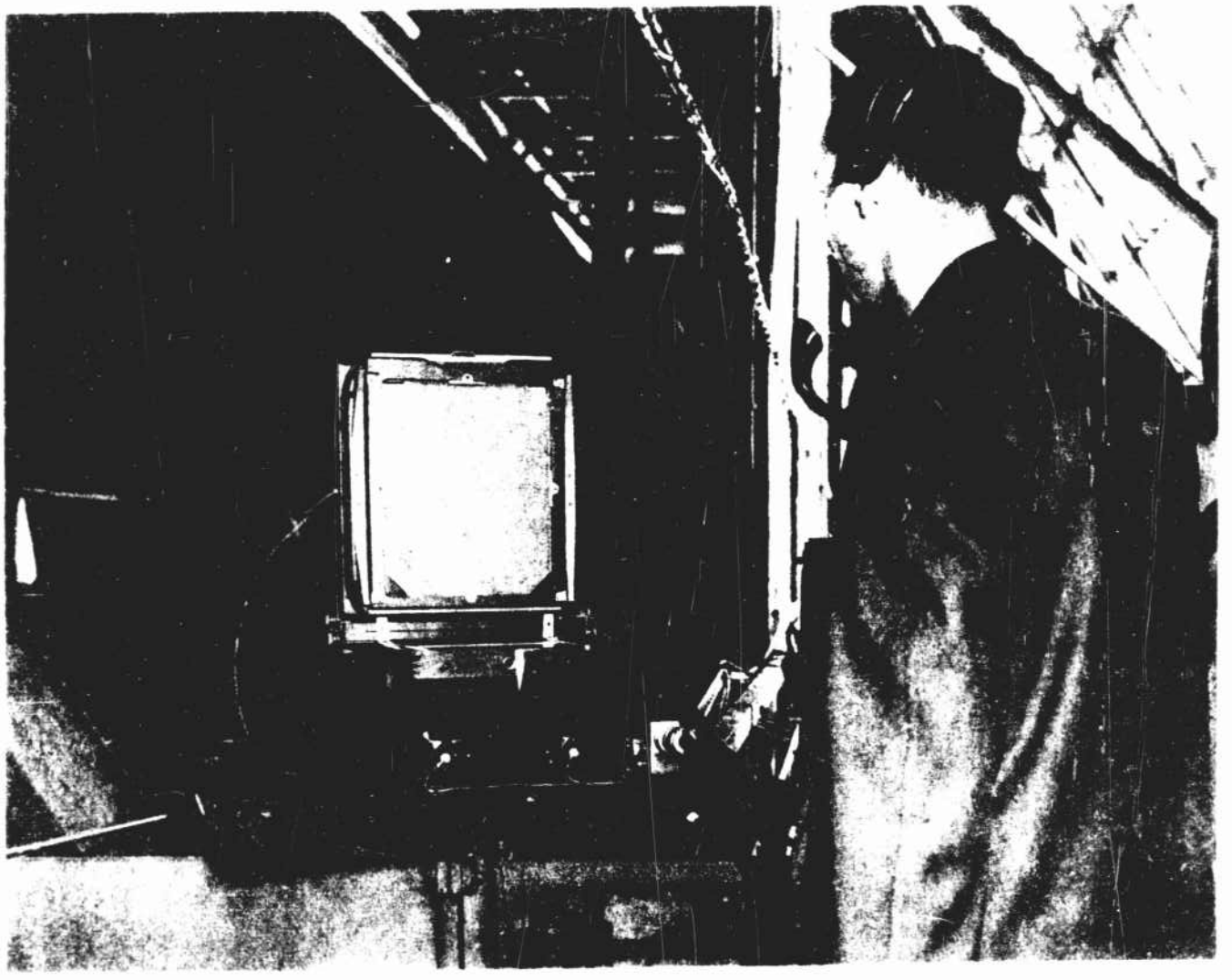

Figure 6 - View of west camera installation in the GAC airship dock.

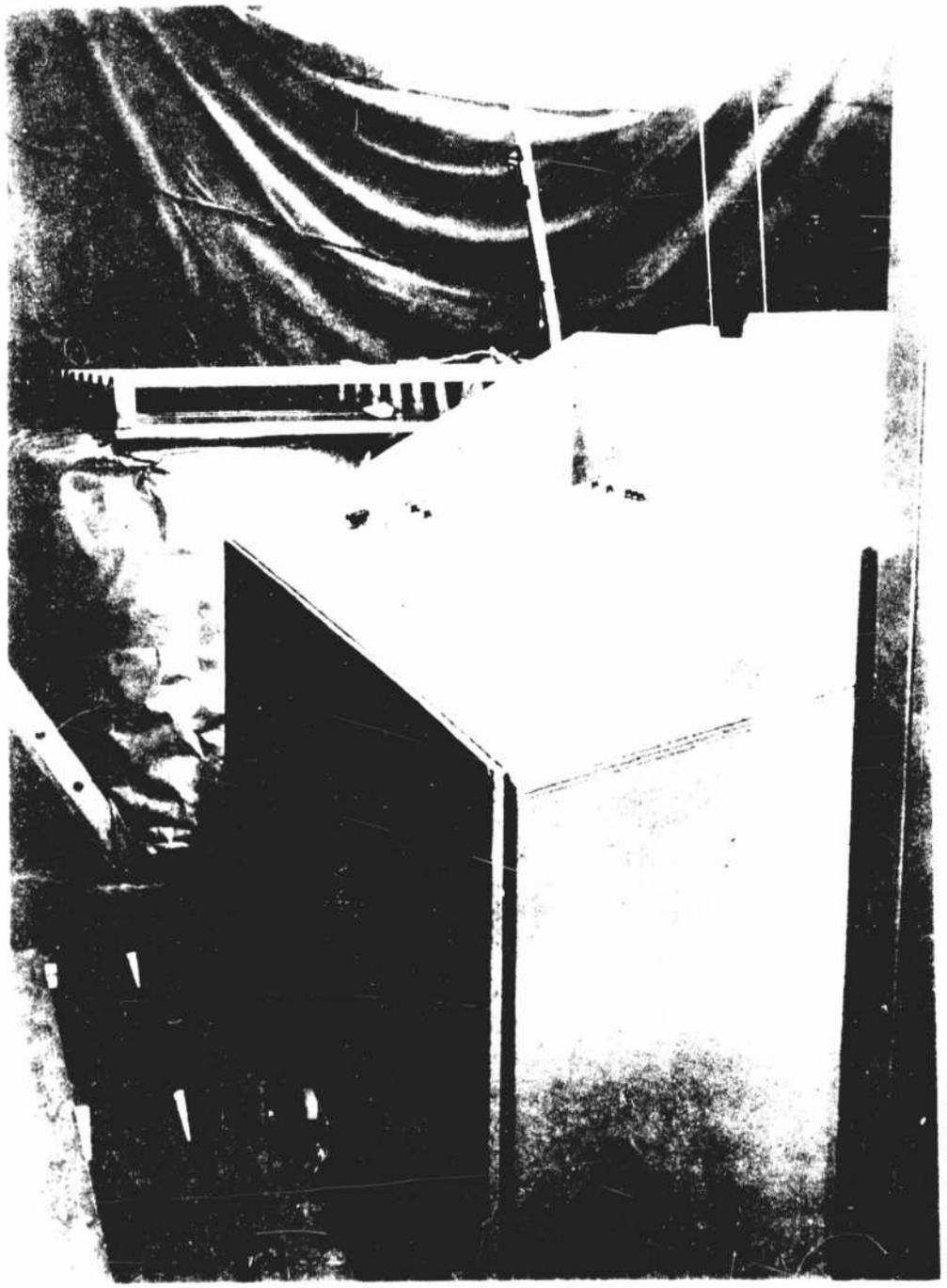

Figure 7 - View of control panel for the parachute drop-test program.

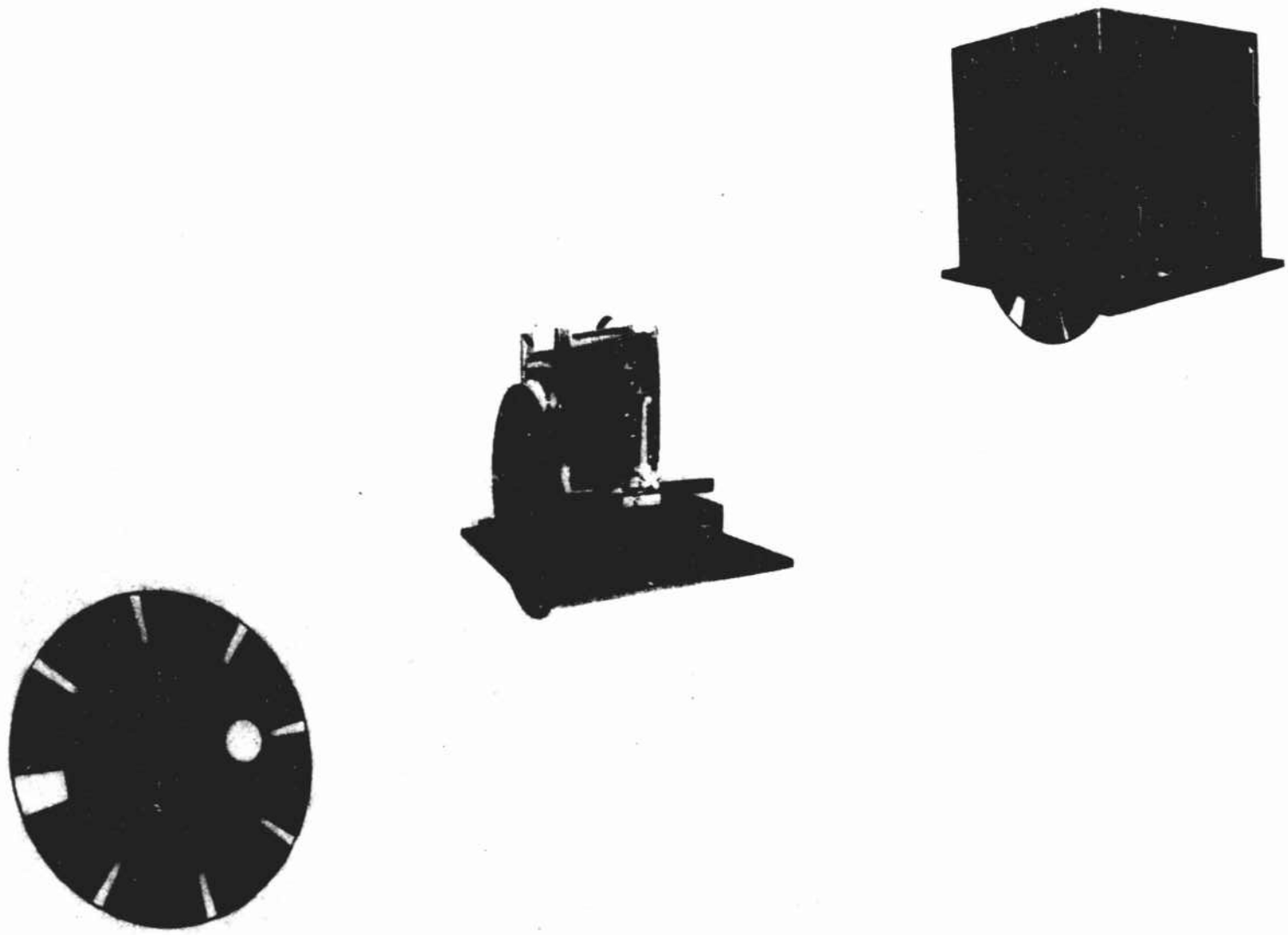

Figure 8 - Composite of parachute drop-test photographic assembly accentuating the timing-disk construction and the protective housing.

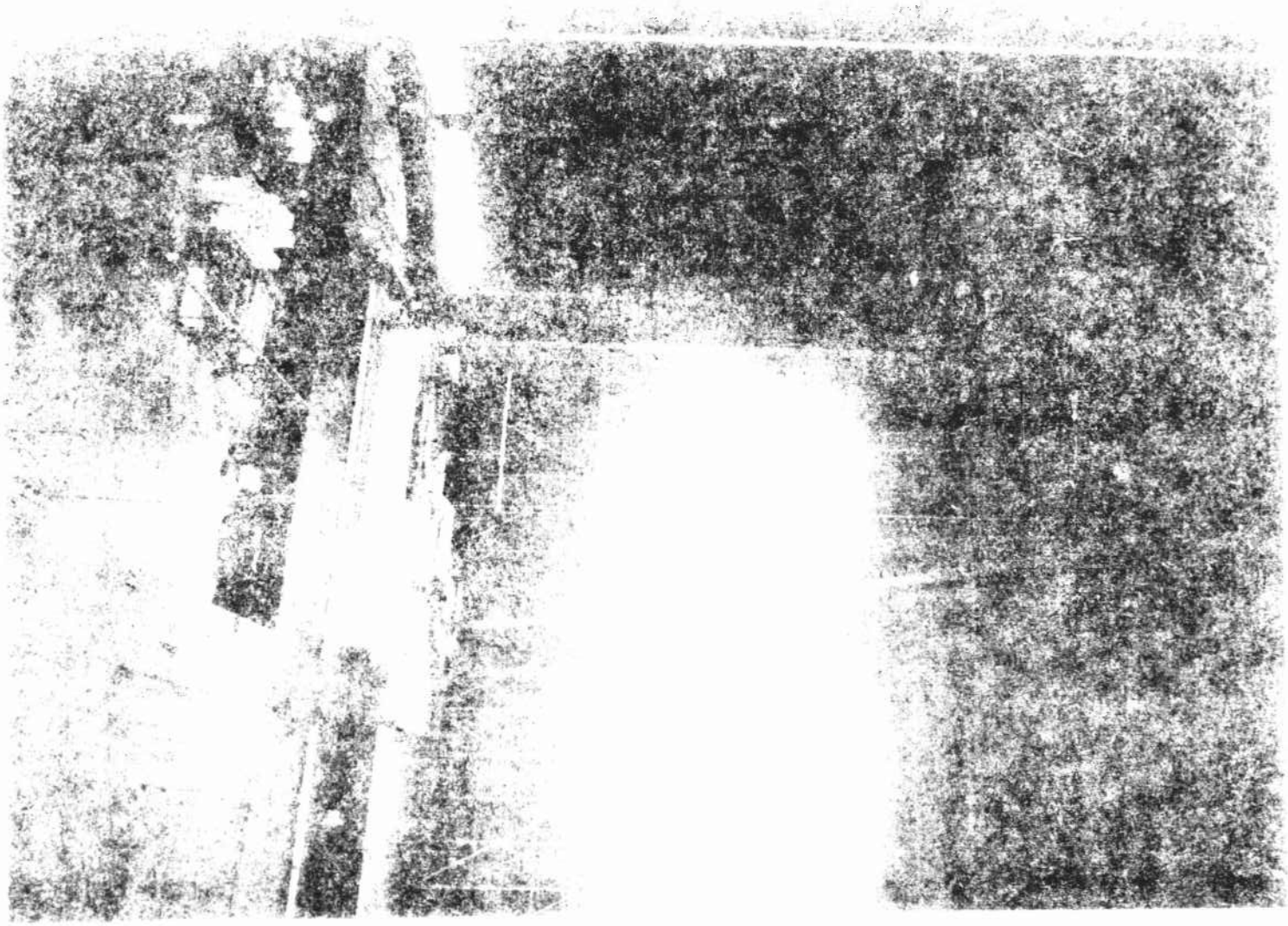

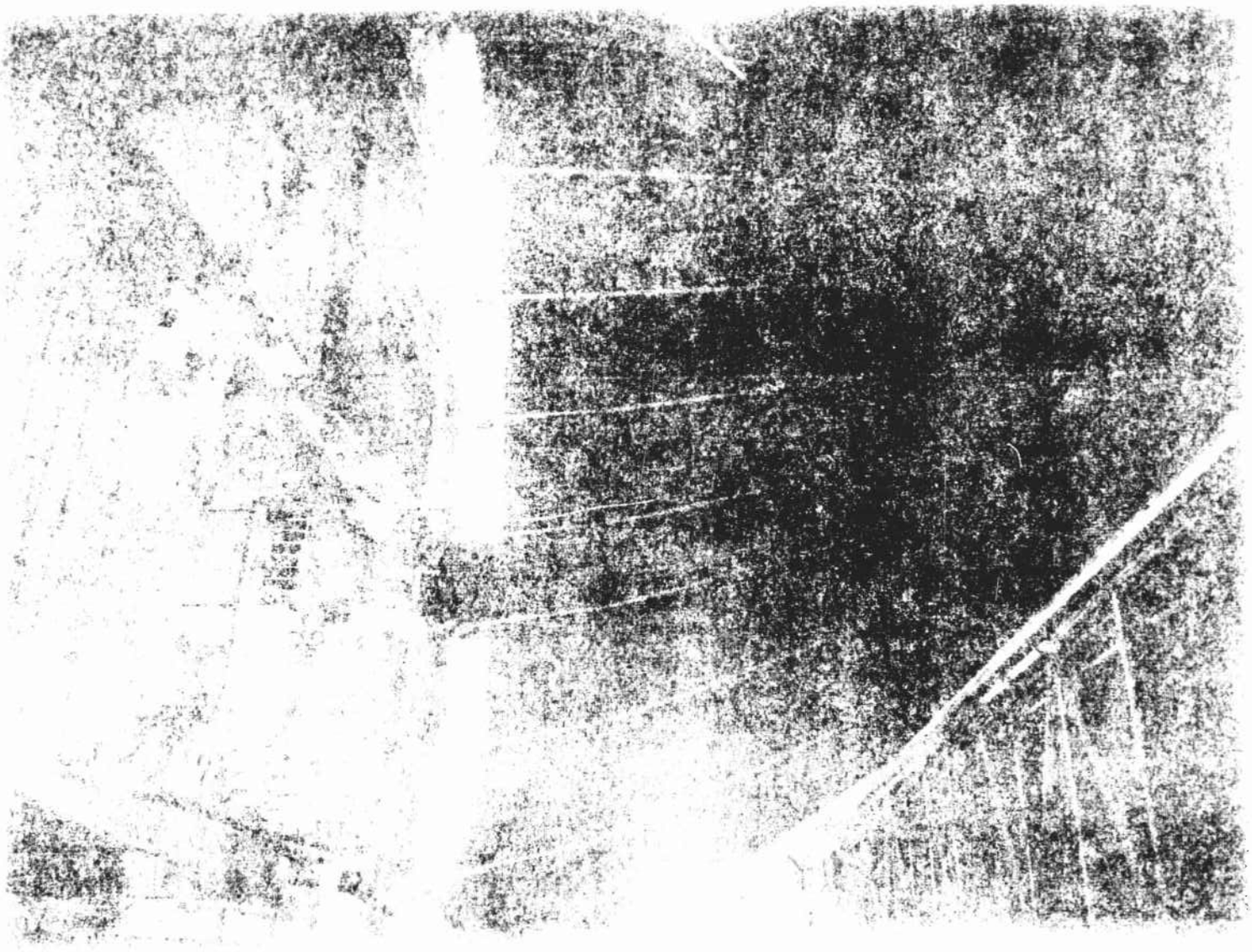

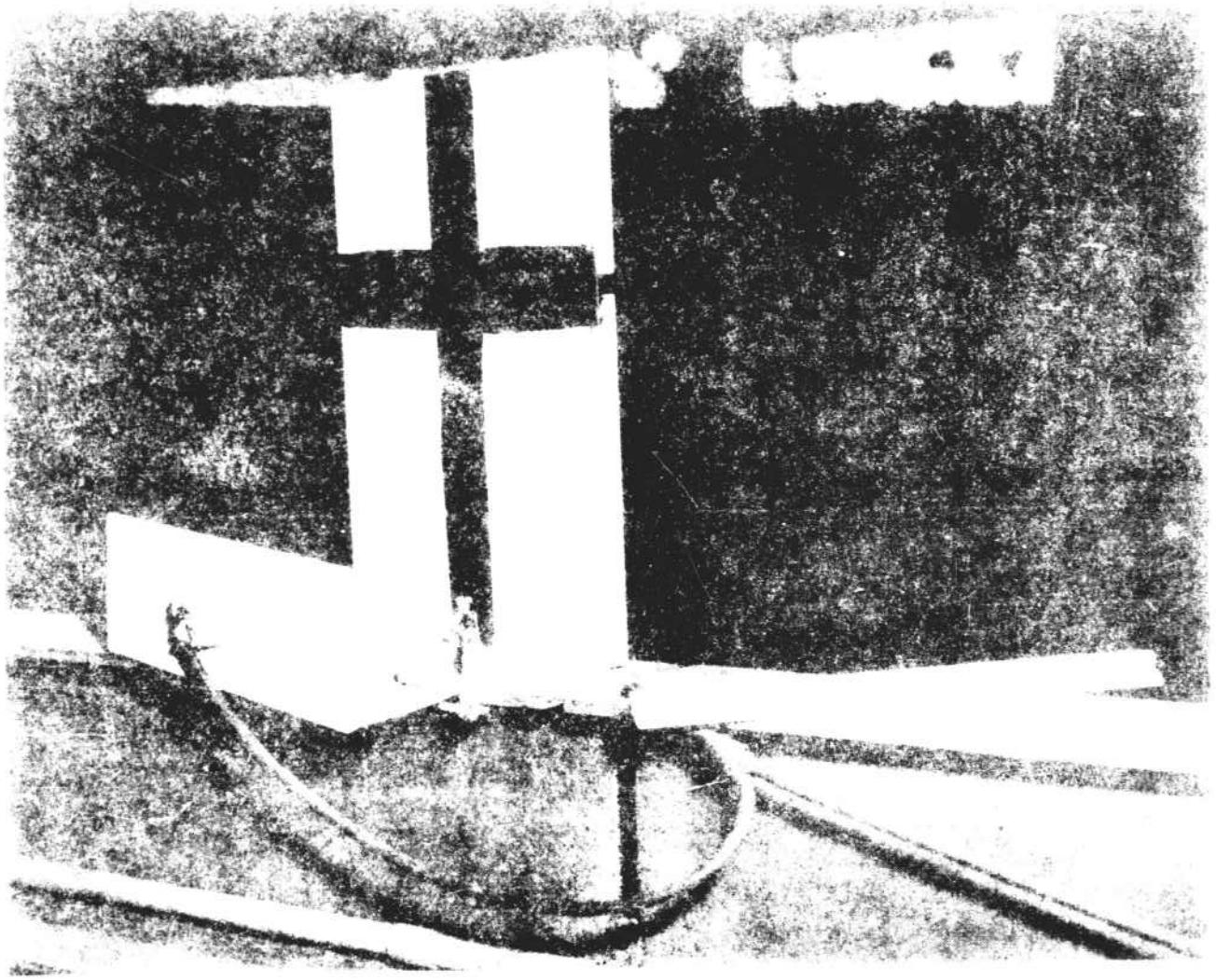

Figure 11 - Parachute drop-test-position sign for locating negative ion analyzer.

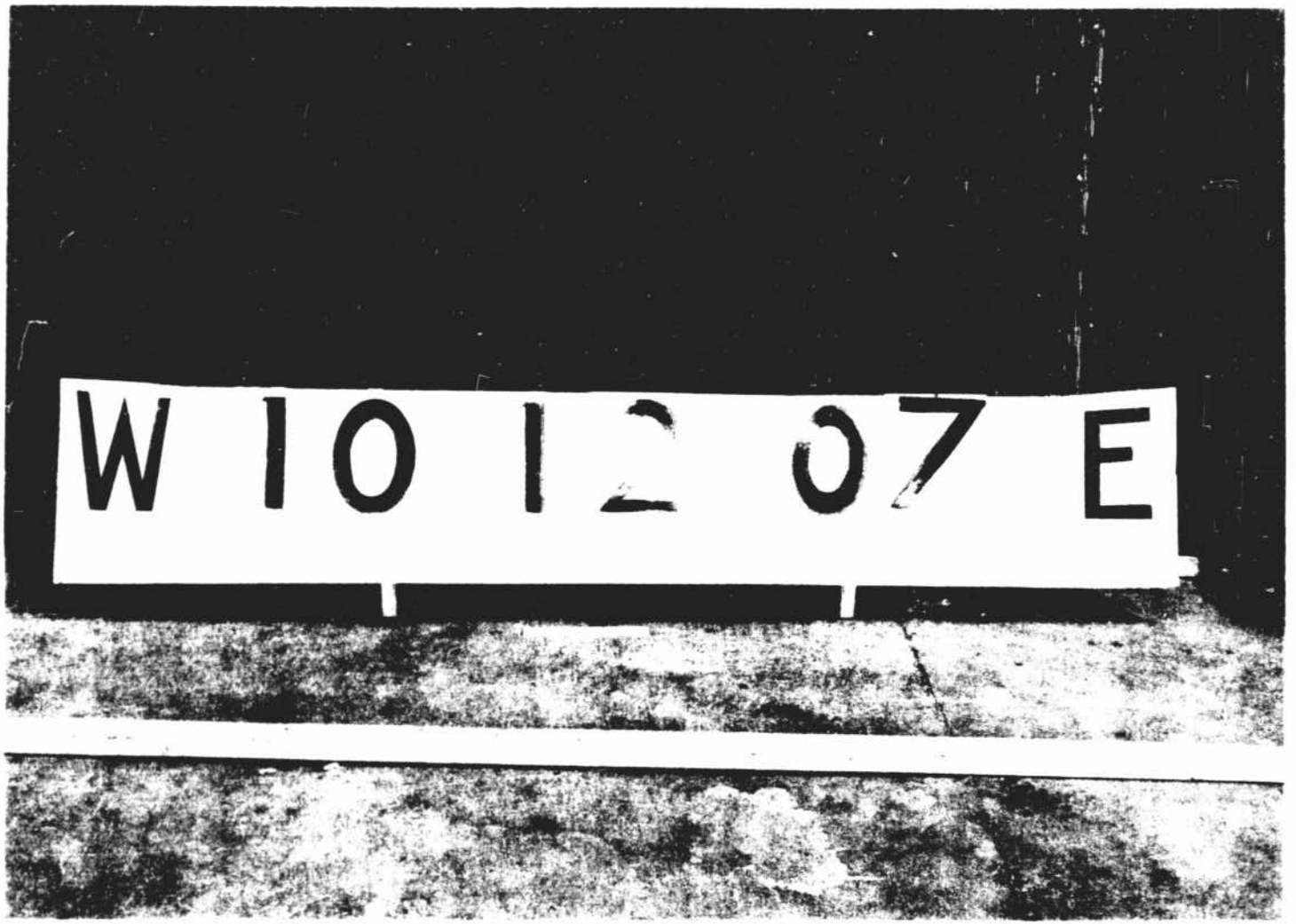

Figure 12 - Parachute drop-test marking sign giving the month, day of month, and number of drop respectively, along with camera identification letters.

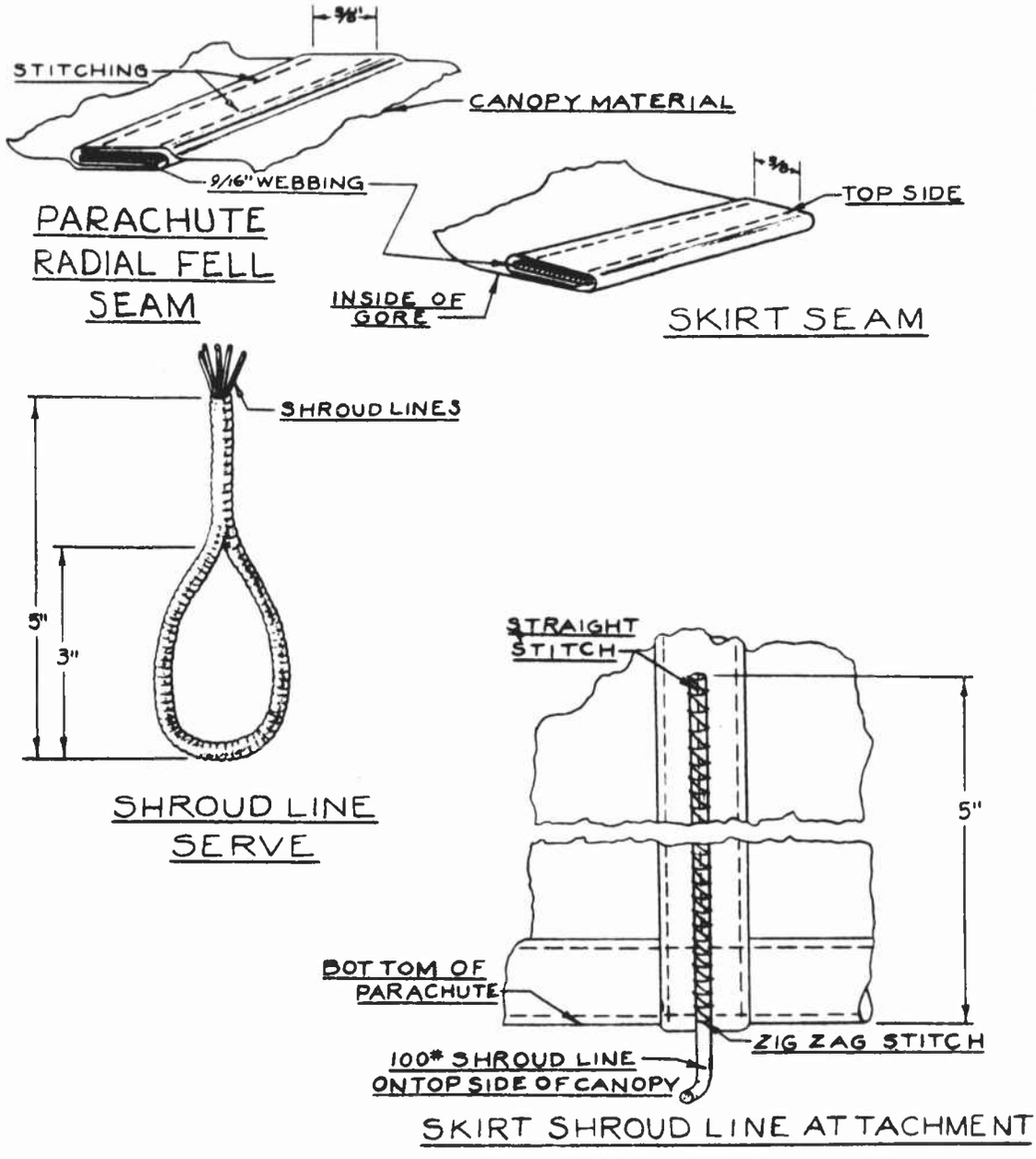

Figure 13 - Schematic diagram of model construction details on the parachute drop-test program.

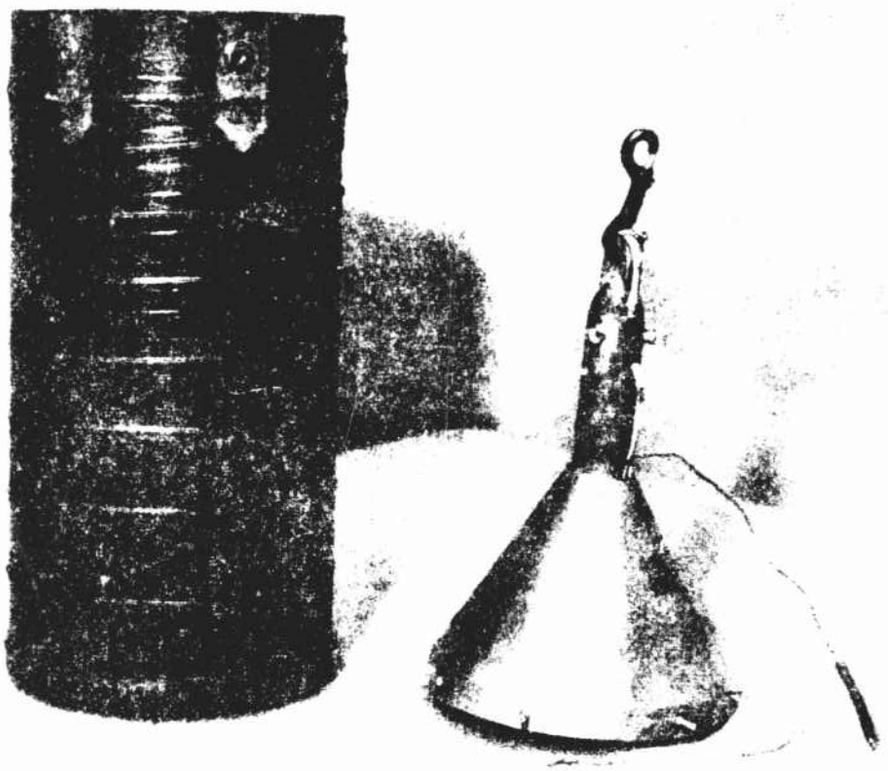

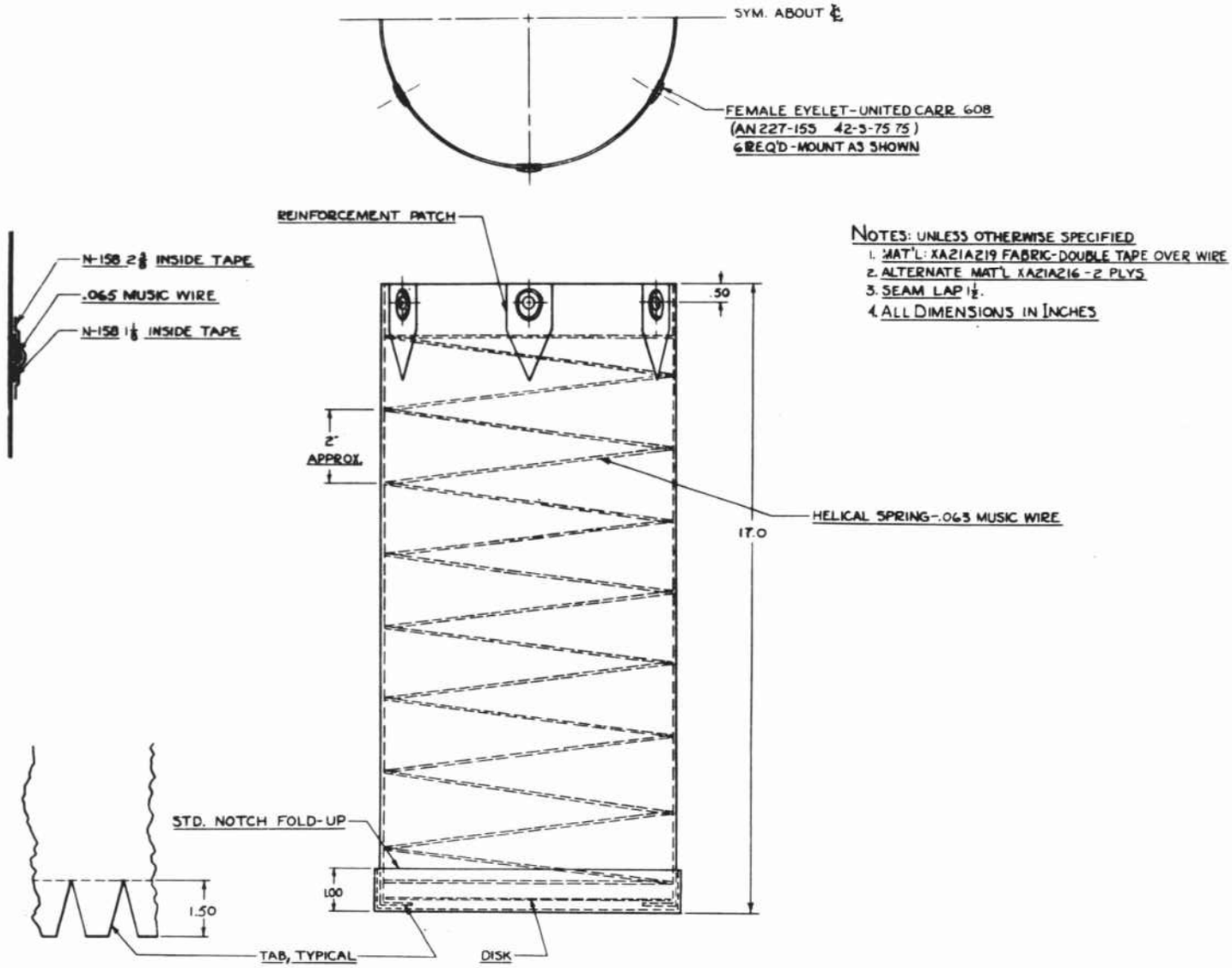

Figure 15 - Sketch of reinforced fabric bag of the parachute drop-test weight instrument.

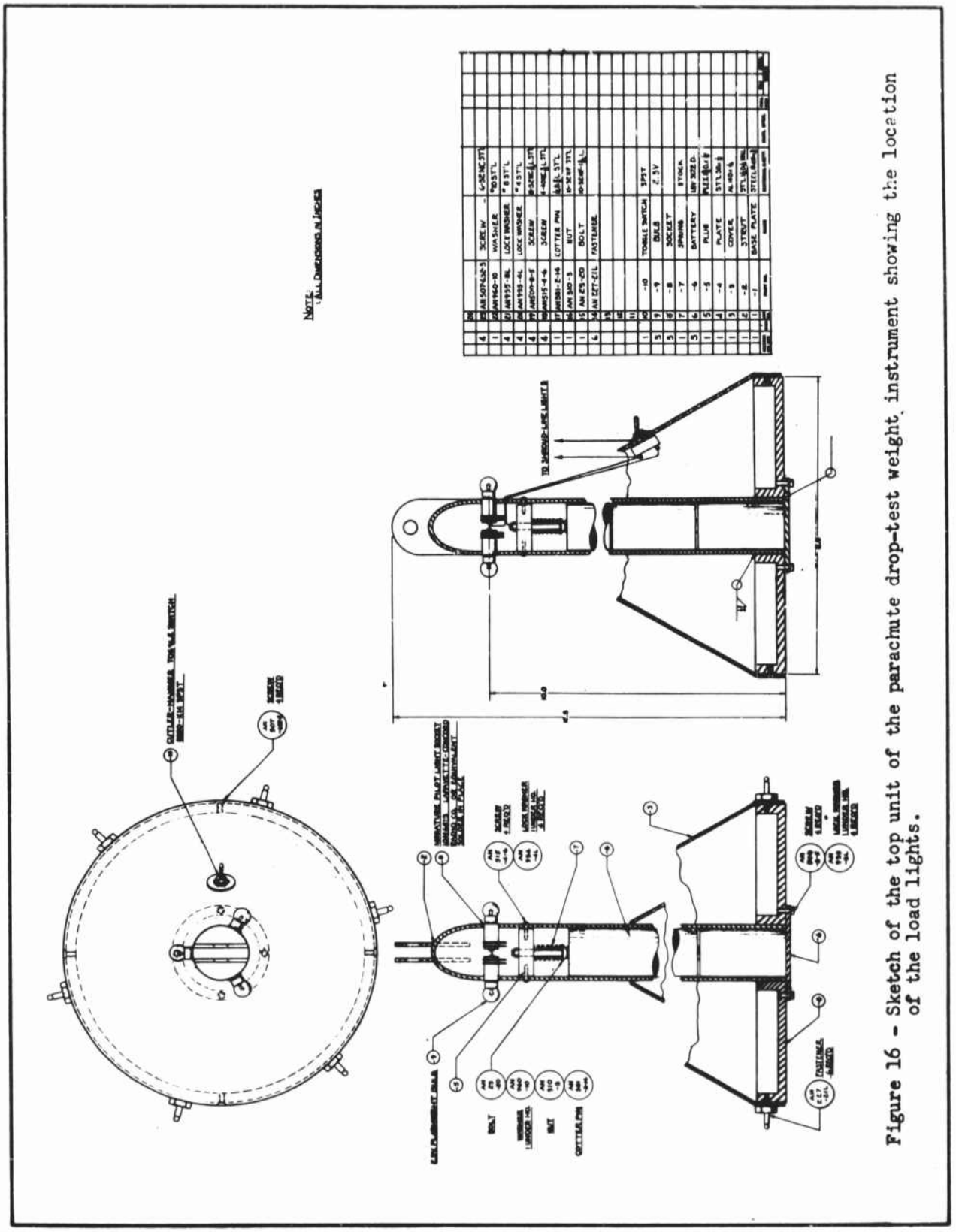

Figure 16 - Sketch of the top unit of the parachute drop-test weight instrument showing the location of the load lights.

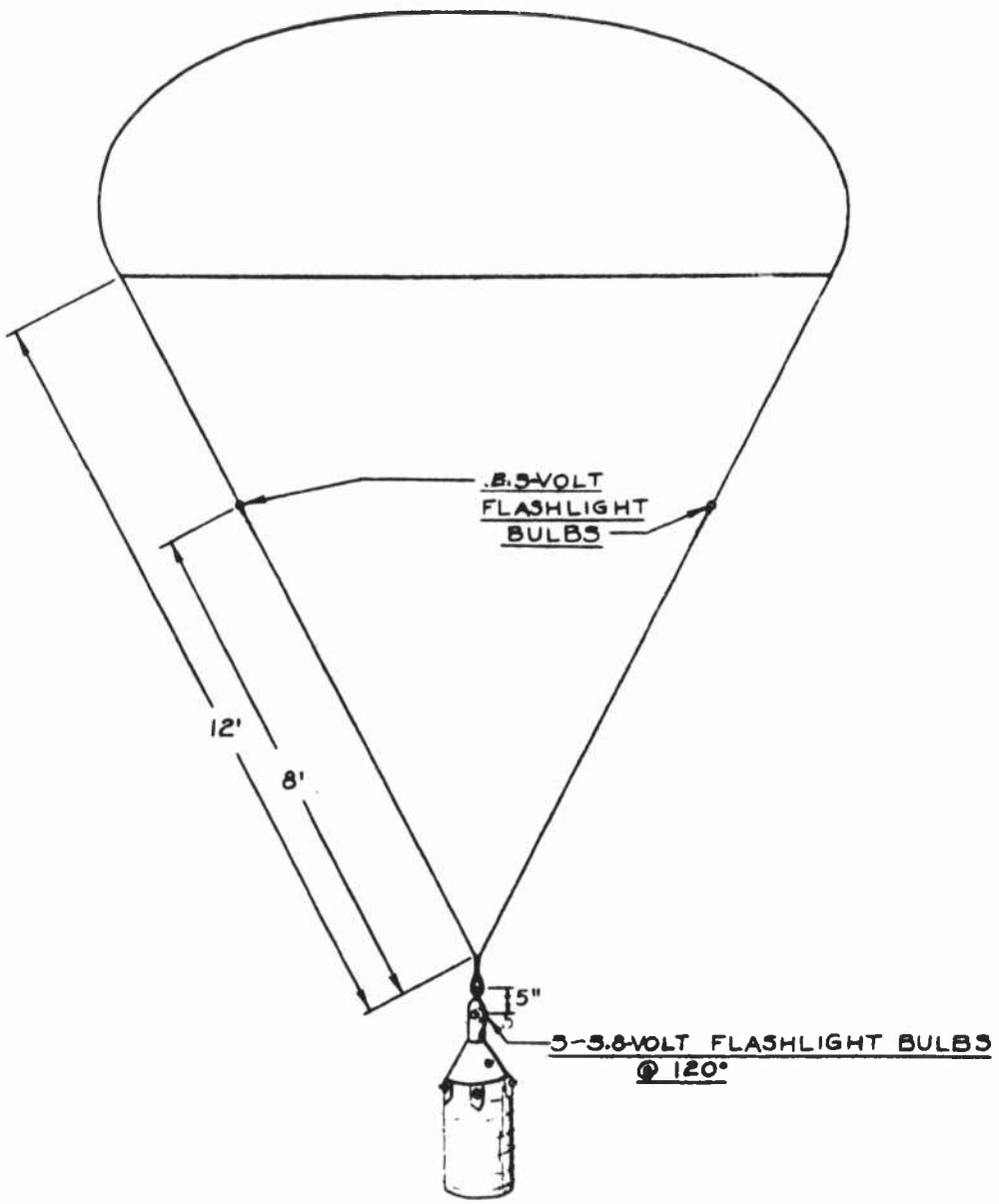

Figure 17 - Schematic diagram showing location of light bulbs for circular and square parachute systems where the upper lights are placed on diametrically opposite shroud lines.

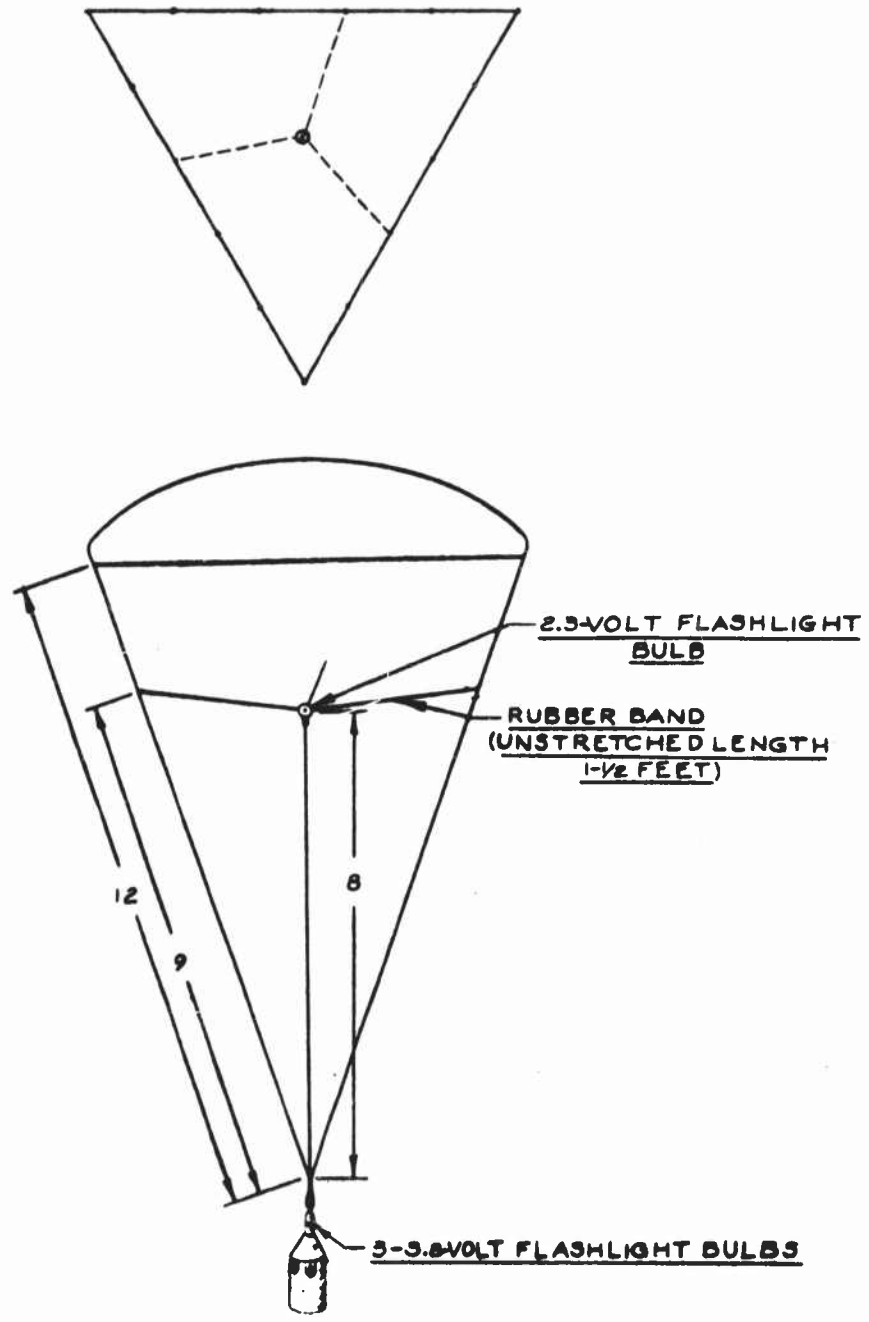

Figure 18 - Schematic diagram showing location of light bulbs for triangular parachute systems.

Figure 19 - Parachute-model bulk tester with calibrated cubic-inch scale attached.

Figure 20 - FRAZIER fabric permeability machine as used for determining the average porosity of the parachute canopy.

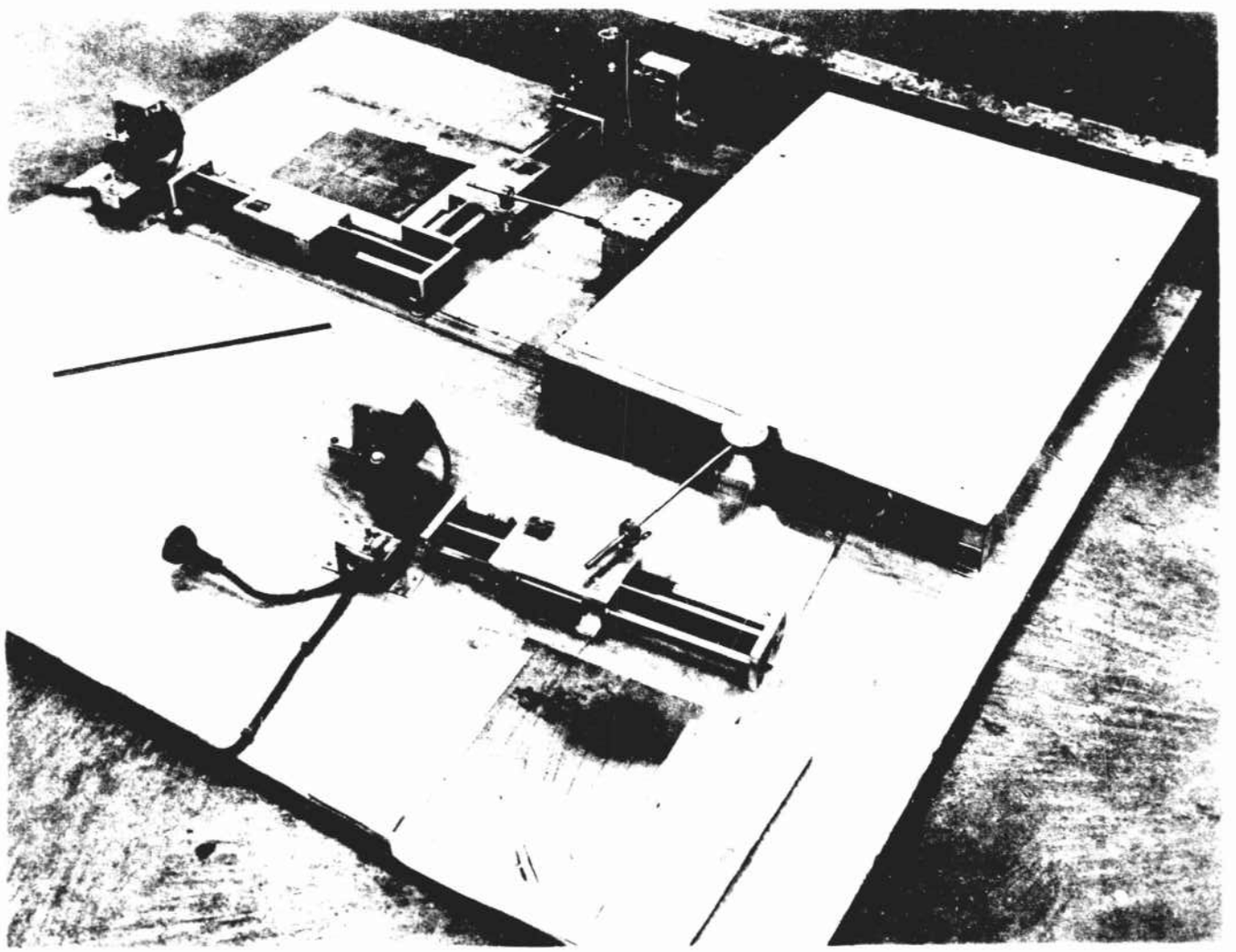

Figure 21 - Parachute drop-test analyzer for the two-camera system of recording.

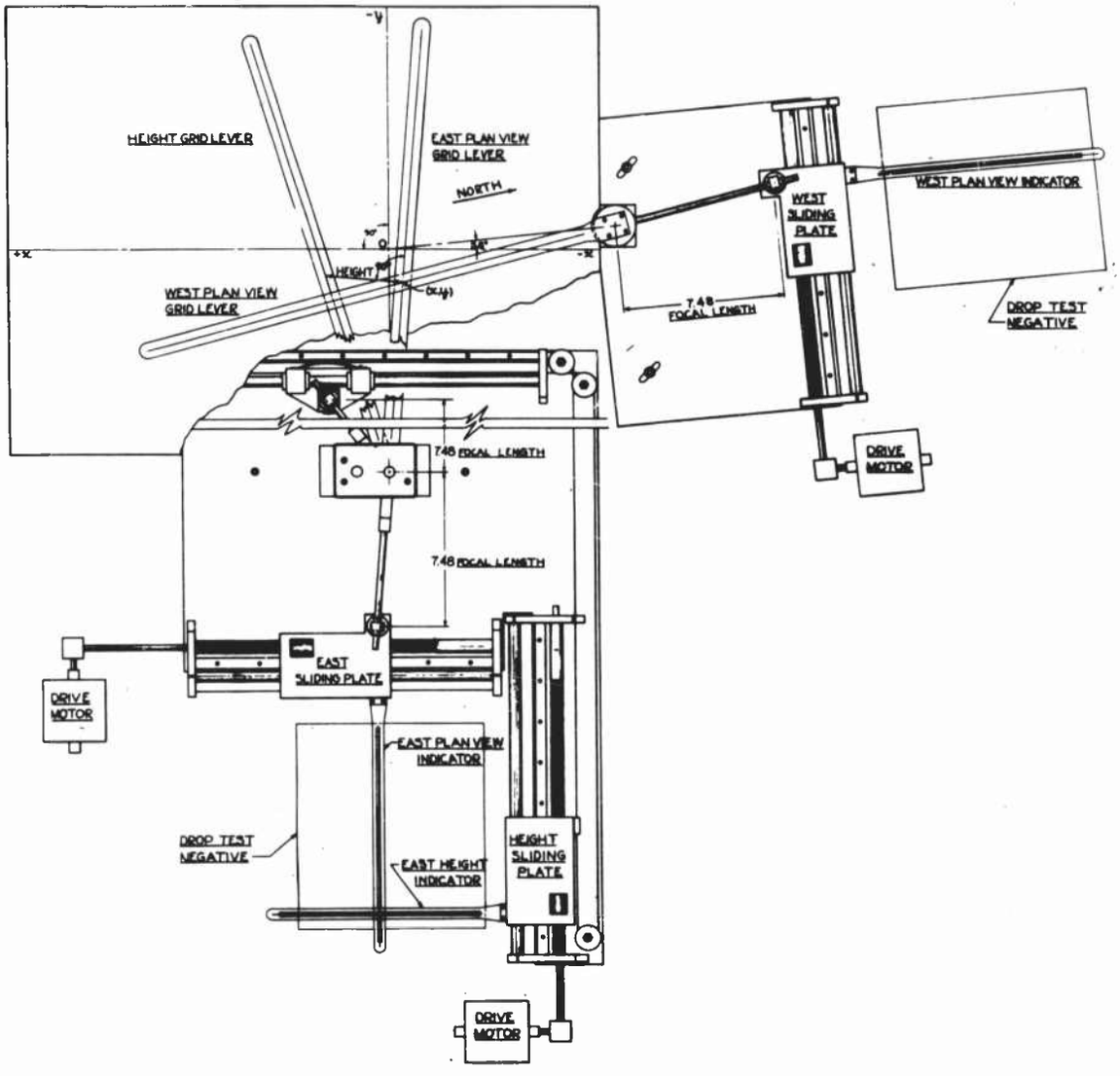

Figure 22 - Sketch of the parachute drop-test analyzer showing characteristic definitions and dimensions.

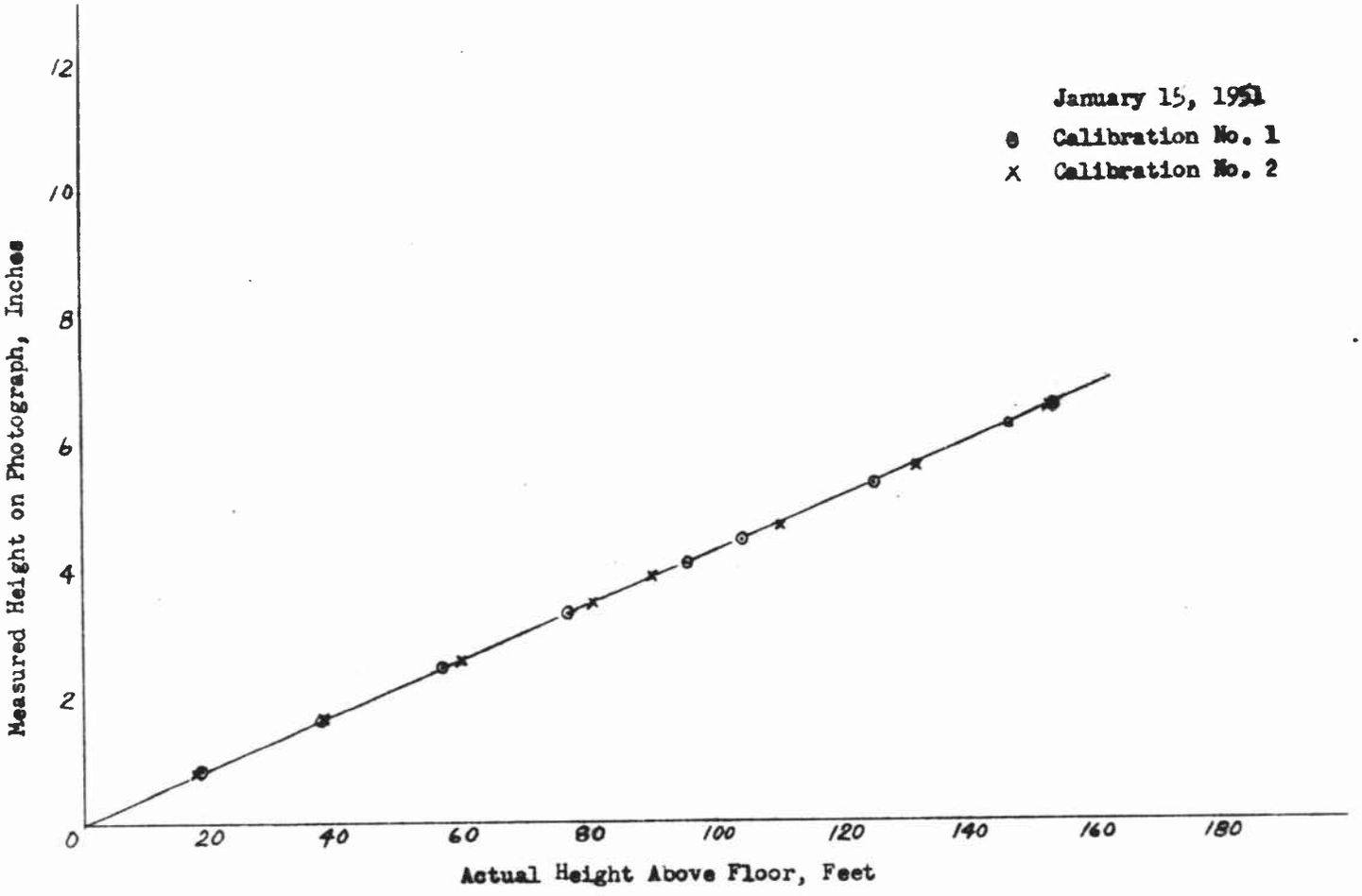

Figure 23 - Typical camera calibration curve showing relationship of the actual height measurement and the measured distance on the drop-test photograph.

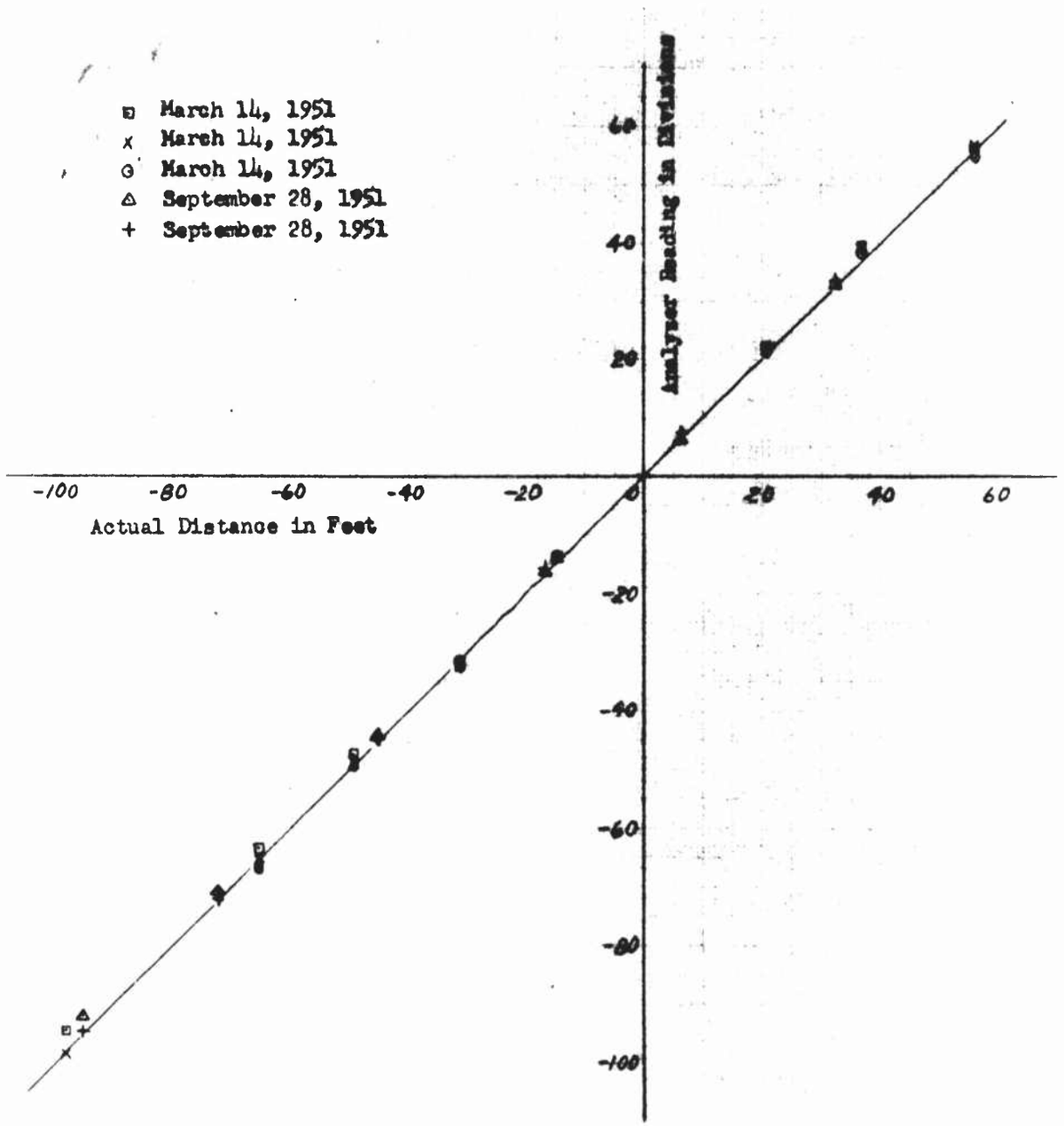

Figure 24 - Typical analyzer calibration curve showing that one division on the analyzer equals one foot of distance in drop-test area.

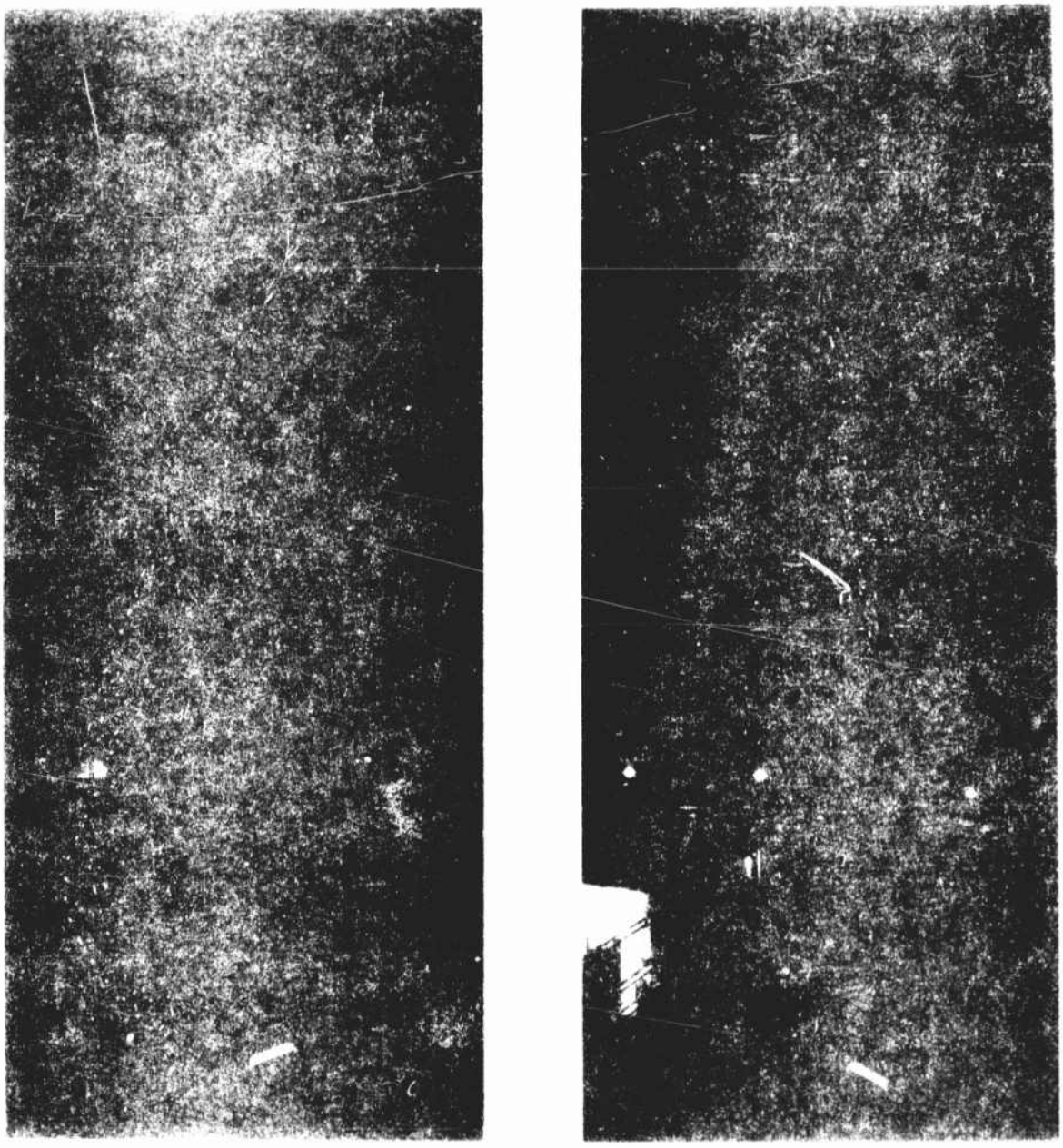

View from East Camera

View from West Camera

Figure 2.8 - Photographic copy of a set of representative drop-test negatives showing the actual dots produced by the data recording system.

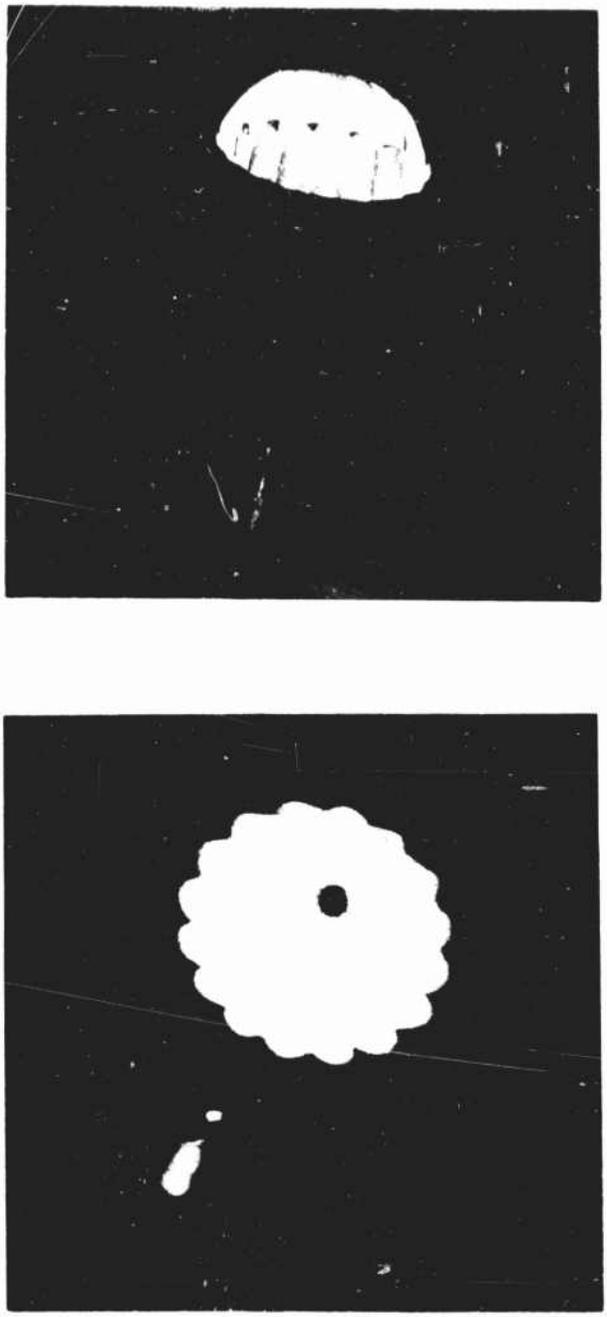

Figure 25 - Photograph of the solid-flat-circular parachute model (No. 1) during descent at approximately 20 feet per second.

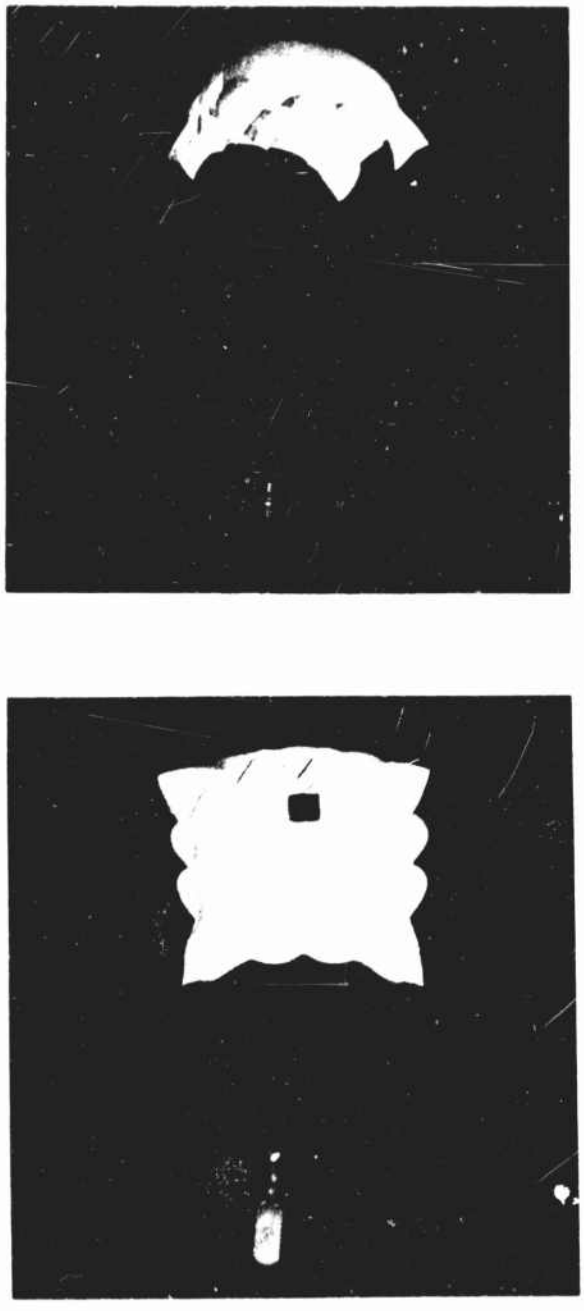

Figure 26 - Photograph of the solid-flat-square pocketed parachute model (No. 2) during descent at approximately 20 feet per second.

Figure 27 - Photograph of the solid-flat-triangular pocketed parachute model (No. 3) during descent at approximately 20 feet per second.

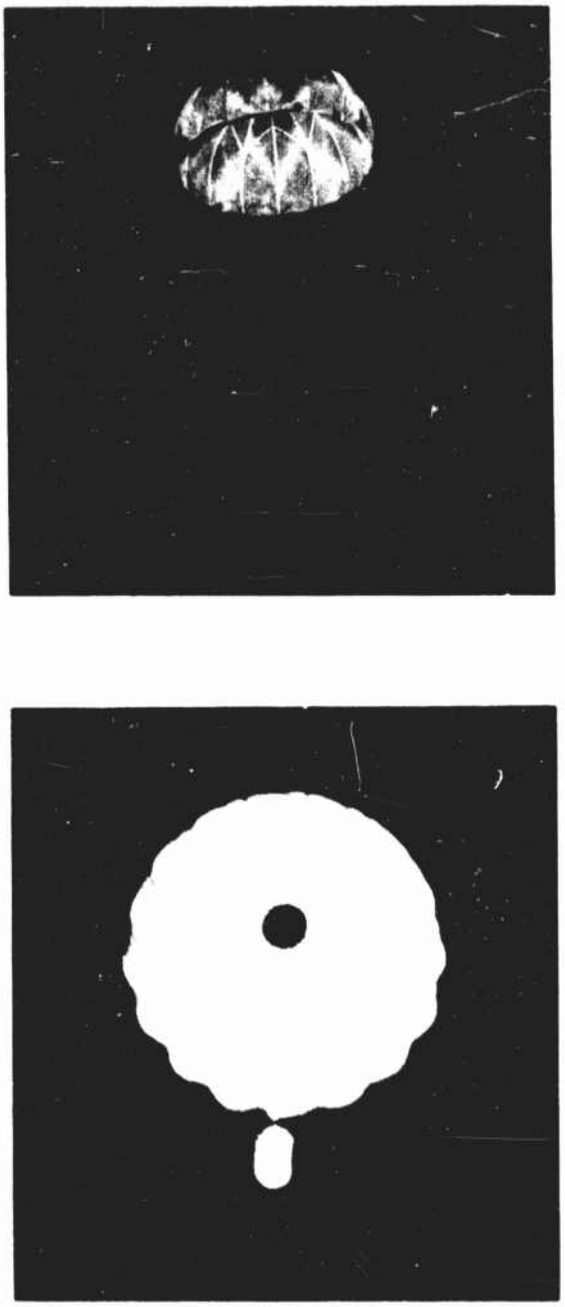

Figure 28 - Photograph of the solid-flat 10% extended-skirt parachute model (No. 4) during descent at approximately 20 feet per second.

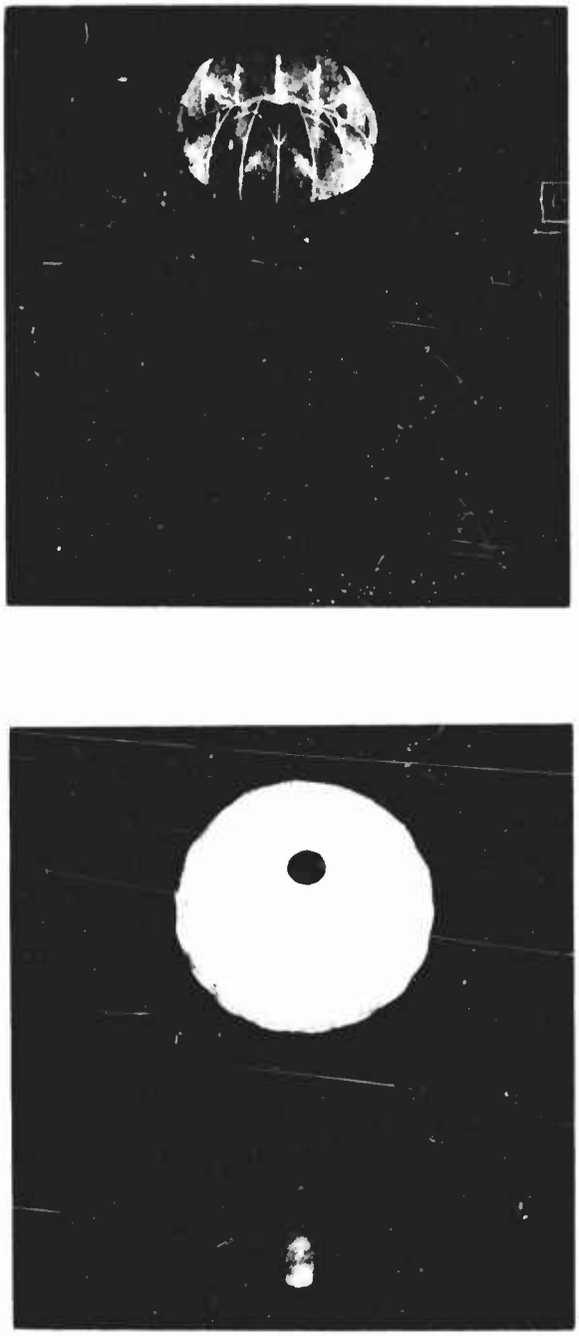

Figure 29 - Photograph of the solid-flat 12½% extended-skirt parachute model (No. 5) during descent at approximately 20 feet per second.

Figure 30 - Photograph of the solid-flat fully extended-skirt parachute model (No. 6) during descent at approximately 20 feet per second.

Figure 31 - Frame from film of the 50% vent airfoil parachute model (No. 7) during descent at approximately 20 feet per second.

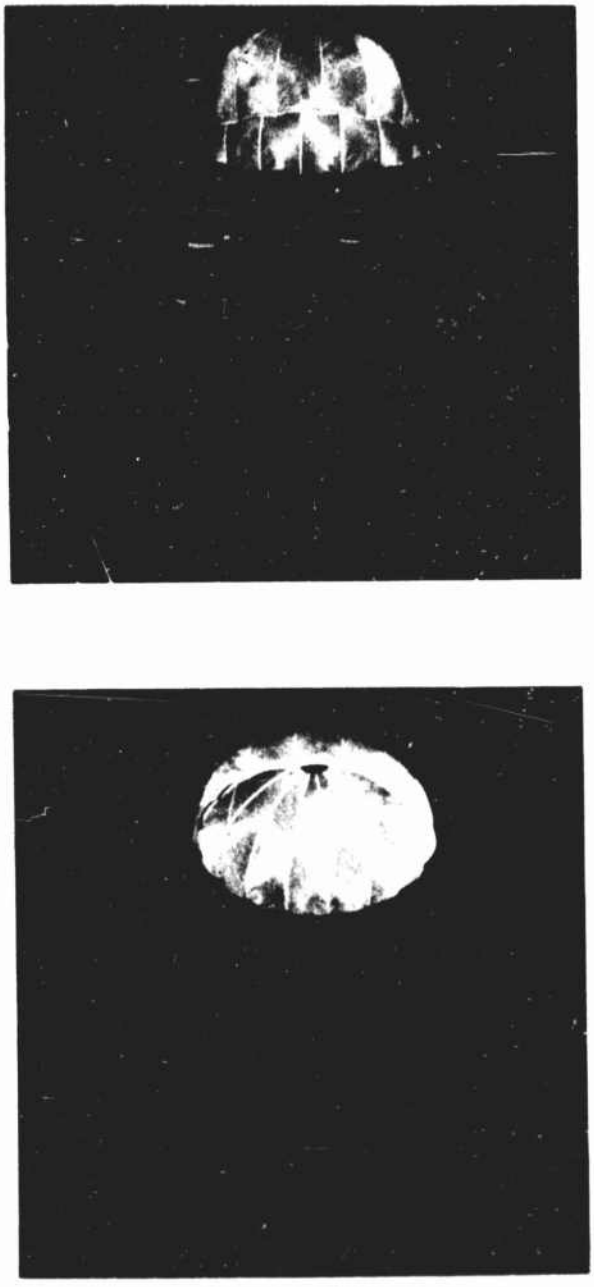

Figure 32 - Photograph of the ½ sphere circular parachute model (No. 8) during descent at approximately 20 feet per second.

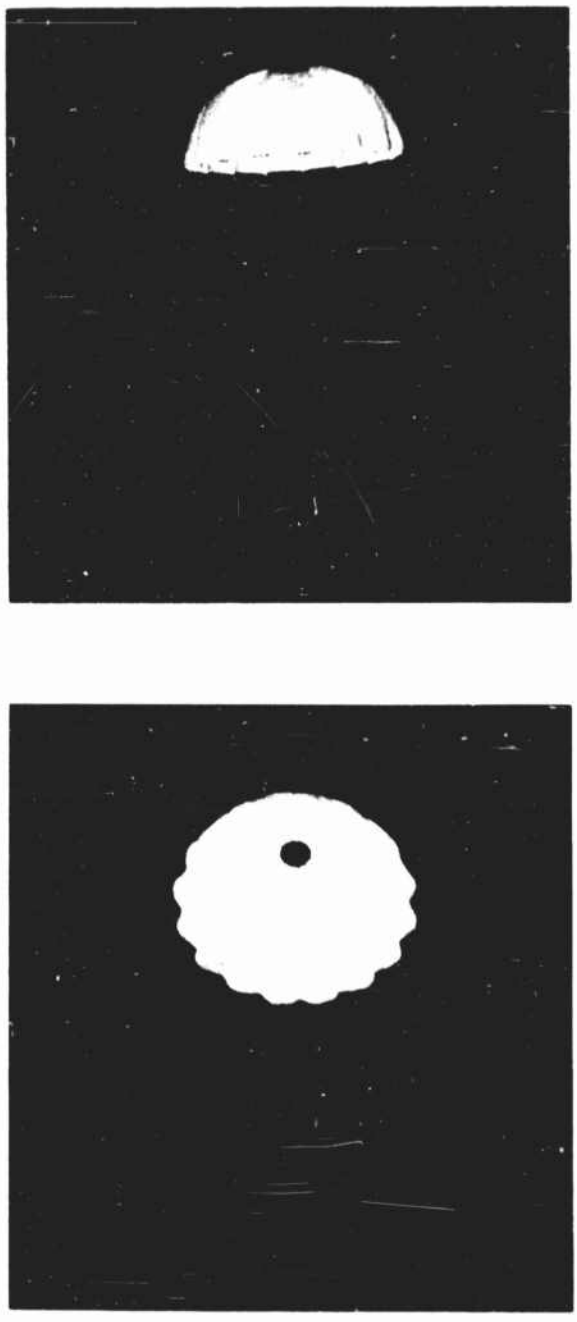

Figure 33 - Photograph of the $\frac{1}{4}$ sphere circular parachute model (No. 9) during descent at approximately 20 feet per second.

Figure 34 - Photograph of the $\frac{1}{4}$ sphere square parachute model (No. 10) during descent at approximately 20 feet per second.

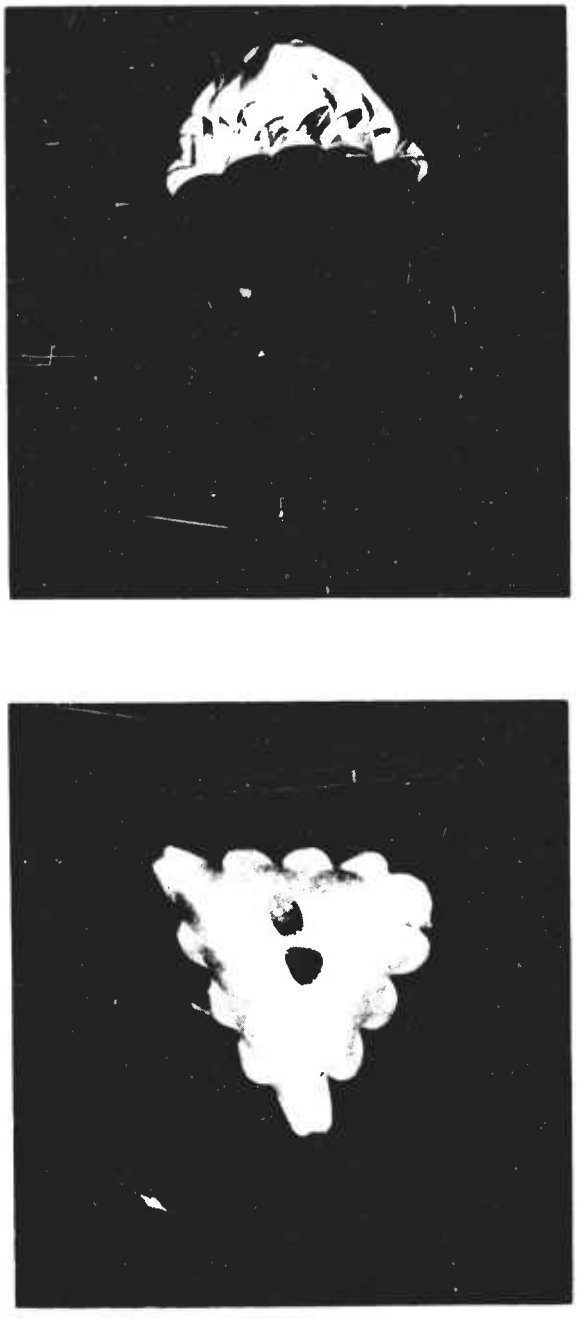

Figure 35 - Photograph of the $\frac{1}{4}$ sphere triangular parachute model (No. 11) during descent at approximately 20 feet per second.

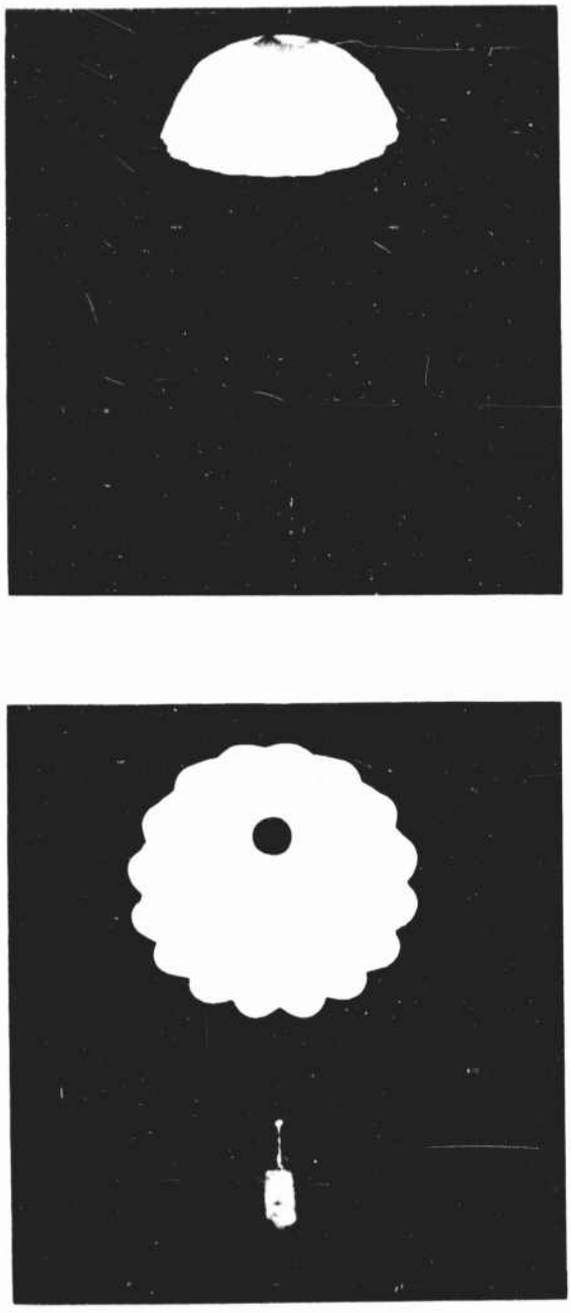

Figure 36 - Photograph of the 30° circular conical parachute model (No. 12) during descent at approximately 20 feet per second.

Figure 37 - Photograph of the 30° square conical parachute model (No. 13) during descent at approximately 20 feet per second.

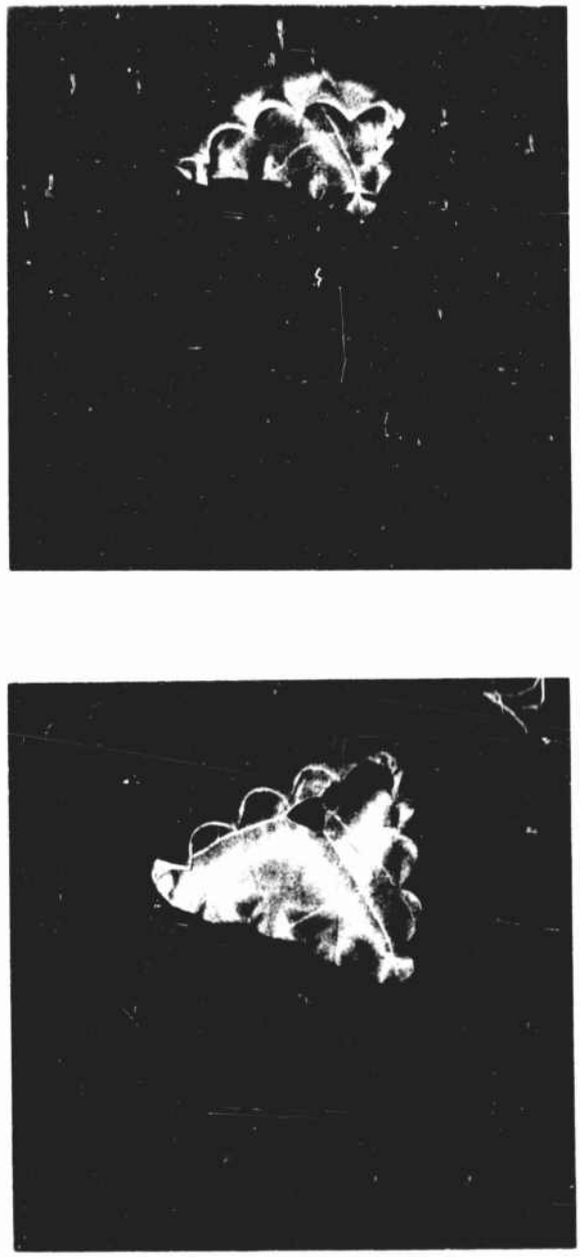

Figure 38 - Photograph of the 30° triangular conical parachute model (No. 14) during descent at approximately 20 feet per second.

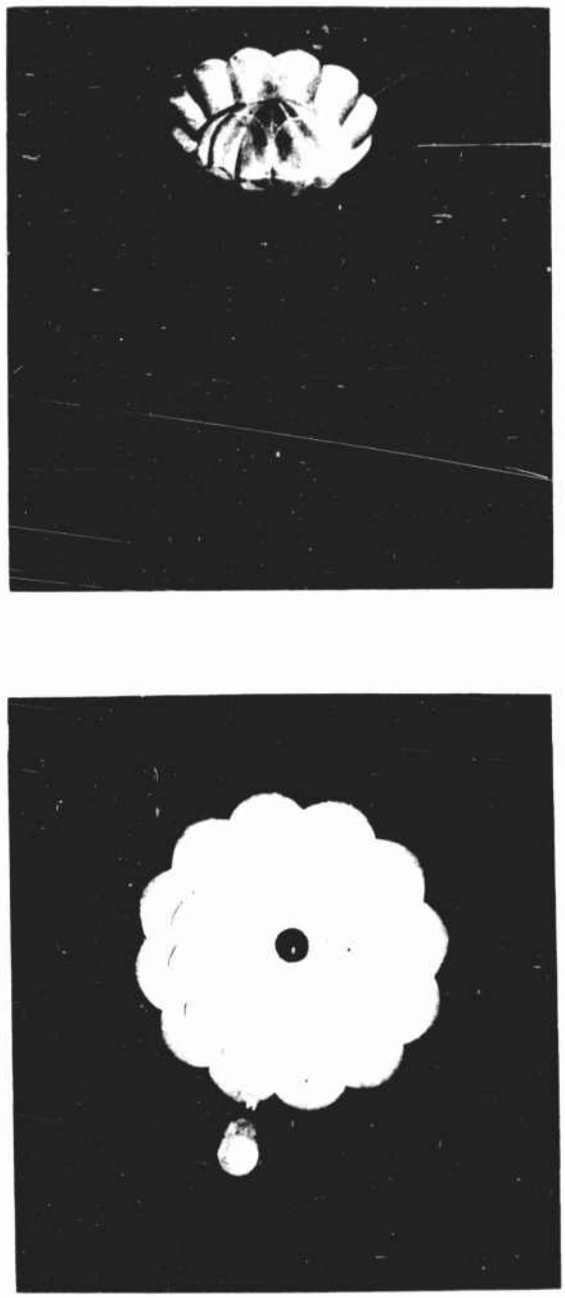

Figure 39 - Photograph of the medium-construction brake-type guide-surface parachute model (No. 16) during descent at approximately 20 feet per second.

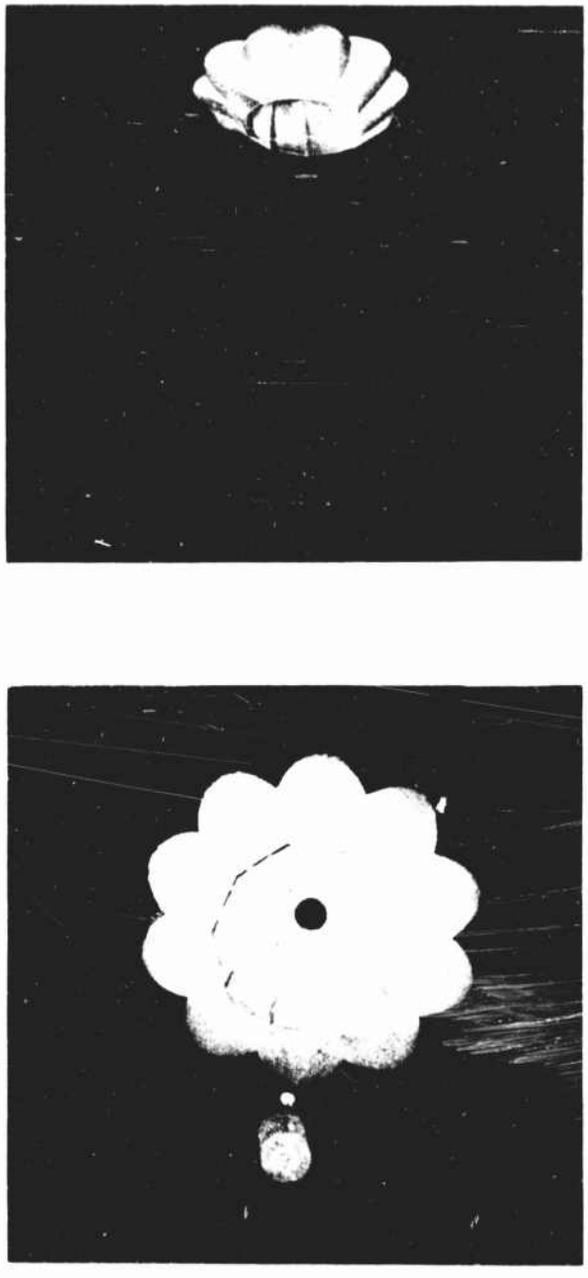

Figure 40 - Photograph of the stabilization-type guide-surface parachute model (No. 17) during descent at approximately 20 feet per second.

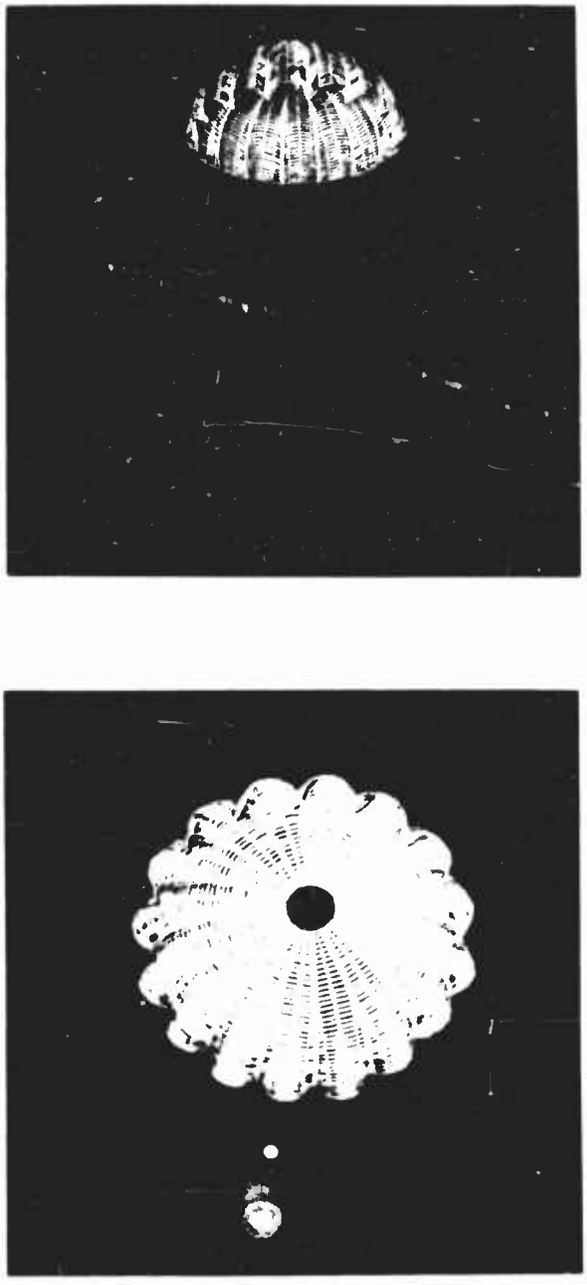

Figure 41 - Photograph of the circular brake-type FIST ribbon parachute model (No. 21) during descent at approximately 20 feet per second.

Figure 42 - Photograph of the square ribbon parachute model (No. 22) during descent at approximately 20 feet per second.

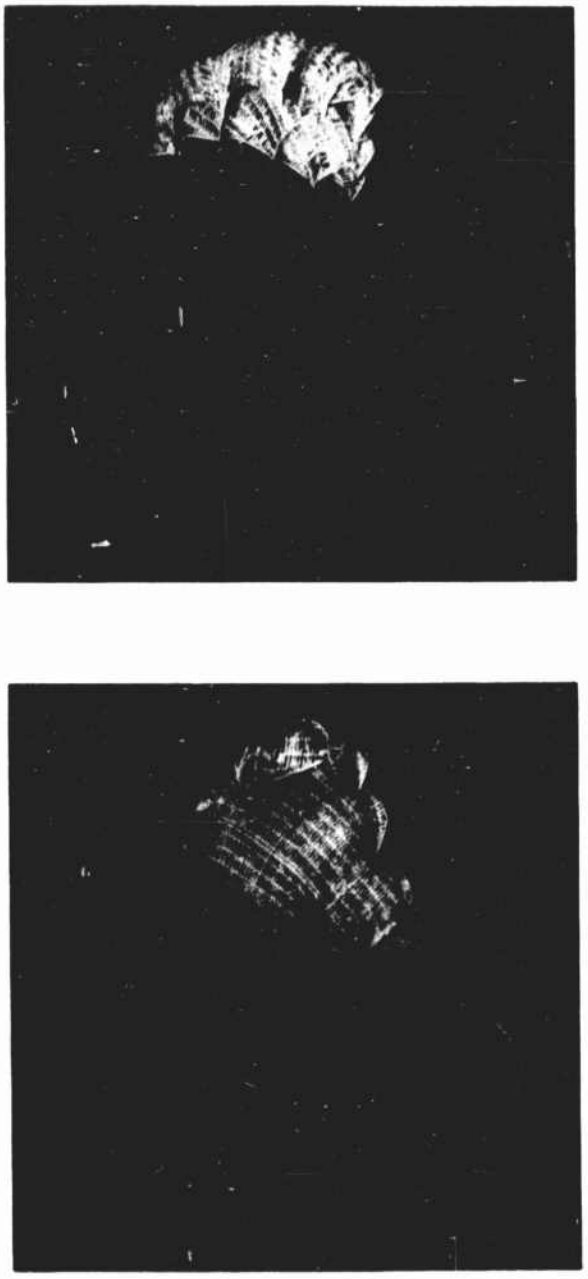

Figure 43 - Photograph of the triangular ribbon parachute model (No. 23) during descent at approximately 20 feet per second.

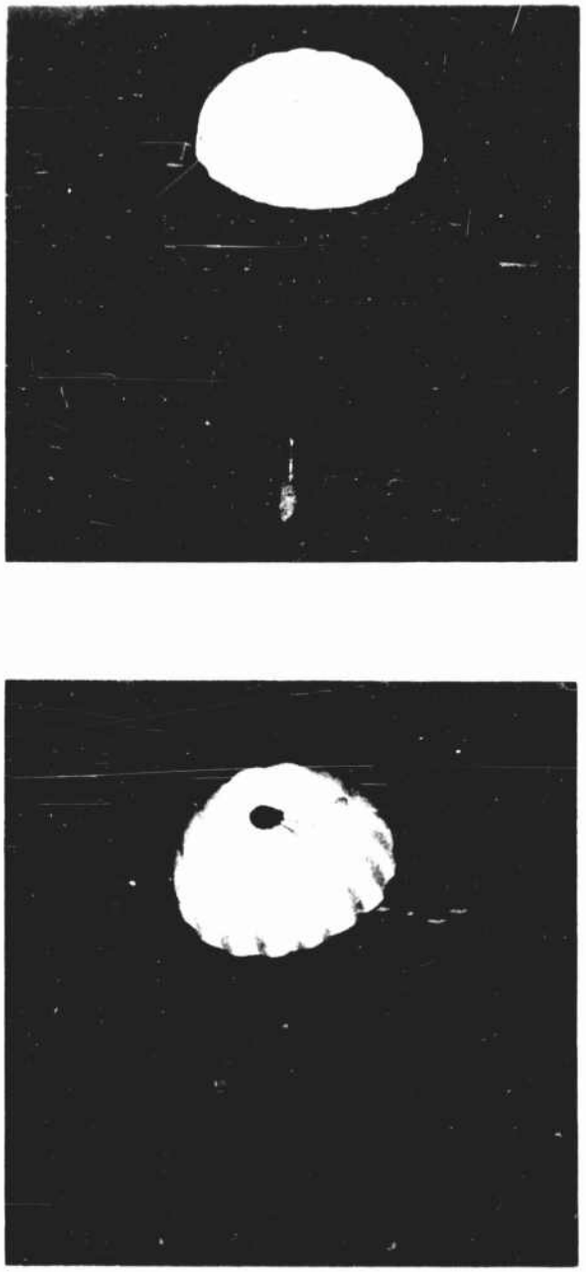

Figure 44 - Photograph of the Exeter Type-12 shaped parachute model (No. 24) during descent at approximately 20 feet per second.

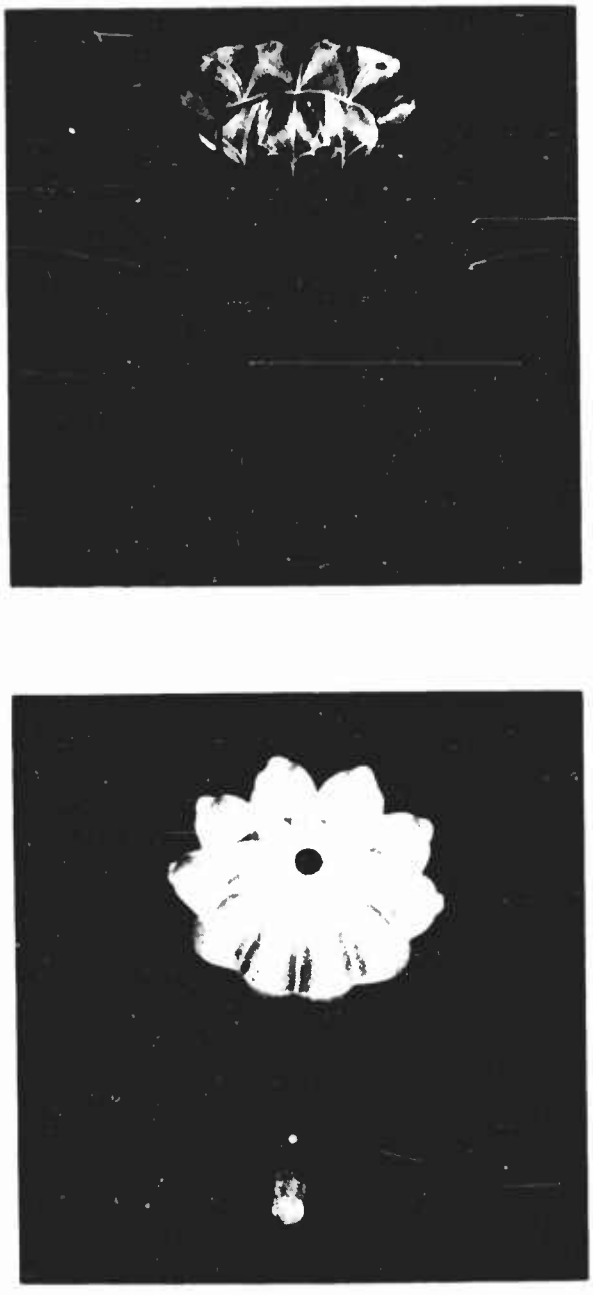

Figure 45 - Photograph of the universal-type ribless guide-surface parachute model (No. 25) during descent at approximately 20 feet per second.

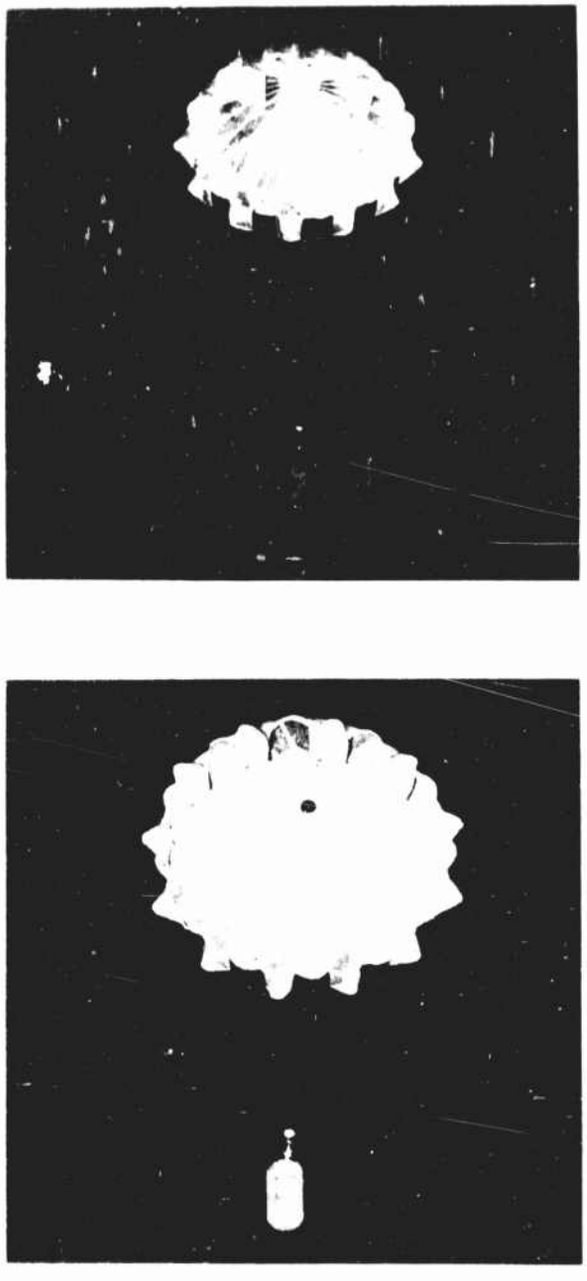

Figure 46 - Photograph of the personnel-type guide-surface parachute model (No. 26) during descent at approximately 20 feet per second.

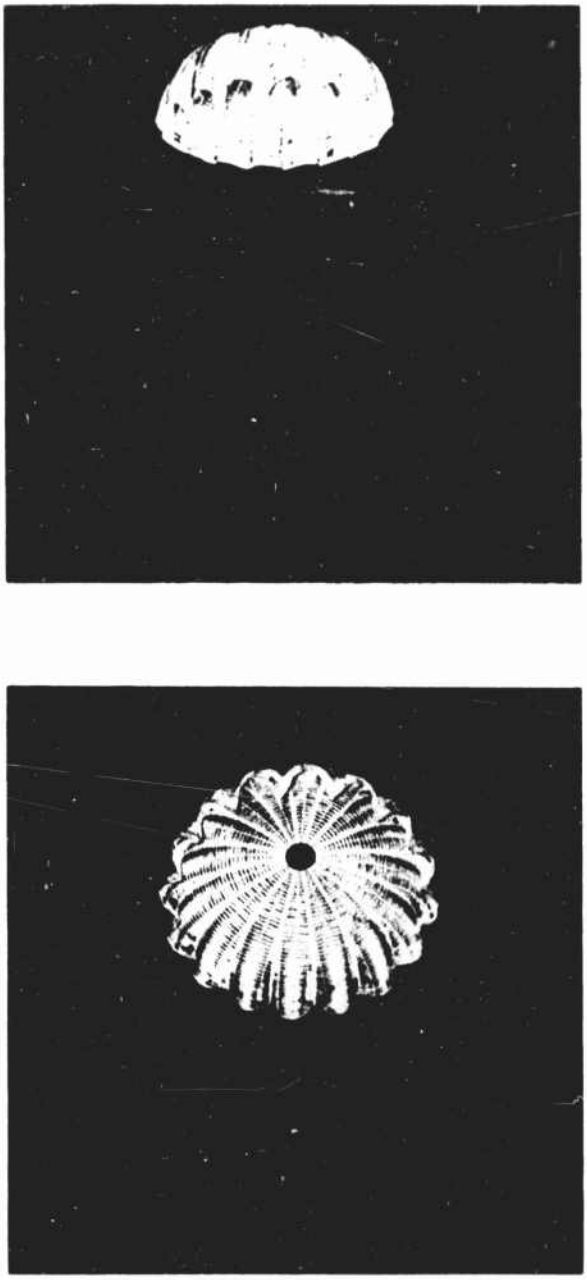

Figure 47 - Photograph of the FIST ribbon parachute model (20% total porosity)(No. 27) during descent at approximately 20 feet per second.

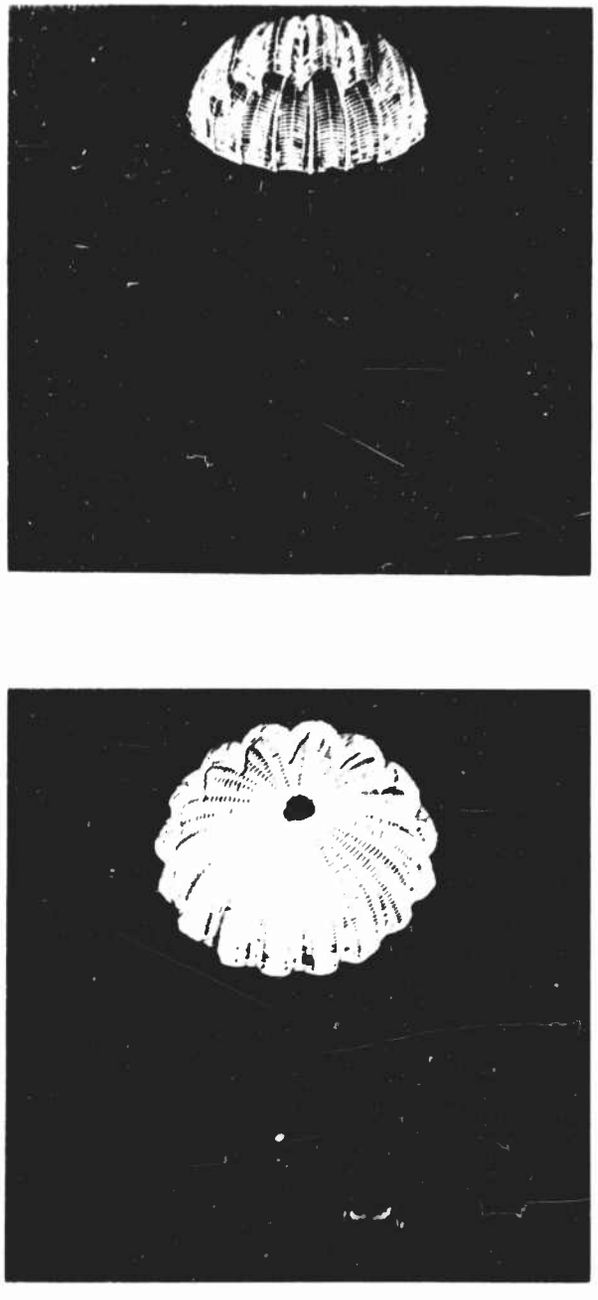

Figure 48 - Photograph of the FIST ribbon parachute model (25% total porosity)(No. 28) during descent at approximately 20 feet per second.

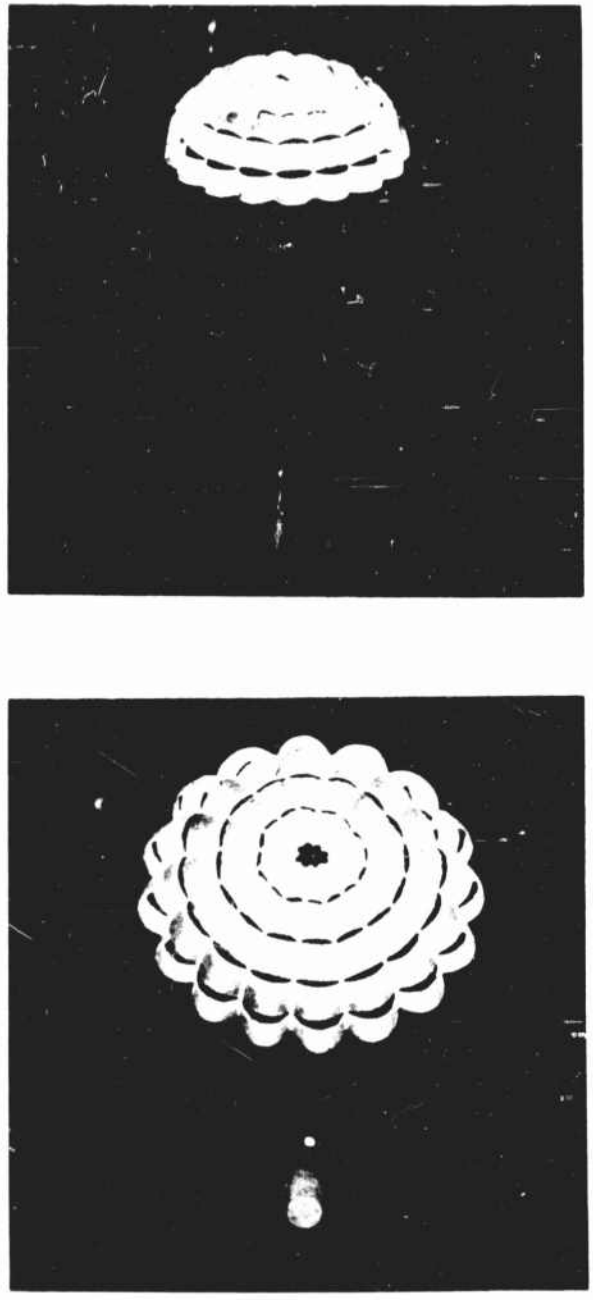

Figure 49 - Photograph of the ring-slot parachute model (10% total porosity) (No. 29) during descent at approximately 20 feet per second.

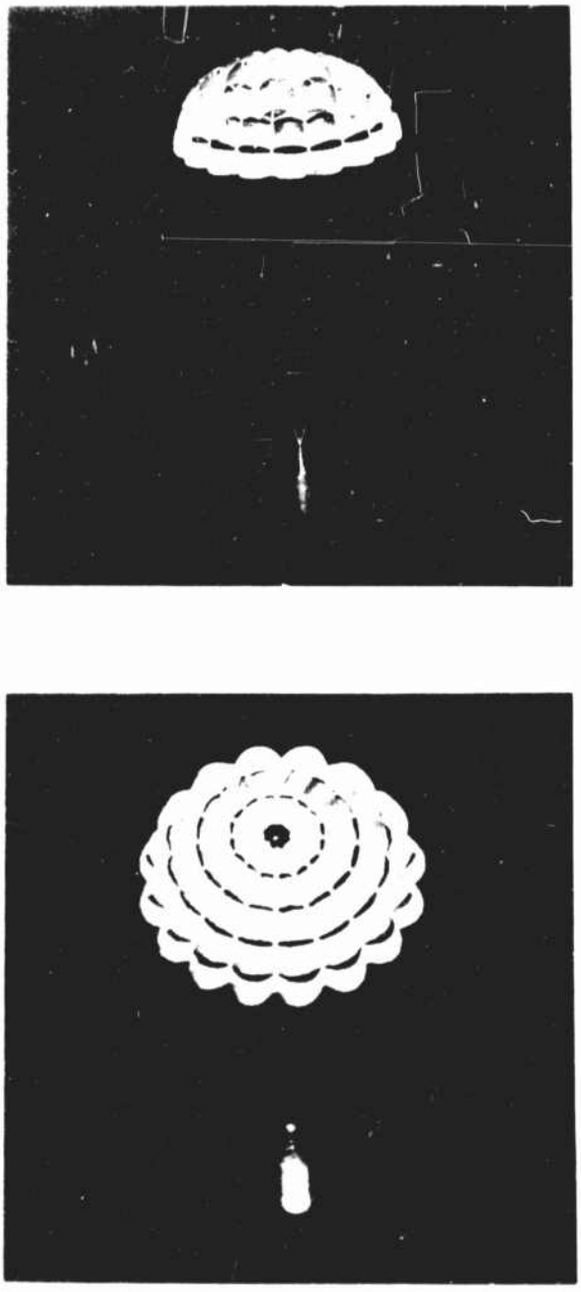

Figure 50 - Photograph of the ring-slot parachute model (13.5% total porosity) (No. 30) during descent at approximately 20 feet per second.

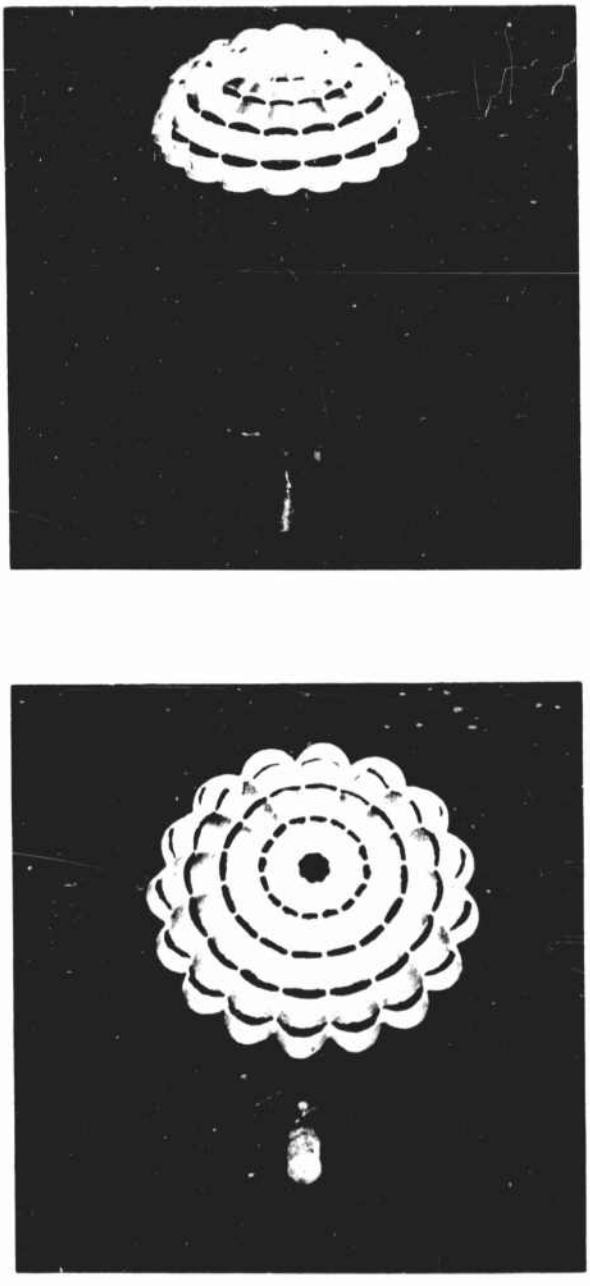

Figure 51 - Photograph of the ring-slot parachute model (17% total porosity) (No. 31) during descent at approximately 20 feet per second.

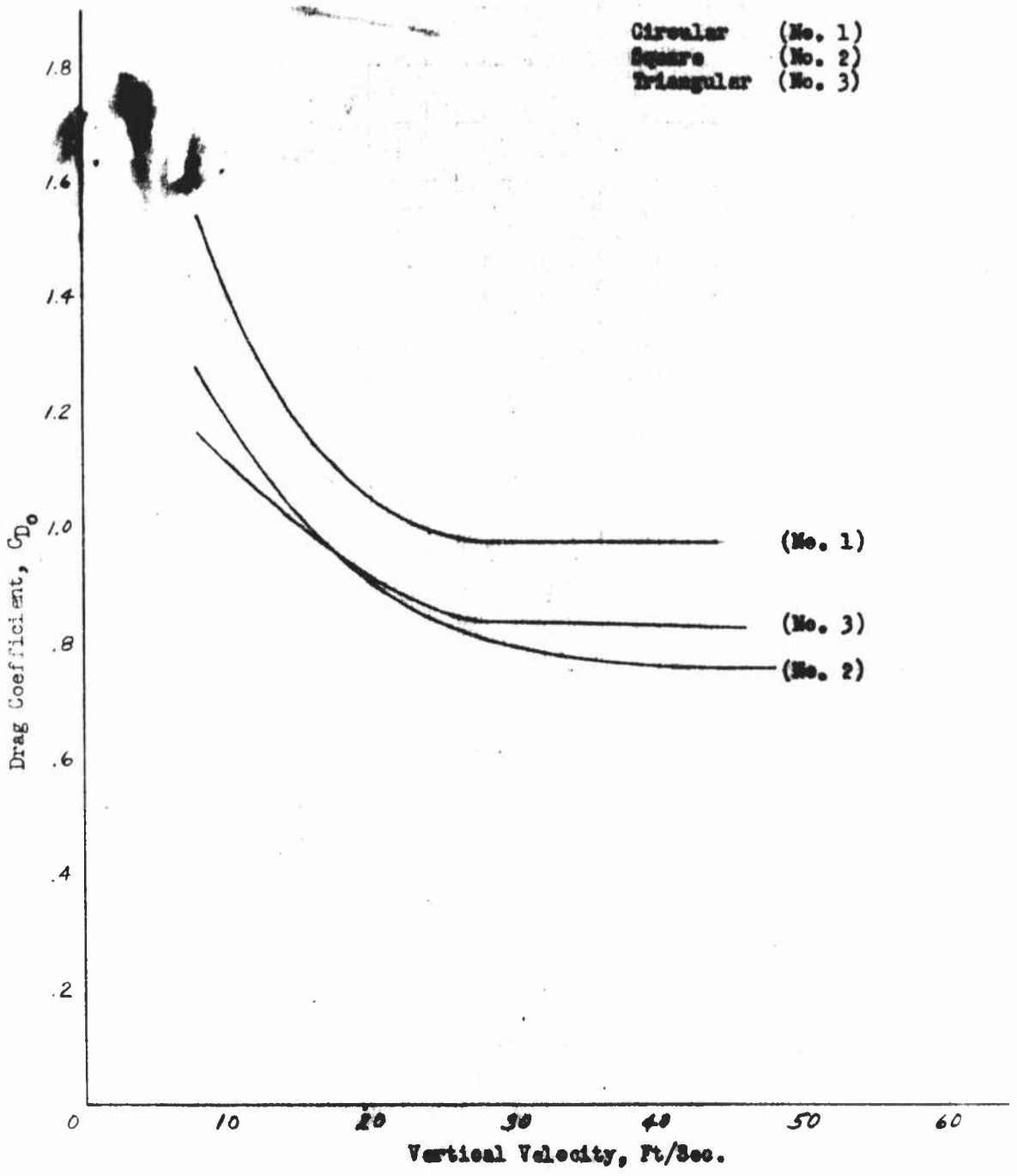

Figure 52 - Summary curves of drag coefficient versus vertical velocity for the models of the solid-flat parachute family.

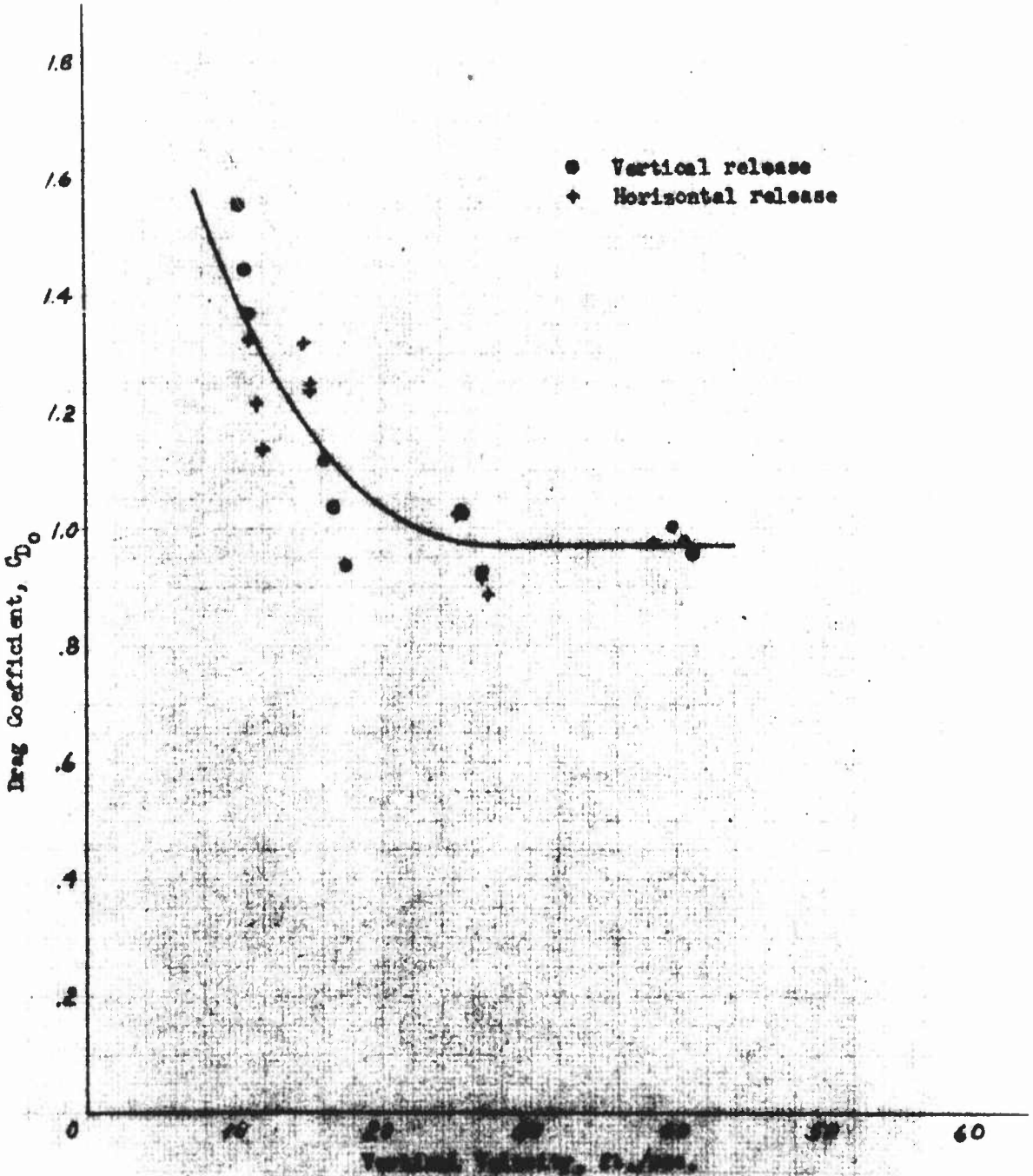

Figure 53- [illegible] vertical velocity for the solid-flat- [illegible] during free fall [illegible] and horizontal types of release.

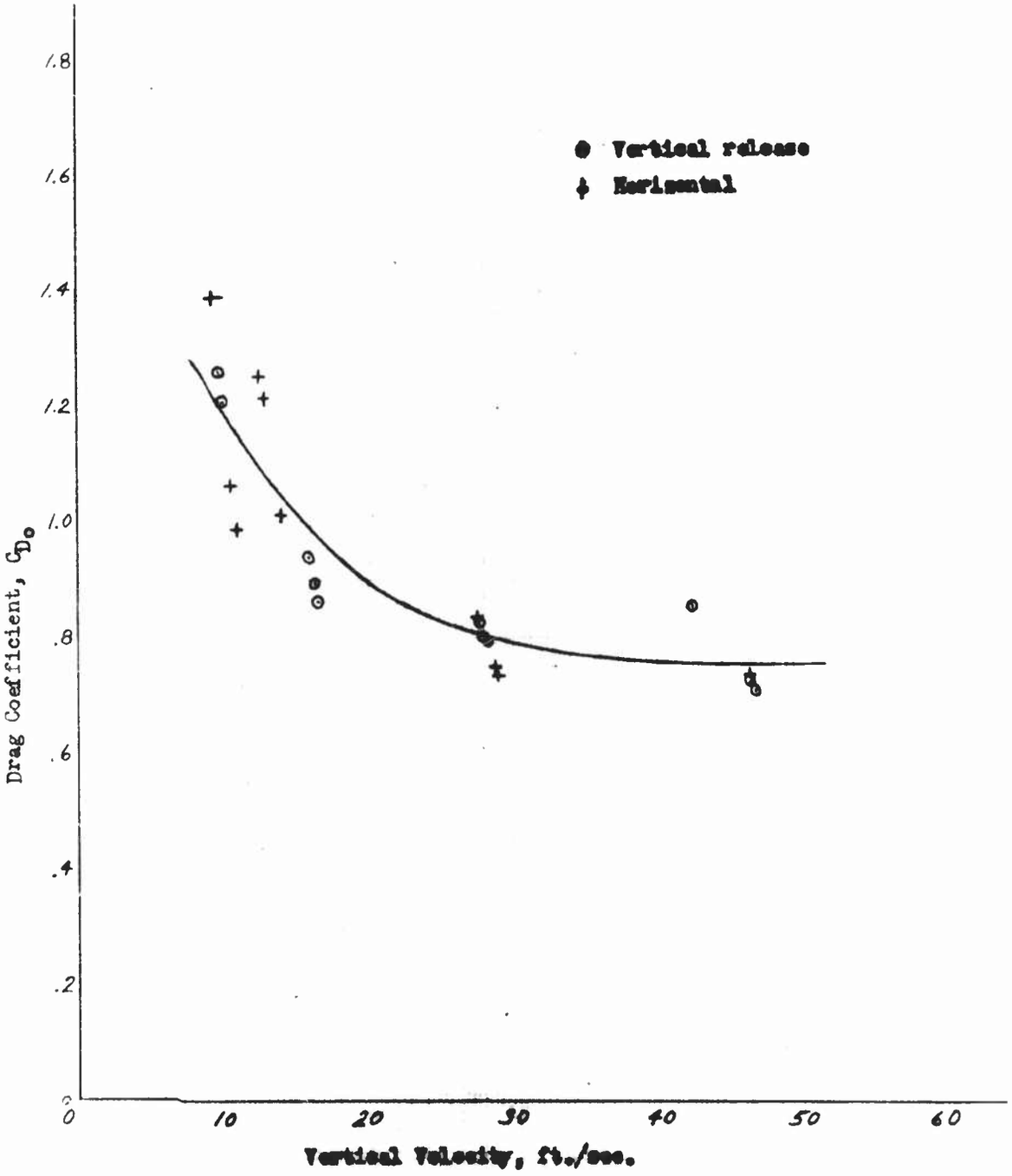

Figure 54 - Drag coefficient versus vertical velocity for the solid-flat-square pedestal parachute model (No. 2) measured during free fall after both vertical and horizontal types of release.

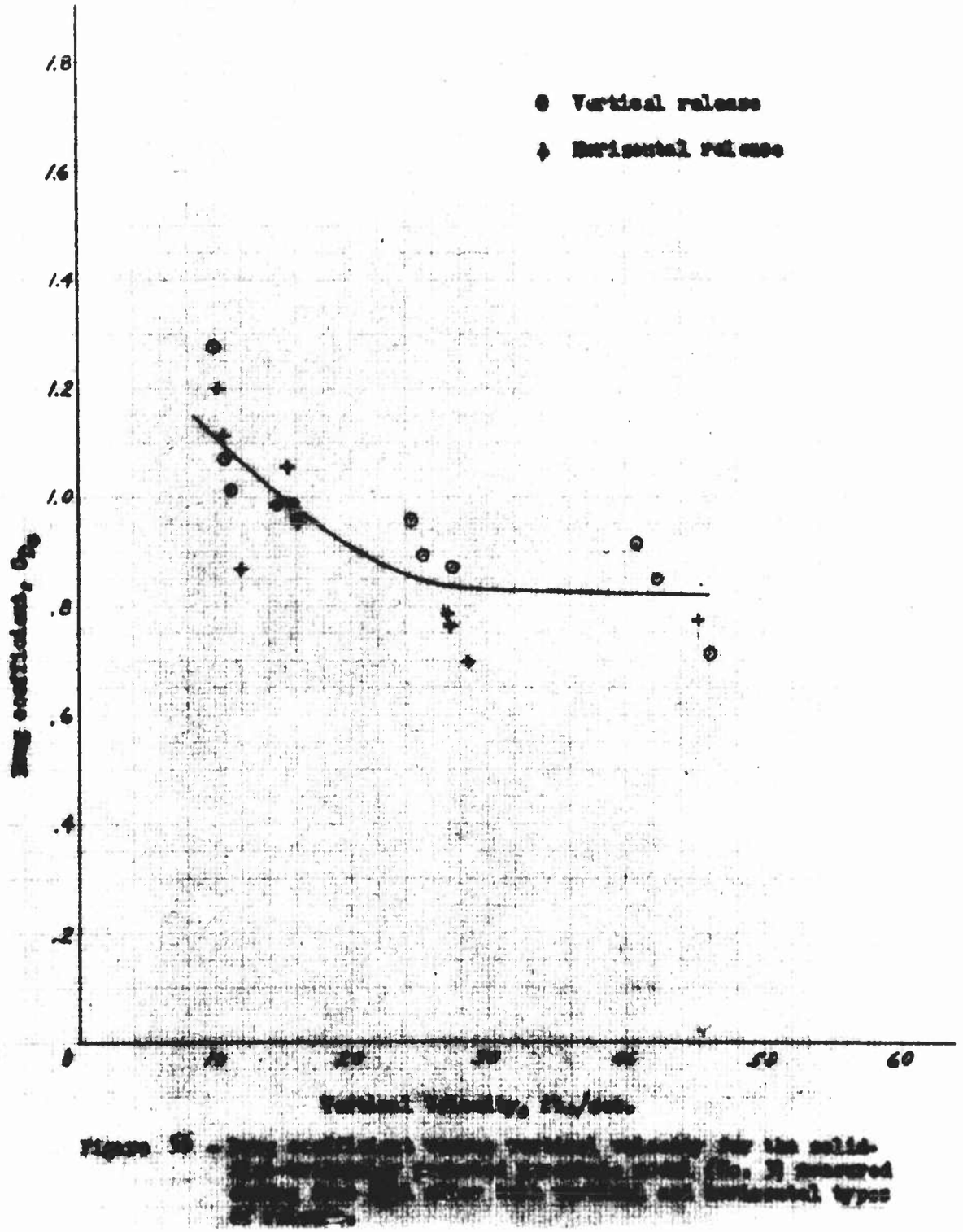
Vertical release
Horizontal release
1.8
1.6
1.4
1.2
1.0
.8
.6
.4
.2
0
10
20
30
40
50
60

Figure 56 -

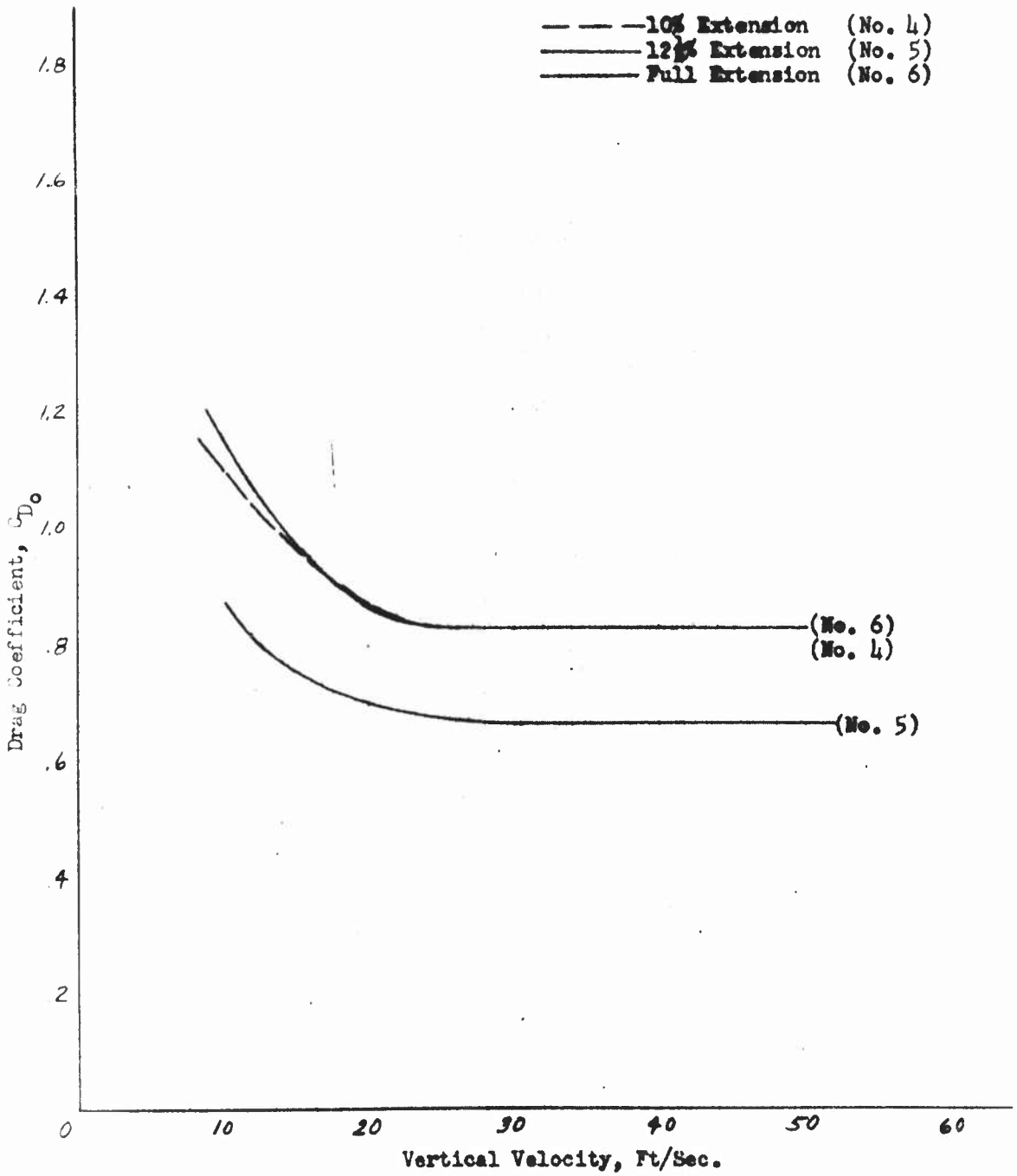

Figure 56 - Summary curves of drag coefficient versus vertical velocity for the models of the solid, extended-skirt parachute family

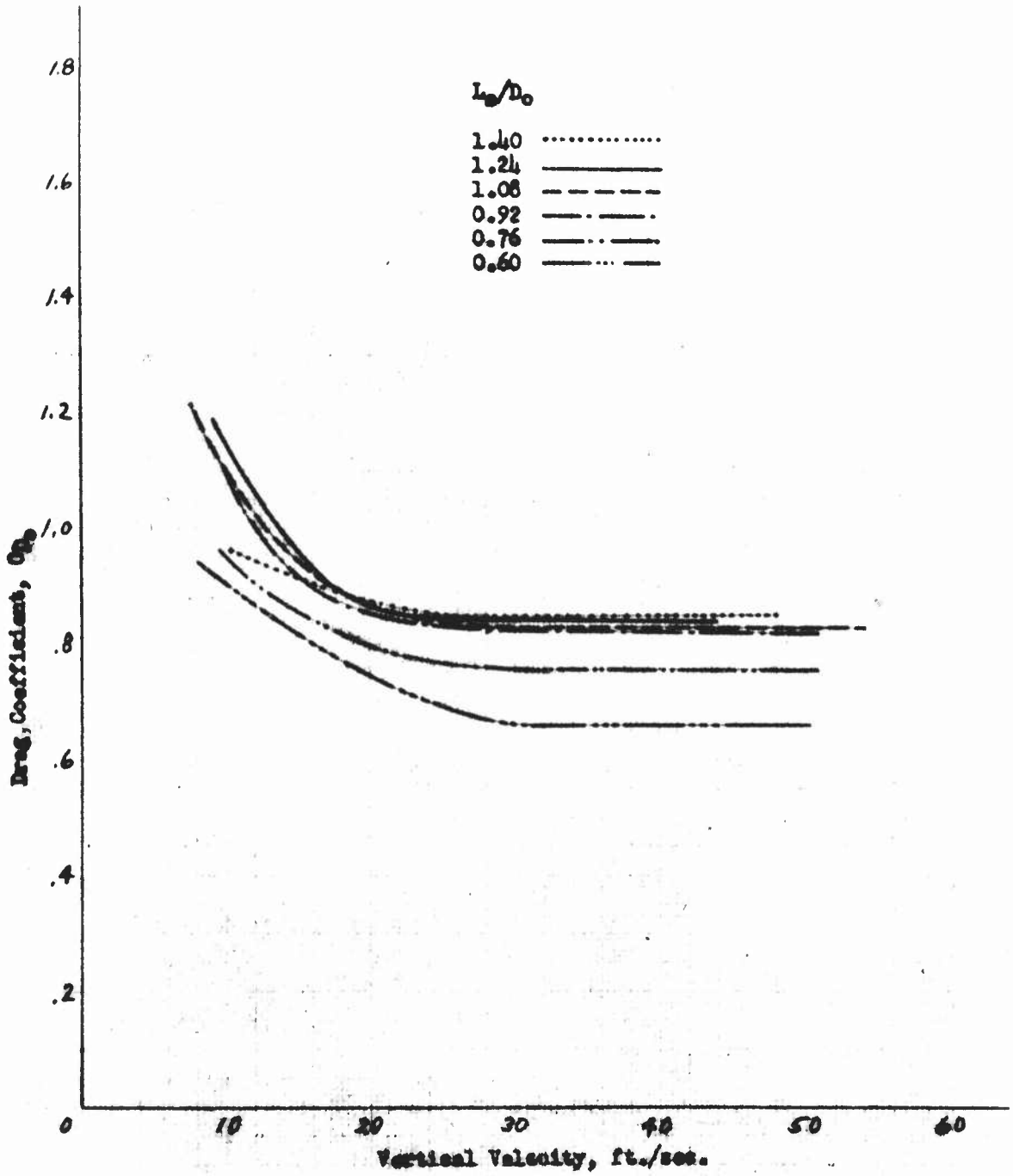

Figure 57 - Summary curves of drag coefficient versus vertical velocity for the solid-flat 10% extended-skirt parachute model (No. 4) for the various suspension line ratios investigated.

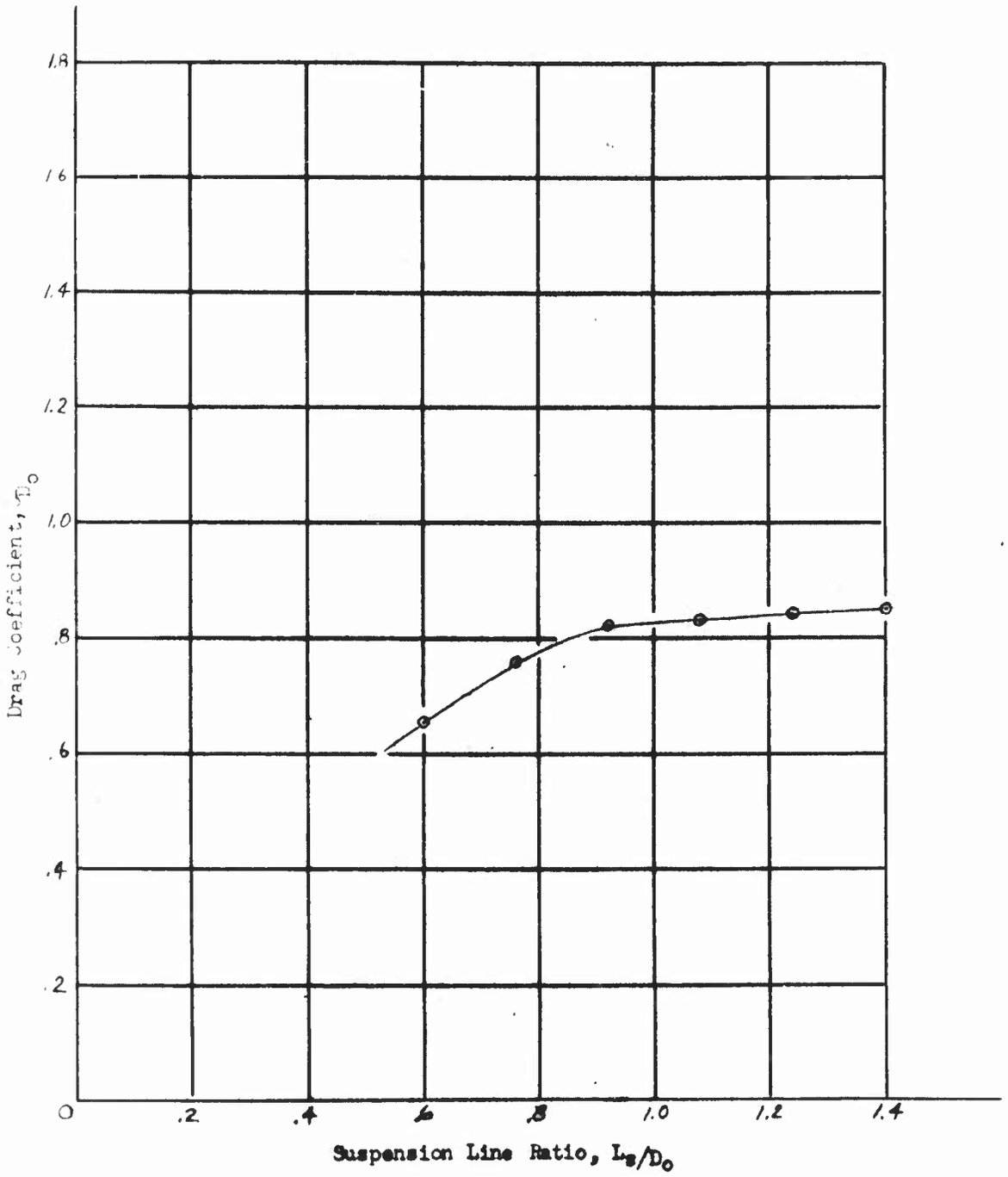

Figure 58 - Drag coefficient versus suspension line ratio for the solid-flat 10% extended-skirt parachute model (No. 4) measured during free fall after both vertical and horizontal types of release.

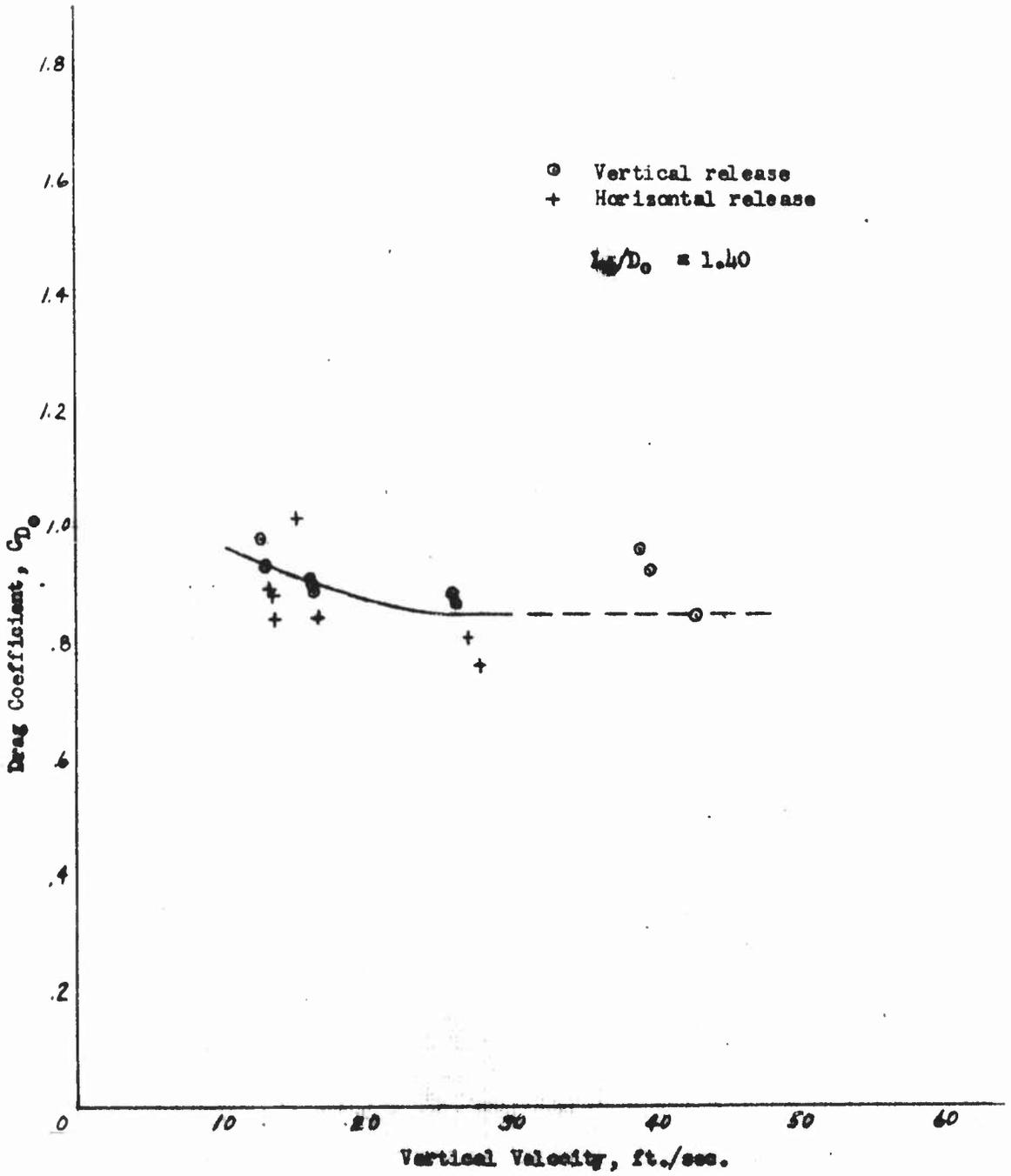

Figure 59 - Drag coefficient versus vertical velocity for the solid-flat 10% extended-skirt parachute model (No. 4) with a shroud-line length of 16 feet 8 inches, measured during free fall after both vertical and horizontal types of release

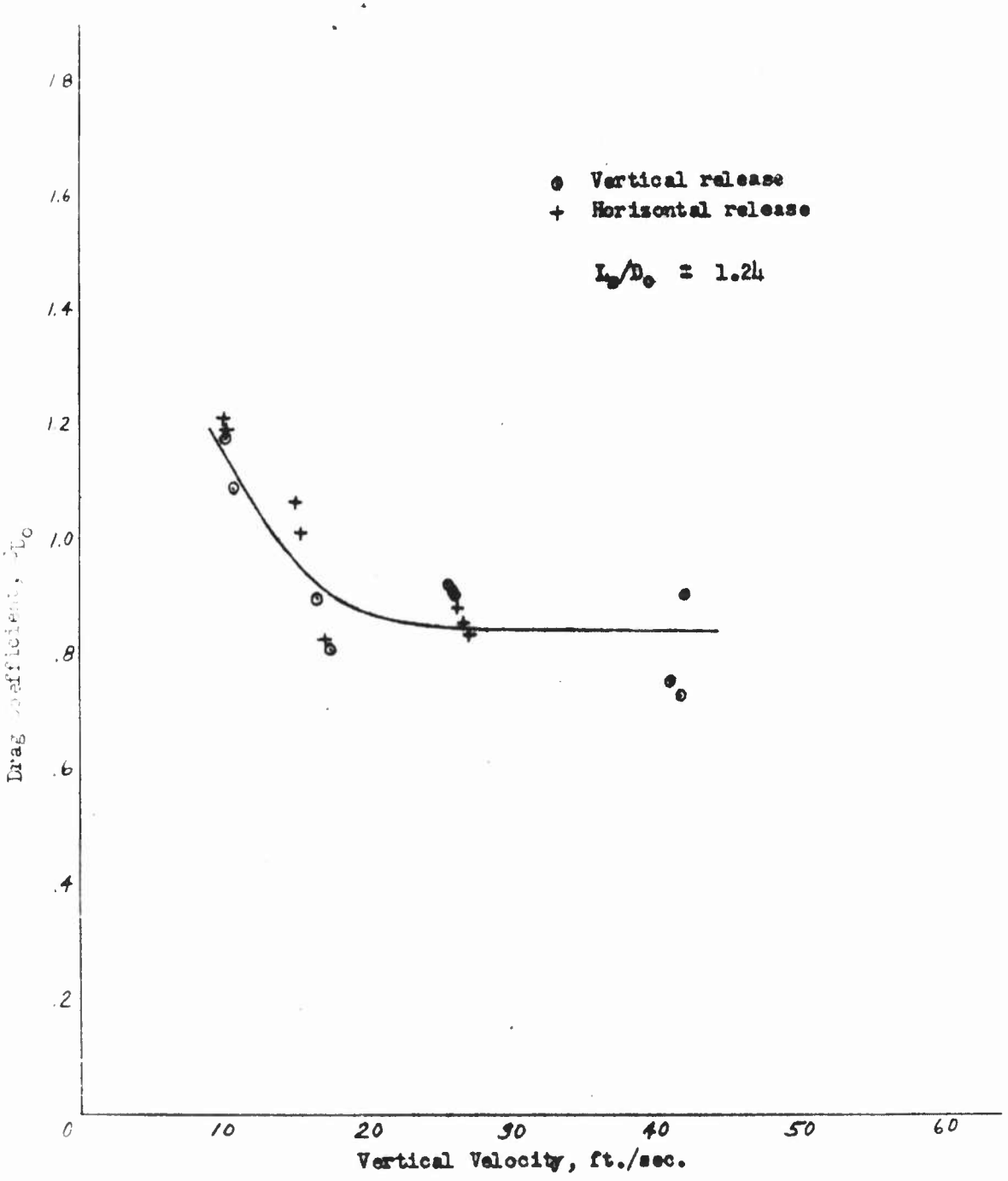

Figure 60 - Drag coefficient versus vertical velocity for the solid-flat 10% extended-skirt parachute model (No. 4) with a shroud-line length of 14 feet 9 inches, measured during free fall after both vertical and horizontal types of release

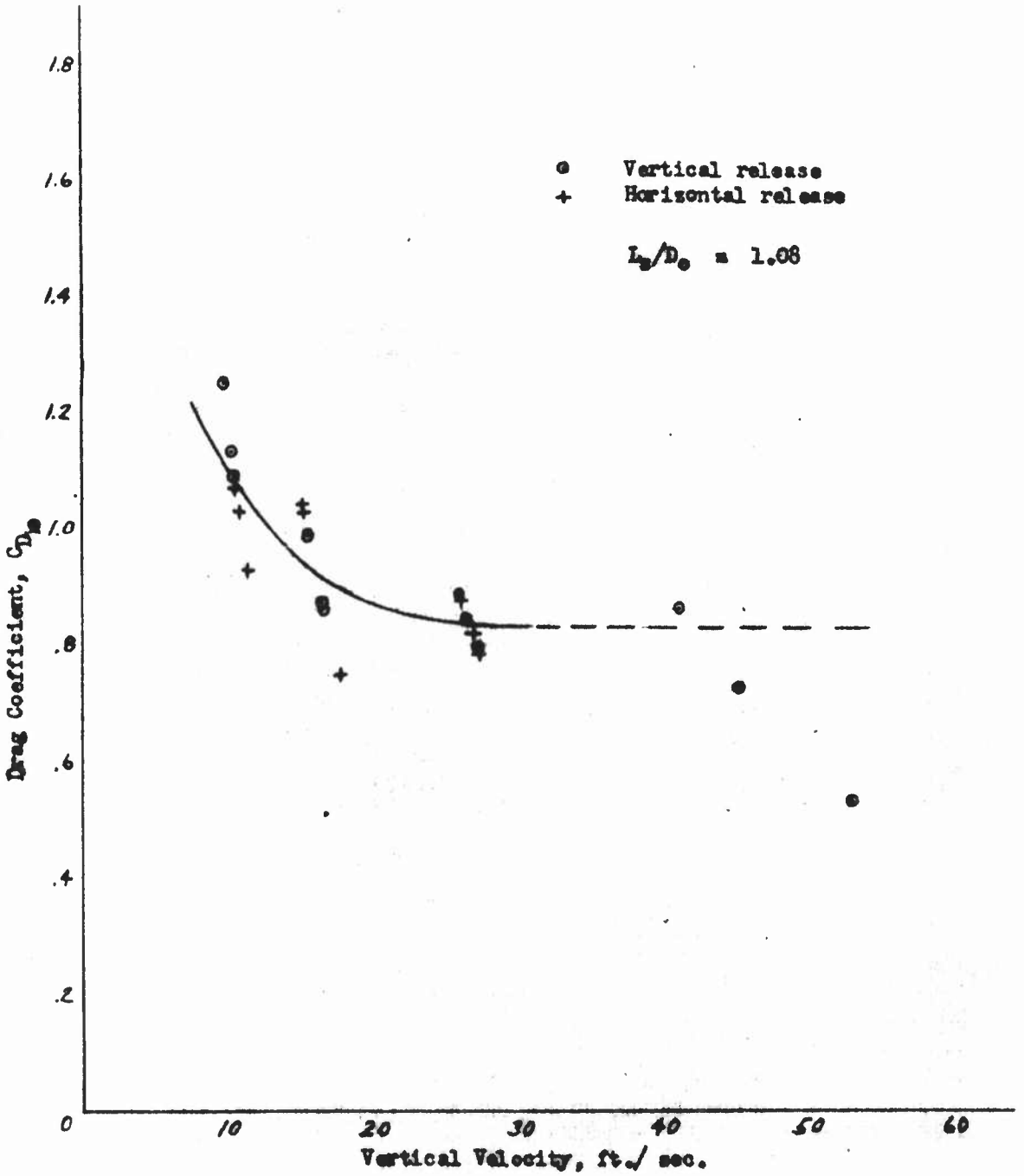

Figure 61 - Drag coefficient versus vertical velocity for the solid-flat 10% extended-skirt parachute model (No. 4) with a shroud-line length of 12 feet 10 inches, measured during free fall after both vertical and horizontal types of release.

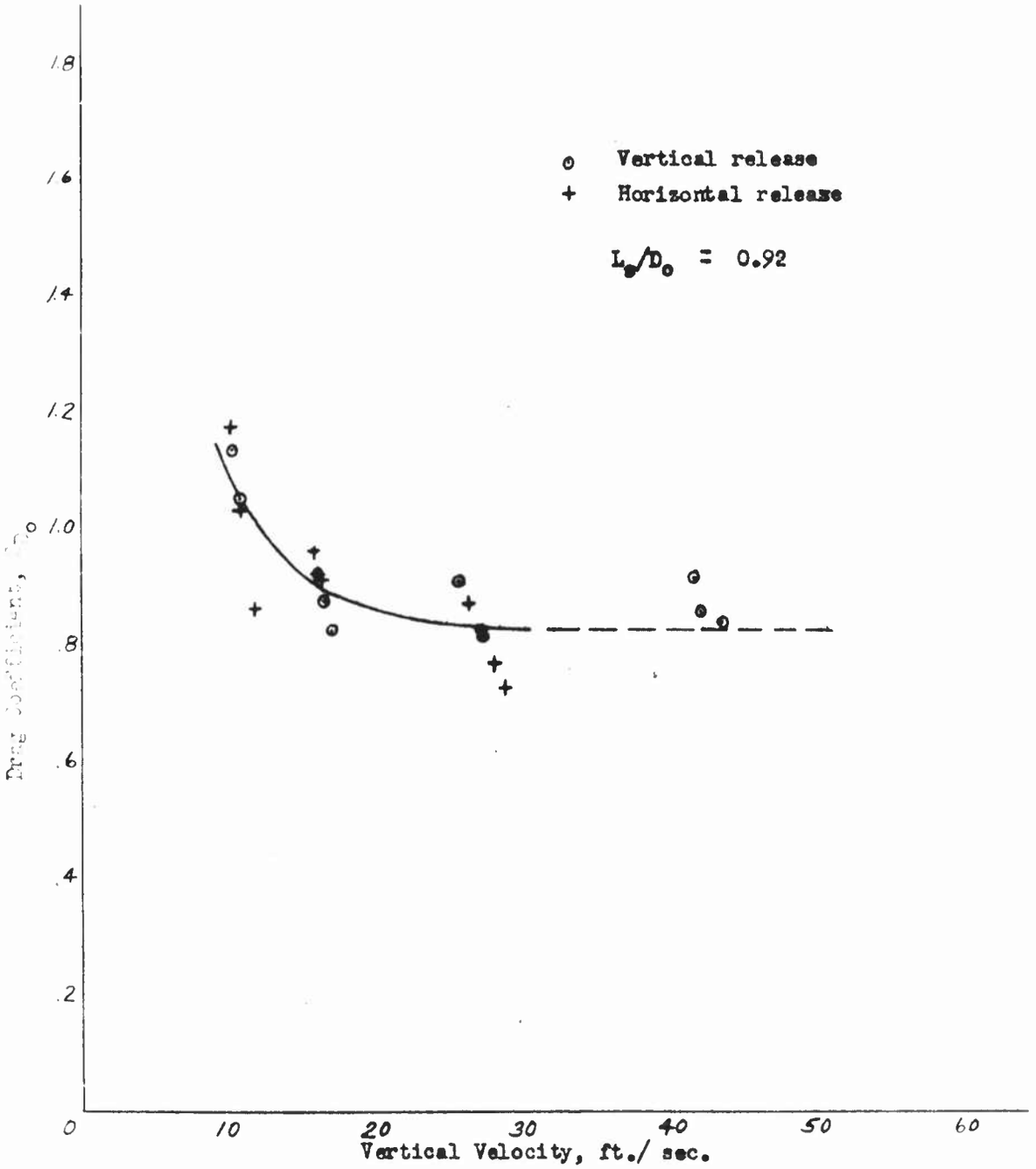

Figure 62 - Drag coefficient versus vertical velocity for the solid-flat 10% extended-skirt parachute model (No. 4) with a shroud-line length of 10 feet 11 inches, measured during free fall after both vertical and horizontal types of release.

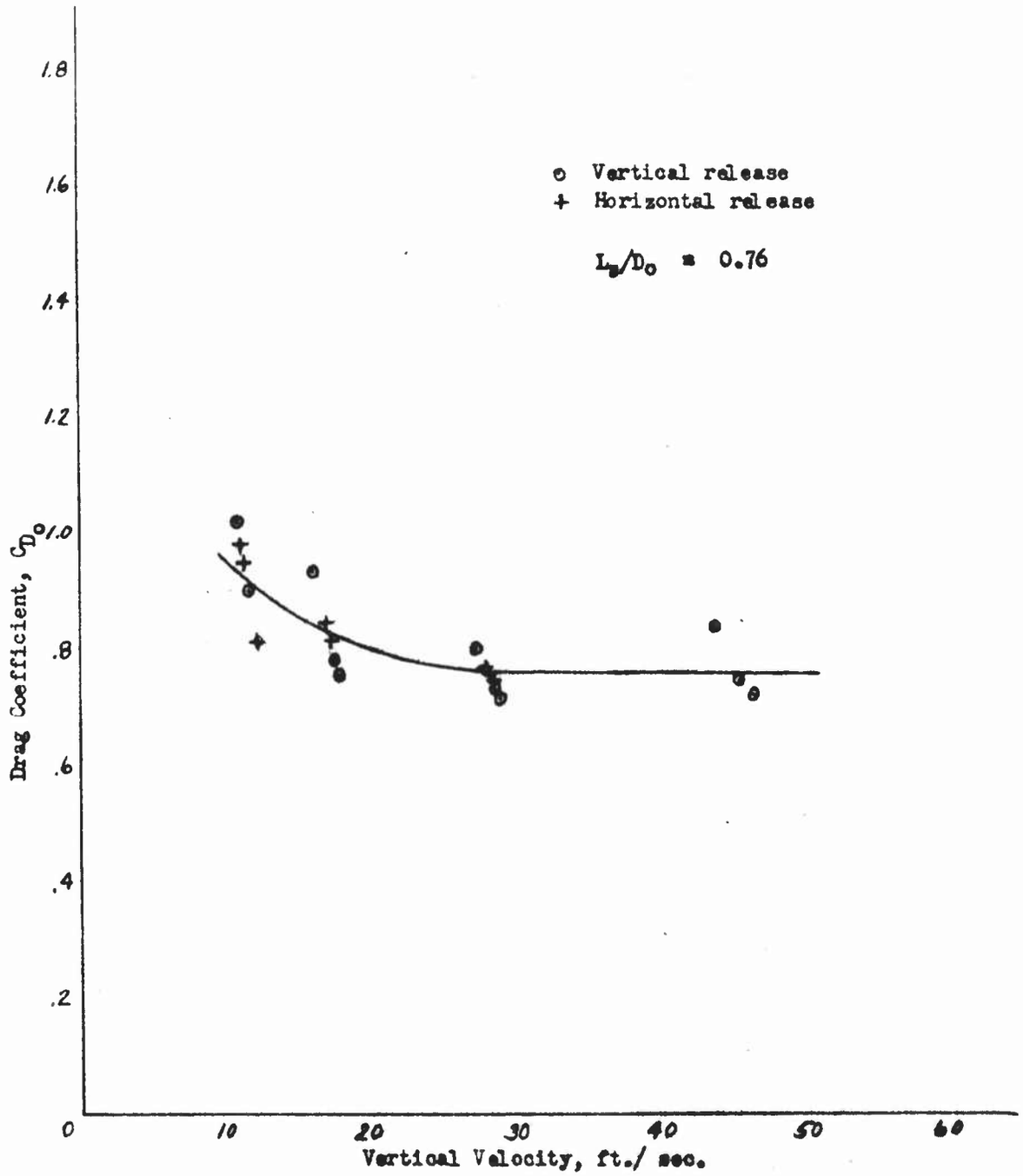

Figure 63 - Drag coefficient versus vertical velocity for the solid-flat 10% extended-skirt parachute model (No. 4) with a shroud-line length of 9 feet 1 inch, measured during free fall after both vertical and horizontal types of release.

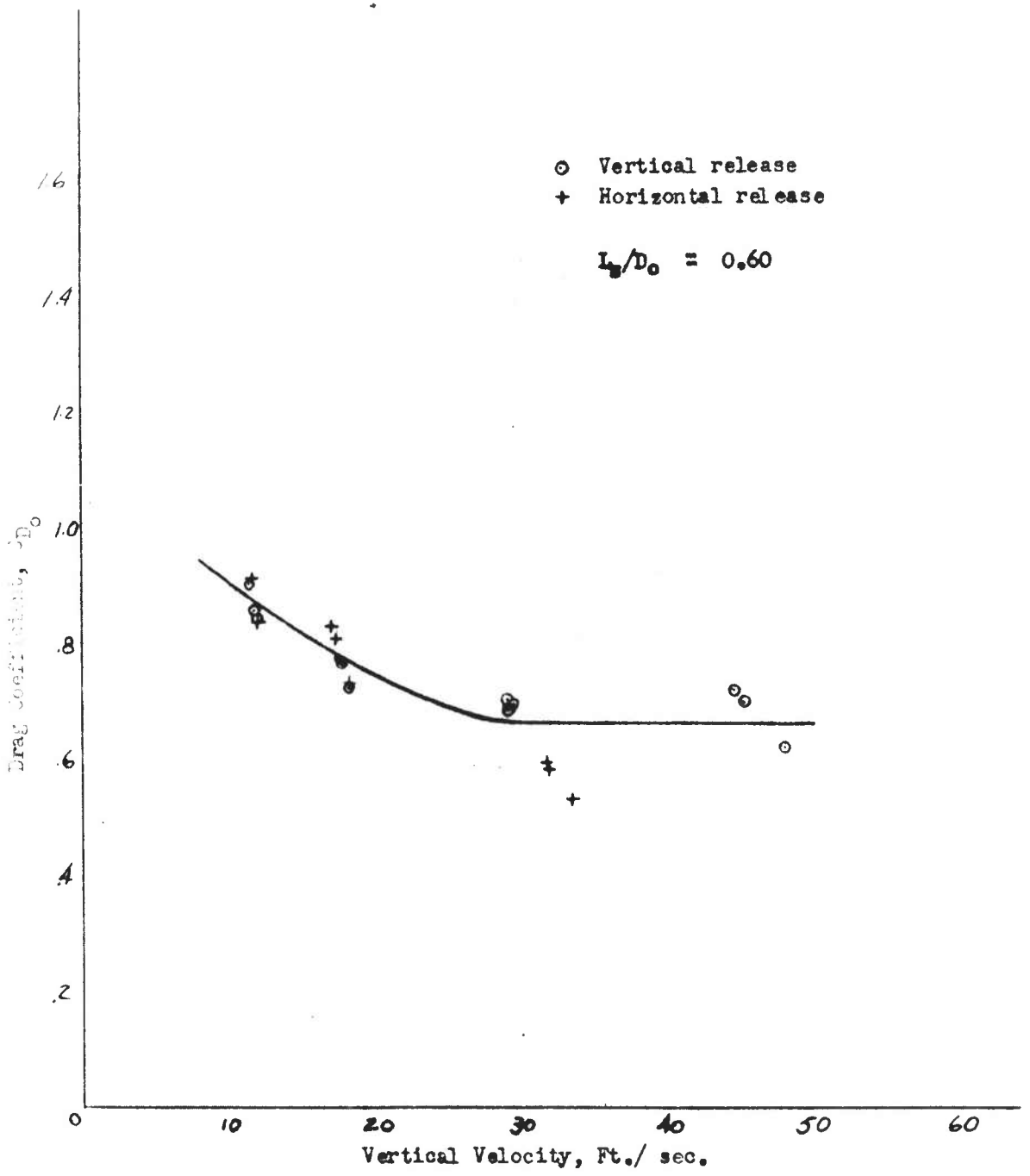

Figure 64 -Drag coefficient versus vertical velocity for the solid-flat 10% extended-skirt parachute model (No. 4) with a shroud-line length of 7 feet 2 inches, measured during free fall after both vertical and horizontal types of release.

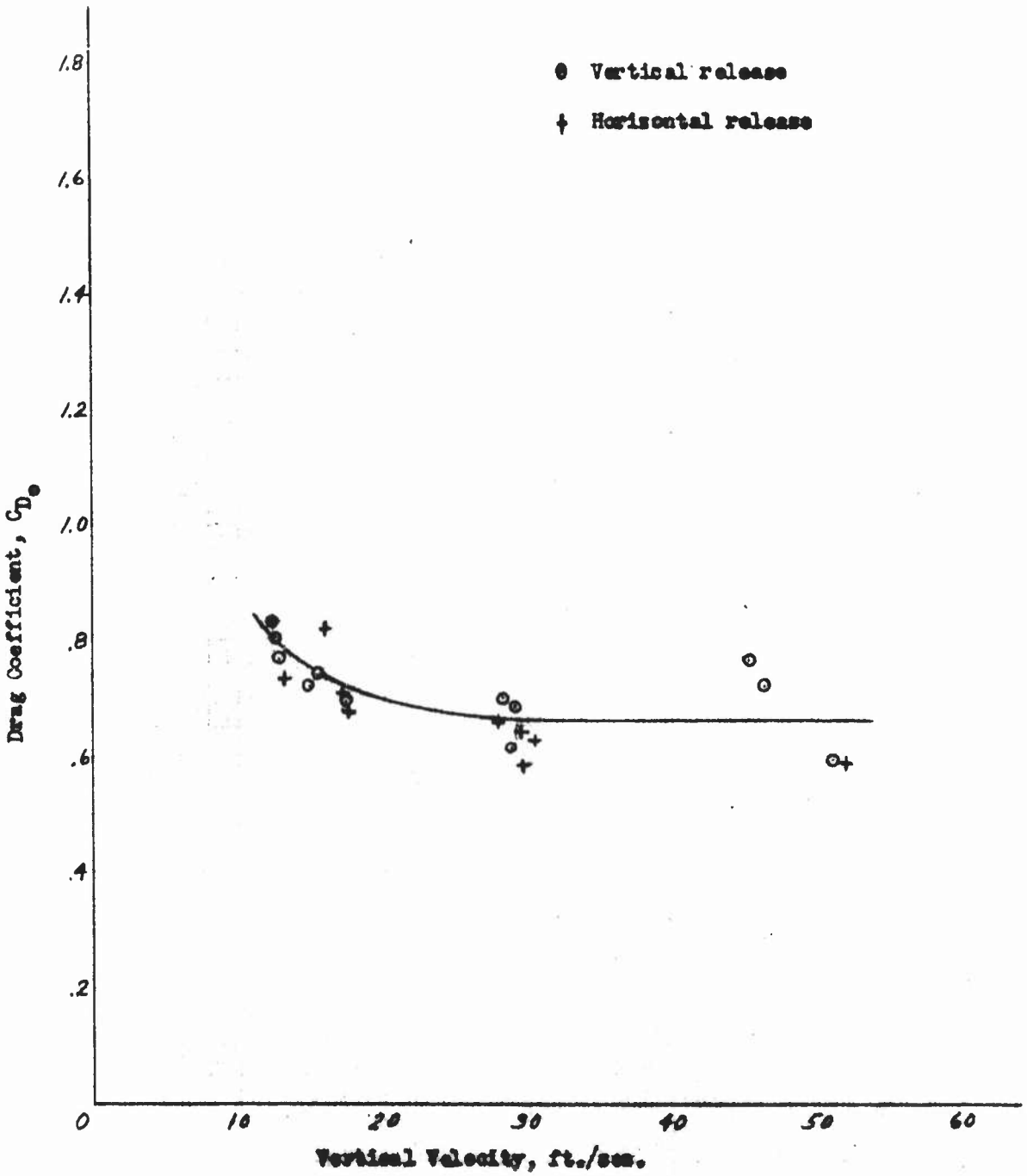

Figure 65 - Drag coefficient versus vertical velocity for the solid-cloth 1/8 extended-skirt parachute model (No. 5) measured during free fall after both vertical and horizontal types of release.

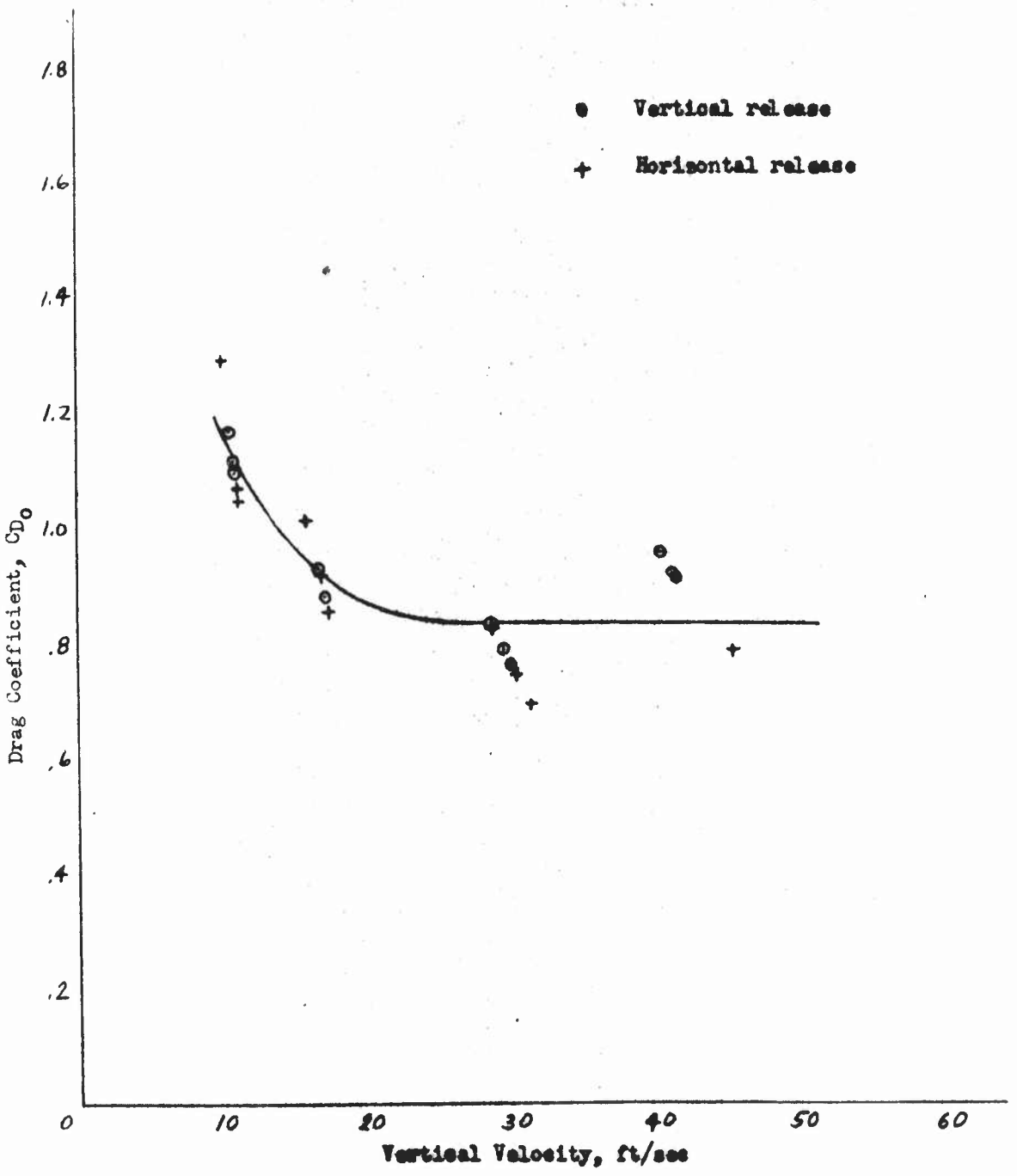

Figure 66 - Drag coefficient versus vertical velocity for the solid-flat fully extended-skirt parachute model (No. 6) measured during free fall after both vertical and horizontal types of release.

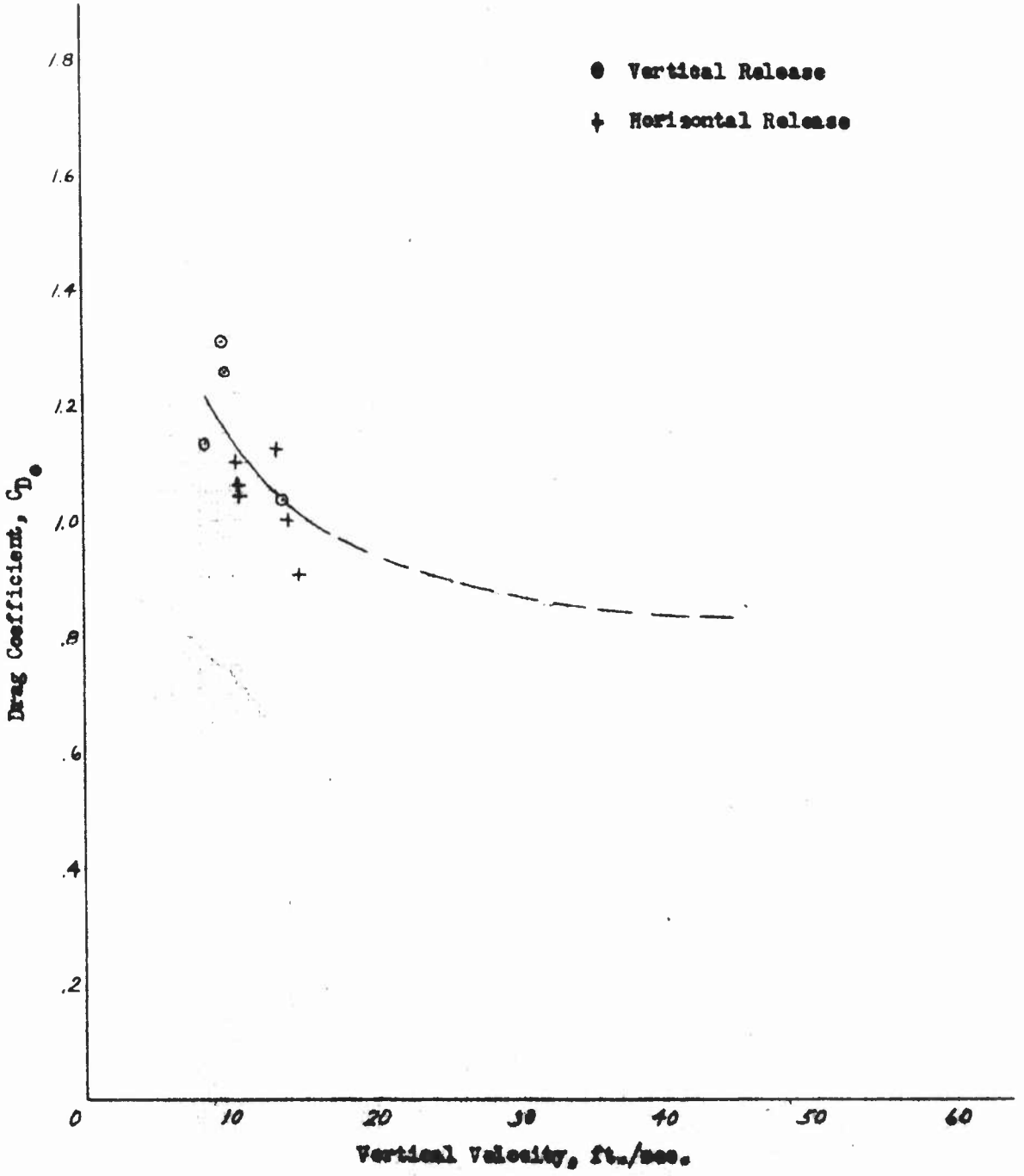

Figure 67 - Drag coefficient versus vertical velocity for the 50% vent airfoil parachute model (No. 7) measured during free fall after both vertical and horizontal types of release.

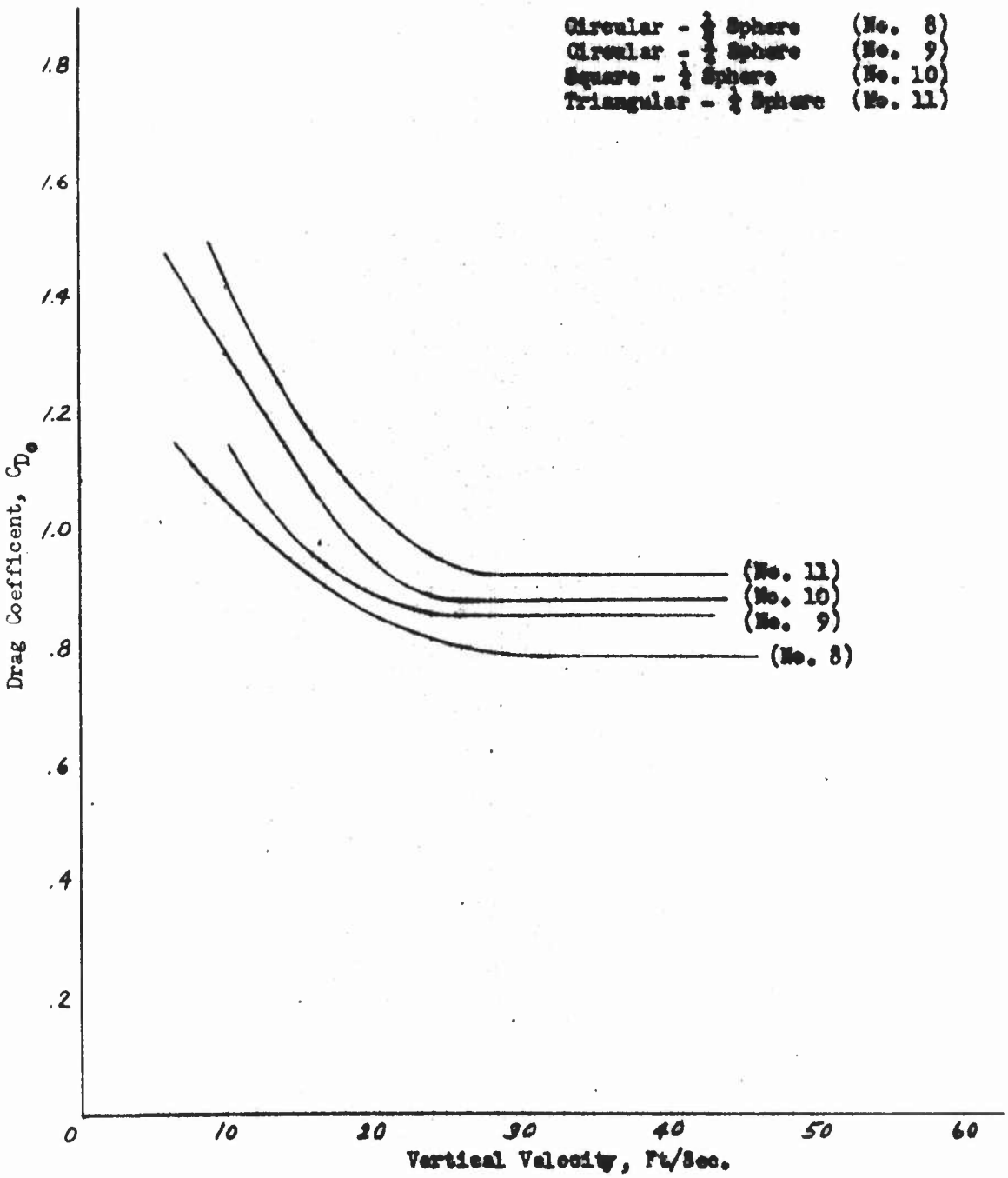

Figure 68 - Summary curves of drag coefficient versus vertical velocity for the models of the solid spherical parachute family.

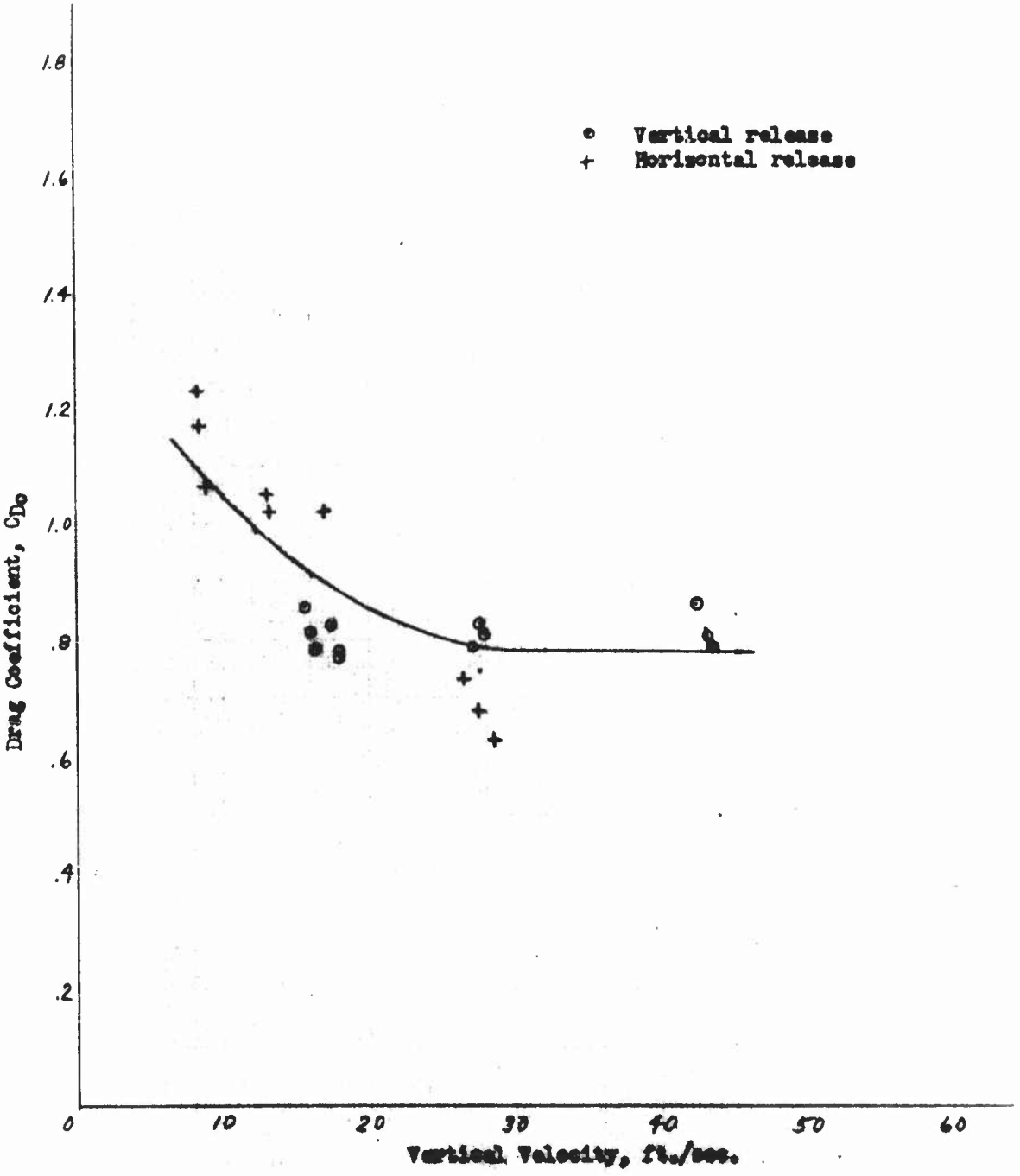

Figure 69 - Drag coefficient versus vertical velocity for the 3 sphere circular symmetric model (No. 8) measured during free fall after both vertical and horizontal types of release.

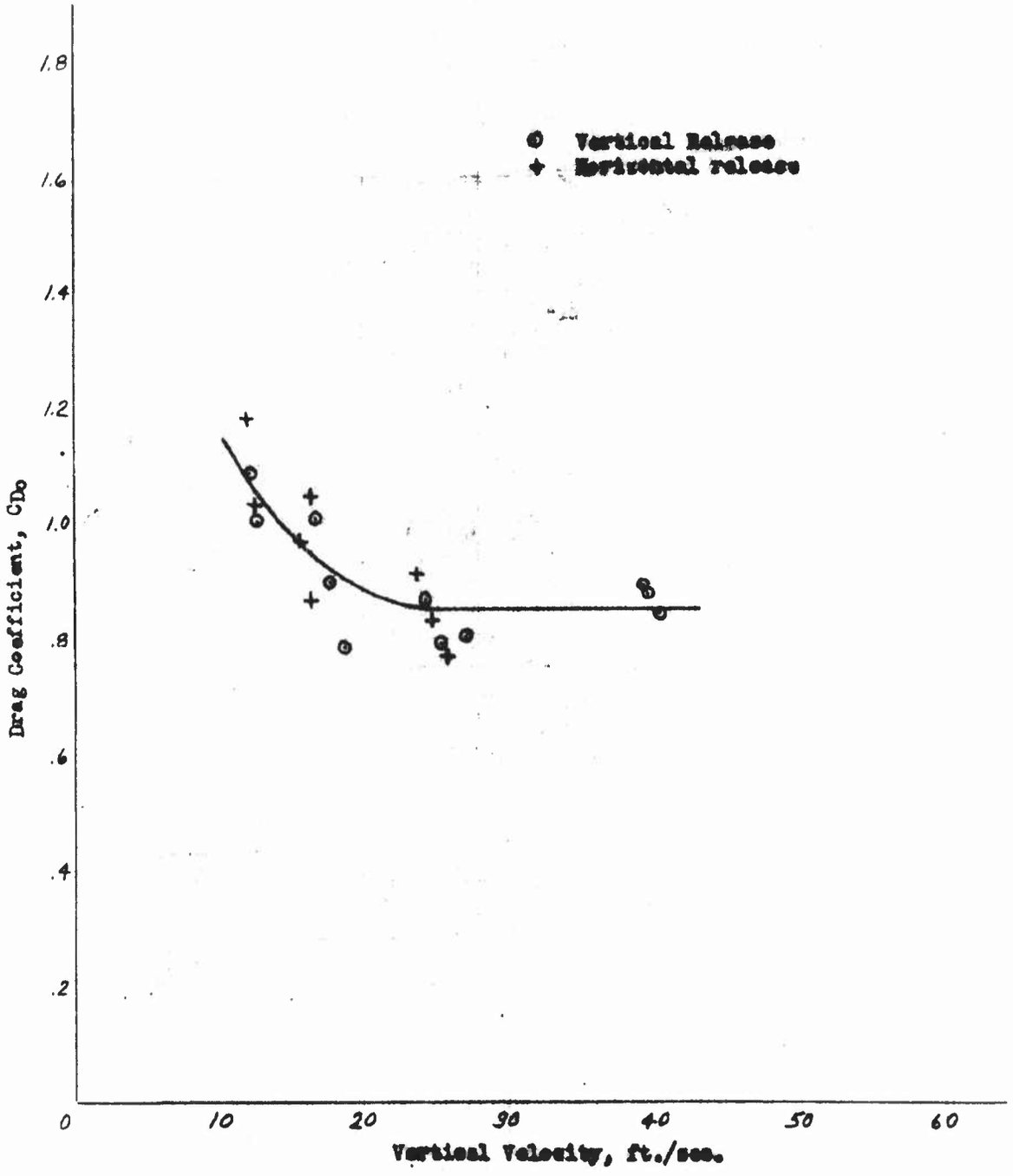

Figure 70 - Drag coefficient versus vertical velocity for the ½ sphere circular [illegible] model (No. 9) measured during free fall after both vertical and horizontal types of release.

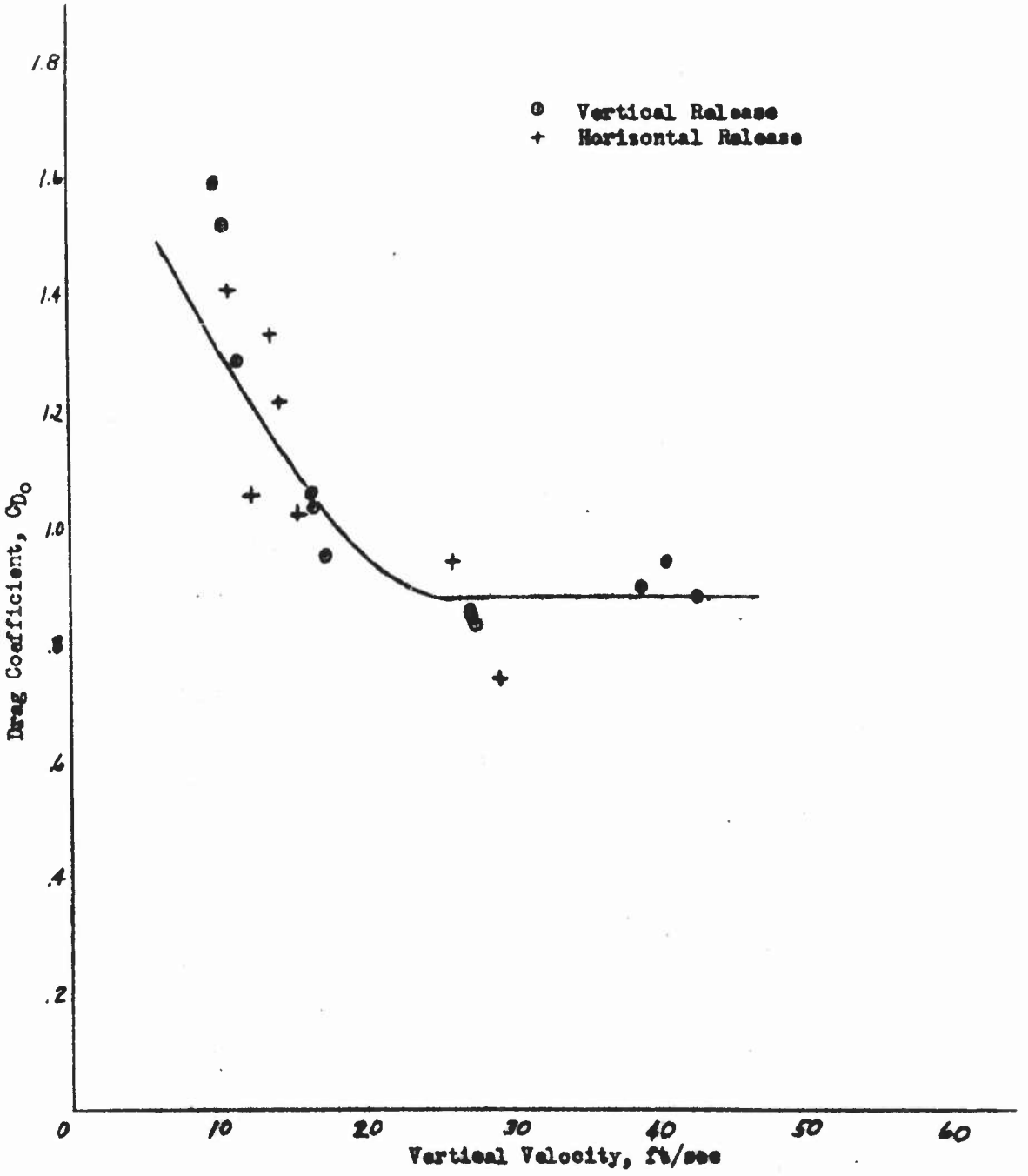

Figure 71 - Drag coefficient versus vertical velocity for the ½ sphere square parachute model (No. 10) measured during free fall after both vertical and horizontal types of release.

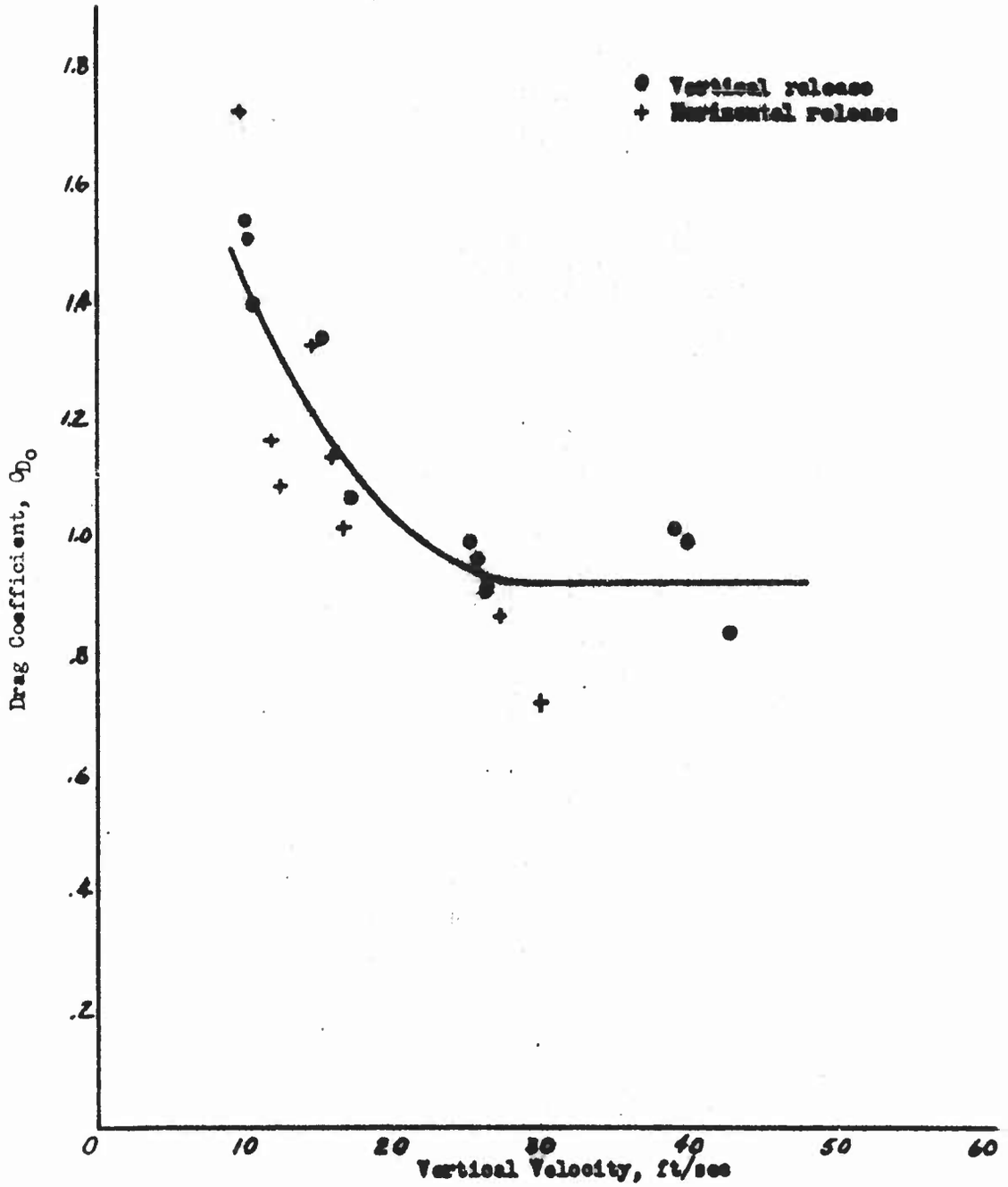

Figure 72 - Drag coefficient versus vertical velocity for the ¼ sphere triangular parachute model (No. 11) measured during free fall after both vertical and horizontal types of release.

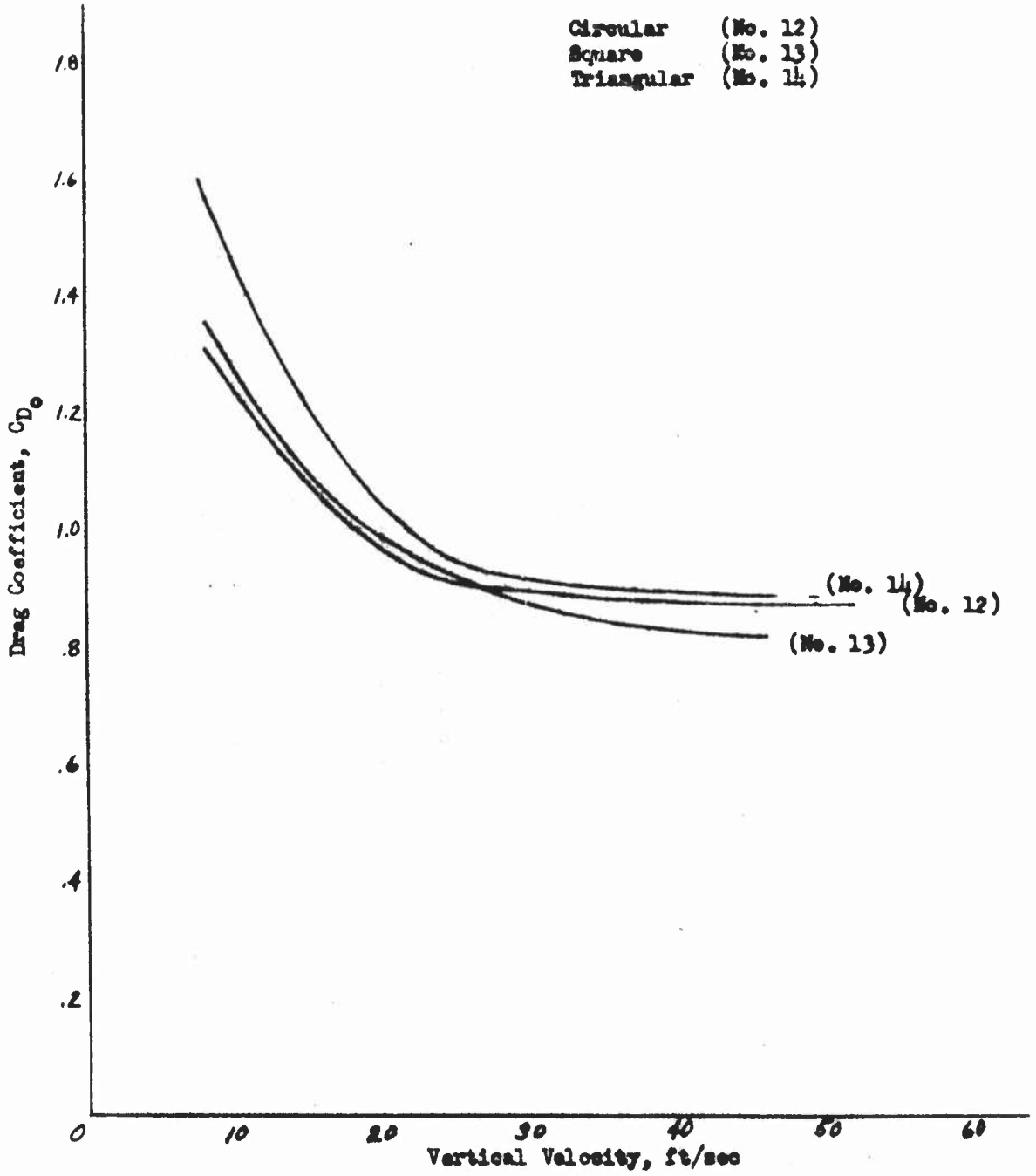

Figure 73 - Summary curves of drag coefficient versus vertical velocity for the models of the 30° solid conical parachute family

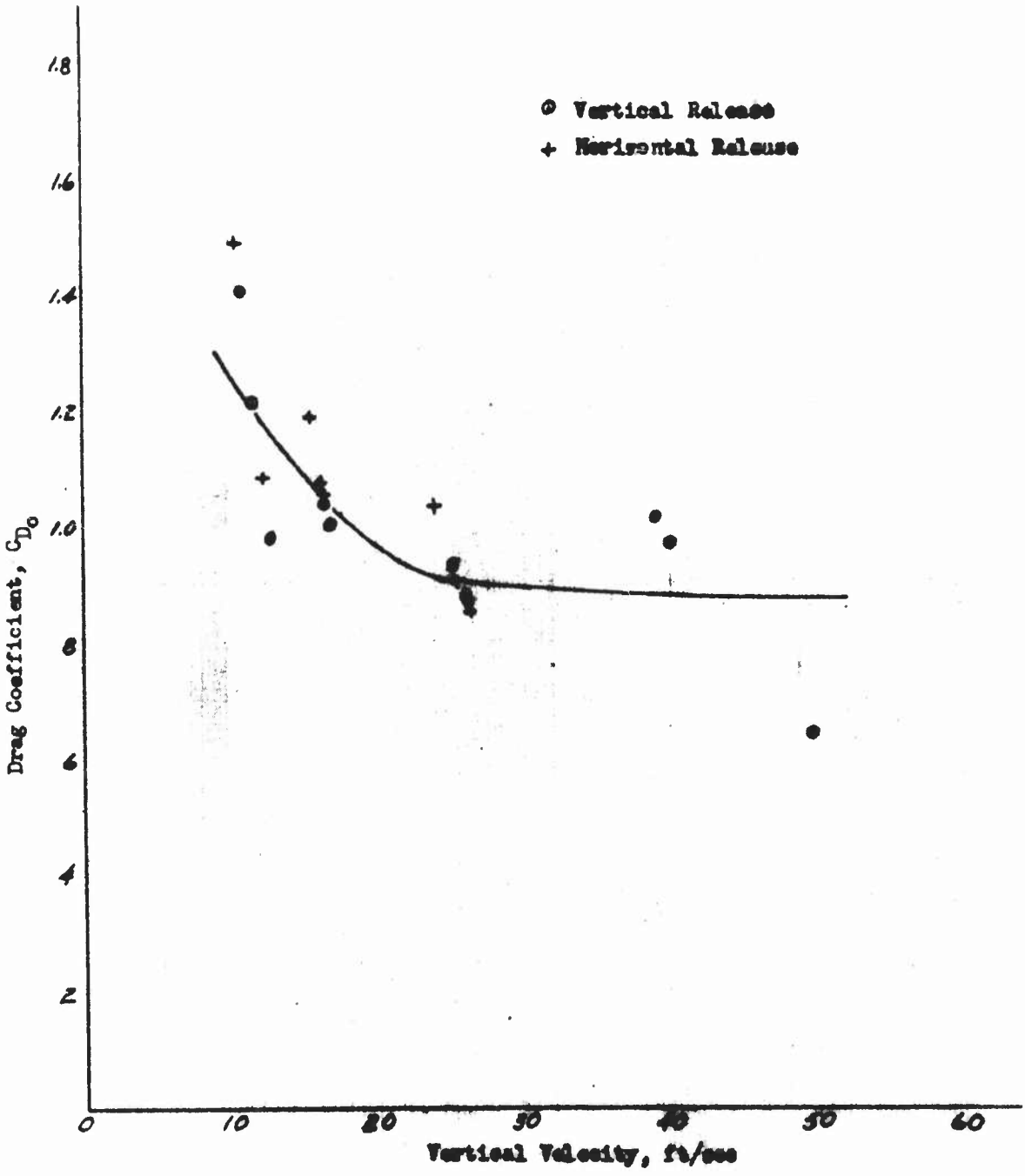

Figure 74 - Drag coefficient versus vertical velocity for the 30° circular conical parachute model (No. 12) measured during free fall after vertical and horizontal types of release.

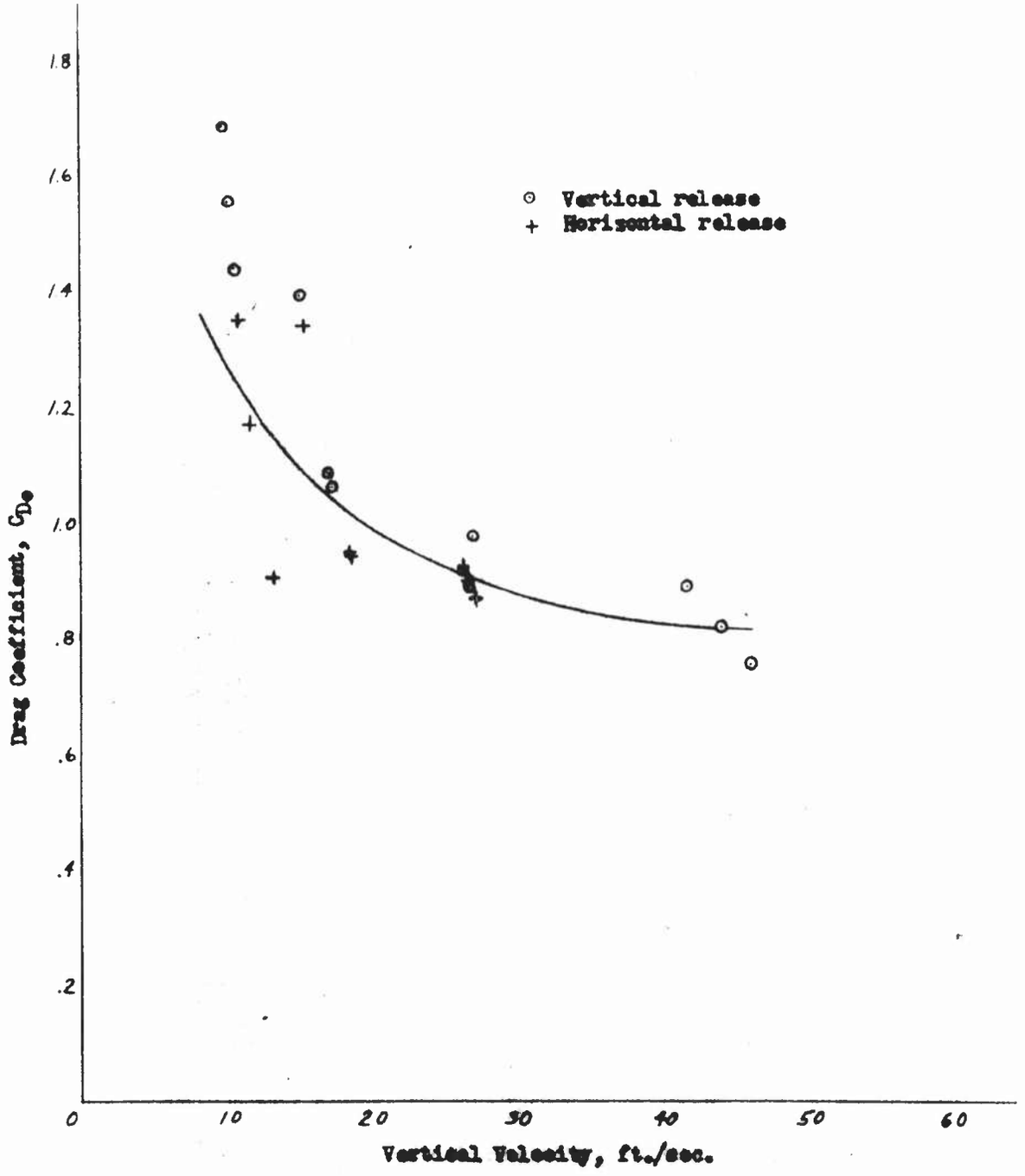

Figure 75 - Drag coefficient versus vertical velocity for the 30° square conical parachute model (No. 13) measured during free fall after both vertical and horizontal types of release.

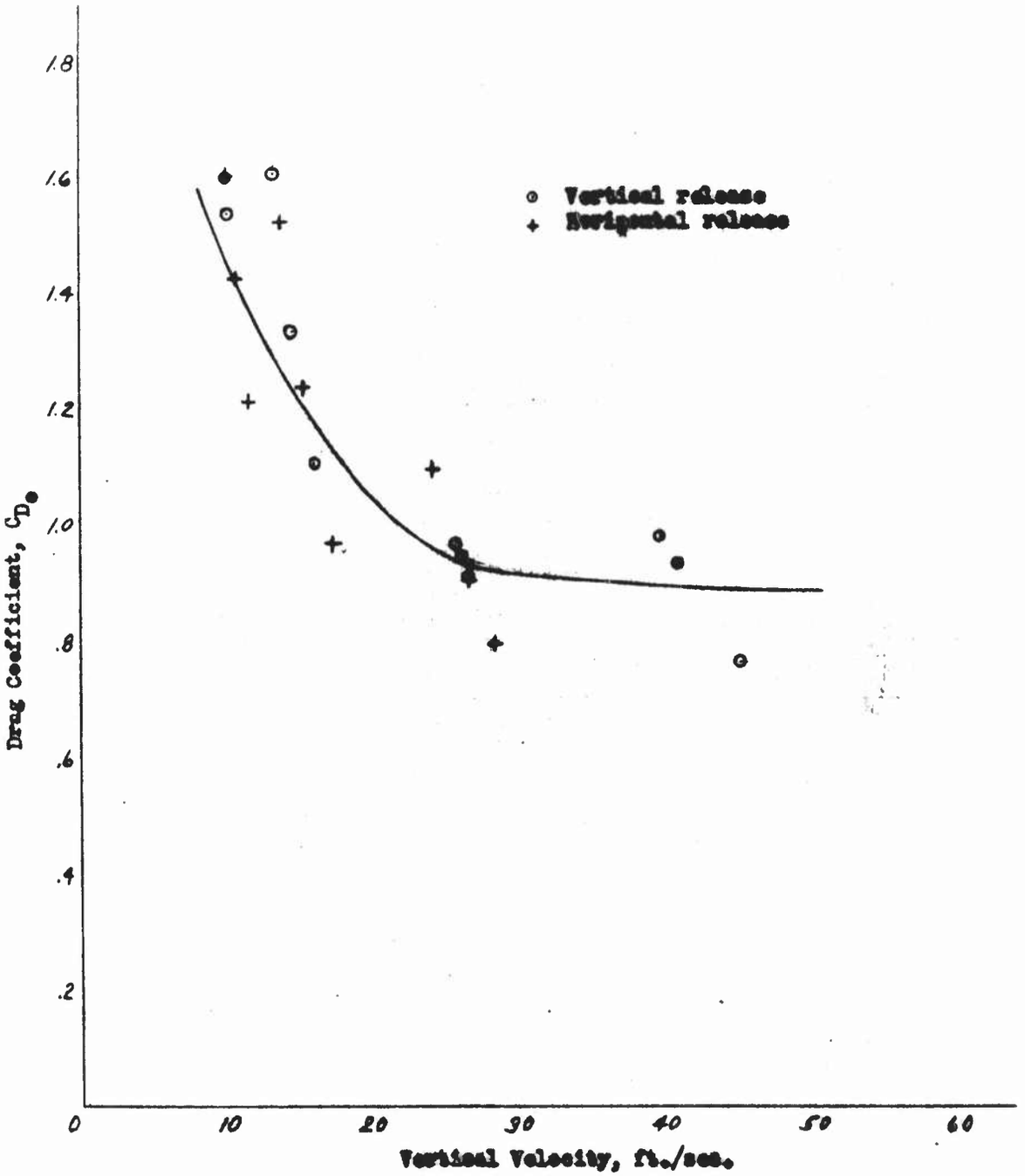

Figure 76 - Drag coefficient versus vertical velocity for the 30° triangular confined parachute model (No. 14) measured during free fall after both vertical and horizontal types of release.

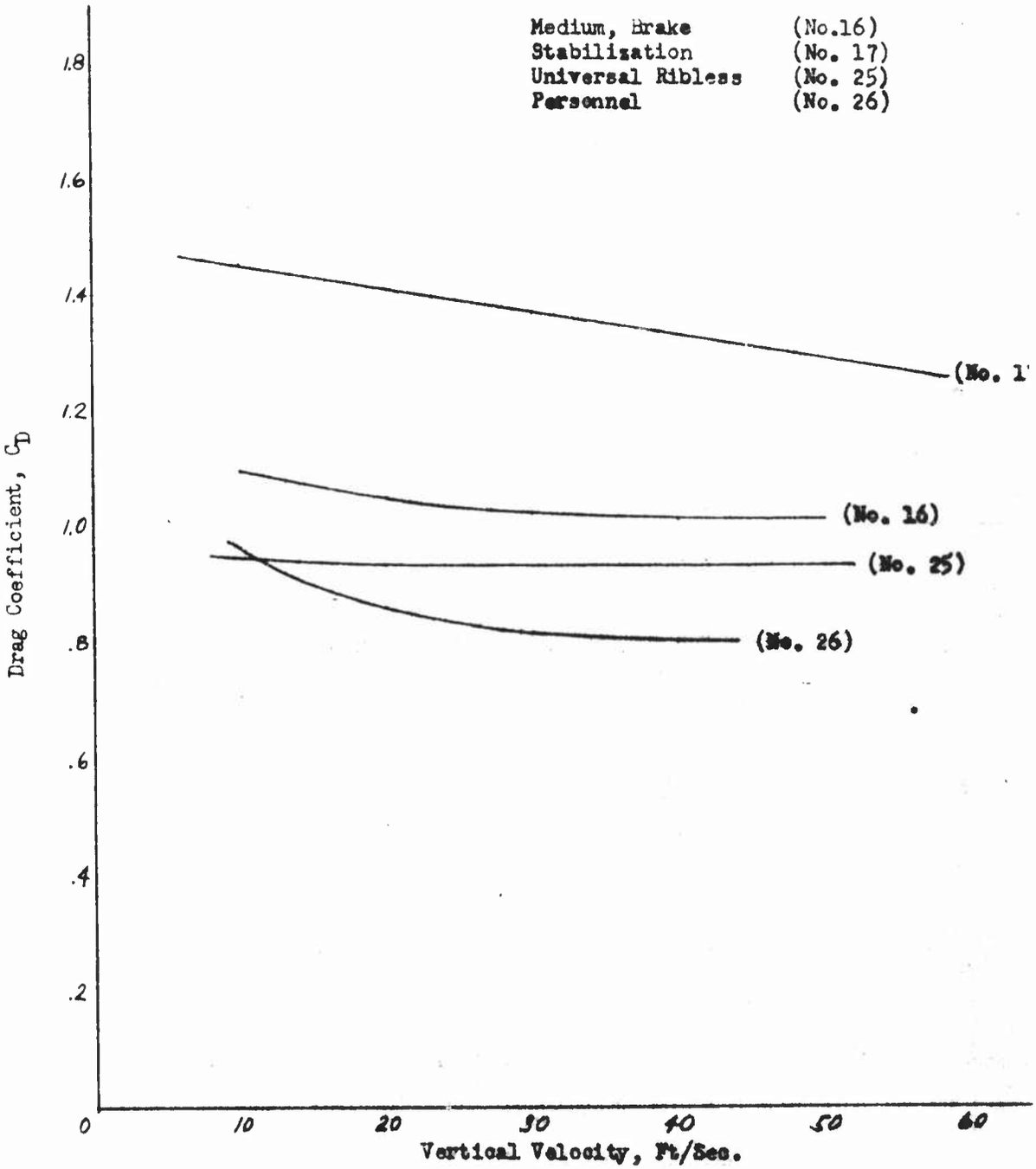

Figure 77 - Summary curves of drag coefficient versus vertical velocity for the models of the guide surface parachute family.

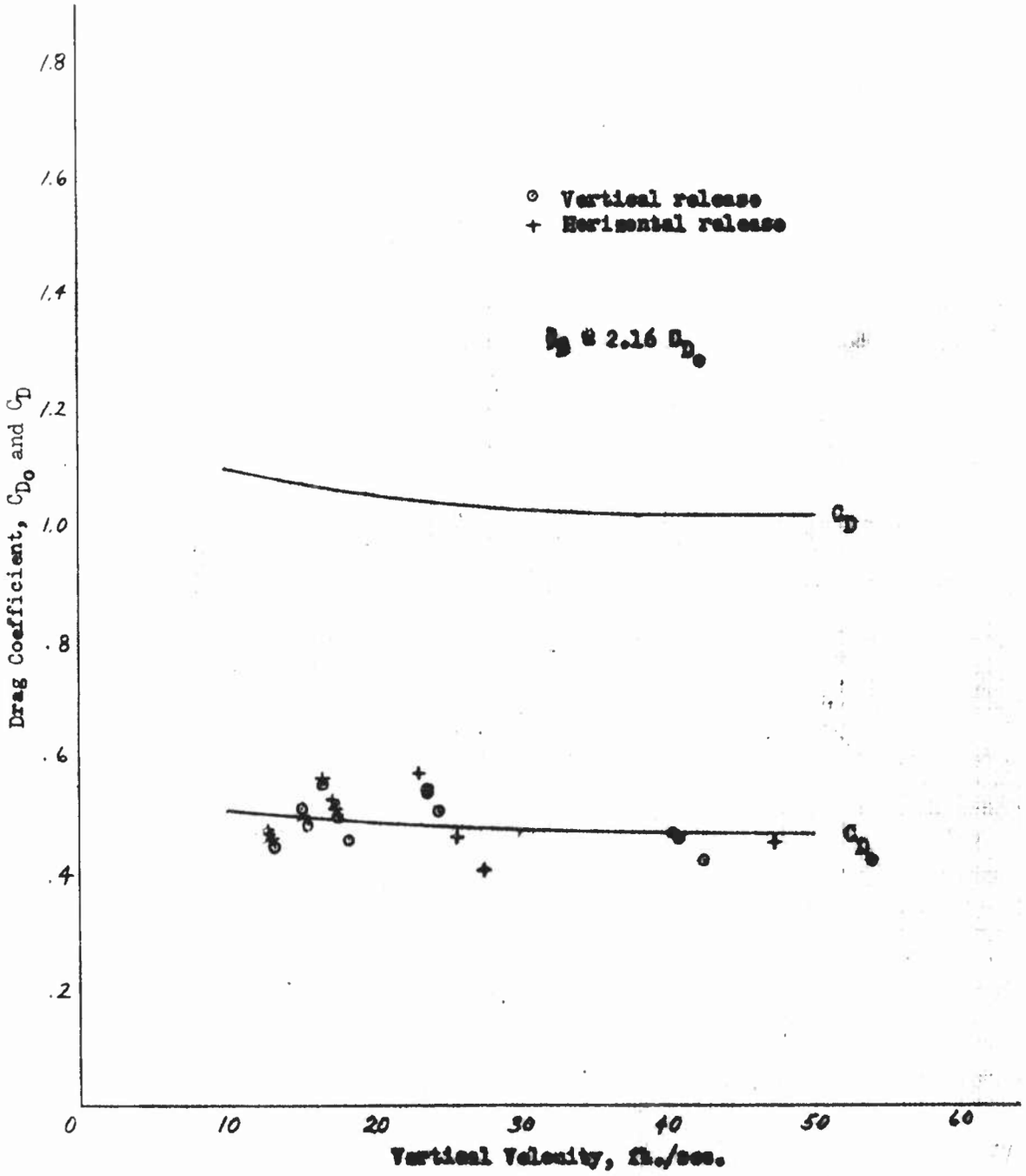

Figure 78 - Drag coefficient versus vertical velocity for the medium-construction brake-type guide-surface parachute model (No. 16) measured during free fall after both vertical and horizontal types of release.

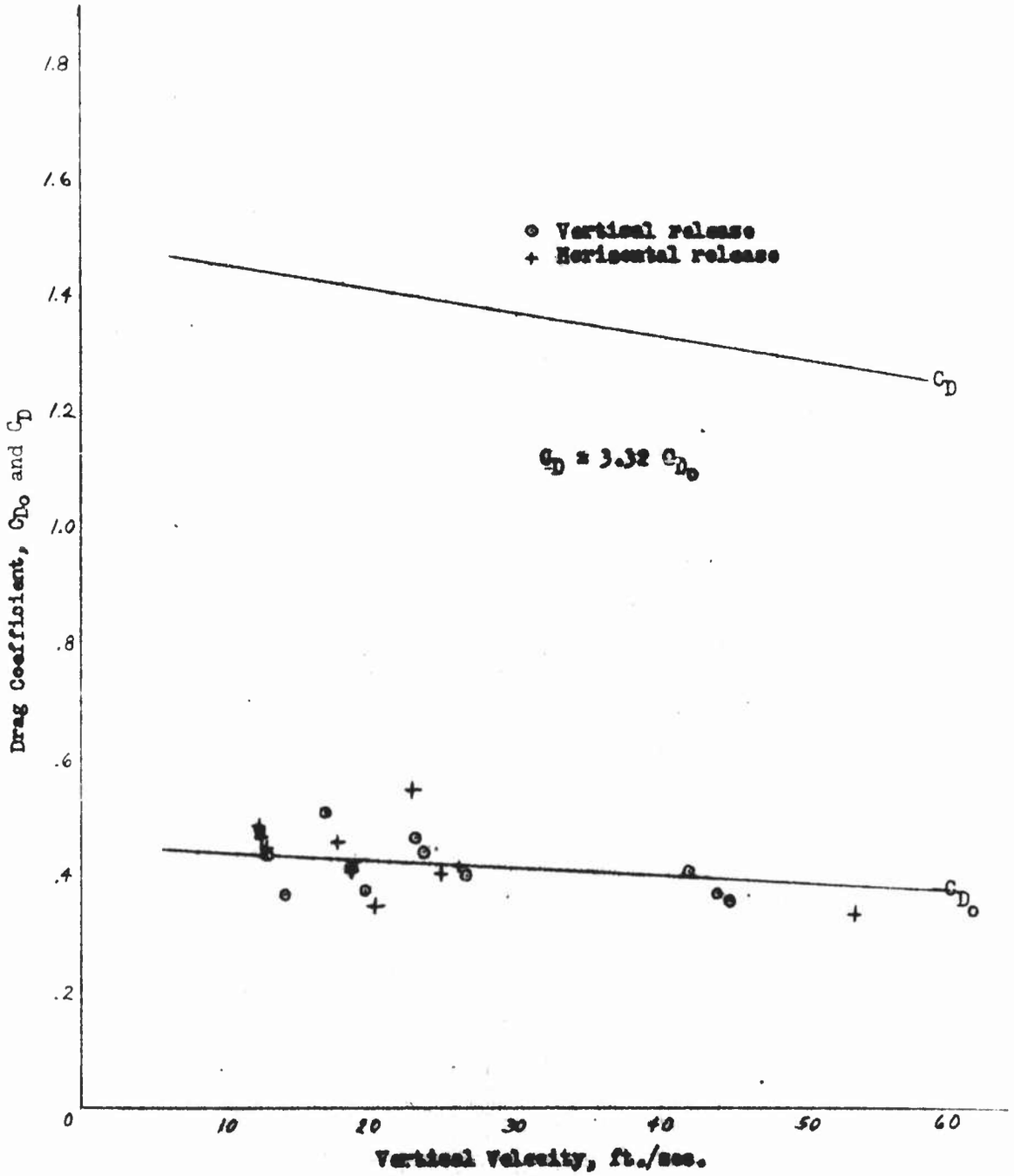

Figure 79 - Drag coefficient versus vertical velocity for the stabilization-type guide-surface parachute model (No. 17) measured during free fall after both vertical and horizontal types of release.

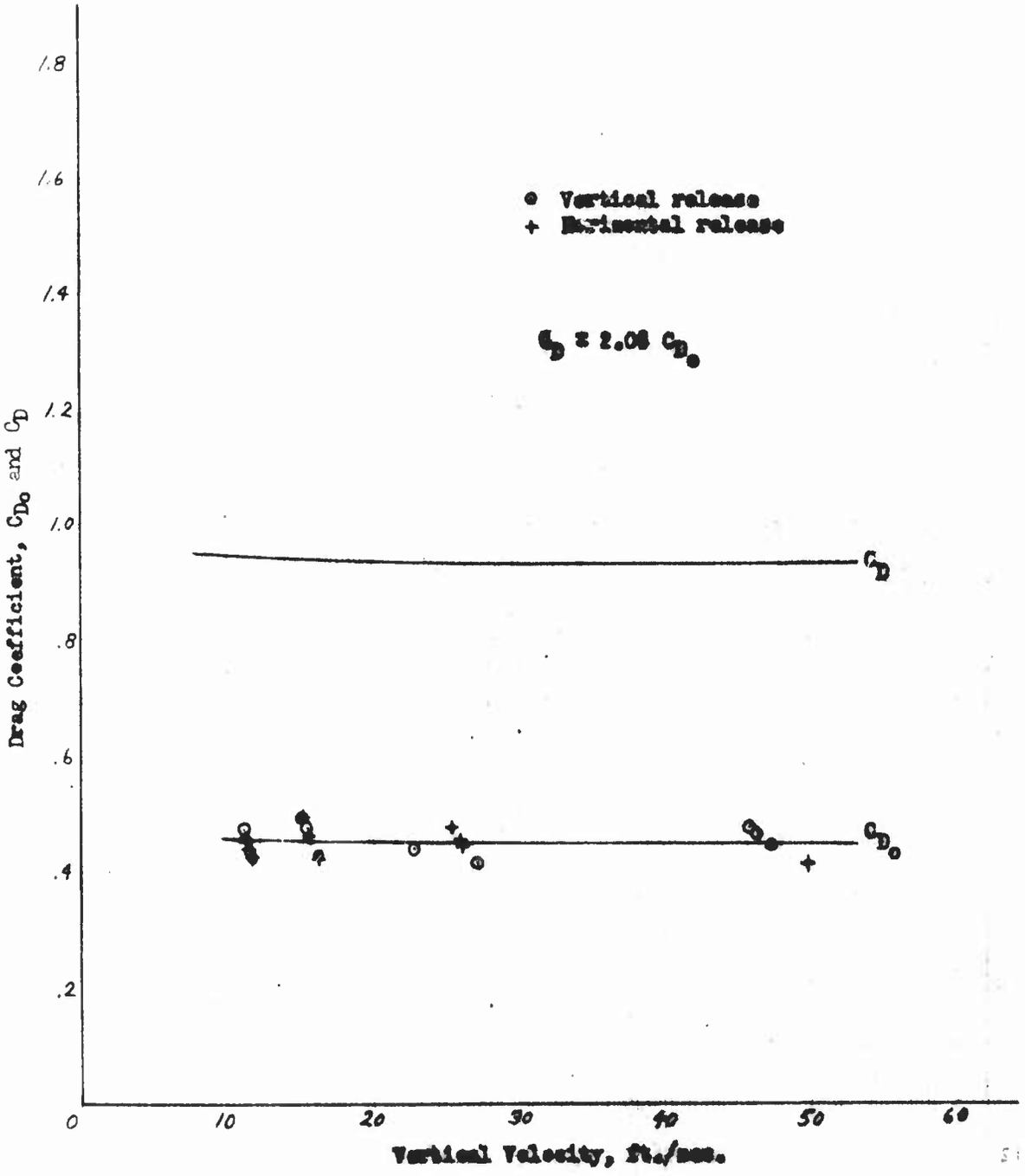

Figure 80 - Drag coefficient versus vertical velocity for the universal-type ribless guide-surface parachute model (No. 25) measured during free fall after both vertical and horizontal types of release.

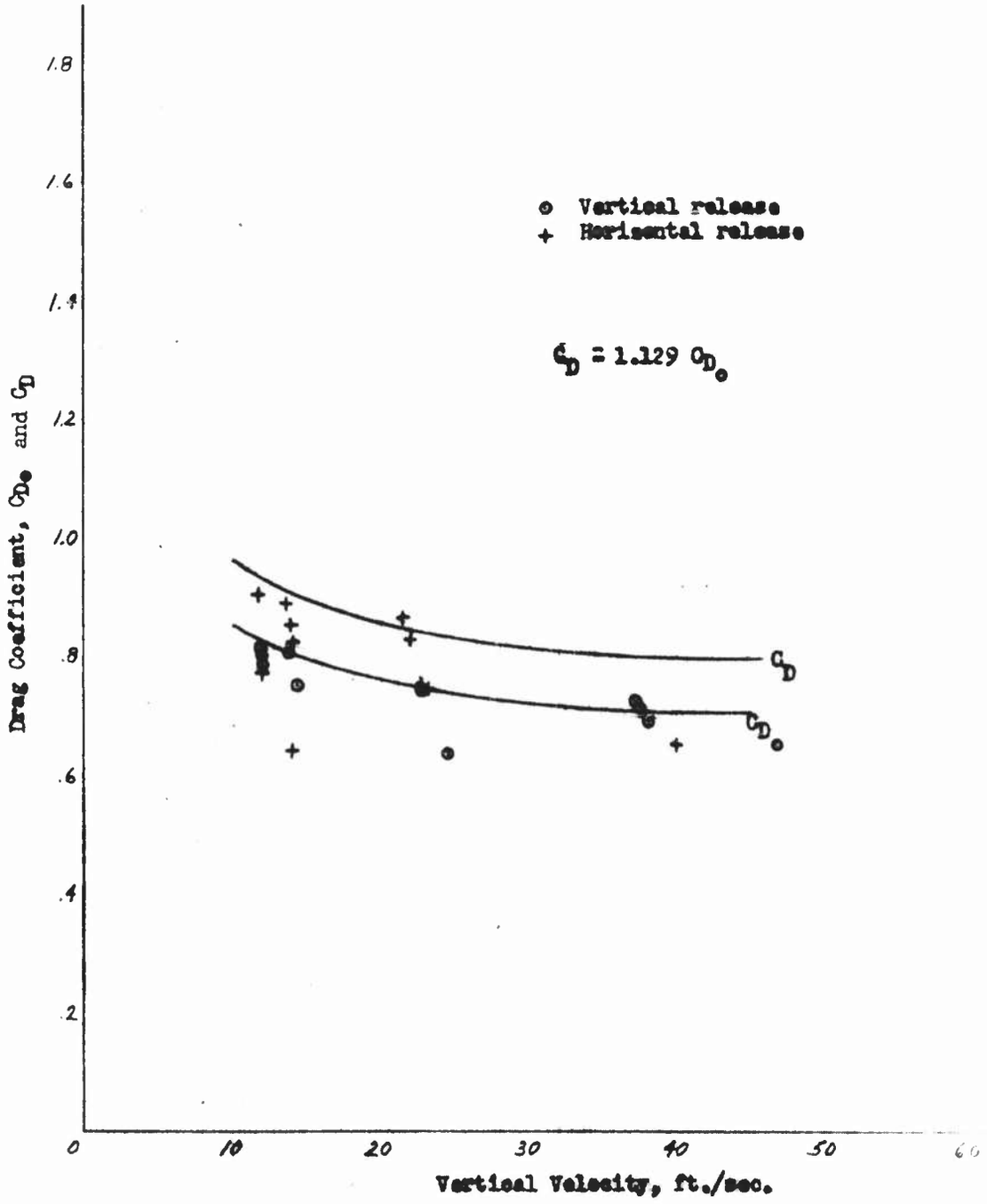

Figure 81 - Drag coefficient versus vertical velocity for the personnel-type guide-surface parachute model (No. 26) measured during free fall after both vertical and horizontal types of release.

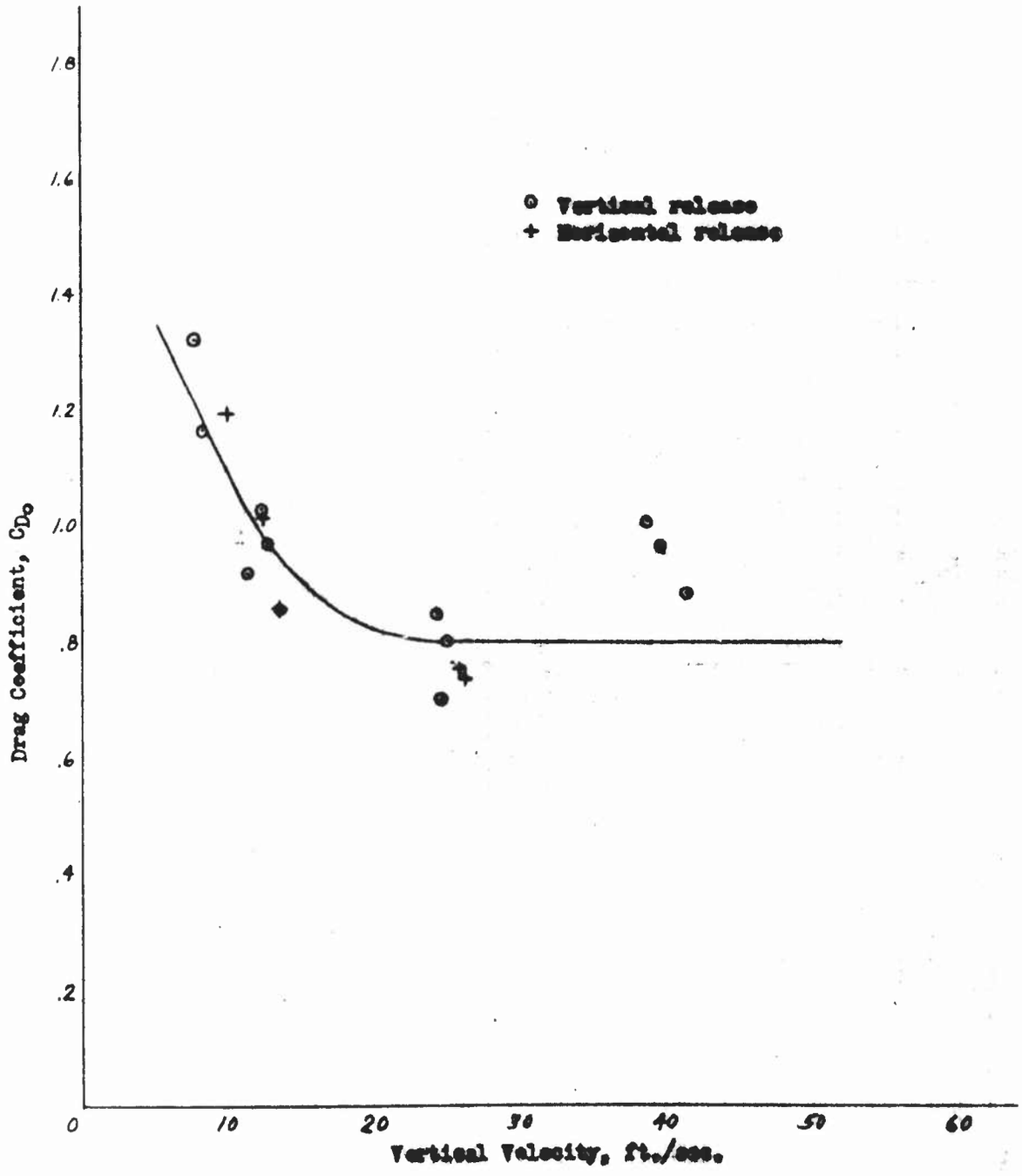

Figure 82 - Drag coefficient versus vertical velocity for the Exeter Type-12 shaped pancreatic model (No. 8) measured during free fall after both vertical and horizontal types of release.

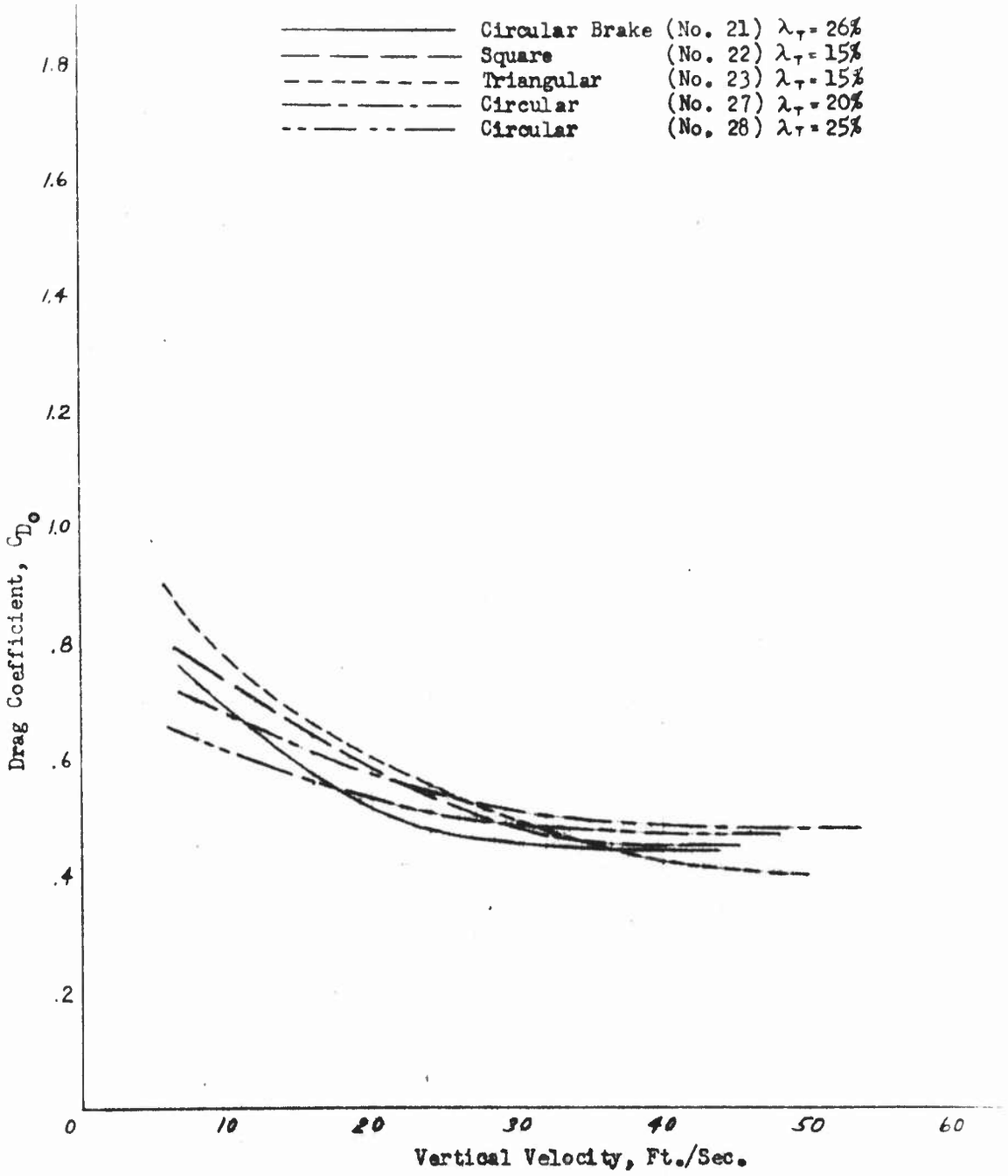

Figure 83- Summary curves of drag coefficient versus vertical velocity for the models of the FIST type ribbon parachute family.

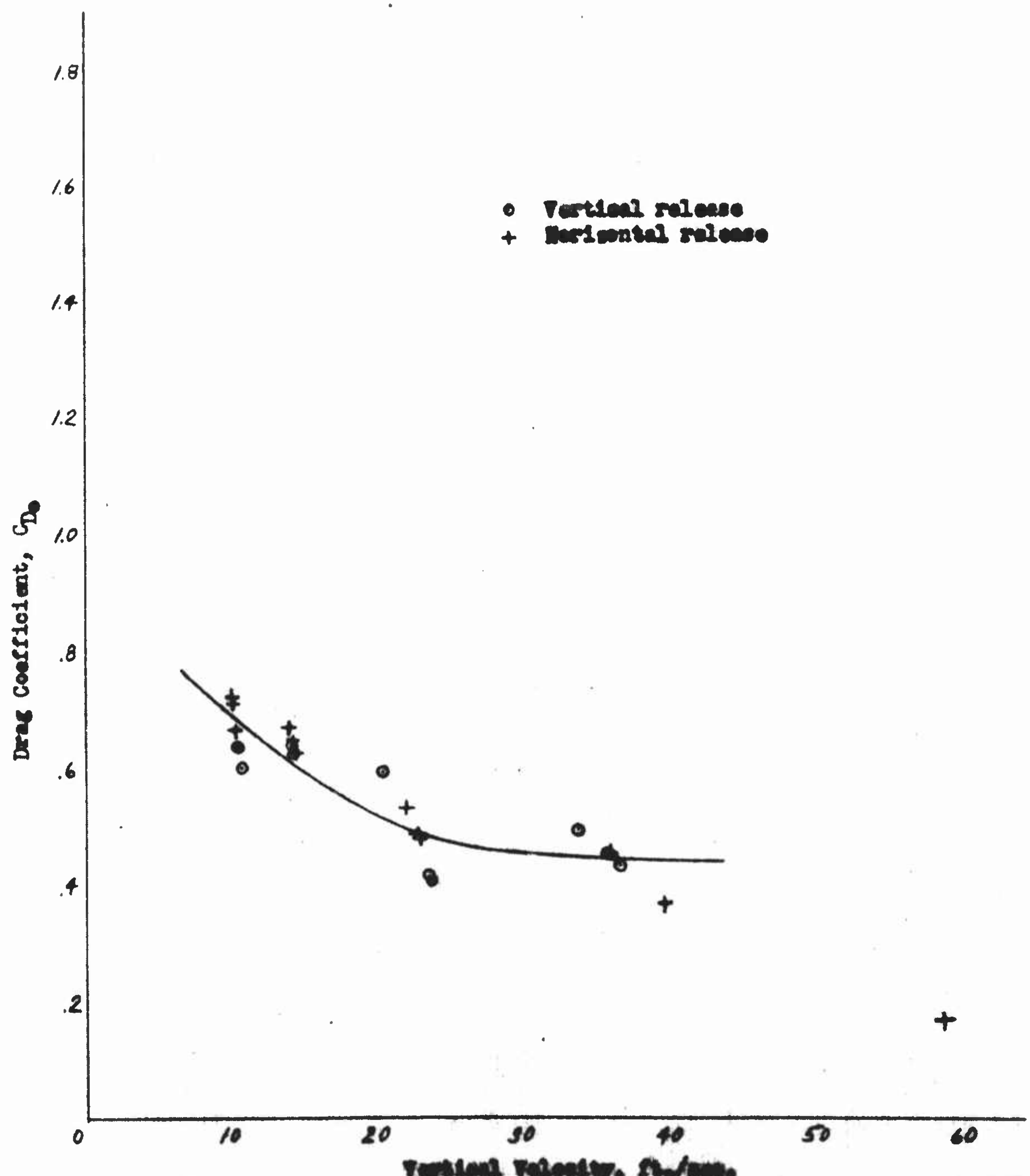

Figure 84 - Drag coefficient versus vertical velocity for the circular [illegible] ribbon parachute model ([illegible]) measured during free fall after both vertical and horizontal types of release.

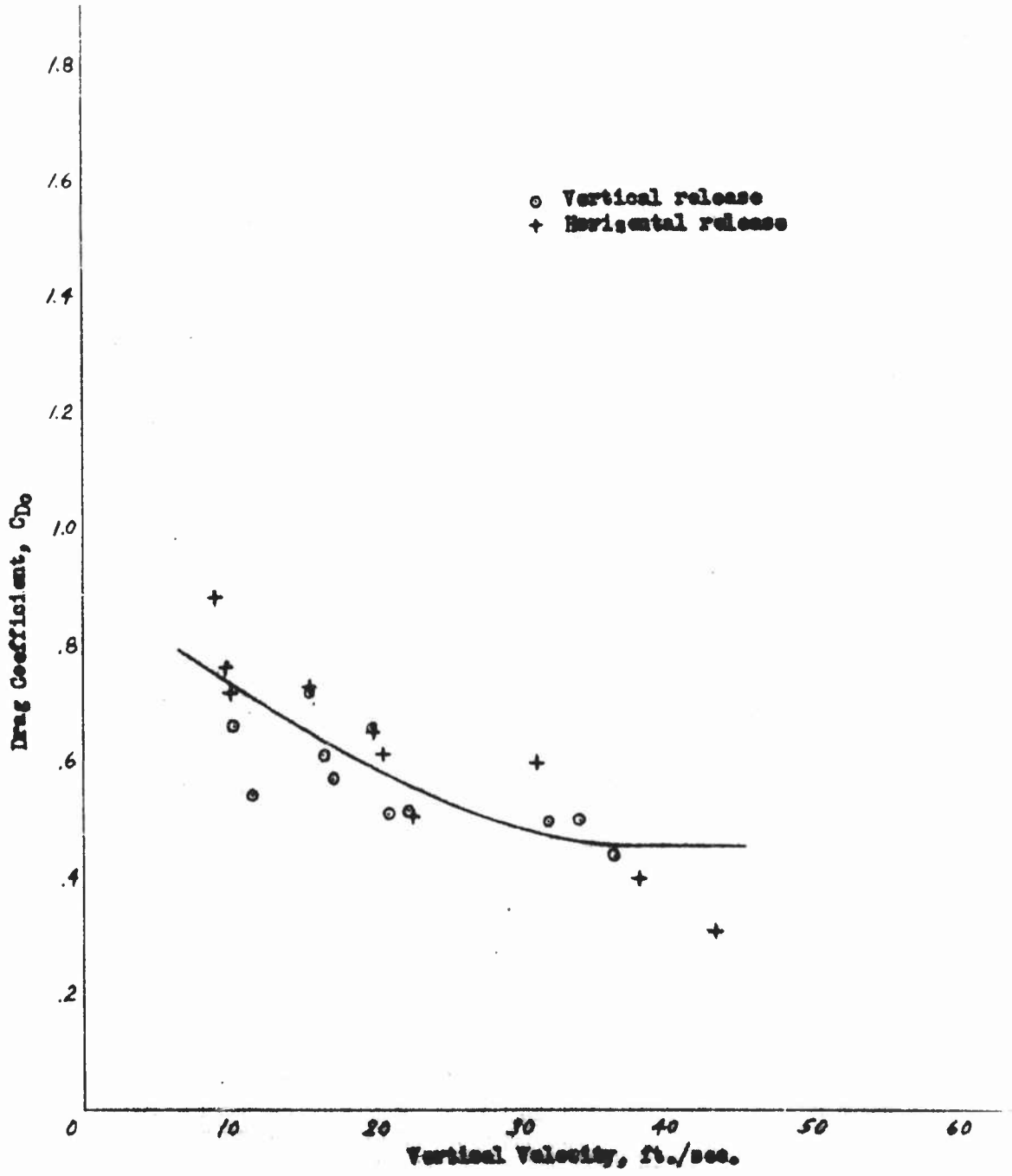

Figure 85 - Drag coefficient versus vertical velocity for the square ribbon parachute metal (No. 22) measured during free fall after both vertical and horizontal types of release.

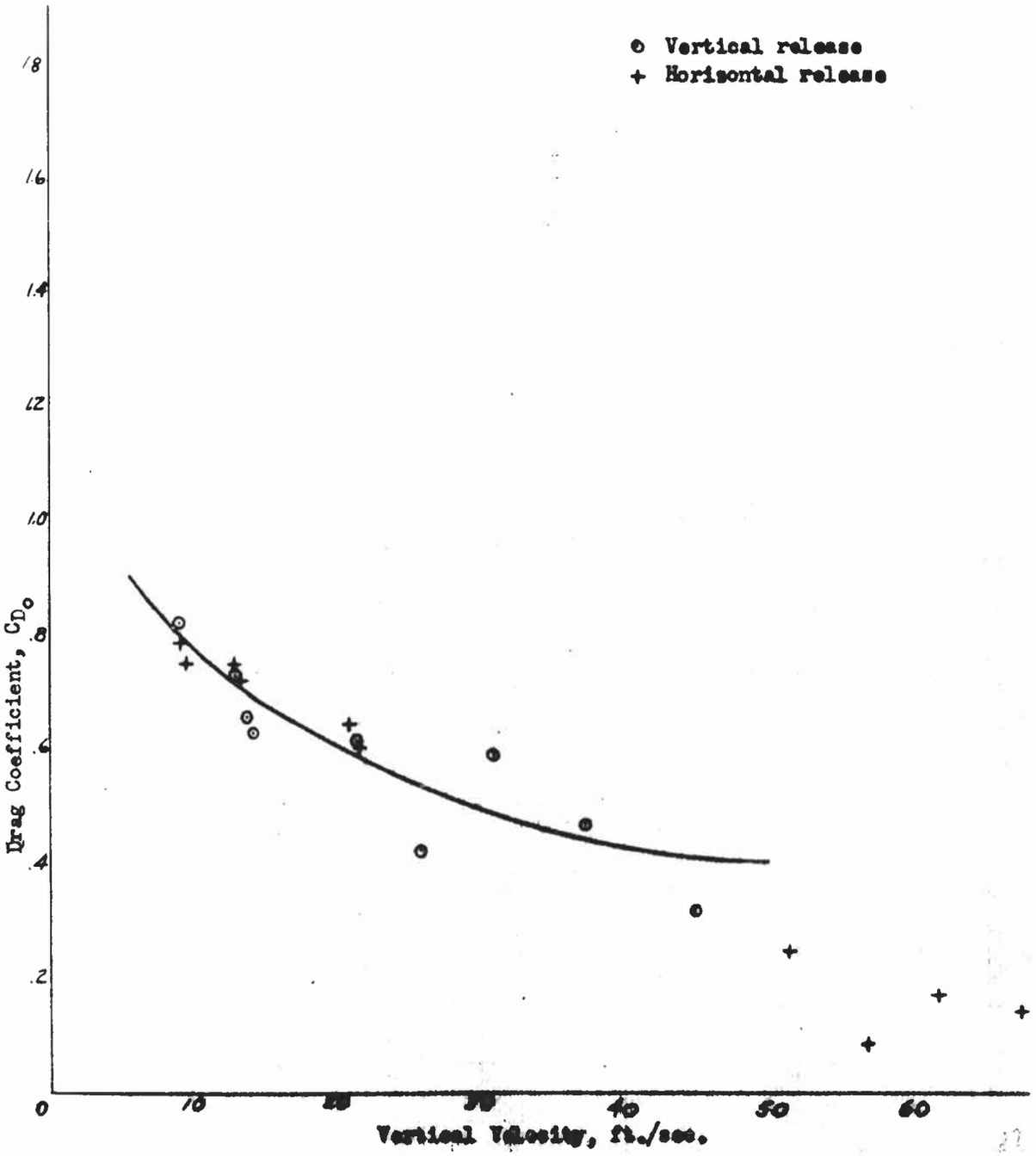

Figure 86 - Drag coefficient versus vertical velocity for the triangular ribbon parachute model (No. 23) measured during free fall after both vertical and horizontal types of release.

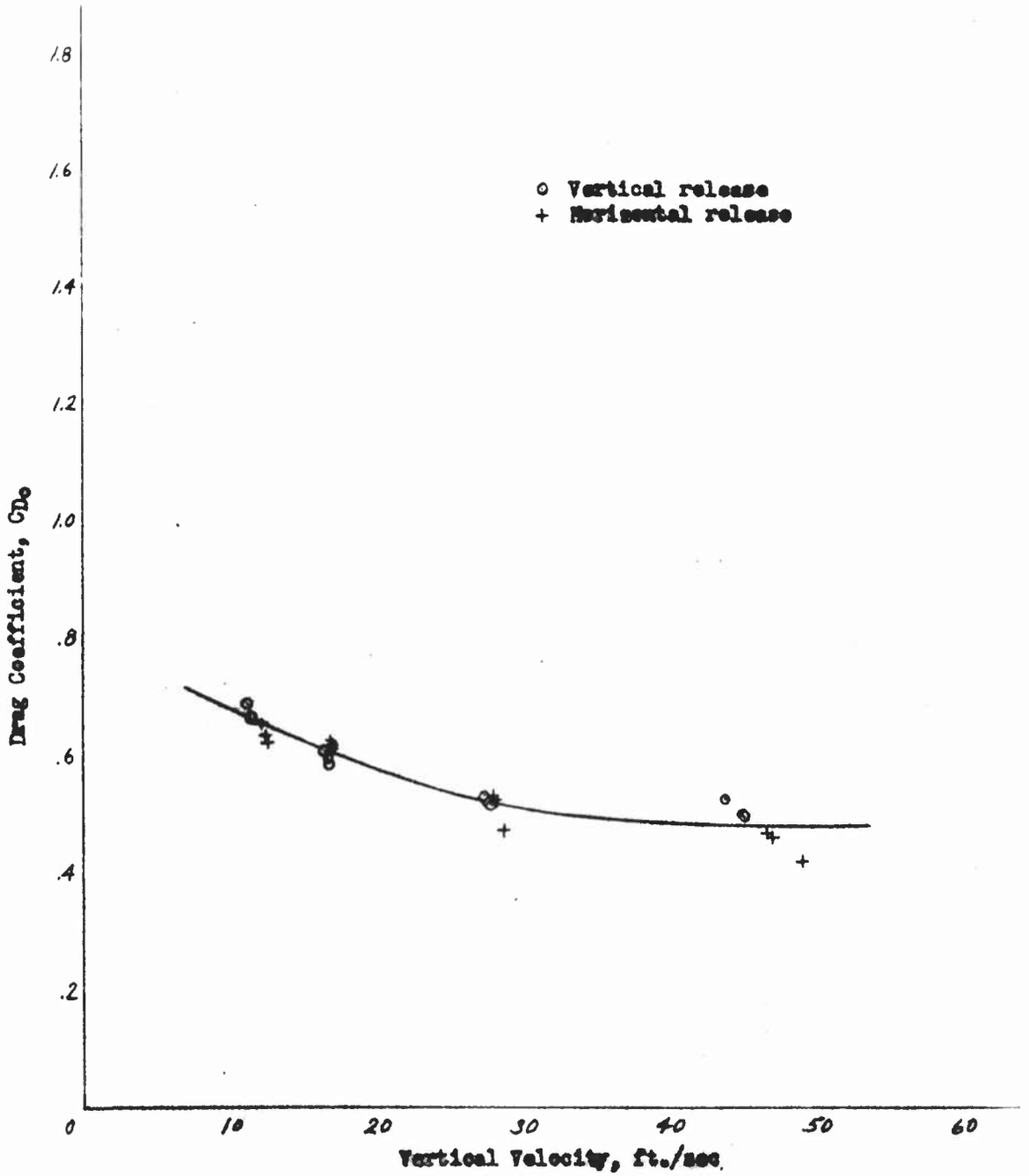

Figure 87 - Drag coefficient versus vertical velocity for the FIST ribbon parachute model (20% total porosity) (No. 27) measured during free fall after both vertical and horizontal types of release.

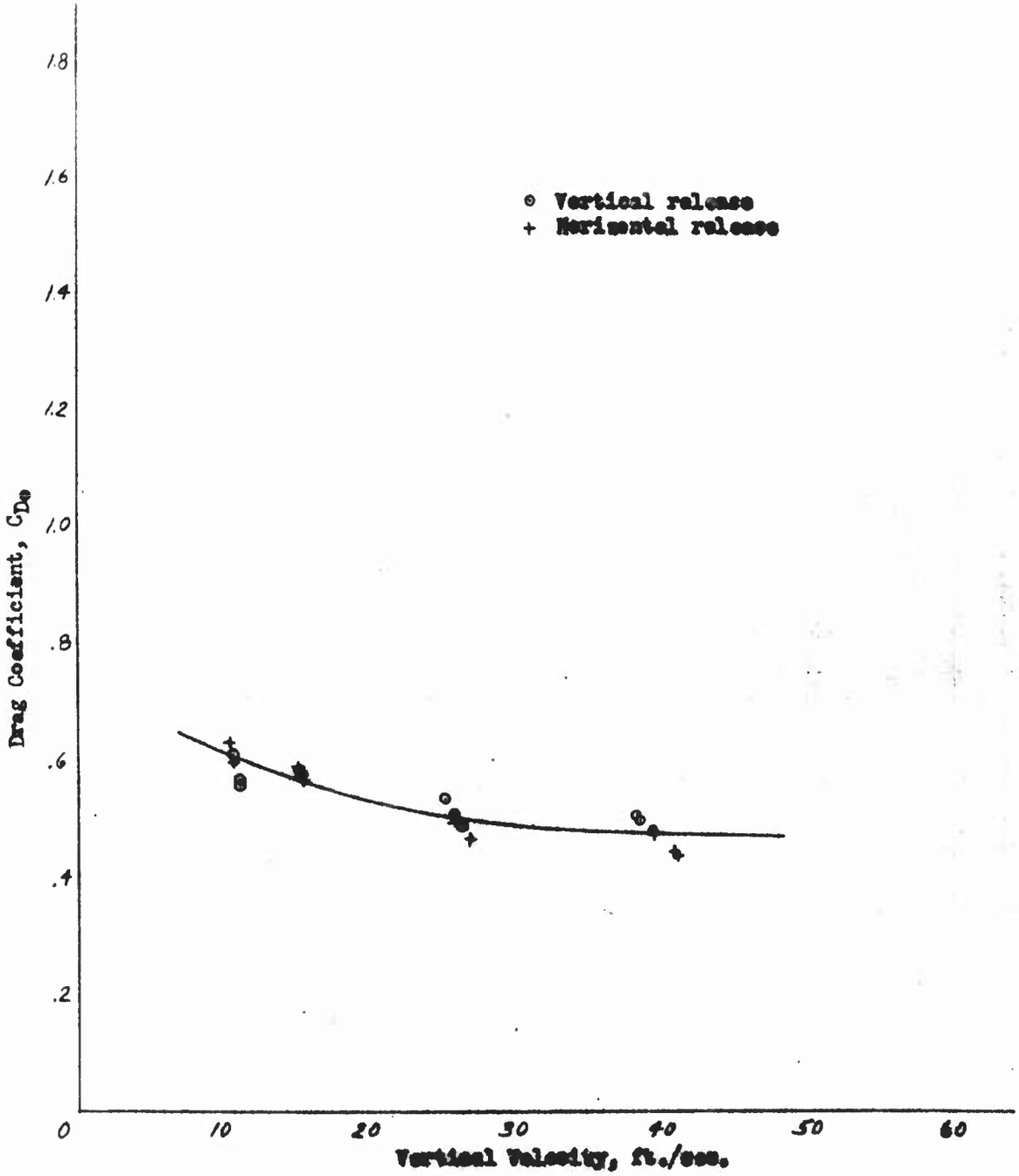

Figure 88 - Drag coefficient versus vertical velocity for the FIST ribless parachute model (35% total porosity) (No. 28) measured during free fall after both vertical and horizontal types of release.

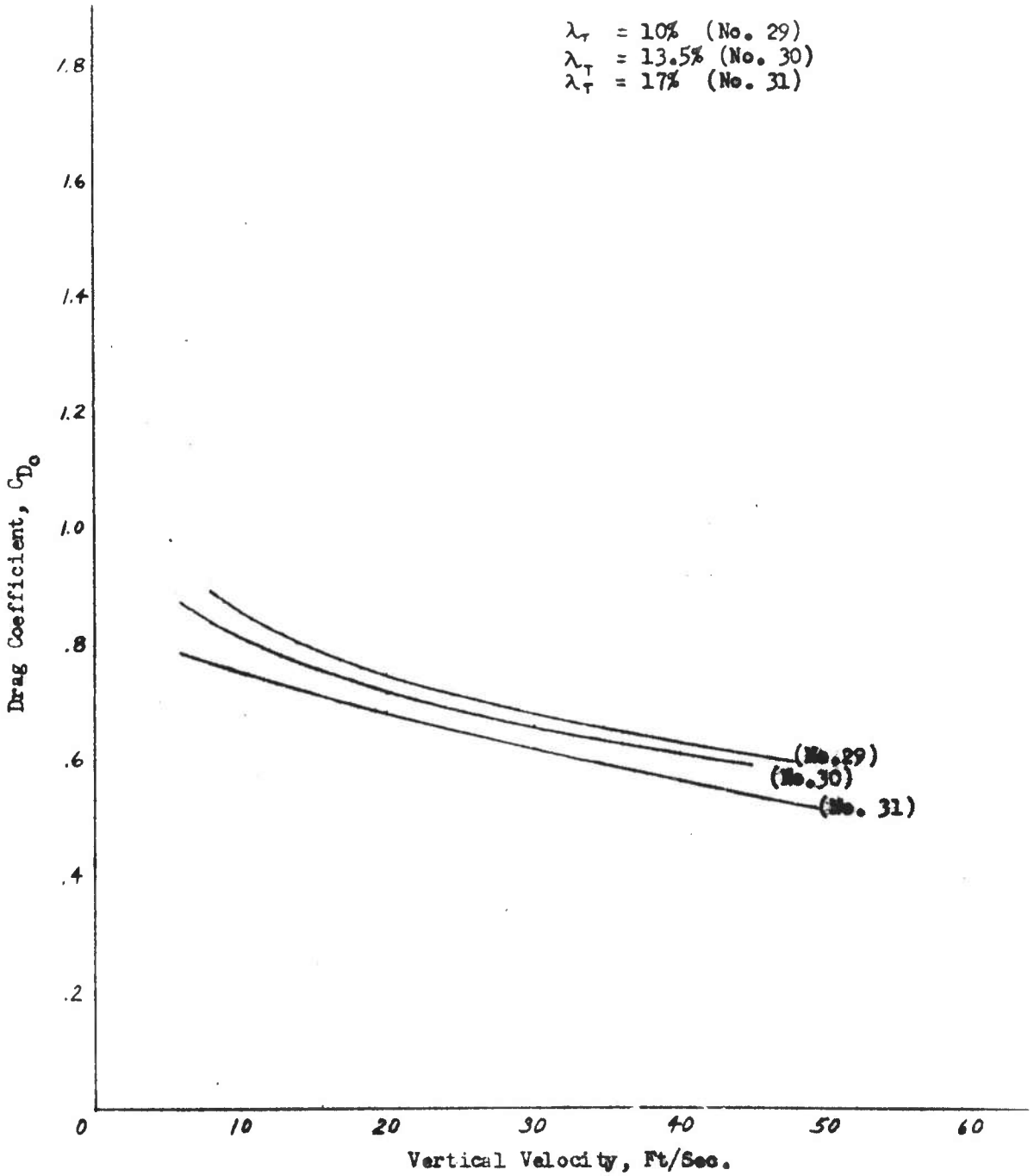

Figure 89 - Summary curves of drag coefficient versus vertical velocity for the circular models of the ring-slot parachute family

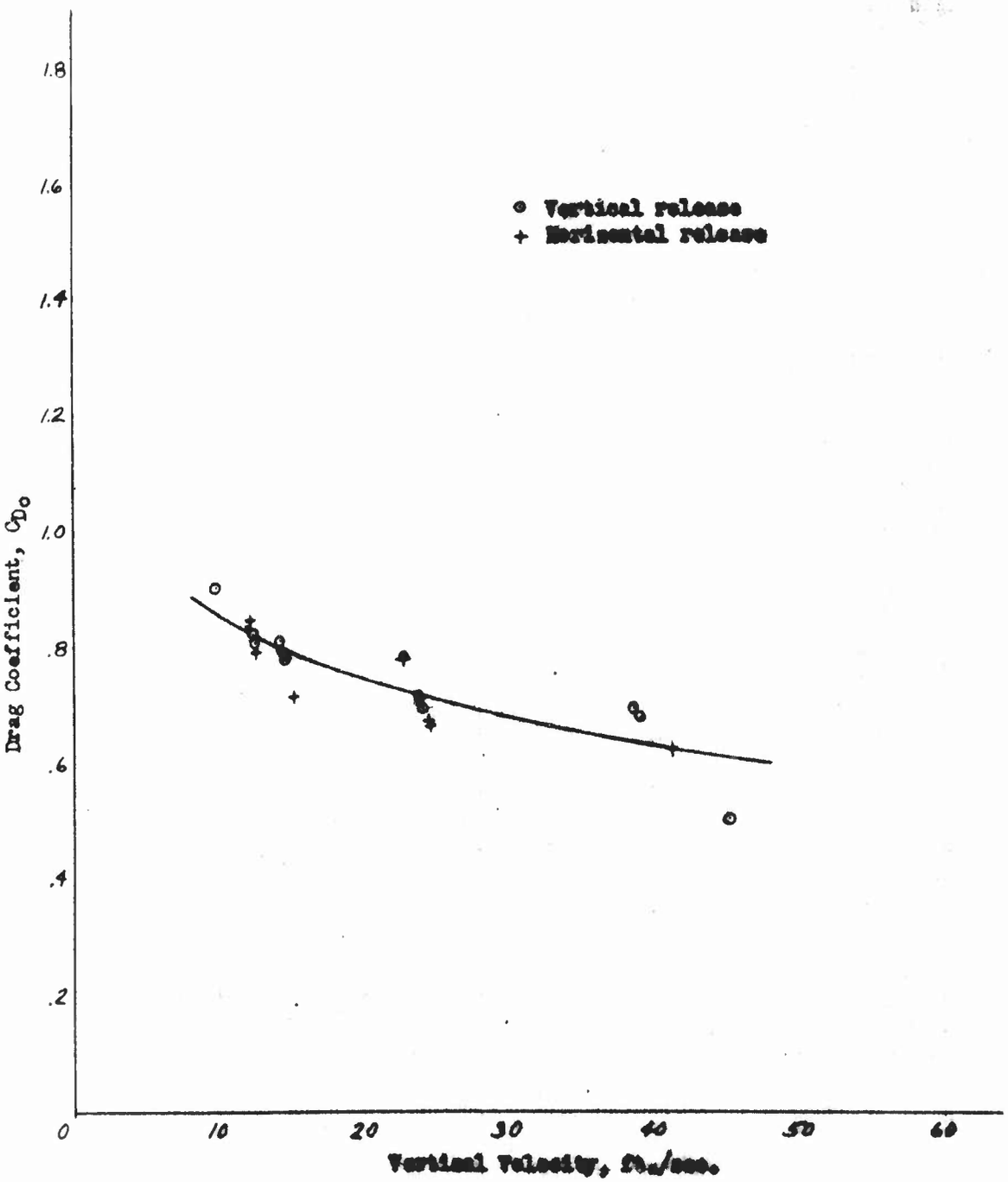

Figure 90 - Drag coefficient versus vertical velocity for the ring-slot parachute model (10% total porosity) (No. 29) measured during free fall after both vertical and horizontal types of release.

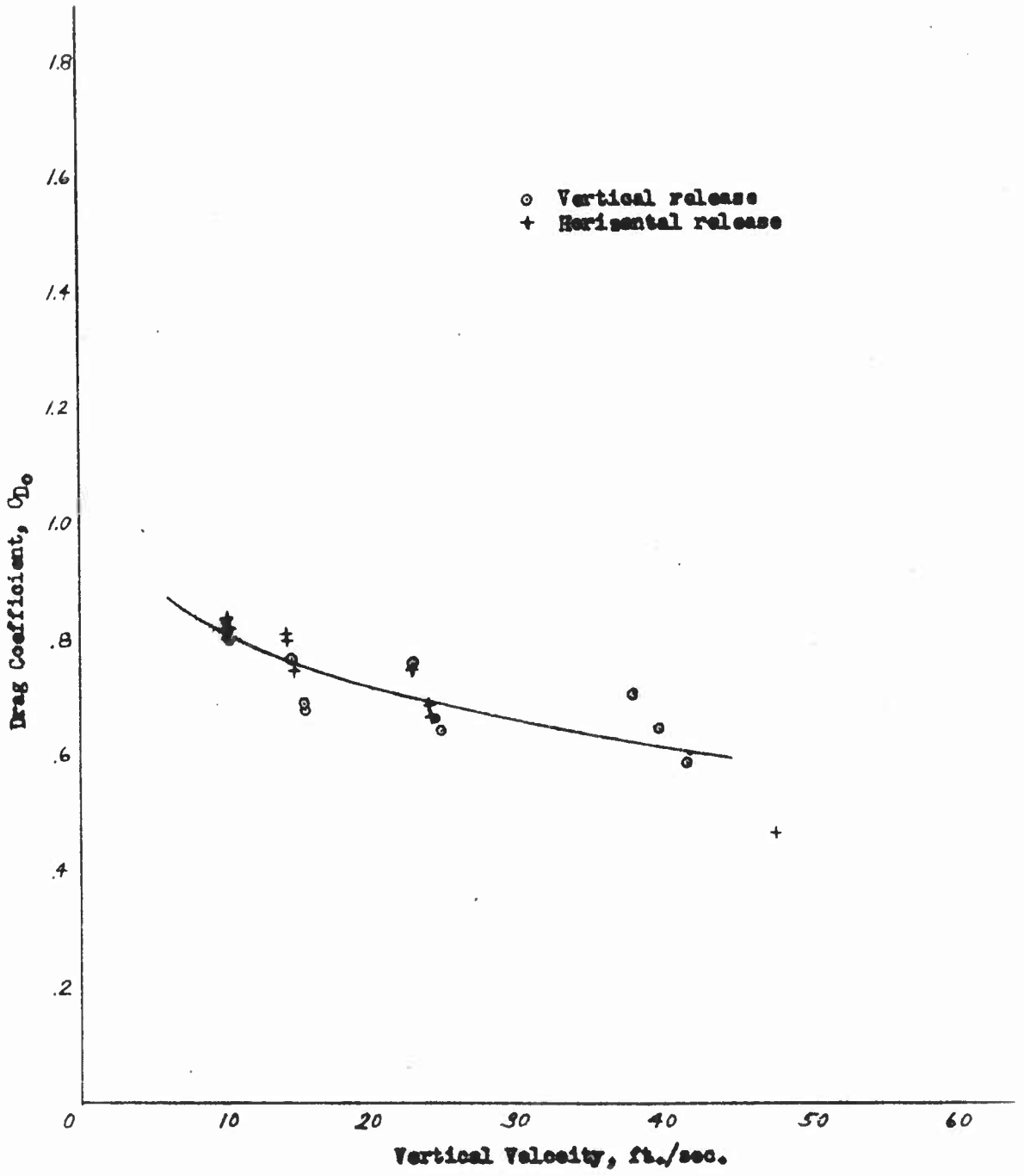

Figure 91 - Drag coefficient versus vertical velocity for the ring-slot parachute model (13.5% total porosity) (No. 30) measured during free fall after both vertical and horizontal types of release.

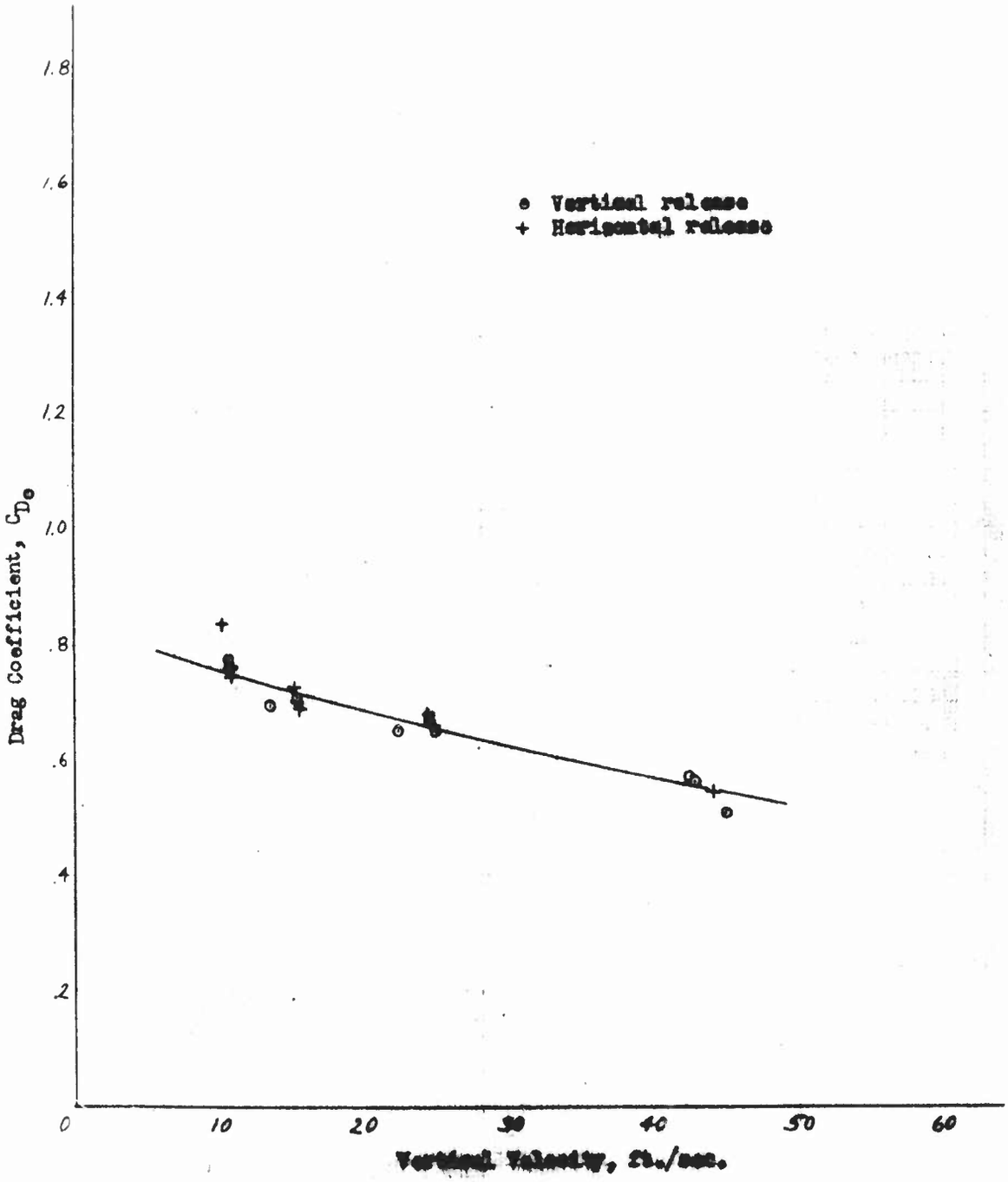

Figure 92 - Drag coefficient versus vertical velocity for the ring-slot parachute model (17% total geometric) (No. 31) measured during free fall after both vertical and horizontal types of release.

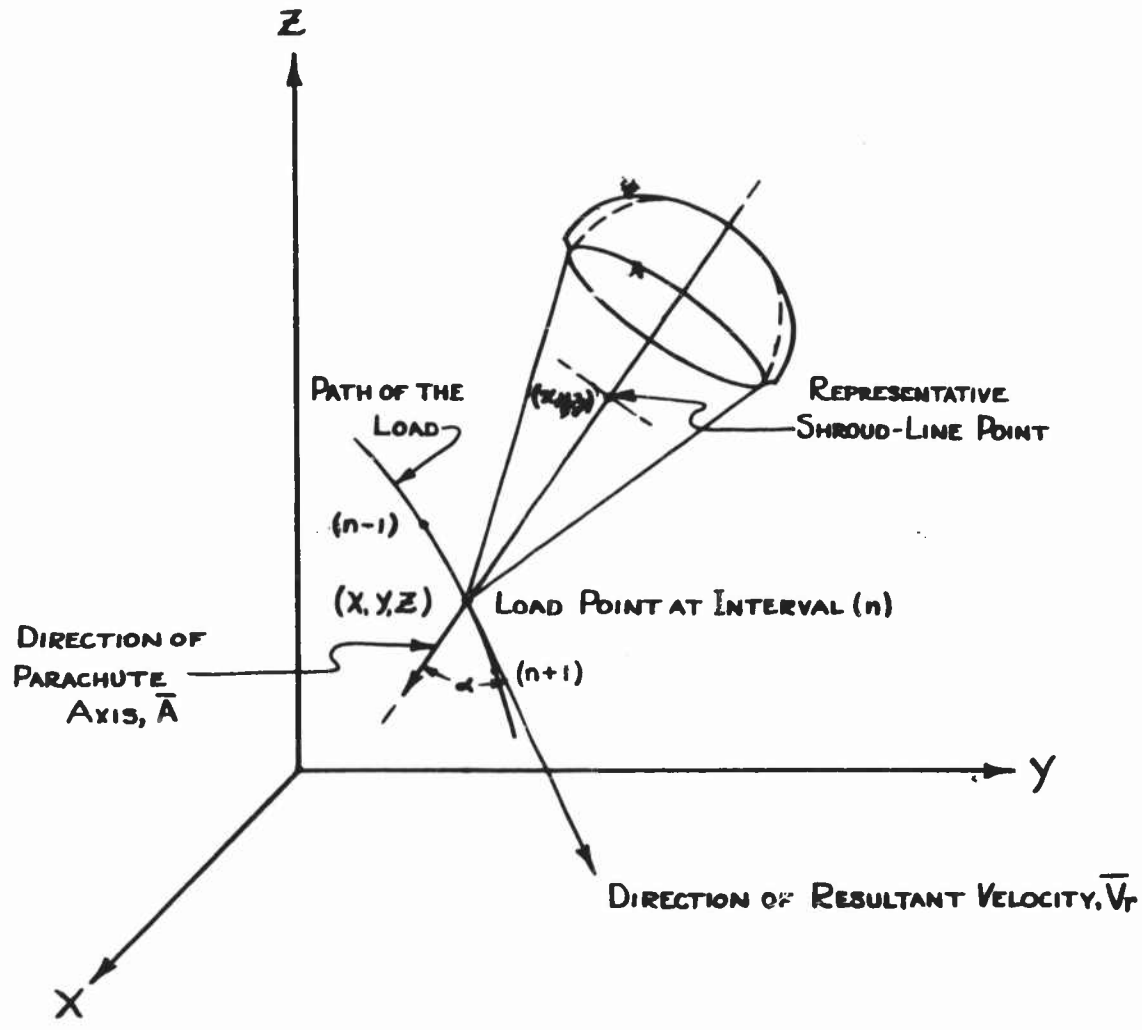

AT POINT (n):

$$\bar{A} = (X-x)i + (Y-y)j + (Z-z)k$$

$$\bar{V}_r = (X_{n+1} - X_{n-1})i + (Y_{n+1} - Y_{n-1})j + (Z_{n+1} - Z_{n-1})k$$

$$\cos\alpha = \frac{\bar{A}\cdot\bar{V}_r}{A\cdot V_r}$$

Figure 93 - Definitions of axes, vectors, and parachute system as used in the angle of attack determination.

Drop No. 1

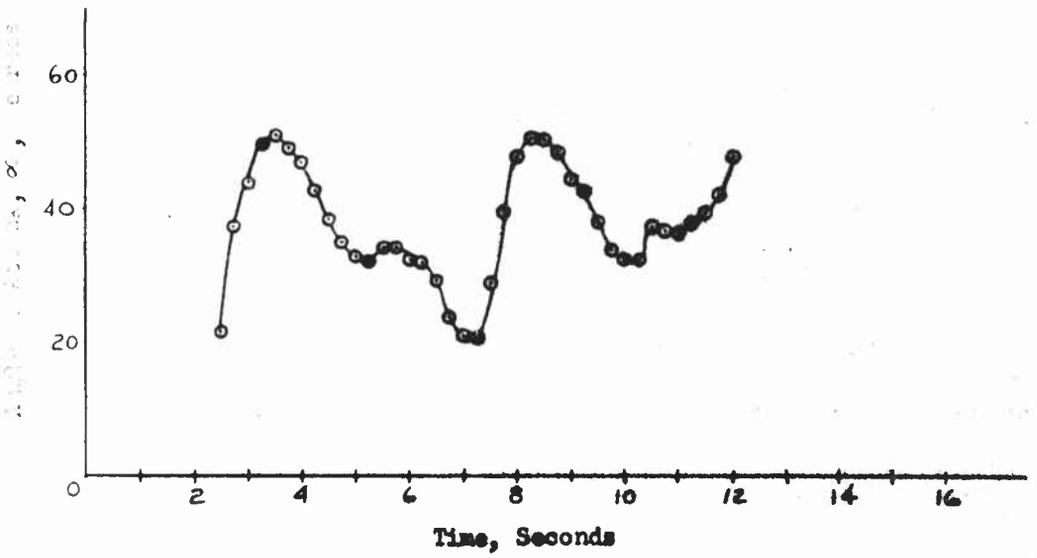

Figure 94 - Angle of attack of the parachute measured at the load versus time for the solid-flat-circular parachute model (No. 1) in free fall at a vertical terminal velocity of 10.4 feet per second after a vertical release.

Drop No. 4

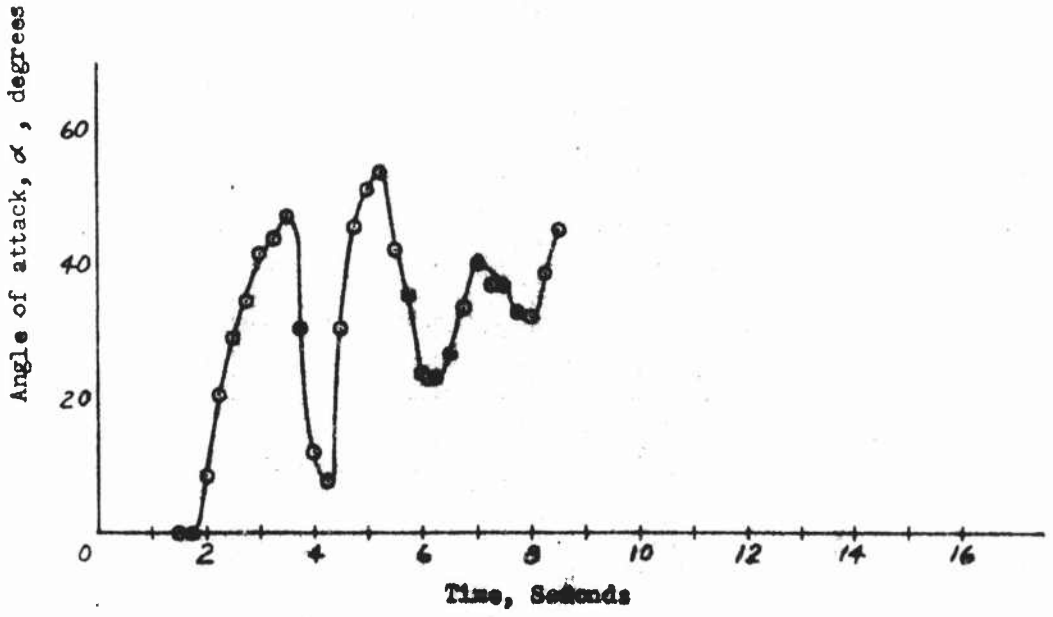

Figure 95 - Angle of attack of the parachute measured at the load versus time for the solid-flat-circular parachute model (No. 1) in free fall at a vertical terminal velocity of 16.8 feet per second after a vertical release.

Drop No. 8

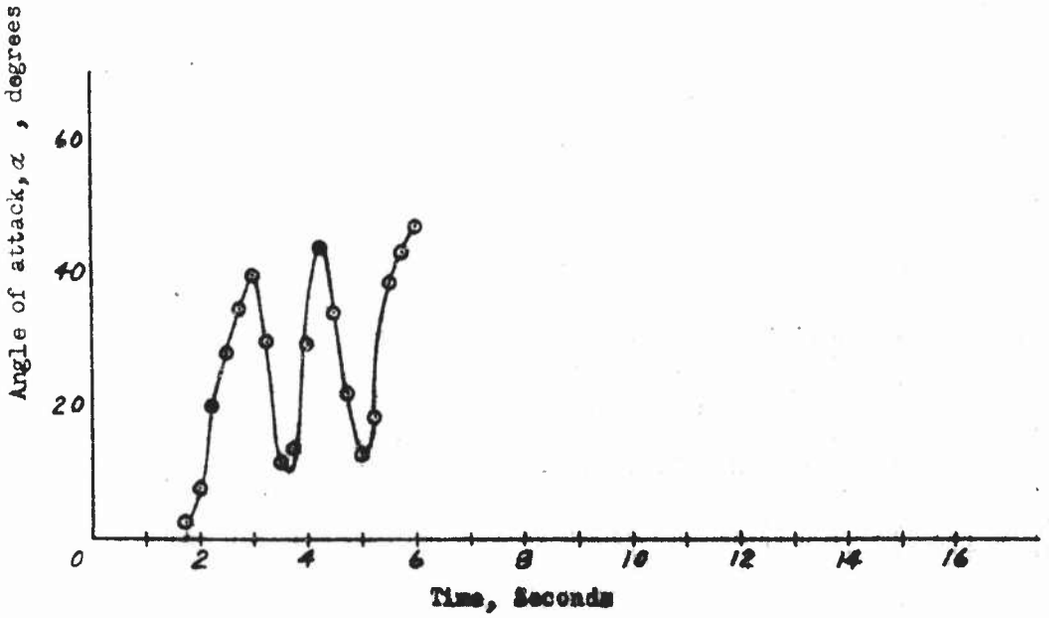

Figure 96 - Angle of attack of the parachute measured at the load versus time for the solid-flat-circular parachute model (No. 1) in free fall at a vertical terminal velocity of 26.8 feet per second after a vertical release.

Drop No. 11

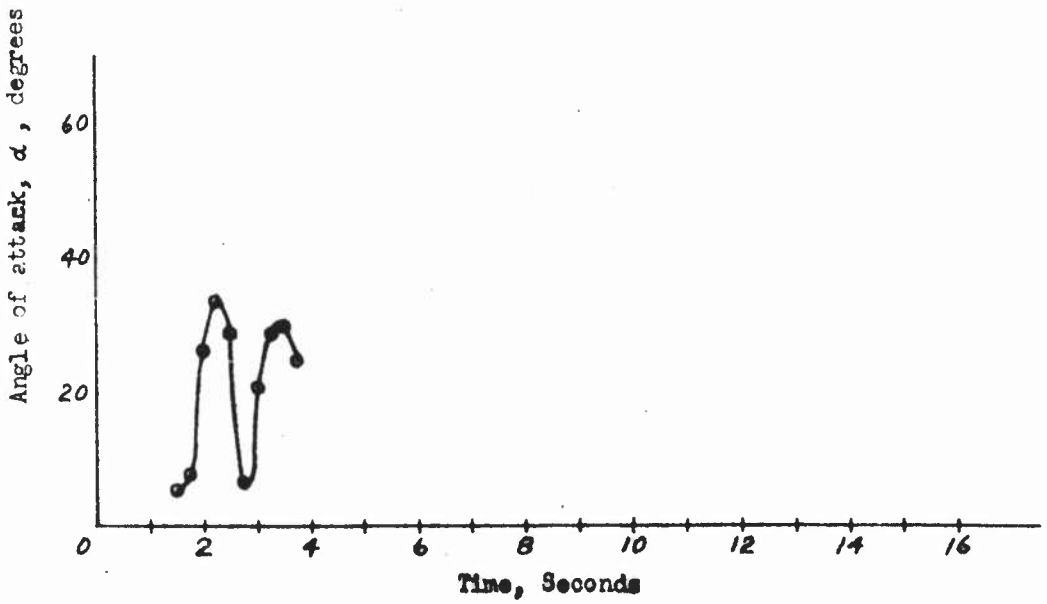

Figure 97 -Angle of attack of the parachute measured at the load versus time for the solid-flat-circular parachute model (No. 1) in free fall at a vertical terminal velocity of 41.1 feet per second after a vertical release.

Drop No. 15

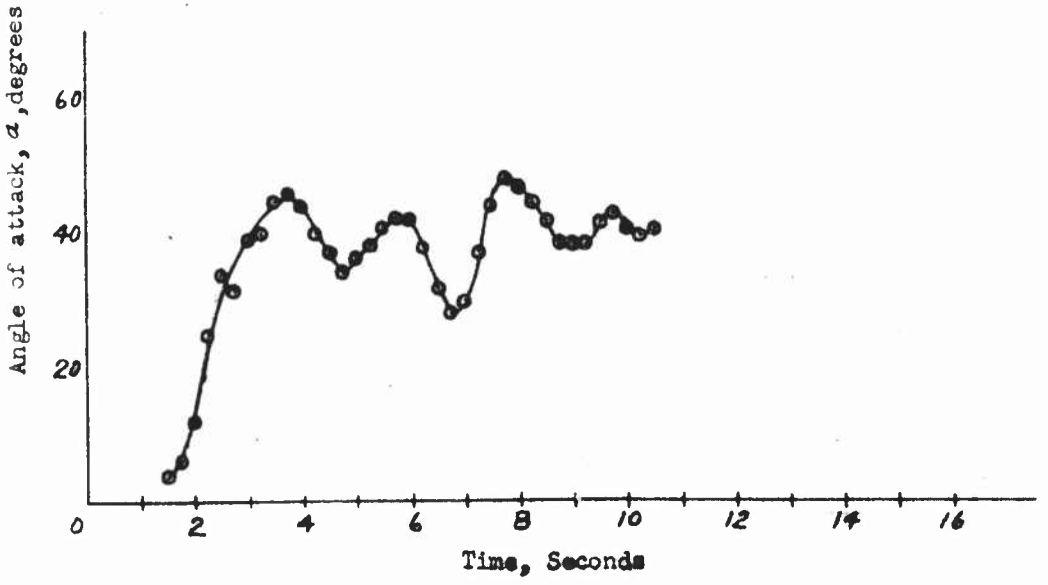

Figure 98 - Angle of attack of the parachute measured at the load versus time for the solid-flat-circular parachute model (No. 1) in free fall at a vertical terminal velocity of 11.2 feet per second after a horizontal release.

Drop No. 16

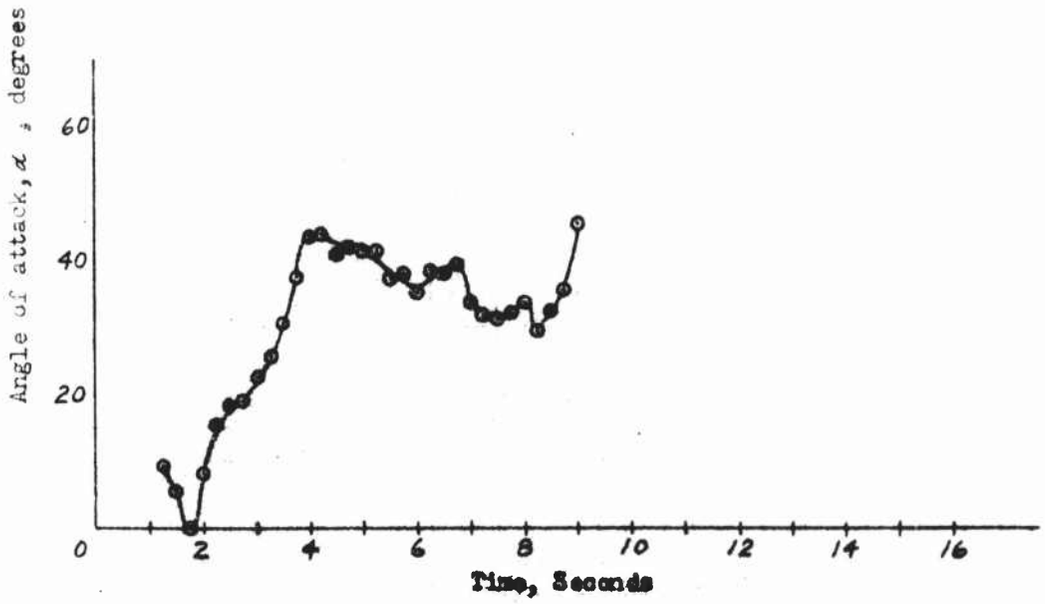

Figure 99.-Angle of attack of the parachute measured at the load versus time for the solid-flat-circular parachute model (No. 1) in free fall at a vertical terminal velocity of 15.2 feet per second after a horizontal release.

Drop No. 20

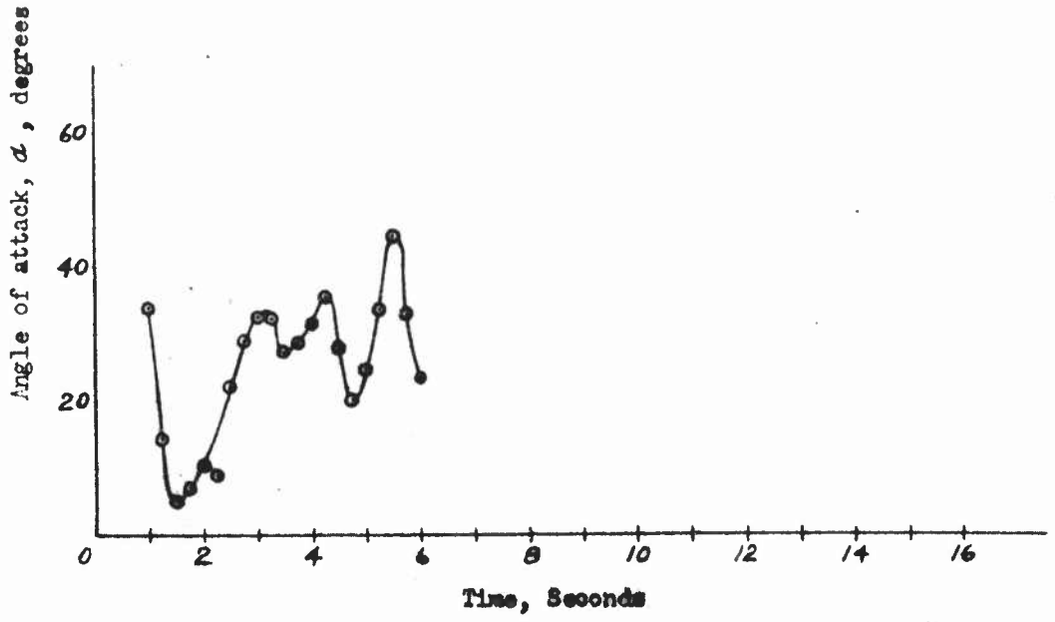

Figure 100 - Angle of attack of the parachute measured at the load versus time for the solid-flat-circular parachute model (No. I) in free fall at a vertical terminal velocity of 27.2 feet per second after a horizontal release.

Drop No. 22

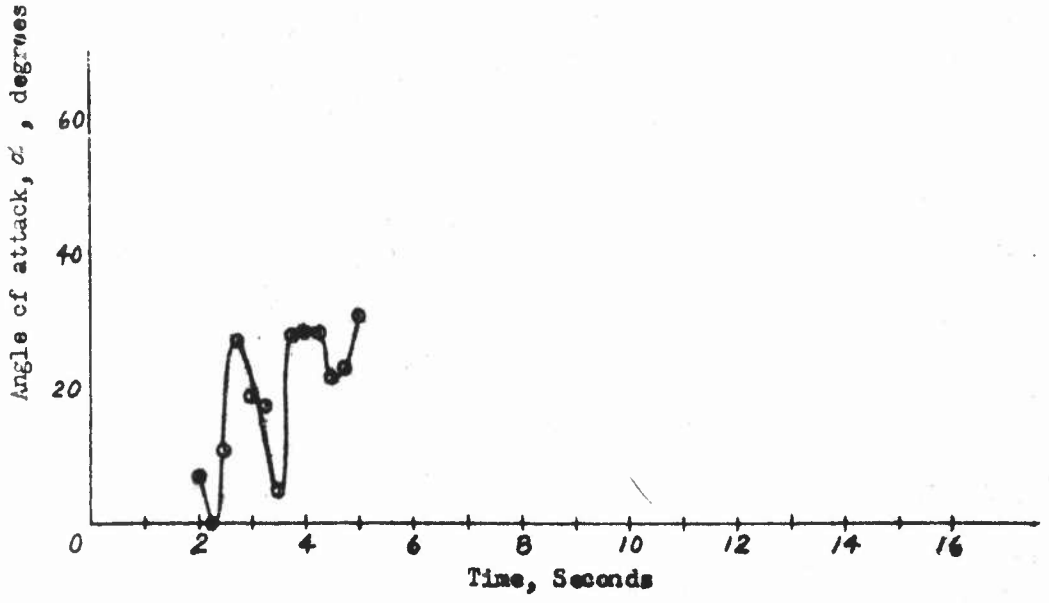

Figure 101-Angle of attack of the parachute measured at the lead versus time for the solid-flat-circular parachute model (No. T) in free fall at a vertical terminal velocity of 38.5 feet per second after a horizontal release.